



UNIVERSITY
OF HULL

| ENERGY AND ENVIRONMENT
INSTITUTE

Ecological Responses to Climate Change:
Using the Common Ragworm
(*Hediste diversicolor*)
as an Indicator for Benthic Ecosystems

Thesis submitted for the Degree of Doctor of Philosophy
(Ph.D).

By

Jennifer James

Contents

List of figures.....	4
Abstract.....	19
Synopsis.....	20
Acknowledgements.....	26
1.0. Introduction and Literature Review	27
1.1. Mass Extinction.....	27
1.2. Ocean Acidification and Climate Change in the Marine Environment	31
1.3. Impacts on Marine Organisms	38
1.3.1. Calcification Issues.....	40
1.3.2. Physiology and Larval Development	41
1.3.3. Chemical Communication	45
1.3.5. Growth rate and Mortality	51
1.3.6. Multi-stressor Effects: Temperature and Pollution	52
1.3.6. Energetic costs of climate change	55
1.3.7. Bioturbation.....	59
1.3.8. Evolution of Bioturbation and the Expansion of Accessible Habitat.....	60
1.3.9. Loss of Bioturbation	63
1.3.10. <i>Hediste diversicolor</i>	64
1.4. Past Mass Extinctions and the Modern Day Link.....	67
1.5. Permian-Triassic Mass Extinction	70
1.5.1. Background Information.....	70
1.5.2. Environmental Conditions During the PTME – Based on Fossil Records.	73
1.5.3. Environmental Conditions during the PTME – Based on Isotope Analysis	76
Rationale for Research.....	80
2.0. Chapter 2.....	83
2.1. The Future of Chemical Cues: Responses of the polychaete <i>Hediste diversicolor</i> to artificial food cues in an warm, acidic ocean.....	84
2.1.1. Abstract	84
2.1.2. Introduction	86
2.1.3. Method	90
2.1.4. Results	96
2.1.5. Discussion	110
2.1.6. Conclusion.....	125

3.0. Chapter 3.....	128
3.2. Acid Reflux: How Temperature and pH Alter Oxygen Dynamics in Bioturbated Sediments.....	129
3.2.1. Abstract.....	129
3.2.2. Introduction	130
3.2.3. Methods	134
3.2.4. Results	142
3.2.5. Discussion.....	149
4.0. Chapter 4.....	157
4.1. Mucus production in future climatic conditions	158
4.1.1. Abstract	158
4.1.2. Introduction	159
4.1.3. Method	161
4.1.4. Results	167
4.1.5. Discussion	170
5.0. Conclusion	179
5.1. Chemical Communication and Environmental Change	179
5.2. Burrow Oxygen and Environmental Change	183
5.3. Mucous Production and Environmental Change.....	188
5.4. Climate change and polychaetes	190
Supplementary materials - Chapter 2.....	193
Supplementary Materials – Chapter 3.....	211
References.....	236

List of figures

FIGURE 1.1 : A) SENSITIVITY OF MARINE ORGANISMS TO MODERN CLIMATE CHANGE BASED ON EXPERIMENTAL DATA (REDDIN ET AL., 2020). B) MODELLED PERCENTAGE EXTINCTION BY LATITUDE IN THE MARINE ENVIRONMENT BY 2300 BASED ON RCP 8.5 CLIMATE SCENARIOS (PENN AND DEUTCH, 2022). C) PAST AND FUTURE SPECIES RICHNESS IN THE MARINE ENVIRONMENT. PAST SPECIES RICHNESS IS BASED ON FOSSIL RECORDS RELATIVE TO TODAY. FUTURE PROJECTIONS BASED ON MODEL EXTINCTION RISKS, AVERAGED (LINES) AND VARYING (SD, SHADINGS) ACROSS EARTH SYSTEM MODELS AND COLONIZATION SCENARIOS.	28
FIGURE 1.2: A) LOW LATITUDE WARMING IN THE PERMIAN TRIASSIC AND B) PALAEOCENE EOCENE BOUNDARIES. MODERN SEA SURFACE TEMPERATURE RANGE IS SHOWN IN GREEN. RED DOTTED LINES SHOW UPPER MEDIAN THERMAL LIMITS FOR MODERN MARINE FAUNA. BLUE PANEL SHOWS DURATION OF PERMIAN TRIASSIC MASS EXTINCTION. YELLOW CIRCLES SHOW PALAEOCENE-EOCENE SEA SURFACE TEMPERATURES (BASED ON $\Delta 18\text{O}$, MG/CA AND TEX-86 PROXIES). RED DIAMONDS SHOWS EQUATORIAL SEA SURFACE TEMPERATURES (FROM BIOMARKER PALEOTHERMOMETRY), SHOWING A TEMPERATURE INCREASE OF CA. 13°C WARMING IN EQUATORIAL OCEAN TEMPERATURES DURING THE 500,000 YEARS LEADING UP TO THE PERMIAN-TRIASSIC BOUNDARY (OR 2.6°C PER 100,000 YEARS) (BOND AND SUN, 2021).	30
FIGURE 1.3: NATURAL FLUCTUATIONS IN PCO_2 IN COASTAL AND OCEAN SYSTEMS. A) DAILY CYCLE CAUSED BY THE PHOTOSYNTHESIS-TO-RESPIRATION RATIO IN COASTAL INTERTIDAL, SUBTIDAL AND KELP FOREST HABITATS. B) TEMPORARY, SHORT TERM LOW ALKALINITY/LOW SALINITY AND HIGH PCO_2 CONDITIONS CAUSED BY FRESHWATER RUNOFF. C) UPWELLING OF HIGH- PCO_2 WATER ON A SEASONAL BASIS FOR PERIODS OF DAYS/WEEKS IN TEMPERATE REGIONS. D) OPEN OCEANS HAVE MORE STABLE PCO_2 WITH GRADUAL LONGER TERM (DECADAL) CHANGES CAUSED BY OCEAN ACIDIFICATION. TAKEN FROM VARGAS ET AL. (2022).	32
FIGURE 1.4: ANNUAL, GLOBAL MEAN OCEAN PH SINCE 1950 AND MODELLED FUTURE CHANGE BASED ON TWO SCENARIOS: RCP2.6 (BLUE) ASSUMES A SIGNIFICANT DECLINE IN GREENHOUSE GAS EMISSION AFTER 2020, RCP 8.5 (RED) ASSUMES THAT EMISSIONS WILL CONTINUE TO INCREASE THROUGH THE 2100S (IPCC, 2022). INSET: TIME SERIES OF UPPER 200M OCEAN HEAT CONTENT CHANGE IN ZJ RELATIVE TO 2000-2010 AVERAGE. OBSERVATIONS ARE SHOWN IN MAGENTA AND SIMULATED HISTORICAL VALUES ARE SHOWN IN TAN. PROJECTIONS SHOW RCP2.6 IN BLUE AND RCP8.5 (BINDOFF ET AL., 2019).....	33

FIGURE 1.5: A) PROJECTED SEA SURFACE WARMING PER CENTURY BY DEPTH (GRAPH) AND BY GLOBAL DISTRIBUTION (MAP) B) SPATIAL DISTRIBUTION OF SIMULATED CHANGE IN SURFACE PH, UPPER 100 M FOR THE PERIOD 1900 TO 2100 (MAP) AND TIMESCALE OF UNCERTAINTY PERCENTAGE IN PROJECTIONS (GRAPH). FROM BINDOFF ET AL. (2019).	35
FIGURE 1.6: A) OPEN OCEAN TIME SERIES SHOWING HISTORICAL GLOBAL MEAN SEA SURFACE TEMPERATURE (TAN) AND PROJECTED GLOBAL MEAN SEA SURFACE TEMPERATURES BASED ON RCP2.6 (BLUE) AND RCP8.5 (RED). PROJECTIONS ARE MAPPED ON TO COLOUR BARS SHOWING ASSESSMENT OF HABITAT RISK RANGING FROM VERY HIGH IN PURPLE TO UNDETECTABLE IN WHITE. ASTERISKS ADJACENT TO BARS SHOW CONFIDENCE LEVELS (****= VERY HIGH, ***=HIGH, **=MEDIUM, *=LOW) B)LEVEL OF RISK ASSOCIATED WITH CLIMATE CHANGE IN COASTAL ECOSYSTEMS RANGING FROM VERY HIGH IN PURPLE TO UNDETECTABLE IN WHITE. ASTERISKS ADJACENT TO BARS SHOW CONFIDENCE LEVELS (****= VERY HIGH, ***=HIGH, **=MEDIUM, *=LOW) (BINDOFF ET AL., 2019).	37
FIGURE 1.7: RATIO OF THE MEAN EFFECT OF ACIDIFICATION TREATMENT TO MEAN EFFECT IN CONTROL GROUP (LN RR) AND ΔPCO_2 (μATM). GREY SQUARES ARE FROM EXPERIMENT ON EGGS AND LARVAE. OPEN SQUARES ARE FROM EXPERIMENTS ON JUVENILES AND ADULTS. DASH LINES ARE 95% CONFIDENCE INTERVALS (A) CLAMS, (B) OYSTERS, (C) GASTROPODS, (D) SEA URCHINS, (E) CRUSTACEANS, (F) CORALS, (G) SCALLOPS, AND (H) MUSSELS. FROM VARGAS ET AL. (2022).....	39
FIGURE 1.8: PHOTOGRAPH ILLUSTRATING THE DISSOLUTION OF LIMACINA HELICINA WHEN HELD IN SEAWATER SIMULATING THE PCO_2 CONCENTRATIONS IN 2100, BASED ON A ‘BUSINESS AS USUAL’ (IS92A) SCENARIO (IPCC, 2013, ORR ET AL., 2005). IMAGE TAKEN FROM HTTPS://WWW.PMEL.NOAA.GOV/CO2/FILE/PTEROPOD+SHELL+EXPERIMENT	40
FIGURE 1.9: MECHANISMS BY WHICH INCREASED OCEAN PCO_2 CAN AFFECT A MARINE ORGANISM. FROM THE WATER, CO_2 DIFFUSES INTO INTRACELLULAR AND EXTRACELLULAR COMPARTMENTS INFLUENCING THE PH. THIS AFFECTS TISSUES, CELLS AND PHYSIOLOGICAL PROCESSES. THE CAPACITY AN ORGANISM HAS TO ALTER ION REGULATION AND ACID-BASE REGULATION MAY BE CRITICAL IN DETERMINING THEIR ABILITY TO TOLERATE OCEAN ACIDIFICATION (WITTMANN AND PÖRTNER, 2013).....	43
FIGURE 1.10. A TYPICAL INVERTEBRATE OLFACTORY SENSILLUM (VOSSHALL AND STOCKER, 2007).....	48
FIGURE 1. 11: ANTERIOR SECTION OF A TYPICAL NEREIDID SHOWING SENSORY AND CIRCULATORY FEATURES. BUC = BUCCAL ORGAN;	

DBV = DORSAL BLOOD VESSEL; IBV = INTESTINAL BLOOD VESSEL; LANT = LATERAL ANTENNA; LBV = LATERAL BLOOD VESSEL; NEP = NEPHRIDIUM; NUC = NUCHAL ORGAN; OEG = OESOPHAGEAL GLAND; OES = OESOPHAGUS; PALP = PALP; PAR = PARAPODIA; PER =PERISTOMIUM; PROS = PROSTOMIUM; SEP = SEPTUM, TCI = TENTACULAR CIRRI; VBV = VENTRAL BLOOD VESSEL (BEESLEY ET AL., 2000). B) SCHEMATIC OF THE OVERVIEW OF THE SUPAGEAL GANGLION WITHIN THE HEAD OF HEDISTE DIVERSICOLOR. PROSTOMIAL TENTACLES (PT), PARTS OF THE TENTACLE NERVES (TN), CENTRAL NEUROPIIL REGION (CN), MURAESOPHSHROOM BODIES (MB) ARE EFFERENTS FROM THE ANTERIOR (AE) AND POSTERIOR EYES (PE) FUSE TO FORM THE OPTIC NEUROPIIL (ON), PALPS (PA), PROSTOMIAL CIRRI (PC), PALPAL NERVE (PN)	49
FIGURE 1. 12: SCHEMATIC OF THE HOLOTYPE OF GUANSHANCHAETA FELICIA GEN. ET SP. NOV. POLYCHAETE FROM CAMBRIAN-ERA FOSSILS FOUND IN CHINA. SHOWING ALL CHARACTERISTICS OF THE SPECIMEN: SEGMENTS ARE NUMBERED 1, 2, 3. AC ACICULA, BS BIFID STRUTURE, BT BUCCAL TUBE, CH CHAETAE, NOPOD. NOTOPODIUM, NUPOD. NEUROPODIUM, NOCH. NOTOCHAETAE, NUCH. NEUROCHAETAE, PH PHARYNX, SED. SEDIMENT, TT. TENTACLE (LIU ET AL., 2015).	50
FIGURE 1.13: THE IMPACT OF [CO ₂] (PPM) ON THE BIOMASS (G, MEAN+S.E.) OF ALITTA VIRENS UNDER AMBIENT TEMPERATURE CONDITIONS (GODBOLD AND SOLAN, 2013).....	52
FIGURE 1.14: APPROXIMATE NUMBER OF STUDIES CONDUCTED ON MARINE ORGANISMS EXPOSED TO MULTIPLE STRESSORS FROM A 2015 REVIEW PAPER BY GUNDERSON ET AL. (2016).	54
FIGURE 1.15: EXAMPLES OF THE RANGE OF TYPES OF BIOTURBATION AND THE VARIETY ORGANISMS THAT PERFORM THIS IMPORTANT SERVICE. (A) MOLE TRACK (THOMOMYS TALPOIDES MACROTIS) (B) MOLE TRACK IN PRAIRIE GRASSLANDS. (C) DUGONG (DUGONG DUGONG) FEEDING ON RHIZOMES (D) FEEDING PIT ATTRIBUTED TO THE BLUE-SPOTTED STINGRAY (TAENIURA LYMMA) (E) FORAGING BLUE-SPOTTED STINGRAY (F) THE COMMON EARTHWORM (LUMBRICUS TERRESTRIS). IN THE MARINE ENVIRONMENT, THE DOMINANT BIOTURBATATORS ARE DEPOSIT-FEEDING POLYCHAETES AND BURROWING CRUSTACEANS. INVERTEBRATES HAVE A SMALL PER CAPITA IMPACT, BUT DUE TO THEIR POPULATION DENSITY THEY ARE DOMINANT FROM A GLOBAL PERSPECTIVE. FROM MEYSMAN ET AL. (2006).	61
FIGURE 1.16: CONCEPTUAL ILLUSTRATION SHOWING THE TRANSITION BETWEEN EDIACARAN MATGROUND HABITAT WITH MICROBIAL MATT COVERED SEDIMENTS TO CAMBRIAN MIXGROUND WHERE THE SEDIMENT IS MIXED DUE TO COMPLEX BURROW NETWORKS. BURROW FLUSHING ALLOWS OXYGEN TRANSPORTATION DEEP INTO SEDIMENTS. INSET PHOTOGRAPH SHOWS ARENICOLA MARINA	

WITH A LIGHT HALO OF OXIDISED SEDIMENT AROUND ITS BURROW AS COMPARED TO GREY BACKGROUND OF REDUCED SEDIMENT. MEYSMAN ET AL. (2006).....	62
FIGURE 1.17: DRAWING OF A TYPICAL RAGWORM WITH PHARYNX EVERTED AND PHOTOGRAPH OF THE COMMON RAGWORM HEDISTE DIVERSICOLOR. FROM HESSELBERG (2007).....	65
FIGURE 1.18: THE OCCURRENCE OF MASS EXTINCTIONS THROUGH GEOLOGICAL TIME DURING THE PHANEROZOIC WITH EXTINCTION RATES GIVEN AS FAMILIES PER MILLION YEARS. THE FIVE MASS- EXTINCTIONS CAN BE SEEN CLEARLY AS PEAKS THAT STAND WELL ABOVE BACKGROUND EXTINCTION LEVELS. A) LATE ORDOVICIAN, B) LATE DEVONIAN, C) END PERMIAN, D) LATE TRIASSIC, E) LATE CRETACEOUS. TAKEN FROM HALLAM AND WIGNALL (1997).	68
FIGURE 1.19: A) CHANGES IN MARINE CARBONATE OVER THE PERMIAN TRIASSIC PERIOD WITH THE MASS EXTINCTION EVENT PERIOD SHADED IN BLUE. B) DIAGRAMS ILLUSTRATING THE MAIN ENVIRONMENTAL IMPACTS OF THERMOGENIC (TOP) AND VOLCANIC (BOTTOM) GASSES DURING THIS TIME. C) THE IMPACT OF ENVIRONMENTAL CHANGE ILLUSTRATED IN B ON BIOTA (DAL CORSO ET AL., 2022).	71
FIGURE 1.20: A) VULNERABILITY TO EXTINCTION FOR DIFFERENT GROUPS OF MARINE ORGANISMS BASED ON SUSCEPTIBILITY TO CLIMATE CHANGE. B) EXTINCTION MAGNITUDE FOR DIFFERENT GROUPS OF MARINE ORGANISMS DURING THE PERMIAN TRIASSIC MASS EXTINCTION EVENT WITH NON-MOTILE, BENTHIC, UNBUFFERED TAXA AS WELL AS BRACHIOPODS SUFFERING THE HIGHEST EXTINCTION RATES. C) SELECTIVITY OF GROUPS OF MARINE ORGANISMS TO A RANGE OF CONDITIONS. FROM DAL CORSO ET AL. (2022).	72
FIGURE 1.21: TIME SERIES OF FOSSIL GROUPS USED TO RECONSTRUCT PALEOTEMPERATURES. GRAY LINES SHOW THE TEMPORAL RANGE OF GROUP (BIVALVES, BRACHIOPODS, FORAMINIFERS, AND FISH ARE EXTANT); BLUE LINES SHOW STRATIGRAPHIC RANGE WHERE EACH GROUP HAS PALEOTHERMOMETRY APPLICATIONS. NOTE JAWLESS FISH ARE NOT INCLUDED AS THEY ARE NOT USEFUL FOR OXYGEN ISOTOPE PALEOTHERMOMETRY. TAKEN FROM BOND AND SUN (2021).....	74
FIGURE 1.22: GLOBAL OCEAN DISTRIBUTION OF OXYGEN ISOTOPE COMPOSITION SHOWING LARGE LATITUDINAL VARIATION IN SEAWATER $\Delta^{18}\text{O}$. $\Delta^{18}\text{O}$ OF SEAWATER REFLECTS BOTH REGIONAL EVAPORATION AND PRECIPITATION AS WELL AS THE GLOBAL CHANGE IN CONTINENTAL ICE VOLUME. IN ADDITION $\Delta^{18}\text{O}$ CAN BE USED TO ASSESS PALEOTHERMOMETRY DUE TO DIFFERENCES IN THE ENERGY REQUIRED TO BREAK BONDS IN THE HEAVIER VERSUS LIGHTER ISOTOPES. THIS LEADS TO PREDICTABLE ISOTOPE FRACTIONATION WHICH IS RECORDED IN THE SHELL MATERIAL	

WHEN IT IS PRECIPITATED FROM SEAWATER IN EQUILIBRIUM AND IS A FUNCTION OF TEMPERATURE. TAKEN FROM BOND AND SUN (2021), ORIGINALLY FROM SCHMIDT (1999). 77

FIGURE 2. 1: A. BIOASSAY SETUP– TEN WORMS WERE ADDED TO EACH ASSAY CONTAINER. THEY WERE GIVEN ONE HOUR TO CREATE A BURROW WITH WATER CYCLING ON. WORMS WERE PRE-WEIGHED PRIOR TO THE ASSAYS. EACH WORM WAS IN AN INDIVIDUAL GLASS CONTAINER TO ALLOW INDIVIDUAL MONITORING AND CONTAINERS WERE CAPPED WITH MESH TO PREVENT ESCAPE. EACH CONTAINER HAD ITS OWN SYRINGE TO ALLOW ACCURATE CUE DELIVERY. BEFORE ADDING THE CHEMICAL CUE, MESH WAS REMOVED TO ALLOW A CLEAR LINE OF SIGHT FOR RECORDING. ASSAYS WERE CONDUCTED 1 HOUR AFTER ‘SUNSET’, WHEN THE LIGHTS WERE TURNED OFF. B. NUMERICAL LAYOUT OF THE TEST TUBES IN THE ASSAY CONTAINER TO ALLOW INDIVIDUAL MONITORING OF WORMS. 94

FIGURE 2. 2: RESPONSE OF RAGWORMS (HEDISTE DIVERSICOLOR) TO THE CHEMICAL FOOD CUE DIMETHYL SULPHIDE. ACTIVITY WAS MEASURED AS THE PERCENTAGE OF TIME SPENT OUT OF THE BURROW DURING A 30 MINUTE RECORDING, N=20 FOR EACH CONDITION. RESPONSE WAS TESTED IN FOUR PH/ TEMPERATURE CONDITIONS, NAMELY PH 8.1, 18°C; PH8.1, 22°C; PH7.3, 18°C; PH7.3, 22°C. CUE CONCENTRATIONS RANGING FROM $1 \times 10^{-2} \text{M}$ TO $1 \times 10^{-9} \text{M}$ WERE TESTED AT TEN TIMES DILUTION BETWEEN CONCENTRATIONS. A CONTROL WAS TESTED WITH THE ADDITION OF WATER ALONE. POINTS SHOW THE GROUP MEAN AND BARS SHOW STANDARD ERROR. SIGNIFICANCE STARS SHOW THOSE POINTS THAT ARE SIGNIFICANTLY DIFFERENT TO THE CONTROL (SIGNIF. CODES: *** = $P < 0.001$, ** = $P < 0.01$, * = $P < 0.05$) 96

FIGURE 2. 3: RESPONSE OF RAGWORMS (HEDISTE DIVERSICOLOR) TO THE CHEMICAL FOOD CUE ATP. ACTIVITY WAS MEASURED AS THE PERCENTAGE OF TIME SPENT OUT OF THE BURROW DURING A 30 MINUTE RECORDING, N=20 FOR EACH CONDITION. RESPONSE WAS TESTED IN THREE PH/ TEMPERATURE CONDITIONS, NAMELY PH 8.1, 18°C; PH8.1, 22°C; PH7.3, 18°C. CUE CONCENTRATIONS RANGING FROM $1 \times 10^{-2} \text{M}$ TO $1 \times 10^{-9} \text{M}$ WERE TESTED AT TEN TIMES DILUTION BETWEEN CONCENTRATIONS. A CONTROL WAS TESTED WITH THE ADDITION OF WATER ALONE. POINTS SHOW THE GROUP MEAN AND BARS SHOW STANDARD ERROR. SIGNIFICANCE STARS SHOW THOSE POINTS THAT ARE SIGNIFICANTLY DIFFERENT TO THE CONTROL (SIGNIF. CODES: *** = $P < 0.001$, ** = $P < 0.01$, * = $P < 0.05$) 99

FIGURE 2. 4: RESPONSE OF RAGWORMS (HEDISTE DIVERSICOLOR) TO THE CHEMICAL FOOD CUE TAURINE. ACTIVITY WAS MEASURED AS THE PERCENTAGE OF TIME SPENT OUT OF THE BURROW DURING A

30 MINUTE RECORDING, N=20 FOR EACH CONDITION. RESPONSE WAS TESTED IN THREE PH/ TEMPERATURE CONDITIONS, NAMELY PH 8.1, 18°C; PH8.1, 22°C; PH7.3, 18°C; PH7.3, 22°C. CUE CONCENTRATIONS RANGING FROM $1 \times 10^{-2} \text{M}$ TO $1 \times 10^{-9} \text{M}$ WAS TESTED AT TEN TIMES DILUTION BETWEEN CONCENTRATIONS. A CONTROL WAS TESTED WITH THE ADDITION OF WATER ALONE. POINTS SHOW THE GROUP MEAN AND BARS SHOW STANDARD ERROR. POINTS SHOW THE GROUP MEAN AND BARS SHOW STANDARD ERROR. SIGNIFICANCE STARS SHOW THOSE POINTS THAT ARE SIGNIFICANTLY DIFFERENT TO THE CONTROL (SIGNIFICANT. CODES: *** = $P < 0.001$, ** = $P < 0.01$, * = $P < 0.05$) 101

FIGURE 2. 5: RESPONSE OF RAGWORMS (HEDISTE DIVERSICOLOR) TO THE CHEMICAL FOOD CUE GSH. ACTIVITY WAS MEASURED AS THE PERCENTAGE OF TIME SPENT OUT OF THE BURROW DURING A 30 MINUTE RECORDING, N=20 FOR EACH CONDITION. RESPONSE WAS TESTED IN THREE PH/ TEMPERATURE CONDITIONS, NAMELY PH 8.1, 18°C; PH8.1, 22°C; PH7.3, 18°C; PH7.3, 22°C. CUE CONCENTRATIONS RANGING FROM $1 \times 10^{-2} \text{M}$ TO $1 \times 10^{-9} \text{M}$ WAS TESTED AT TEN TIMES DILUTION BETWEEN CONCENTRATIONS. A CONTROL WAS TESTED WITH THE ADDITION OF WATER ALONE. POINTS SHOW THE GROUP MEAN AND BARS SHOW STANDARD ERROR. SIGNIFICANCE STARS SHOW THOSE POINTS THAT ARE SIGNIFICANTLY DIFFERENT TO THE CONTROL (SIGNIF. CODES: *** = $P < 0.001$, ** = $P < 0.01$, * = $P < 0.05$) .. 103

FIGURE 2.6: RESPONSE OF RAGWORMS (HEDISTE DIVERSICOLOR) TO THE CHEMICAL CUE CHONDROITIN SULPHATE. ACTIVITY WAS MEASURED AS THE PERCENTAGE OF TIME SPENT OUT OF THE BURROW DURING A 30 MINUTE RECORDING, N=20 FOR EACH CONDITION. RESPONSE WAS TESTED IN FOUR PH/ TEMPERATURE CONDITIONS, NAMELY PH 8.1, 18°C; PH8.1, 22°C; PH7.3, 18°C; PH7.3, 22°C. CUE CONCENTRATIONS RANGING FROM $1 \times 10^{-2} \text{M}$ TO $1 \times 10^{-9} \text{M}$ WAS TESTED AT TEN TIMES DILUTION BETWEEN CONCENTRATIONS. A CONTROL WAS TESTED WITH THE ADDITION OF WATER ALONE. POINTS SHOW THE GROUP MEAN AND BARS SHOW STANDARD ERROR. POINTS SHOW THE GROUP MEAN AND BARS SHOW STANDARD ERROR. SIGNIFICANCE STARS SHOW THOSE POINTS THAT ARE SIGNIFICANTLY DIFFERENT TO THE CONTROL (SIGNIF. CODES: *** = $P < 0.001$, ** = $P < 0.01$, * = $P < 0.05$) 106

FIGURE 2. 7: RESPONSE OF RAGWORMS (HEDISTE DIVERSICOLOR) TO THE CHEMICAL CUE UREA. ACTIVITY WAS MEASURED AS THE PERCENTAGE OF TIME SPENT OUT OF THE BURROW DURING A 30 MINUTE RECORDING, N=20 FOR EACH CONDITION. RESPONSE WAS TESTED IN FOUR PH/ TEMPERATURE CONDITIONS, NAMELY PH 8.1, 18°C; PH8.1, 22°C; PH7.3, 18°C; PH7.3, 22°C. CUE CONCENTRATIONS RANGING FROM $1 \times 10^{-2} \text{M}$ TO $1 \times 10^{-9} \text{M}$ WAS TESTED AT TEN TIMES DILUTION BETWEEN CONCENTRATIONS. A CONTROL WAS TESTED WITH THE ADDITION OF WATER ALONE. POINTS SHOW THE GROUP

MEAN AND BARS SHOW STANDARD ERROR. POINTS SHOW THE GROUP MEAN AND BARS SHOW STANDARD ERROR. SIGNIFICANCE STARS SHOW THOSE POINTS THAT ARE SIGNIFICANTLY DIFFERENT TO THE CONTROL (SIGNIF. CODES: *** = $P < 0.001$, ** = $P < 0.01$, * = $P < 0.05$).....	108
FIGURE 2. 8: RELATIVE ABUNDANCE OF INDIVIDUAL PROTONATION STATES OF TAURINE ALONG WITH THE PERCENTAGE CHANGE ACROSS THE PH SCALE. PROPORTIONS ARE SHOWN FOR PROTONATION STATES PRESENT BETWEEN PH 0 AND 14. THE GREEN SHADED AREA INDICATES THE PH RANGE TESTED IN THIS STUDY; FROM PH 8.1 TO PH 7.3.	121
FIGURE 2. 9: RELATIVE ABUNDANCE OF INDIVIDUAL PROTONATION STATES OF GSH ALONG WITH THE PERCENTAGE CHANGE ACROSS THE PH SCALE. PROPORTIONS ARE SHOWN FOR PROTONATION STATES PRESENT BETWEEN PH 0 AND 14. THE GREEN SHADED AREA INDICATES THE PH RANGE TESTED IN THIS STUDY; FROM PH 8.1 TO PH 7.3.	123
FIGURE 3. 1: SCHEMATIC DIAGRAM OF PH CONTROL SYSTEM USED TO HOUSE HEDISTE DIVERSICOLOR. JBL PROFLOA CONTROL UNITS WERE USED TO AUTOMATICALLY ADJUST THE PH OF THE WATER BY TRIGGERING THE RELEASE OF CO ₂ IF THE WATER PH ROSE BY 0.05 PH UNITS ABOVE THE SET LEVEL. A PH PROBE (1) AND TEMPERATURE PROBE (2) WERE USED TO FEED INFORMATION TO THE PH CONTROL UNIT. AN AIR PUMP AND AIR STONE (3) BUBBLED AIR THROUGH THE WATER TO MAINTAIN OXYGEN LEVELS. A SECOND AIR STONE (4) WAS USED TO BUBBLE THE CO ₂ FROM A TANK. 4CM DEPTH OF WASHED 3MM CORAL SAND (5) WAS USED AS SEDIMENT. TANKS WERE FILLED WITH 18‰ SALINITY (±1‰) WATER DILUTED WITH PURIFIED WATER (6). ALL TANKS WERE HOUSED IN A CLIMATE-CONTROLLED ROOM IN ORDER TO MAINTAIN CONSTANT TEMPERATURE, DAILY LIGHT/ DARK CYCLES AND MONTHLY MOON CYCLES.....	135
FIGURE 3. 2: SCHEMATIC ILLUSTRATING THE SIX PH/ TEMPERATURE CONDITIONS USED IN THIS STUDY. IN EACH CONDITION BURROWS WERE ANALYSED FOR IN-BURROW OXYGEN LEVELS AND OXYGEN PENETRATION DEPTH.....	137
FIGURE 3. 3: SCHEMATIC DIAGRAM OF THE SETUP FOR OPCODE SENSOR FOIL EXPERIMENTS. THE HEADER TANK (45CM X 25CM X 25CM) CONTAINED SEAWATER WHICH WAS PH ADJUSTED WITH A JBL PROFLOA CONTROL UNIT, WHICH BUBBLED CO ₂ TO REDUCE WATER PH. THE EXPERIMENTAL TANK (25CM X 8CM X 25CM) CONTAINED NATURAL, FILTERED SEDIMENT (3) AND 18‰ (±1‰) SEAWATER. FLOAT SWITCHES (1) WERE USED TO PREVENT OVERFLOW AND MINI WATER PUMPS (2) WERE USED TO CIRCULATE	

THE WATER BETWEEN THE HEADER TANK AND THE EXPERIMENTAL TANK.	139	
FIGURE 3. 4: EXAMPLE IMAGES OF THE BURROWS USED FOR ANALYSIS. A) PH 8.1, TEMPERATURE 18°C, 45MM VERTICAL DEPTH. B) PH 8.1, TEMPERATURE 22°C, 47MM VERTICAL DEPTH. C) PH 7.7, TEMPERATURE 18°C 48MM VERTICAL DEPTH. D) PH 7.7, TEMPERATURE 22°C, 48MM VERTICAL DEPTH. E) PH 7.3, TEMPERATURE 18°C 46MM VERTICAL DEPTH. F) PH 7.3, TEMPERATURE 22°C, 48MM VERTICAL DEPTH.		144
FIGURE 3. 5: TIME SERIES OF THE IN-BURROW O ₂ FLUCTUATIONS OVER A 12-HOUR IMAGE ACQUISITION PERIOD FOR EACH PH/ TEMPERATURE REGIME (N=1 FOR EACH REGIME). INSET ON EACH GRAPH IS AN IMAGE OF THE BURROW WITH THE BURROW BORDER DRAWN IN WHITE.		145
FIGURE 3.6: BOXPLOT COMPARING THE BURROW O ₂ RATIO ACROSS THE SIX PH AND TEMPERATURE REGIMES. O ₂ RATIO WAS CALCULATED USING THE RATIO BETWEEN IN-BURROW OXYGEN AND OVERLYING WATER OXYGEN LEVELS. LOWER RATIOS INDICATE A HIGHER DIFFERENCE BETWEEN OXYGEN IN THE BURROW AND THE OXYGEN IN THE OVERLYING WATER. BLACK CIRCLES INDICATE OUTLIERS. N=5 FOR EACH PH/ TEMPERATURE CONDITION. A SIGNIFICANT DIFFERENCE WAS FOUND BETWEEN EACH PH REGIME (ROBUST FACTORIAL ANOVA WITH TRIMMED MEAN (0.2), P=0.001) BUT NOT BETWEEN TEMPERATURE REGIMES (P=0.147). THE INTERACTION EFFECT (TEMPERATURE~PH WAS SIGNIFICANT (P=0.004), THEREFORE AN MCP2ATM POST-HOC TEST WAS RUN TO INVESTIGATE INDEPENDENT EFFECTS (MAIR AND WILCOX, 2020) (P=0.002 FOR PH 7.7 VS. PH 8.1, P=0.004 FOR PH 7.3 VS. PH 8.1, P=0.0001 FOR PH7.3 VS PH 7.7 AS WELL AS A SIGNIFICANT DIFFERENCE BETWEEN THE TWO TEMPERATURES AT PH 7.7 (P = 0.0009) AND PH 8.1 (P=0.04) BUT NOT AT PH 7.3 (P=0.4)). SIGNIFICANCE LEVELS; P<0.05 (*), P<0.01 (**), P<0.001(***)).		146
FIGURE 3. 7: BOXPLOT COMPARING THE AVERAGE O ₂ PENETRATION DEPTH (MM) INTO THE SEDIMENT SURROUNDING BURROW WALLS ACROSS THE SIX PH AND TEMPERATURE REGIMES. BLACK DOTS INDICATE OUTLIERS. A SIGNIFICANT DIFFERENCE WAS FOUND FOR TEMPERATURE (P=0.015) AND PH (P=0.004) BUT NO SIGNIFICANCE WAS FOUND FOR THE PH: TEMPERATURE INTERACTION (P=0.58), BASED ON ANOVA WITH TRIMMED MEAN (0.2) USING THE WSM PACKAGE IN R. SIGNIFICANCE LEVELS; P<0.05 (*), P<0.01 (**), P<0.001(***)).		148
FIGURE 3. 8: SCATTER GRAPH COMPARING THE AVERAGE WIDTH OF EACH BURROW WITH OXYGEN PENETRATION DEPTH INTO THE SEDIMENT SURROUNDING THE BURROW. NO CORRELATION WAS FOUND (SPEARMAN'S RANK = 0.098, P-VALUE = 0.2603).		149

FIGURE 4. 1: GLUCOSE CALIBRATION CURVE (DISSOLVED IN DISTILLED WATER) MEASURED AT 490 NM ACCORDING TO PROTOCOL. . EACH CALIBRATION POINT REPRESENTS THE AVERAGE OF 3 TECHNICAL REPLICATES. THE BLUE LINE REPRESENTS LINEAR FIT OF THE MEASURED POINTS CALCULATED BY THE LEAST SQUARES METHOD. THE LINEAR REGRESSION EQUATION ($Y = AX + B$) REPRESENTS CALIBRATION EQUATION SLOPE (A) AND INTERCEPT (B). THE R ² COEFFICIENT WAS CALCULATED BY THE LEAST SQUARES METHOD.	166
FIGURE 4. 2: BAR PLOT ILLUSTRATING THE MEAN (\pm STANDARD DEVIATION) MUCUS PRODUCTION PER GRAM OF BIOMASS BY THE HARBOUR RAGWORM HEDISTE DIVERSICOLOR AT DIFFERENT PH/ TEMPERATURE CONDITIONS. FOR EACH CONDITION N=3.....	167
FIGURE 4. 3: : LOESS SMOOTHING FUNCTION (BLUE LINE) SHOWING THE RELATIONSHIP BETWEEN DRY MASS OF MUCUS PRODUCED AND BIOMASS OF WORMS (HEDISTE DIVERSICOLOR) AND 95% CONFIDENCE INTERVALS (GREY SHADING).	168
FIGURE 4. 4: BOXPLOT ILLUSTRATING THE CARBOHYDRATE CONTENT IN MUCUS SAMPLES PRODUCED BY THE HARBOUR RAGWORM HEDISTE DIVERSICOLOR AT DIFFERENT PH/ TEMPERATURE CONDITIONS. FOR EACH CONDITION N=3.....	169
FIGURE 5. 1: NUMBER OF OCCURRENCES OF THE CLASS POLYCHAETA THROUGHOUT THE PHANEROZOIC BASED ON FOSSIL RECORDS. CM = CAMBRIAN, O = ORDOVICIAN, S = SILURIAN, D = DEVONIAN, C= CARBONIFEROUS, P= PERMIAN, T= TRIASSIC, J = JURASSIC, K = CRETACEOUS PG = PALEOGENE, (PALEOBIOLOGY DATABASE, 2019) RANGE THROUGH DIVERSITY (DOTTED LINE) SHOWS EACH TAXON AS PRESENT FROM ITS FIRST OCCURRENCE TO ITS LAST OCCURRENCE, WHETHER OR NOT IT WAS EVER FOUND IN THE FOSSIL RECORD IN THE INTERVENING INTERVALS. ORIGINATION AND EXTINCTION RATES (GREEN AND RED LINES) ARE ESTIMATED HERE USING THE "PER-CAPITA RATE" METHOD OF (FOOTE, 2000) ..	191
FIGURE S2. 1: DOSE RESPONSE FITTED CURVES FOR RESPONSE OF HEDISTE DIVERSICOLOR TO DMS A) PH8.1, 18C, GOODNESS OF FIT = 0.001. B) PH8.1, 22C, GOODNESS OF FIT <0.0001. C) PH7.3, 18C, GOODNESS OF FIT <0.0001. D) PH7.2, 22C, GOODNESS OF FIT <0.0001.	195
FIGURE S2. 2: DOSE RESPONSE FITTED CURVES FOR RESPONSE OF HEDISTE DIVERSICOLOR TO ATP A) PH8.1, 18C, GOODNESS OF FIT = 0.001. B) PH8.1, 22C, GOODNESS OF FIT <0.0001. C) PH7.3, 18C, GOODNESS OF FIT =0.003.	198

FIGURE S2. 3: DOSE RESPONSE FITTED CURVES FOR RESPONSE OF HEDISTE DIVERSICOLOR TO TAURINE A) PH8.1, 18C, GOODNESS OF FIT < 0.0001. B) PH8.1, 22C, GOODNESS OF FIT <0.0001. C) PH7.3, 18C, GOODNESS OF FIT <0.0001. D) PH7.2, 22C, GOODNESS OF FIT <0.0001.	201
FIGURE S2. 4: DOSE RESPONSE FITTED CURVES FOR RESPONSE OF HEDISTE DIVERSICOLOR TO GSH A) PH8.1, 18C, GOODNESS OF FIT < 0.0001. B) PH8.1, 22C, GOODNESS OF FIT< 0.0001. C) PH7.3, 18C, GOODNESS OF FIT < 0.0001. D) PH7.2, 22C, GOODNESS OF FIT = 0.0017.	204
FIGURE S2. 5: DOSE RESPONSE FITTED CURVES FOR RESPONSE OF HEDISTE DIVERSICOLOR TO UREA AT PH7.2, 22C, GOODNESS OF FIT , 0.0001.	207
FIGURE S2. 6: DOSE RESPONSE FITTED CURVES FOR RESPONSE OF HEDISTE DIVERSICOLOR TO CHONDROITIN SULPHATE A) PH8.1, 22C, GOODNESS OF FIT < 0.0001. B) PH7.3, 18C, GOODNESS OF FIT = 0.0059. C) PH7.3, 22C, GOODNESS OF FIT = 0.0029.....	210
FIGURE S3. 1: HISTOGRAMS AND QQ PLOTS FOR ASSESSMENT OF NORMALITY ON OXYGEN RATIO FOR EACH OF THE CONDITIONS TESTED.	215
FIGURE S3. 2: OUTPUT IMAGES FROM VARIOUS STAGES OF THE PYTHON IMAGE ANALYSIS SCRIPT USED TO COMPUTE OXYGEN PENETRATION DEPTH INTO THE SEDIMENT.	222
FIGURE S3. 3: HISTOGRAMS AND QQ PLOTS FOR ASSESSMENT OF NORMALITY ON OXYGEN PENETRATION DEPTH	234

List of tables

TABLE 2. 1: THE CONCENTRATION OF CUE THAT ELICITED 10% ACTIVITY COMPARED TO THE CONTROL LEVEL (EC ₁₀) WAS CALCULATED TO ALLOW COMPARISON OF CUE RESPONSE BETWEEN THE PH/ TEMPERATURE CONDITIONS TESTED.....	98
TABLE 2. 2: THE CONCENTRATION OF CUE THAT ELICITED 10% ACTIVITY COMPARED TO THE CONTROL LEVEL (EC ₁₀) WAS CALCULATED TO ALLOW COMPARISON OF CUE RESPONSE BETWEEN THE PH/ TEMPERATURE CONDITIONS TESTED.....	100
TABLE 2. 3: THE CONCENTRATION OF CUE THAT ELICITED 10% ACTIVITY COMPARED TO THE CONTROL LEVEL (EC ₁₀) WAS CALCULATED TO ALLOW COMPARISON OF CUE RESPONSE BETWEEN THE PH/ TEMPERATURE CONDITIONS TESTED.....	102
TABLE 2. 4: THE CONCENTRATION OF CUE THAT ELICITED 10% ACTIVITY COMPARED TO THE CONTROL LEVEL (EC ₁₀) WAS	

CALCULATED TO ALLOW COMPARISON OF CUE RESPONSE BETWEEN THE PH/ TEMPERATURE CONDITIONS TESTED.....	105
TABLE 2. 5: THE CONCENTRATION OF CUE THAT ELICITED 10% ACTIVITY COMPARED TO THE CONTROL LEVEL (EC ₁₀) WAS CALCULATED TO ALLOW COMPARISON OF CUE RESPONSE BETWEEN THE PH/ TEMPERATURE CONDITIONS TESTED. DUE TO LACK OF RESPONSE IN PH8.1, 18°C, EC ₁₀ COULD NOT BE CALCULATED AND EC ₅ WAS CALCULATED INSTEAD.....	107
TABLE 2. 6: THE CONCENTRATION OF CUE THAT ELICITED 10% ACTIVITY COMPARED TO THE CONTROL LEVEL (EC ₁₀) WAS CALCULATED TO ALLOW COMPARISON OF CUE RESPONSE BETWEEN THE PH/ TEMPERATURE CONDITIONS TESTED.....	109
TABLE 4. 1: RESULTS OF A TWO WAY FACTORIAL ANOVA TESTING FOR DIFFERENCES IN MUCUS PRODUCTION BY THE HARBOUR RAGWORM HEDISTE DIVERSICOLOR IN DIFFERENT PH/ TEMPERATURE CONDITIONS. NO SIGNIFICANT DIFFERENCES WERE OBSERVED.	168
TABLE 4. 2: TOTAL BIOMASS OF THE FIVE WORMS USED IN EACH OF THE PH/ TEMPERATURE CONDITIONS TESTED.....	169
TABLE 4. 3: : RESULTS OF A TWO WAY FACTORIAL ANOVA TESTING FOR DIFFERENCES IN CARBOHYDRATE CONTENT OF MUCUS PRODUCED BY THE HARBOUR RAGWORM HEDISTE DIVERSICOLOR IN DIFFERENT PH/ TEMPERATURE CONDITIONS. SIGNIFICANCE CODES: 0 = '***', 0.001 = '**', 0.01 = '*',	170
TABLE S2. 1: RESULTS OF ROBUST FACTORIAL REPEATED MEASURES ANOVA USING WRS2 PACKAGE IN R	193
TABLE S2. 2: : RESULTS OF NONPARAMETRIC MULTIPLE COMPARISON DUNN'S TEST FOR PH8.1, 18C	194
TABLE S2. 3:: RESULTS OF NONPARAMETRIC MULTIPLE COMPARISON DUNN'S TEST FOR PH8.1, 22C	194
TABLE S2. 4: RESULTS OF NONPARAMETRIC MULTIPLE COMPARISON DUNN'S TEST FOR PH7.3, 18C	194
TABLE S2. 5: RESULTS OF NONPARAMETRIC MULTIPLE COMPARISON DUNN'S TEST FOR PH7.3, 22C	195
TABLE S2. 6: RESULTS OF NONPARAMETRIC MULTIPLE COMPARISON DUNN'S TEST FOR PH8.1, 18C	196
TABLE S2. 7: RESULTS OF NONPARAMETRIC MULTIPLE COMPARISON DUNN'S TEST FOR PH8.1, 22C	196
TABLE S2. 8: RESULTS OF NONPARAMETRIC MULTIPLE COMPARISON DUNN'S TEST FOR PH7.3, 18C	197
TABLE S2. 9: RESULTS OF ROBUST FACTORIAL REPEATED MEASURES ANOVA USING WRS2 PACKAGE IN R	199
TABLE S2. 10: RESULTS OF NONPARAMETRIC MULTIPLE COMPARISON DUNN'S TEST FOR PH8.1, 18C	199

TABLE S2. 11: RESULTS OF NONPARAMETRIC MULTIPLE COMPARISON DUNN'S TEST FOR PH8.1, 22C	199
TABLE S2. 12: RESULTS OF NONPARAMETRIC MULTIPLE COMPARISON DUNN'S TEST FOR PH7.3, 18C	200
TABLE S2. 13: RESULTS OF NONPARAMETRIC MULTIPLE COMPARISON DUNN'S TEST FOR PH7.3, 22C	200
TABLE S2. 14: RESULTS OF ROBUST FACTORIAL REPEATED MEASURES ANOVA USING WRS2 PACKAGE IN R	202
TABLE S2. 15: RESULTS OF NONPARAMETRIC MULTIPLE COMPARISON DUNN'S TEST FOR PH8.1, 18C	202
TABLE S2. 16: RESULTS OF NONPARAMETRIC MULTIPLE COMPARISON DUNN'S TEST FOR PH8.1, 22C	202
TABLE S2. 17: RESULTS OF NONPARAMETRIC MULTIPLE COMPARISON DUNN'S TEST FOR PH7.3, 18C	203
TABLE S2. 18: RESULTS OF NONPARAMETRIC MULTIPLE COMPARISON DUNN'S TEST FOR PH7.3, 22C	203
TABLE S2. 19: RESULTS OF ROBUST FACTORIAL REPEATED MEASURES ANOVA USING WRS2 PACKAGE IN R	205
TABLE S2. 20: RESULTS OF NONPARAMETRIC MULTIPLE COMPARISON DUNN'S TEST FOR PH8.1, 18C	205
TABLE S2. 21: RESULTS OF NONPARAMETRIC MULTIPLE COMPARISON DUNN'S TEST FOR PH8.1, 22C	205
TABLE S2. 22: RESULTS OF NONPARAMETRIC MULTIPLE COMPARISON DUNN'S TEST FOR PH7.3, 18C	206
TABLE S2. 23: RESULTS OF NONPARAMETRIC MULTIPLE COMPARISON DUNN'S TEST FOR PH7.3, 22C	206
TABLE S2. 24: RESULTS OF ROBUST FACTORIAL REPEATED MEASURES ANOVA USING WRS2 PACKAGE IN R	207
TABLE S2. 25: RESULTS OF NONPARAMETRIC MULTIPLE COMPARISON DUNN'S TEST FOR PH8.1, 18C	208
TABLE S2. 26: RESULTS OF NONPARAMETRIC MULTIPLE COMPARISON DUNN'S TEST FOR PH8.1, 22C	208
TABLE S2. 27: RESULTS OF NONPARAMETRIC MULTIPLE COMPARISON DUNN'S TEST FOR PH7.3, 18C	209
TABLE S2. 28: RESULTS OF NONPARAMETRIC MULTIPLE COMPARISON DUNN'S TEST FOR PH7.3, 22C	209
TABLE S3. 1: AVERAGE OXYGEN LEVEL IN THE WATER ABOVE THE ANALYSED BURROW. COMPUTED USING A REGION OF INTEREST IN THE VISISENS ANALYTICAL.	211
TABLE S3. 2: MONITORING OF TEMPERATURE, PH AND SALINITY IN WORM CULTURE TANKS WAS DONE THREE TIMES PER WEEK WHEN POSSIBLE. THE DATA IS SHOWN BELOW AND WAS USED TO CALCULATE VARIATION (STANDARD ERROR) IN THESE VARIABLES.	211

TABLE S3. 3: : RESULTS OF SHAPIRO-WILK’S TEST OF NORMALITY FOR THE OXYGEN RATIO VARIABLE GENERATED IN R (CENTRE= MEDIAN) FOR EACH PH/ TEMPERATURE GROUP. ALL GROUPS ARE SIGNIFICANTLY NON-NORMAL.	215
TABLE S3. 4: RESULTS OF SHAPIRO-WILK’S TEST OF NORMALITY FOR THE OXYGEN RATIO VARIABLE GENERATED IN R (CENTRE= MEDIAN) FOR ALL DATA. THE DATA DOES NOT CONFORMS TO A NORMAL DISTRIBUTION (P<0.05).....	215
TABLE S3. 5: RESULTS OF LEVENE’S TEST FOR HOMOGENEITY OF VARIANCE (CENTRE=MEDIAN) FOR O ₂ RATIO VARIABLE.	216
TABLE S3. 6: RESULTS OF ROBUST INDEPENDENT FACTORIAL ANOVA TEST WITH TRIMMED MEANS (0.2) USING THE WRS2 PACKAGE AND T2WAY FUNCTION FOR OXYGEN RATIO VARIABLE.	216
TABLE S3. 7: TABLE SHOWING ONE OF THREE REPRESENTATIVE IMAGES USED FOR EACH BURROW REPEAT IN O ₂ PENETRATION DEPTH CALCULATION ALONG WITH THE CORRESPONDING ‘MASK’ IMAGE AFTER PROCESSING FOR SET RGB COLOUR THRESHOLDS IN PYTHON. THE MASK IMAGES WERE THEN USED TO <i>QUANTIFY O₂ PENETRATION DEPTH BY COUNTING THE NUMBER OF WHITE PIXELS IN EACH ROW AND AVERAGING.</i>	223
TABLE S3. 8: O ₂ PENETRATION DEPTH (IN MM) USED IN ANALYSIS	230
TABLE S3. 9: RESULTS OF SHAPIRO-WILK’S TEST OF NORMALITY GENERATED IN R (CENTRE= MEDIAN) FOR EACH PH/ TEMPERATURE GROUP FOR O ₂ PENETRATION DEPTH. THE PH7.2/ 18C REGIME WAS SIGNIFICANTLY NON-NORMAL.	234

Abstract

Climate change is projected to have a negative impact on biodiversity over the next century. Similar drivers of change have been observed in the geological past and were also associated with loss of species, particularly in the marine environment. This research uses the common ragworm *Hediste diversicolor* as a model organism to investigate the physiological and ecological impacts of changing temperature and pH on hardy, benthic species. *H. diversicolor* is a keystone species in estuarine habitats in Europe and North America and their bioturbating activities likely have a crucial effect on ecosystem functioning. Here we demonstrate that future pH and temperature conditions will impact the chemosensory abilities of *H. diversicolor* as well as the production of mucus and oxygen-sediment penetration. These results indicate that projected future climate change could have population level impacts on *H. diversicolor*. Additionally, the changes in mucus production and oxygen penetration identified here may alter the rate of nutrient cycling and sediment cohesion with potential ecosystem level effects. The complex behavioural, ecological and physiological impacts of pH and temperature change identified in this research can also contribute to the understanding of kill mechanisms that led to the extreme mass extinctions observed in the geological past.

Synopsis

Increasing concentrations of greenhouse gasses released to the atmosphere since the late 19th century have led to an increase in global mean surface temperature of 1.09°C (Bindoff et al., 2019). Marine environments have experienced a global mean increase in sea surface temperatures of 0.88°C (Bindoff et al., 2019). Rising levels of atmospheric CO₂ since pre-industrial times has had a corresponding impact on ocean pCO₂ (Pörtner et al., 2019). The pH of the world's oceans has decreased by a mean of 0.1 and a further decrease of up to 0.32 by 2100 is predicted by IPCC modelling (IPCC, 2013b, Pörtner et al., 2019).

In the geological past, periods of environmental and climatic change have been causally linked to each of the greatest mass extinctions in the fossil record. The Permian-Triassic mass extinction (PTME) was particularly severe in the marine environment, manifesting as the extinction of more than 90% of marine species (Erwin, 1994). During this period burrowing infauna populations reduced dramatically and eventually burrowing habitat was replaced by microbial mudflats (Cribb and Bottjer, 2020, Pruss et al., 2006). The PTME was not confined to oceanic taxa, there was also a profound effect on terrestrial ecology. The Permian Triassic boundary was marked by a transition from diverse seed ferns to low diversity conifers and lycopsids. The 'coal gap' that begins in the late Permian (~250Mya) and continues to Mid Triassic (~243Mya) is indicative of the loss of peat-forming plants during this interval (Retallack et al., 1996). Variation in paleosols (fossilised soils) from Antarctica indicate a transition to low-productivity ecosystems with high proportions of stress-tolerant opportunistic plants during the EPME (Retallack & Krull, 1999). Loss of coniferous

vegetation in Europe also led to a degraded ecosystem where lycopsids dominated for ca. 4-5My (Looy et al., 1999)

Temperature and postulated ocean pH changes during this period were likely driven by large scale volcanic activity in the Siberian Trap large igneous province (LIP) (Courtillet and Renne, 2003), (Bond and Grasby, 2017, Wignall, 2001, Wignall et al., 2009). The total CO₂ release from Siberian Traps LIP has been estimated at 30,000 Gt (Courtillet and Renne, 2003). Anthropogenic CO₂ input to the atmosphere currently stands at about 37 Gt per year. At current levels of emissions, it would take around 800 years for humans to input the same mass of CO₂ into the atmosphere as was generated by 0.9 million years (My) of Siberian Traps volcanism (Courtillet and Renne, 2003, Bond and Grasby, 2017).

Boron isotope analysis suggests that late Permian ocean pH reduced by 0.7 pH in ca. 10,000 years and temperatures increased by 8°C in low-latitude surface waters (Clarkson et al., 2015). Although these figures are more extreme than the conditions predicted by the end of this century by the IPCC, the timescales are much longer, suggesting a slower rate of change (Clarkson et al., 2015). Understanding the mechanisms driving population decline and extinction in marine benthic species can help clarify whether the same forces that led to extreme mass extinction observed during the Permian-Triassic period could generate a similar biotic response in the coming centuries.

Burrowing estuarine organisms are generally considered to be resilient to the impacts of climate change thanks to the buffering effects of living in sediment as well as their being evolved to cope with regular exposure to pH, salinity and temperature fluctuations (García et al., 2018a, García et al., 2018b). This project uses the common

ragworm (*Hediste diversicolor*) as a model organism to investigate some of the drivers of climate change induced extinction and ecological change. *H. diversicolor* are abundant throughout Europe and North America and their bioturbating activities have a crucial effect on ecosystem functioning (Scaps, 2002, Fang et al., 2021, Gogina et al., 2020). The burrowing, bio-irrigation and associated sediment re-working of *H. diversicolor* has led to their being classed as a keystone species and it has been suggested that the feeding of this species acts as a rate-limiting step in estuarine detritus processing (Moreira et al., 2006, Mermillod-Blondin et al., 2005).

Focusing on the impacts of pH and temperature, this project investigates how changes in the marine environment effect chemical communication, burrow oxygen dynamics and mucus production.

Chemical Communication

Chemical cues are common in the marine environment and are utilised by a myriad of organisms to signal a range of processes including sensing the presence of food and predators (Ashur et al., 2017, Hay, 2009). Here behavioural response of *H. diversicolor* to multiple synthetic chemical cues under present and future ocean pH and temperature scenarios is investigated. The experiments demonstrated for the first time that glutathione (GSH) and dimethyl sulphide (DMS) appear to act as a food cue for *H. diversicolor*. This was also the first time that urea has been observed acting as a predator cue. In addition, this is the first time worms have been observed with varied, and in some cases opposite, responses to chemical cues over a range of pH conditions. The pH and temperature conditions also affected the concentration of chemical cue required to elicit a response as well as impacting the strength of the response to the cue. This could be due to physiological changes in the ragworm or chemical alterations to

the cue molecules in the different pH/ temperature conditions. The pH was found to affect the response of ragworms to chemical cues that are known to alter their protonation state across the pH conditions tested (pH 7.3 and pH 8.1) which suggests that the conformational change induced in these chemical cues' molecules is contributing to altered response levels, potentially by reducing the binding potential between the cue molecule and the associated receptor protein. Urea caused a significant reduction in response compared to the control only at pH 8.1, 18° C, suggesting that it is acting as a predator cue in these conditions. These results suggest that the ability of *H. diversicolor* to respond appropriately to food and predator cues is impacted by pH and temperature. Higher concentrations of cue are required to elicit a response at reduced pH for DMS, taurine and GSH. Higher temperatures were generally associated with higher levels of activity which may be linked to increased metabolic stress causing higher foraging drive. Response to predator cues is altered at different temperatures and pH all of which has the potential to effect survival in future ocean conditions.

Sediment-oxygen Dynamics

Oxygen planar optodes were used to investigate the impact of water temperature and water pH on in-burrow oxygen levels and oxygen penetration depth using *H. diversicolor*. In-burrow oxygen levels were highly variable over a 12-hour period, with some burrows being vacated for short periods leading to a rapid decline in O₂ levels. Even when burrows were uninhabited for short periods, in-burrow oxygen levels remained above those of the surrounding anoxic sediment. Warmer temperatures (22°C) led to slightly higher oxygen ratios (in burrow O₂: surface water O₂) which may be linked to increased O₂ requirements by *H. diversicolor* in these conditions triggering an increased ventilation effort. At pH 7.3 and pH 8.1 the oxygen ratio was reduced suggesting lower ventilation effort and/or reduced oxygen demand by the worms.

Oxygen penetration depth into surrounding sediments reduced with declining pH and temperatures. These results indicate that future climate conditions may cause an decrease in the sediment oxic zone, which in turn may cause alterations in aerobic respiration and organic matter breakdown in marine sediments.

Mucus Production

This project also investigated whether water pH and temperature have an impact on the quantity and carbohydrate levels in the mucus produced by *H. diversicolor* with a view to examine the impacts of future marine conditions based on these climate change scenarios. The quantity and quality of mucus produced might impact the presence and diversity of microbiota, the penetration of oxygen into sediment surrounding burrows and sediment cohesion. No significant difference in dry mass of mucus was observed between pH 8.1 and pH 7.3 or between 18°C and 22°C, suggesting that overall mucus production *H. diversicolor* may be unaffected by these conditions. However, carbohydrate content was significantly lower in mucus produced at lower pH and higher temperatures. This may be due to the energetic costs associated with producing carbohydrates in more stressful environmental conditions. The results of this study suggest that future climatic conditions will be associated with reduced carbohydrate content in the mucus of *H. diversicolor*. Invertebrate mucus has been linked to sediment microbiota and sediment carbohydrate content has been positively associated with nitrification rates (Dale, 2019a, Dale et al., 2019). Both microbial community composition and nitrogen cycling could be affected in future climate scenarios.

Summary

The results of this project provide evidence that the impacts of climate change will lead to increasing energetic costs with the potential to drive population declines in *H. diversicolor*. Similar mechanisms may have contributed to the extreme declines observed during past mass extinctions. The Permian-Triassic mass extinction was associated with similar levels of pH and temperature change as those predicted for the end of this century.

This work highlights that benthic invertebrates, although hardy to short-term environmental fluctuations, are vulnerable to climatic change. The results not only highlight impacts of pH and temperature change, which could have population level effects on the keystone species *H. diversicolor*, but also some of the potential knock-on ecosystem level impacts that may occur. In the past, similar levels of climatic change, over longer timescales have been associated with mass extinction events in the marine environment. The complex behavioural, ecological and physiological impacts of pH and temperature change identified in this research can contribute to the understanding of kill mechanisms that led to the extreme mass extinction observed during the Permian Triassic period as well as contribute to our understanding of, and therefore our response to, the modern phase of environmental change and extinction.

Acknowledgements

Ar gyfer fy nhad Emyr Huw James. Gorffwys mewn hedd.

I am grateful to so many people for their help and guidance throughout this project. First of all, thanks to my supervisors David Bond and Dan Parsons for their expertise. I am also very grateful to the technical team at Hull University, in particular Vic Swetez, Sonia Jennings and Rose Tershack for their patience and help in the lab. A special thanks goes to Christina Roggatz for her support, guidance and encouragement, I couldn't have done it without her.

Thank you to all my PhD peers that have helped along the way including Sojiro Fukado for help with Python, Paula Schirmacher and Lauric Feugre for their input and expertise. Thanks to Jess Hurley and Amber Jones for all the cigarettes and thanks to Victoria Scott for watching the dogs.

I have to give a most special thanks my sister Ann Fitzpatrick for all the therapy sessions, technical advice and gentle encouragement. I couldn't have made it without you. Of course, a most special thanks to my non-academic family Rob Lord for doing everything that academics are completely unable to do as well as Susan James for giving me a bit of perspective along the way and Alice Fillan for her linguistic honesty.

1.0. Introduction and Literature Review

1.1. Mass Extinction

Modern-day anthropogenically induced climate change is causing reduced ocean pH, increased surface water temperatures and associated anoxia (IPCC, 2013b, Pörtner et al., 2019, IPCC, 2022) although the long term impact is difficult to quantify and is heavily dependent on human responses to the crisis (Howarth and Viner, 2022, IPCC, 2022). It is becoming apparent that Earth is undergoing a mass extinction event with current extinction rates up to 1000 times higher than natural background rates and future projections of 10,000 times the natural rate (De Vos et al., 2015). The geological record contains evidence of the consequences of a variety of climate change events, which hold potential for evaluating the drivers of our current extinction crisis.

Mass extinctions are typically described in terms of either rate of extinction per unit time or total magnitude of extinctions (Şengör et al., 2008). Increasingly, research is identifying modern extinction of species (Pereira et al., 2010, Spalding and Hull, 2021); however, documented numbers are likely to be underestimates due to difficulties in recording formal species descriptions as well as confirming species extinction (Barnosky et al., 2011b, Dirzo and Raven, 2003, Ceballos et al., 2015). Despite this difficulty it is becoming apparent that modern day extinction rates are orders of magnitude higher than the expected background rate (De Vos et al., 2015, Pimm et al., 2006, Pimm et al., 1995, Barnosky et al., 2011a, Ceballos et al., 2017). In the marine environment, calcifying organisms are particularly susceptible to the impacts of climate change due to reducing pH and aragonite saturation (see Figure 1.1 A) (Reddin et al., 2020, Penn and Deutsch, 2022). Additional factors such as eutrophication, and hypoxia in aquatic environments, as well as habitat loss and fragmentations for both aquatic and terrestrial environments are all contributing to modern extinction rates (Barnosky et al.,

2011a). Species found at higher latitudes are considered to be more susceptible to extinction due to increased impact of climate change in these regions (Figure 1.1 B) (Penn and Deutsch, 2022).

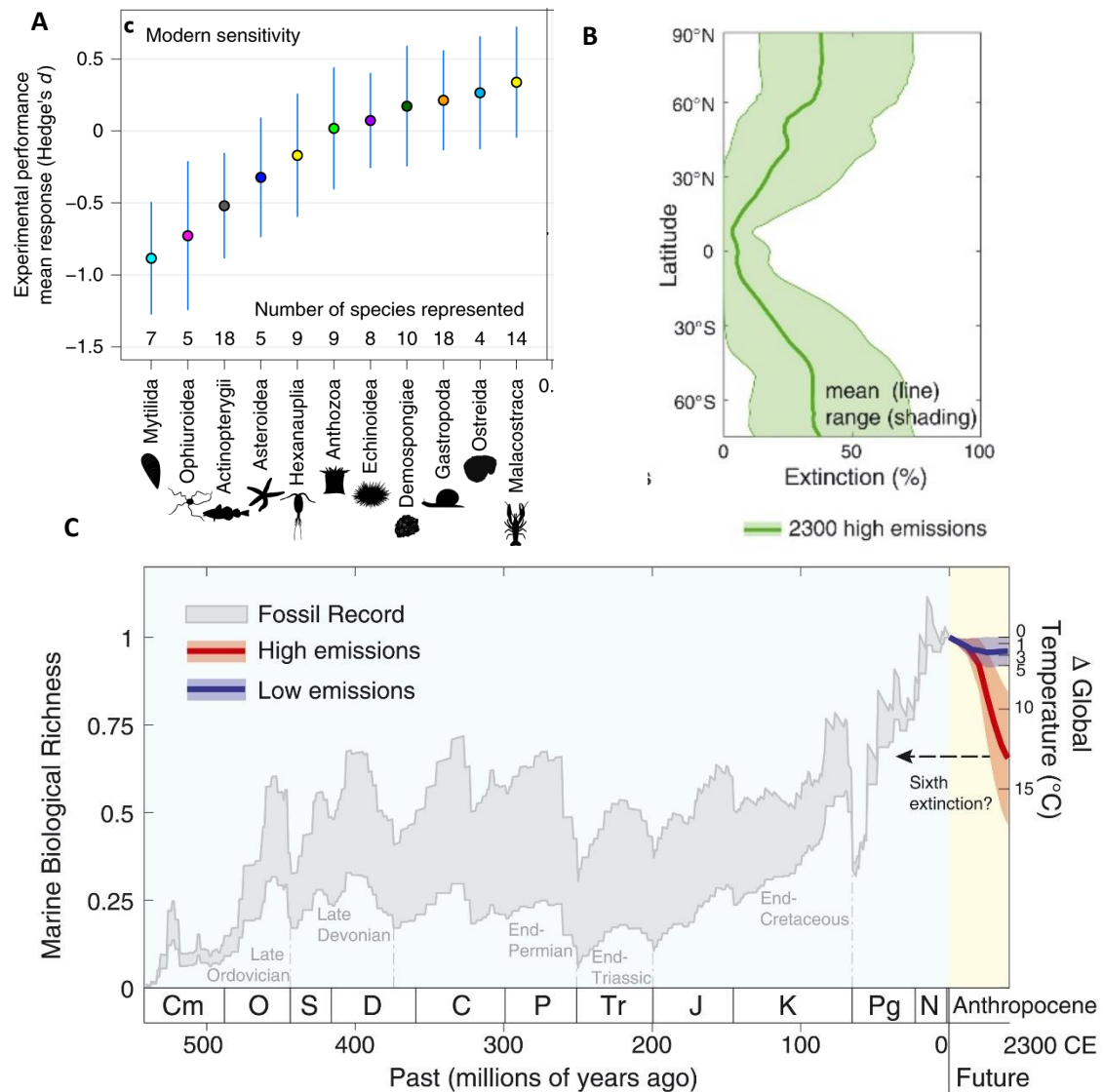


Figure 1.1 : A) Sensitivity of marine organisms to modern climate change based on experimental data (Reddin et al., 2020). B) Modelled percentage extinction by latitude in the marine environment by 2300 based on RCP 8.5 climate scenarios (Penn and Deutsch, 2022). C) Past and future species richness in the marine environment. Past species richness is based on fossil records relative to today. Future projections based on model extinction risks, averaged (lines) and varying (SD, shadings) across Earth system models and colonization scenarios.

Extinction events are marked by widespread reductions in macroscopic biodiversity and act as drivers of major and large scale evolutionary change (Shen et al., 2011, Song et al., 2014, Song et al., 2013). Mass extinction events include the five most severe extinction events found in the geological record plus the present day extinction (See Figure 1.1 C). The Permian-Triassic Mass Extinction (PTME), which occurred ~252.28Ma, is the most severe extinction event in Earth's history, and it profoundly altered marine ecosystems (see Figure 1.2) (Shen et al., 2011; Song et al., 2013). A review of extinction events over the past 300My by Hönisch et al. (2012) identifies the Permian-Triassic Mass Extinction, along with the Paleocene Thermal Maximum and the Triassic-Jurassic mass extinction, as the most analogous to the present day mass extinction. This study based comparisons around: massive CO₂ release, pH decline and aragonite saturation decline (Hönisch et al., 2012). Using such analogues, the impacts of future relevant stressors on ecosystems can be tested via comparison to past events; however, to do so, the degree of severity of the stressors that caused the extinction must be unequivocally identified (Hönisch et al., 2012).

Modern-day rates of CO₂ release are significantly higher than during the PTME (annual carbon release of 9.9PgC today compared to approximately 0.1 to 1PgC in the Permian Triassic interval) (Hönisch et al., 2012). The rate of carbon release can have profound implications on ocean carbonate chemistry (Bates et al., 2014). Slower rates of CO₂ emission to the atmosphere lead to a more limited response in CaCO₃ saturation, potentially causing a very different biotic response, with less harmful effects on calcifying organisms (Hönisch et al., 2012). Although some data suggest that the second phase of the PTME was more extreme and as such CO₂ release rates may have been significantly higher (and therefore closer to today's rates), there is no perfect analogue for modern climate change (Song et al., 2014, Hönisch et al., 2012).

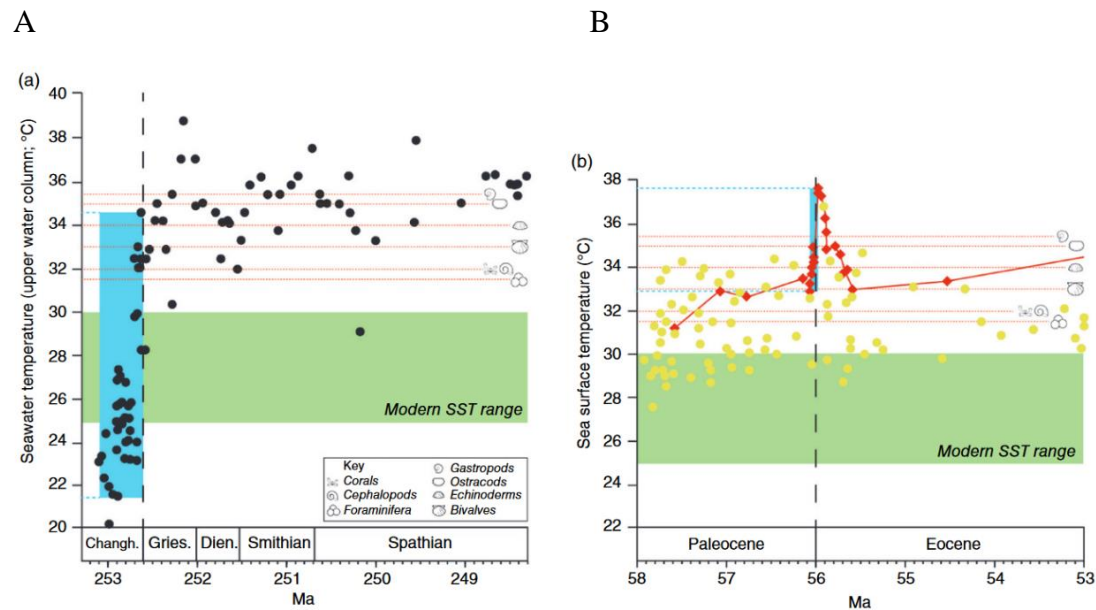


Figure 1.2: A) Low latitude warming in the Permian Triassic and B) Palaeocene Eocene boundaries. Modern sea surface temperature range is shown in green. Red dotted lines show upper median thermal limits for modern marine fauna. Blue panel shows duration of Permian Triassic mass extinction. Yellow circles show Palaeocene-Eocene sea surface temperatures (based on $\delta^{18}O$, Mg/Ca and TEX-86 proxies). Red diamonds shows equatorial sea surface temperatures (from biomarker paleothermometry), showing a temperature increase of ca. 13°C warming in equatorial ocean temperatures during the 500,000 years leading up to the Permian-Triassic boundary (or 2.6°C per 100,000 years) (Bond and Sun, 2021).

Attempting to elucidate the effects of modern climate change is difficult because lab and field experiments are restricted in complexity and duration. Geological records, however, provide long-term data on extinction events and it is plausible that a mixture of experimental biology and geological records can provide novel insight into the mechanisms and outcomes of climate change scenarios. For example an experiment by Benca et al. (2018a) recreated a common pollen mutation found in the bisaccate gymnosperm pollen in the Permian by exposing the dwarf pine (*Pinus mugo*) to increased levels of UV-B radiation. During the PTME, ozone-depleting aerosols led to increased levels of UV-B (Beerling et al., 2007; Seddon et al., 2019). In a recent study

using evidence from experiments on the effects of acidic settings on modern day gastropods, Foster et al. (2022) illustrated that a hypothesised globally acidic ocean during the Triassic is unlikely due to a lack of deformities and repair marks found in Triassic *Hindeodus parvus* Conodont Zone bivalves and gastropods. This study could not rule out acidification events prior to or during the Permian-Triassic extinction, however, the level of acidification did not impact calcification of the fossils examined.

1.2. Ocean Acidification and Climate Change in the Marine Environment

In 2011, the concentrations of greenhouse gases in the atmosphere (CO₂, CH₄ and N₂O) exceeded records from ice cores spanning the past 800,000 years (IPCC, 2013b, IPCC, 2022). While the uptake of CO₂ by surface oceans reduces the levels of atmospheric CO₂ concentrations and mediates climate change somewhat, it is having a significant impact on ocean chemistry. The input of anthropogenic CO₂ into the atmosphere enters the ocean as dissolved inorganic carbon (DIC); not only does this cause hypercapnia, but it also creates more acidic conditions (increased [H⁺]) via the following equation (Doney et al., 2009):



The addition of dissolved CO₂ to the ocean leads to an increase in carbonic acid (H₂CO₃) concentrations, shifting the equilibrium toward the right-hand-side of the equation. This carbonic acid then dissociates to form H⁺ ions (also called protons) along with bicarbonate (HCO₃⁻) and carbonate ions (CO₃²⁻). The increased [H⁺] reduces pH (pH = -log₁₀[H⁺]). Carbonate ions tend to react with the increased concentrations of H⁺ ions, reducing carbonate ion concentration in the ocean (Doney et al., 2009).

In addition to the changing ocean conditions linked to anthropogenically induced climate change, ocean ecosystems are subject to natural daily and seasonal fluctuations (Vargas et al., 2022). Algal photosynthesis and respiration cycles drive CO_2 , O_2 and pH fluctuations in coastal habitats with freshwater discharge and coastal upwellings causing temporary reductions in salinity and pH (see Figure 1.3) (Vargas et al., 2022).

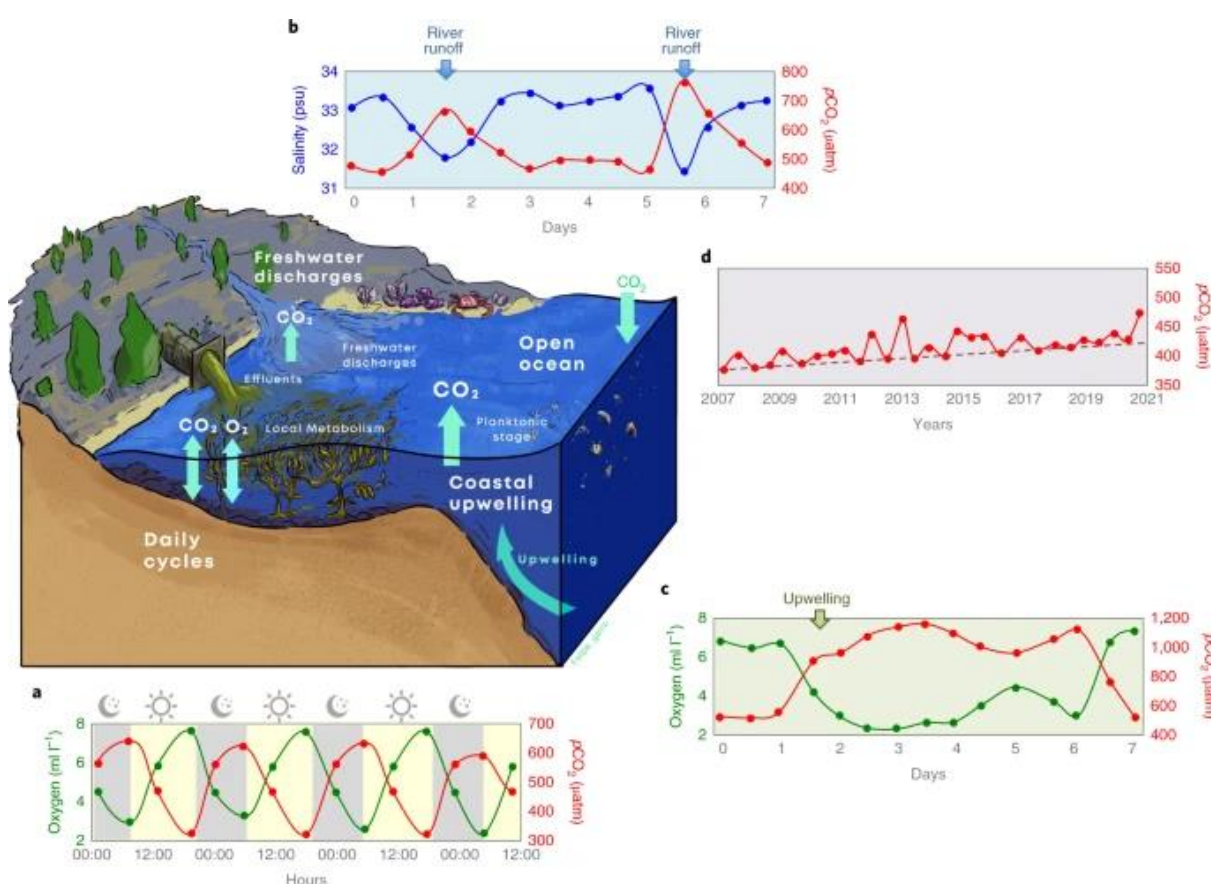


Figure 1.3: Natural fluctuations in pCO_2 in coastal and ocean systems. A) Daily cycle caused by the photosynthesis-to-respiration ratio in coastal intertidal, subtidal and kelp forest habitats. B) Temporary, short term low alkalinity/low salinity and high pCO_2 conditions caused by freshwater runoff. C) Upwelling of high- pCO_2 water on a seasonal basis for periods of days/weeks in temperate regions. D) Open oceans have more stable pCO_2 with gradual longer term (decadal) changes caused by ocean acidification. Taken from Vargas et al. (2022).

Rising levels of atmospheric CO₂ since pre-industrial times and the corresponding impact on ocean pCO₂ has caused a decrease in pH of 0.1 and a further decrease of up to 0.32 by 2100 is predicted (see Figure 1.4) (Pörtner et al., 2019). Because pH is measured on a logarithmic scale, this pH decline represents a 150% increase in H⁺ ions projected by 2100 (Orr et al., 2005).

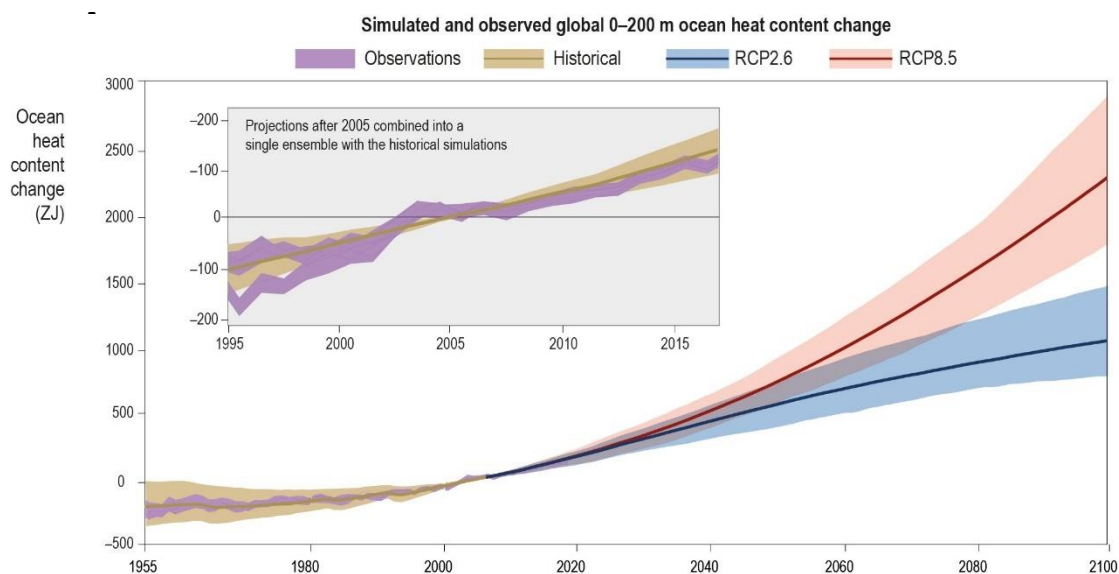


Figure 1.4: Annual, global mean ocean pH since 1950 and modelled future change based on two scenarios: RCP2.6 (blue) assumes a significant decline in greenhouse gas emission after 2020, RCP 8.5 (red) assumes that emissions will continue to increase through the 2100s (IPCC, 2022). Inset: Time series of upper 200m ocean heat content change in ZJ relative to 2000–2010 average. Observations are shown in magenta and simulated historical values are shown in tan. Projections show RCP2.6 in blue and RCP8.5 (Bindoff et al., 2019)

This alteration in ocean chemistry affects marine life through a variety of mechanisms. A significant example of this is the impact of reduced CaCO₃ availability on calcifying organisms, which require calcium carbonate to form skeletons, or shells (e.g. Kleypas and Langdon, 2006, Fabry et al., 2008). Increased CO₂ absorption into the ocean acts to reduce the saturation state (Ω) of CaCO₃ by increasing its solubility in the more acidic environment (Doney et al., 2009). This increased solubility reduces

CO₃²⁻ availability and causes reduced calcification rates in a range of organisms (e.g. Kleypas and Langdon, 2006, Fabry et al., 2008, Cohen and Holcomb, 2009, Gattuso and Buddemeier, 2000). More recent work has identified contradictory evidence suggesting that many calcifiers are tolerant to near-future ocean acidification (Leung et al., 2022). A meta-analysis of 985 research papers found that 70% of observation of growth and calcification were non-negative suggesting that many species may have the capacity for acclimation (Leung et al., 2022). Earlier studies appear to disproportionately focus on deleterious impacts with a bias toward short term exposure (e.g. Marubini et al., 2003, Riebesell et al., 2000, Cornwall et al., 2013). There is mounting evidence that show resilience to ocean acidification. For example, after a 12 week exposure the foraminifera species *Baculogypsina sphaerulata*, *Calcarina gaudichaudii* and *Amphisorus hemprichii* either maintained or increased their shell diameter at 770 µatm CO₂ following 12 week exposure (Fujita et al., 2011). Another example from a study by Melzner et al. (2011) on *Mytilus edulis* exposed to pH 7.7 for seven weeks showed normal shell growth and no shell dissolution. A more recent example from research by Leung et al. (2020) shows the gastropod *Austrocochlea concamerata* are able to maintain shell organic matter content, crystallinity and body condition 940 ppm CO₂. The ability of some calcifiers to maintain calcification in acidified conditions suggests that seawater carbonate chemistry is not strongly associated with calcification (Leung et al., 2020). Calcifying organisms can create localised optimal alkaline condition for precipitating CaCO₃ minerals at the calcification site, in addition, CO₃²⁻ from seawater is not utilised directly, but HCO₃³⁻ or metabolically-produced CO₂ which may mean that seawater carbonate saturation state is not a key limiter for calcification (Leung et al., 2020).

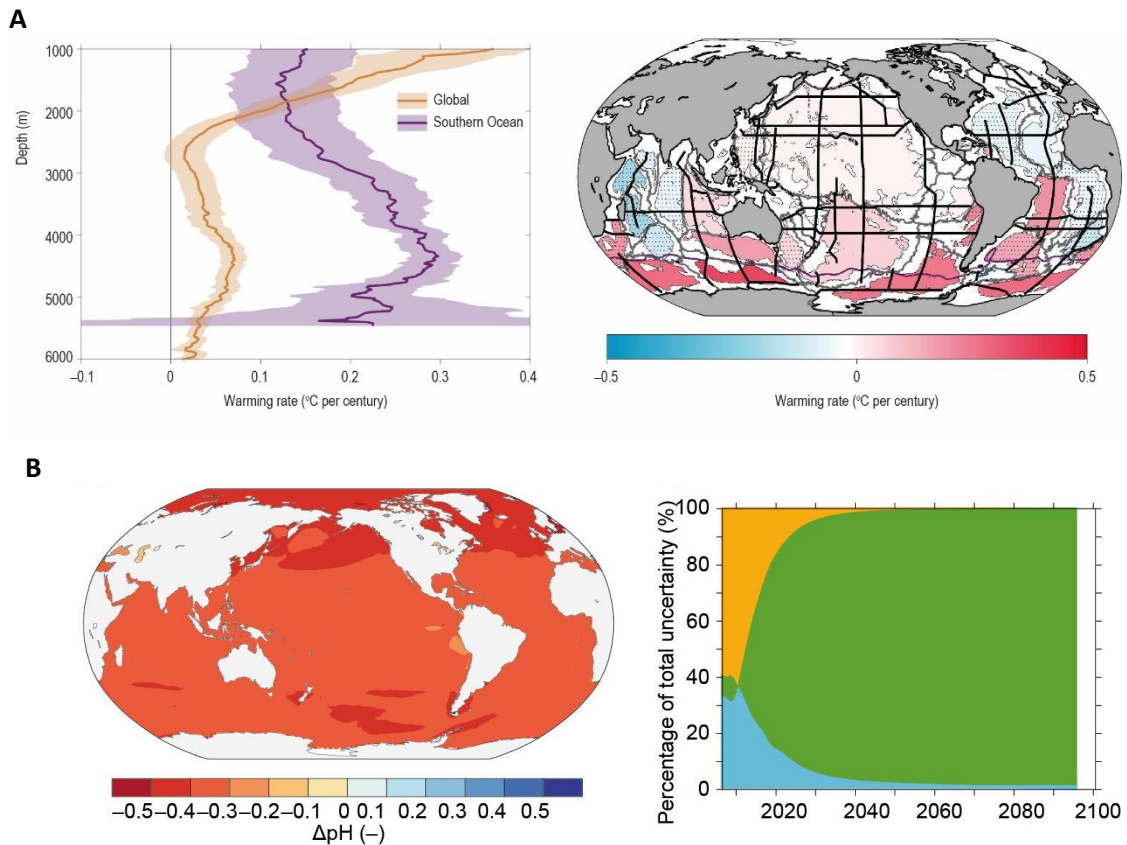


Figure 1.5: A) Projected sea surface warming per century by depth (graph) and by global distribution (map) B) Spatial distribution of simulated change in surface pH, upper 100 m for the period 1900 to 2100 (map) and timescale of uncertainty percentage in projections (graph). From Bindoff et al. (2019).

Increasing global temperatures also have an impact on marine ecology with increasing ocean surface temperatures driving stratification, reduced O₂ and changing biogeography (e.g. mobile species tend to move pole-wards as temperatures increase in search of cooler waters. See Figure 1.5 and 1.6)) (Bindoff et al., 2019). Marine heatwaves, during which temperatures reach the top 1% of recorded conditions (based on the period between 1982 and 2016), have increased in frequency and duration since the 1980s and are likely to continue to increase to the end of the 21st century (Collins M., 2019). Rising temperatures have a myriad of complex effects on marine organisms with overall trends for coastal ecosystems being habitat contraction, migration and

reduced biodiversity and functionality (Bindoff et al., 2019). Ocean warming has increased the pace of coral degradation with more frequent bleaching events occurring since 1996 (Bindoff et al., 2019). Increased temperature has also been found to alter habitat preference for some freshwater larval species (Edeline et al., 2006), but there are no such studies in marine species (Nagelkerken and Munday, 2016). Higher sensitivity to pollutants, such as heavy metals, have been correlated with exposure to higher temperatures in some marine invertebrates (e.g. Heugens et al., 2001, Lu et al., 2018, Holan et al., 2019). However, the compound effect of temperature was found to mitigate the negative effect of pH on egg masses of two intertidal mollusc species (Davis et al., 2013). Early life stages (embryos, larvae and juveniles) are more susceptible to temperature increases in marine species, however, even in adult organism temperature extremes are associated with increased mortality (Pandori and Sorte, 2019).

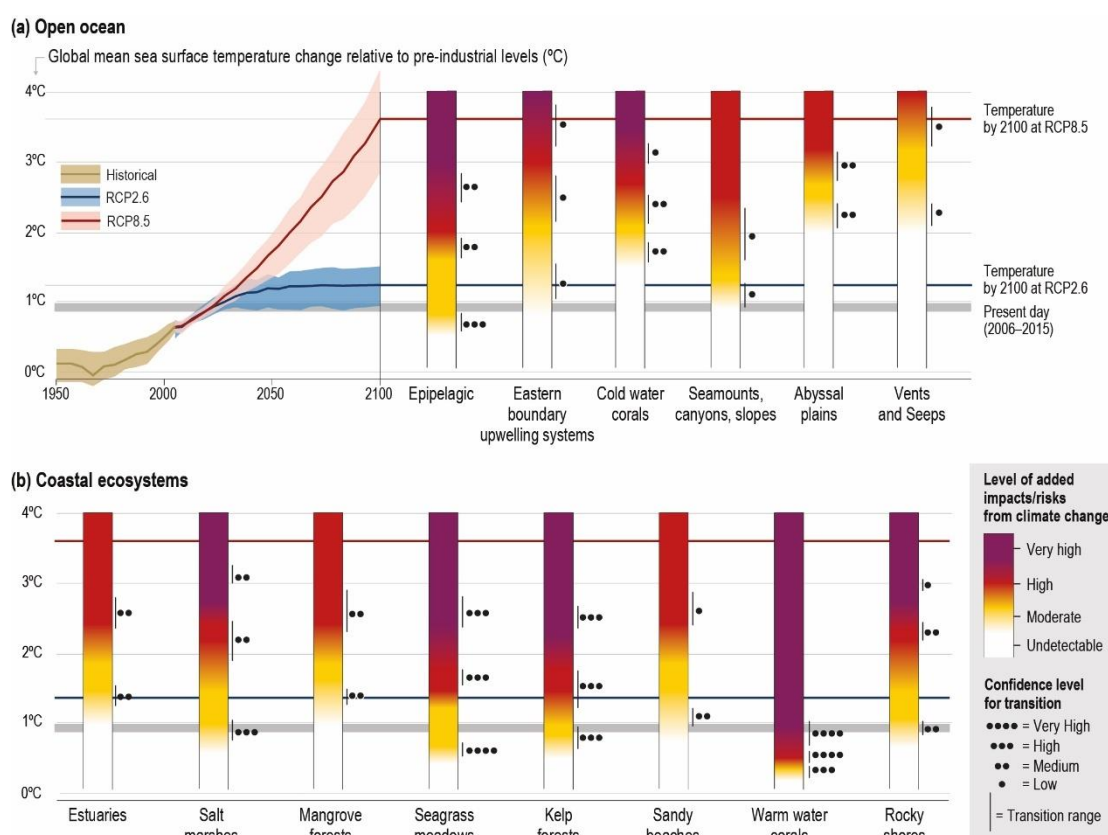


Figure 1.6: A) Open ocean time series showing historical global mean sea surface temperature (tan) and projected global mean sea surface temperatures based on RCP2.6 (blue) and RCP8.5 (red). Projections are mapped on to colour bars showing assessment of habitat risk ranging from very high in purple to undetectable in white. Asterisks adjacent to bars show confidence levels (****= very high, ***=high, **=medium, *=low) B) Level of risk associated with climate change in coastal ecosystems ranging from very high in purple to undetectable in white. Asterisks adjacent to bars show confidence levels (****= very high, ***=high, **=medium, *=low) (Bindoff et al., 2019).

The common ragworm (*Hediste diversicolor*) is used as a model organism in this study. Increased temperature has been found to reduce feeding rate and exacerbate the negative effects of pH on: regenerative capacity, survival, oxidative stress and burrowing behaviour in *H. diversicolor* (Bhuiyan et al., 2021). Oxygen consumption increases with temperature in *H. diversicolor* and some studies have found that growth rate is faster at higher temperatures (Galasso et al., 2020). Studies on similar species, such as a study by Widdicombe and Needham (2007) on the polychaete *Nereis virens* found that elevated CO₂ had no impact on burrow size or density but was associated with increased nitrate uptake and increased ammonium release. Research by Godbold and Solan (2013) highlight the importance of long-term experiments and consideration of the complex temporal fluctuations in natural systems when forecasting ecological consequences. This study on a polychaete species (*Alitta virens*) found that exposure to elevated CO₂ and temperature led to varied responses depending on length of exposure and seasonal fluctuations. Growth was the only variable that was reduced under elevated CO₂, irrespective of duration of exposure (Godbold and Solan, 2013).

1.3. Impacts on Marine Organisms

Ocean pH typically ranges from 7.7 to 8.2 with the highest pH occurring in the summer at high latitude shallow waters and the lowest pH in very deep waters (Brewer Peter et al., 1995). An in-depth study by Bates et al. (2014) suggests that the rate of pH decline at higher northern latitudes is more variable and, therefore, difficult to predict. For example, in the Irminger Sea off the coast of Greenland, pH is declining at almost double the rate of decline in the Iceland Sea (-0.0026 yr^{-1} versus -0.0014 yr^{-1}) (Bates et al., 2014). Local variations in pH are driven by: influx of freshwater from rivers or meltwater; diurnal cycles linked to photosynthesis and respiration of marine organisms; nutrient input via rivers and outflows and associated algal blooms; local temperature fluctuations; rate of surface water mixing linked to local weather conditions; tidal cycles and upwellings (Hofmann et al., 2011). This patchy and regional acidification will lead to some areas being more highly impacted. Tolerance to changing ocean conditions varies between taxonomic groups and life stage as well as between populations, with some being more tolerant to acidification, temperature or pollutants than others (see Figure 1.7) (Doney et al., 2020). Complex interactions between stressors along with behavioural change, phenotypic plasticity, acclimation and adaptation makes for highly varied rates of sensitivity between different marine species (Doney et al., 2020). This complexity also creates an experimental and analytical challenge when attempting to test for the impacts of acidification (Doney et al., 2020). However, the general trend for marine organisms is decreased survival, decreased growth, reduced development and inhibition of calcification (Kroeker et al., 2013).

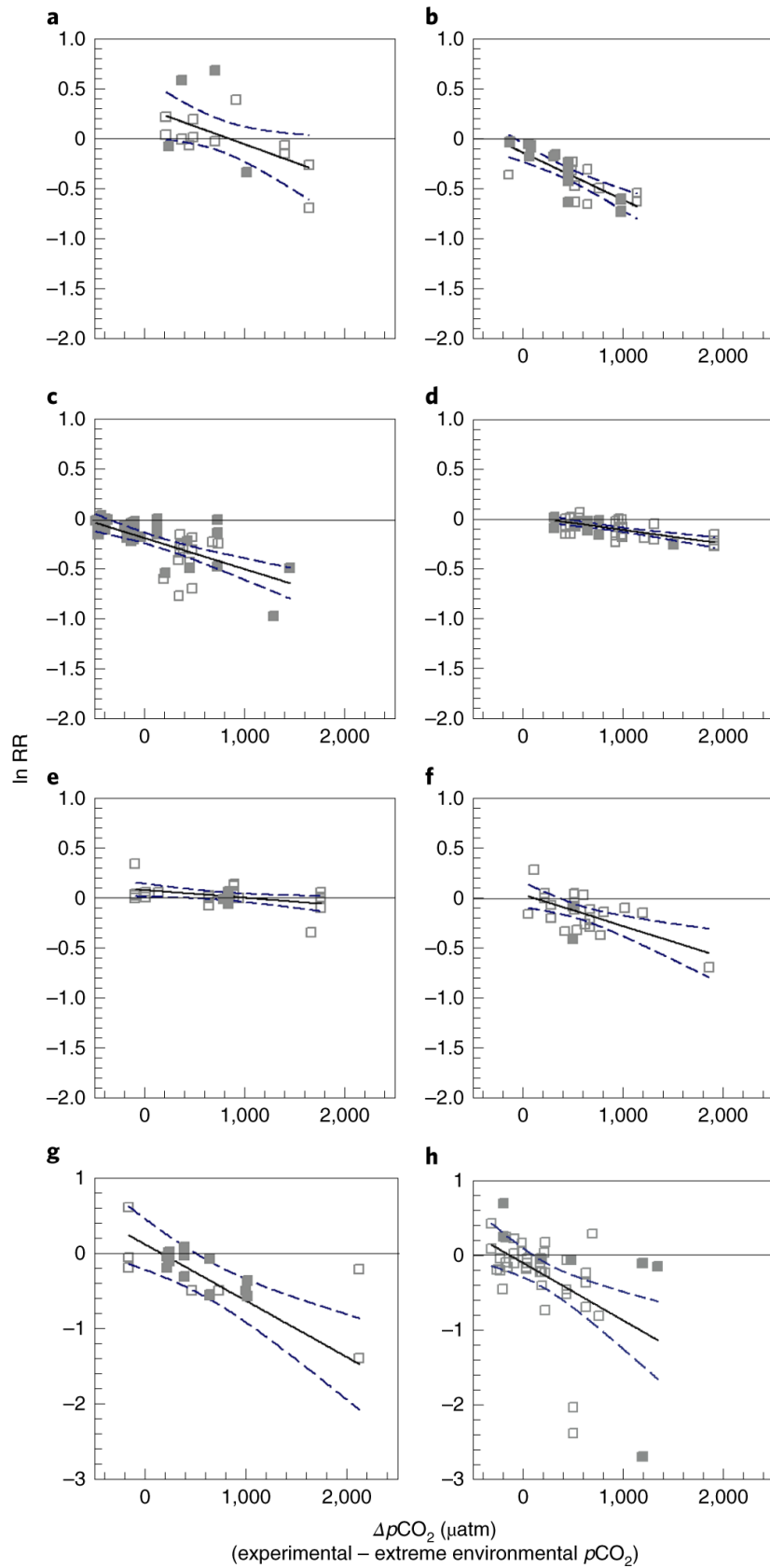
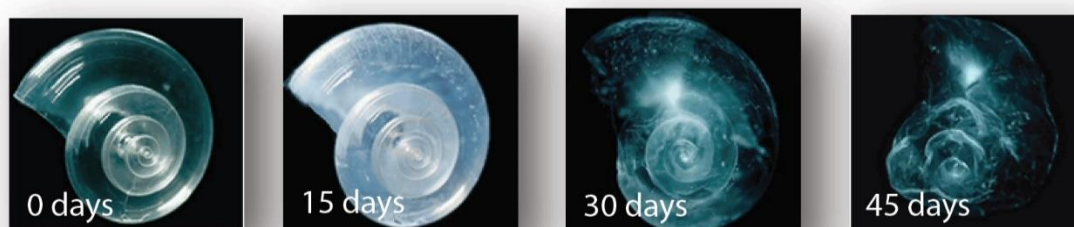


Figure 1.7: Ratio of the mean effect of acidification treatment to mean effect in control group ($\ln RR$) and $\Delta p\text{CO}_2$ (μatm). Grey squares are from experiment on eggs and larvae.

Open squares are from experiments on juveniles and adults. Dash lines are 95% confidence intervals (a) clams, (b) oysters, (c) gastropods, (d) sea urchins, (e) crustaceans, (f) corals, (g) scallops, and (h) mussels. From Vargas et al. (2022)

1.3.1. Calcification Issues

The link between ocean acidification and reduced aragonite and calcite (CaCO_3) saturation was theorised in the 1970s (Fairhall, 1973) and the consequences of this on calcifying organisms were discussed. Since then numerous laboratory and *in situ* studies have concluded that calcification rates are reduced under biologically relevant pH levels, including today's average surface pH of 8.1 (Doney et al., 2009). Calcifying organisms require the availability of calcium and carbonate in order to produce their skeletal structures via active biomineralisation. The increase in dissolved inorganic carbon in the ocean caused by anthropogenically produced CO_2 has reduced the saturation state of CaCO_3 (Ω), which effectively reduces available ions for calcifying organisms (calcification typically occurs at $\Omega > 1$) (Doney et al., 2009). There is a range of stark examples of this (e.g. Figure 1.8), including the complete loss of skeletal structures in corals grown in pH7.4 water based on RCP8.5 scenarios for 2100 (Fine and Tchernov, 2007, IPCC, 2013a, IPCC, 2013b). Due to the serious implications, much research has focused on calcifying organisms and the likely implications reduced calcification rates may have on fitness (Orr et al., 2005).



*Figure 1.8: Photograph illustrating the dissolution of *Limacina helicina* when held in seawater simulating the $p\text{CO}_2$ concentrations in 2100, based on a 'business as usual'*

(IS92a) scenario (IPCC, 2013, Orr et al., 2005). Image taken from <https://www.pmel.noaa.gov/co2/file/Pteropod+shell+experiment>.

Despite these calcification issues there is emerging evidence that calcifiers are tolerant to near-future ocean acidification (Leung et al., 2022). A meta-analysis of 985 research papers found that 70% of observation of growth and calcification were non-negative suggesting that many species may have the capacity for acclimation (Leung et al., 2022). Earlier studies appear to disproportionately focus on deleterious impacts with a bias toward short term exposure (e.g. Marubini et al., 2003, Riebesell et al., 2000, Cornwall et al., 2013). Resilience to reduced pH has been found to vary between species, with experiments identifying positive, negative and zero net effects on calcification rates (Ries et al., 2009). The ability to control the pH and carbonate ion concentration of calcifying fluids at the calcification site in an organism has been proposed as the underlying reason for this variation (Ries, 2011). Another possible explanation highlighted in studies of echinoderms, mollusks, and scleractinian corals suggests that calcification depends on the ability to tightly control intra or extra-cellular compartments where precursors of crystalline aragonite or calcite are formed and grown (Von Euw et al., 2017, Mass et al., 2017). The ability of some calcifiers to maintain calcification in acidified conditions suggests that seawater carbonate chemistry is not strongly associated with calcification (Leung et al., 2020). CO_3^{2-} from seawater is not utilised directly, but HCO_3^- or metabolically-produced CO_2 , which may mean that seawater carbonate saturation state is not a key limiter for calcification (Leung et al., 2020).

1.3.2. Physiology and Larval Development

It is widely agreed that calcifying organisms are particularly susceptible to reduced pH. However, physiologically speaking there is a range of under-researched

stressors caused by acidification that suggest non-calcifying organisms will also be impacted, although to what extent is under investigation (Pörtner et al., 2005). Harsher conditions will have implications on the physiology of all multicellular marine organisms (see Figure 1.9). Maintenance of acid-base balance between extracellular body fluids (such as haemolymph or blood) and intracellular fluids will be affected by increased water pH (Pörtner and Farrell, 2008). Typically, in lower marine invertebrates, bicarbonate ions are used to neutralise acidosis of extracellular fluids associated with reduced water pH (Pörtner and Farrell, 2008, Pörtner et al., 2004). Additional mechanisms of acid-base balance include: metabolic consumption of protons and the active transport of ions that are equivalent to protons out of cells (Michaelidis et al., 2005). Increased concentration of protons can further influence key metabolites and interfere with some enzymatic reactions if the substrates involved differ due to protonation (Pörtner and Bock, 2000). In addition, reduced water pH has been linked to reduced metabolic rate and increased ammonia excretion in a number of species (Michaelidis et al., 2005, Langenbuch and Pörtner, 2002). Different organisms employ different types of metabolic response based on length of exposure to stressors (Strader et al., 2020). The upregulation of genes involved in lipid metabolism is observed in many experiments involving long-term pCO₂ stress response in a variety of taxa (Strader et al., 2020). All of these mechanisms are associated with energetic costs, diverting resources from growth and reproduction (Pörtner and Bock, 2000). Figure 1.9 below (Wittmann and Pörtner, 2013) illustrates the range of effects that ocean acidification can have on the physiology of marine organisms.

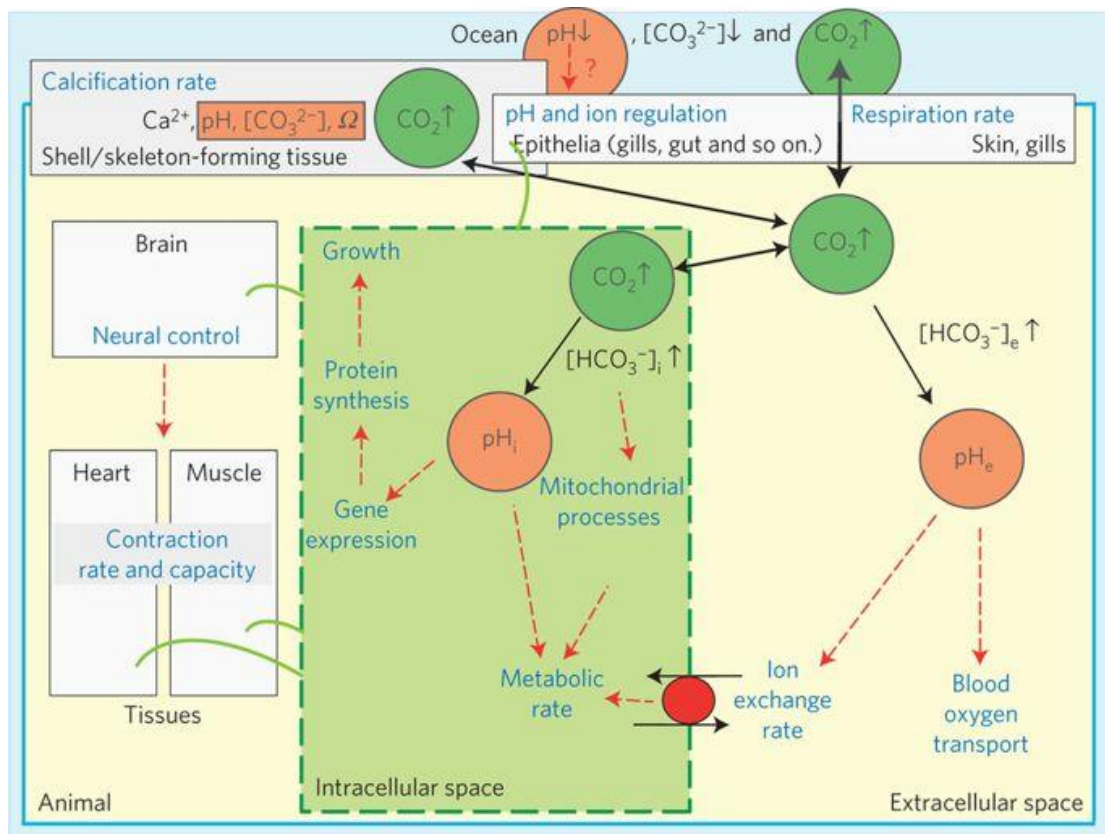


Figure 1.9: Mechanisms by which increased ocean pCO₂ can affect a marine organism. From the water, CO₂ diffuses into intracellular and extracellular compartments influencing the pH. This affects tissues, cells and physiological processes. The capacity an organism has to alter ion regulation and acid-base regulation may be critical in determining their ability to tolerate ocean acidification (Wittmann and Pörtner, 2013).

The larval and juvenile stages of invertebrates have been found to be particularly vulnerable to OA. Calcifying larvae are at risk because they must produce their initial shell in a relatively short period of time and with limited energy provisions (Spalding et al., 2017). The impact on larvae of non-calcifying species is more difficult to quantify. Locating appropriate habitat and avoiding predators is vital for successful larval settlement. Larvae use olfactory, visual and auditory cues to aid in settlement choice (Leis et al., 2011, Huijbers et al., 2012). Research on coral reef fish larvae shows that all three of these sensory systems are impacted by acidification (Nagelkerken and

Munday, 2016). An example of this was demonstrated by Rossi et al. (2015) using larval barramundi where reduced pH caused early metamorphosis, slower swimming speeds and deterrence to auditory settlement cues.

Tolerance to reduced pH varies depending on life stage, with some species being particularly sensitive at gamete, embryo or larval stage. For example, the coral-eating crown of thorn sea star (*Acanthaster planci*) had significantly reduced sperm motility under increased $p\text{CO}_2$ levels (900-1200 μatm) causing reduced fertilisation rates and the development of larvae also reduced significantly (Uthicke et al., 2013). In the stone crab (*Menippe mercenaria*), reduced water pH (7.5 ± 0.05) caused a significant decrease in hatching success and embryonic development compared to control embryos (held in water of pH 8.0 ± 0.06) (Gravinese, 2017). Clements (2016) found that larval dispersal increases when sediments are more acidic in the soft-shell clam (*Mya arenaria*), potentially suggesting avoidance behaviour. Meta-analysis of the literature shows that mollusc larvae are particularly vulnerable to more acidic conditions, however, increased sensitivity at early life stages is not common to all taxa (Kroeker et al., 2013).

Temperature is known to impact development in marine invertebrates (Hoegh-Guldberg and Pearse, 1995, Gangur and Marshall, 2020). Reduced larval development times and smaller adults have been observed when temperatures were elevated in the copepod *Tisbe* sp (Gangur and Marshall, 2020). Shorter development times can impact the dispersal distances that are possible by larvae (Álvarez-Noriega et al., 2020). Investigations into the effect of temperature on larval production have been species specific with some species, such as *Sphaerechinus granularis* producing fewer larvae at temperatures above their natural average (23 and 25°C), while others, such as *Arbacia lixula* producing more (García et al., 2018a, García et al., 2018b). Generally, intertidal species, such as *H. diversicolor* are considered to be robust to temperature

fluctuations thanks to wide thermal tolerances associated with phenotypic plasticity (García et al., 2018b).

Reduced fertilisation and increased frequency of larval abnormalities have been observed in Southern Ocean invertebrates exposed to increased CO₂, with growth rate, feeding and behaviour being unaffected (Hancock et al., 2020). A further concern for marine species is the ingestion of acidic seawater and the subsequent entry to the digestive system (Melzner et al., 2020). This process has been linked to an inability to maintain high pH in the gut due to ion balance systems becoming overwhelmed and digestive efficiency was negatively affected because of this (Hu et al., 2017). Lower feeding rates have been recorded in a range of calcifying marine organisms exposed to increased pCO₂, a factor which may exacerbate the physiological costs of acidification (Clements and Darrow, 2018).

Reproduction in *H. diversicolor* is mediated by photoperiod and temperature, which allows synchronicity of spawning (Wang et al., 2020a). However, a thermal shock of +10°C for one week induced spawning in *H. diversicolor* (Nesto et al., 2018). Wang et al. (2020b) found that embryonic development rate speeds up when temperatures increase from 6.1 to 21.2°C. The reduced time spent in embryonic phase can have impacts later, such as lower adult size (Wang et al., 2020).

1.3.3. Chemical Communication

An understudied impact of ocean acidification is the alteration that increased [H⁺] will have on the perception of dissolved chemical cues. Chemical communication is the oldest form of communication and, for some marine organisms, it is the only form of communication (Hay, 2009). Dissolved chemical cues in the marine environment have been found to influence: settlement; reproduction; foraging; predator avoidance; metamorphosis; conspecific interactions (Ashur et al., 2017, Hay, 2009). The

concentration of a chemical cue can be used by an organism to assess proximity to the source or number of organisms present. Reduced pH can alter the charge density and even the conformation of molecular cues via protonation, which has the potential to reduce their effectiveness or render them ineffective (Roggatz et al., 2016). Alternatively, it is possible that neurotransmitters or receptor molecules themselves alter under reduced pH, making reception of chemical cues much less effective (Chivers et al., 2014). Work by Chivers et al. (2014) illustrated that impairment of neurotransmitter function under near-future CO₂ scenarios inhibited the ability of damselfish to learn predator identities.

In turbid environments, where visual input is limited, dissolved chemicals can be the most important form of communication (Poulin et al., 2018). Primary metabolites such as amino acids, sugars and proteins are purported to act as chemical cues for generalist consumers and there is some evidence to suggest that the ratios of these specific compounds provide information about the source producing it (Hay, 2009, Derby, 2000, Kicklighter et al., 2011). In the lab, behavioural studies using natural products such as fish mucus have been more successful than studies that use individual peptides, pointing towards the importance of blends in chemical cues (Hay, 2009).

Specific chemical foraging cues are notoriously difficult to pinpoint and it is possible that different species interpret chemicals in different ways (Abreu et al., 2016, Chivers and Smith, 1998, Crane et al., 2022). Early studies identified taurine, beta-alanine, glutathione and trimethylamine as potential feeding cues due to the feeding response elicited in the common gulf-weed shrimp (*Leander tenuicornis*) (Johnson and Atema, 1986). Certain scavengers have been found to move towards the source of trimethylamine, essentially using the compound as a food cue (Brown, 2001). Dimethyl

sulphide (DMS) has been recognised as an attractant for procellariiform seabirds and this is linked to its release when zooplankton feed on phytoplankton blooms (Nevitt, 2008). Further work has identified DMS and the related compound Dimethylsulfoniopropionate (DMSP) as a feeding cue for some reef fish, harbour seals and possibly whale sharks (DeBose et al., 2008, Kowalewsky et al., 2005, Martin, 2007). Chondroitin sulphate has been suggested as a predator kairomone for some prey species. Cohen and Forward Jr (2003) found that concentrations of 10^{-5} M of chondroitin sulphate A disaccharides increased larval response to shadowing (a predator avoidance response) in estuarine crab larvae (*Rhithropanopeus harrisi*). Further tests indicated that acetyl-amine containing amino-sugar disaccharides were responsible for this increase in sensitivity to shadowing (Cohen and Forward Jr, 2003).

The complexities of how chemical communication may be hindered in a more acidic ocean and the knock-on effects this might have on populations and community structure is in need of further study. Few feeding cues are fully characterised and this inhibits the ability to conduct in depth studies. In addition, the variability in perception of a cue both within and between species tend to plague behavioural studies with varied responses from organisms (Mutalipassi et al., 2020).

1.3.4. Sensory Systems of Marine Invertebrates

Typically invertebrate chemosensory organs are made up of bipolar neurons with cilia at one end and an axon leading to the central nervous system at the other end (Figure 1.10) (Kamio and Derby, 2017).

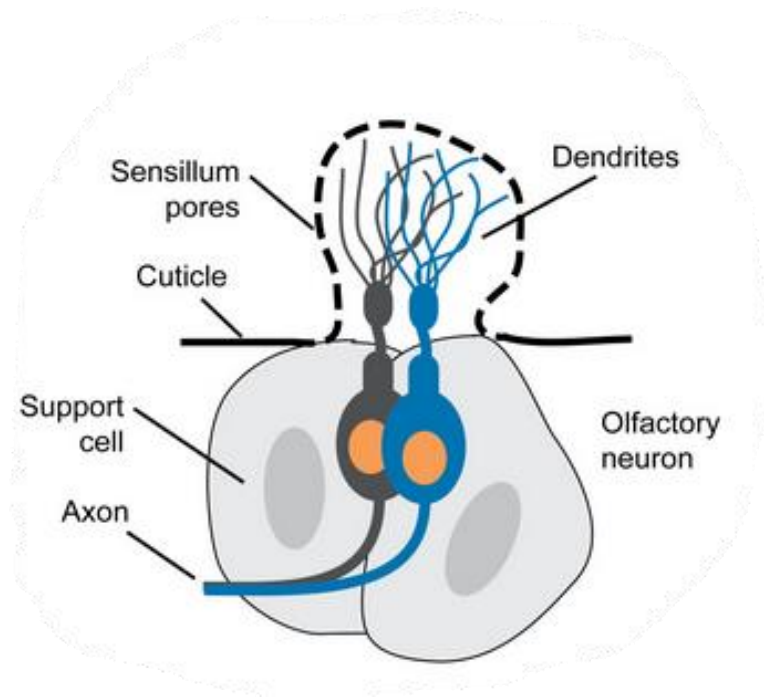


Figure 1.10. A typical invertebrate olfactory sensillum (Vosshall and Stocker, 2007).

Ciliated cells are responsible for collecting a range of sensory information in annelid worms, including visual and chemoreception (Mill, 1978). These ciliated cells may occur in isolation or bunched in groups to form sensory organs such as the nuchal organ (Mill, 1978). Chemoreception is typically considered to be a function of the nuchal organ and histological, structural and positional studies appear to confirm this (e.g. Whittle and Zahid, 1974; Storch and Schlotzer-Schrehardt, 1988; Rhode, 1990; Purschke, 1997). Other than the nuchal organ, several other chemosensory structures have been described in polychaetes such as; epidermal papillae found in *Arenicola marina* (Jouin et al., 1985) and parapodial cirri in nereidid polychaetes (Boilly-Marer, 1972). Compound sensory organs on the prostomial cirri have been identified in *Hediste diversicolor* (Dorsett and Hyde, 1969). These prostomial cirri are encased by the epicuticle the surface of which contains a large number of which extend through the cuticle into the surrounding environment (Dorsett and Hyde, 1969). The chemosensory systems of marine invertebrates

Polychaete worms such as *Hediste diversicolor* have a variety of ciliated cells which are organised into organs such as the apical or nuchal organ (Kamio and Derby, 2017). Nerves from the nuchal organ generally lead directly to the posterior section of the brain (Beesley et al., 2000) (Figure 1.11). Although physiological responses of chemoreceptors to chemical cues has been observed in polychaetes, very few studies have successfully demonstrated behavioural response to chemical cues (Kamio and Derby, 2017). Mechanoreceptor cells also allow relevant sensory input when foraging.

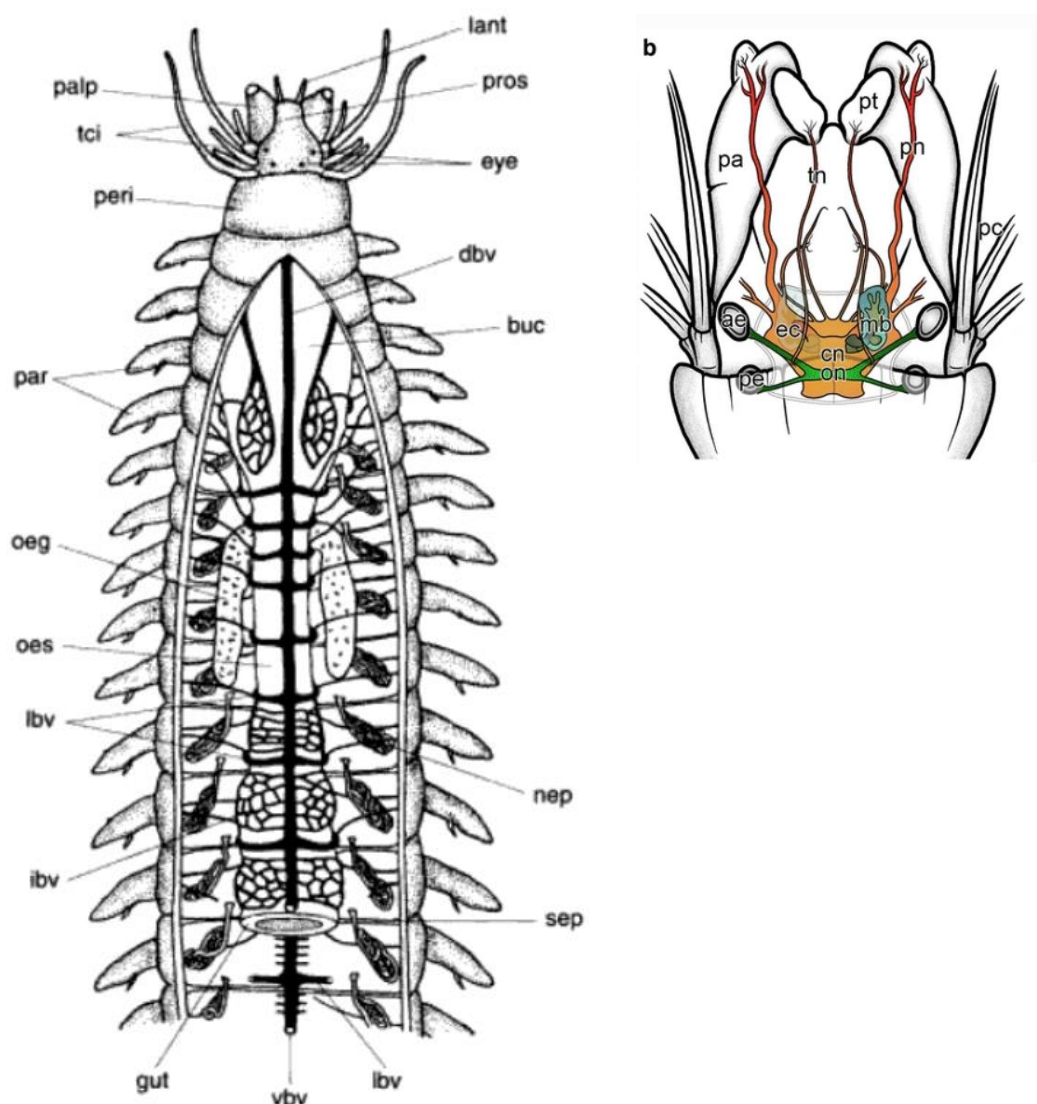


Figure 1. 11: Anterior section of a typical nereidid showing sensory and circulatory features. Buc = buccal organ; dbv = dorsal blood vessel; ibv = intestinal blood vessel;

lant = lateral antenna; *lbv* = lateral blood vessel; *nep* = nephridium; *nuc* = nuchal organ; *oeg* = oesophageal gland; *oes* = oesophagus; *palp* = palp; *par* = parapodia; *per* = peristomium; *pros* = prostomium; *sep* = septum, *tci* = tentacular cirri; *vbv* = ventral blood vessel (Beesley et al., 2000). b) Schematic of the overview of the supageal ganglion within the head of *Hediste diversicolor*. Prostomial tentacles (pt), parts of the tentacle nerves (tn), central neuropil region (cn), muraesophshroom bodies (mb) are efferents from the anterior (ae) and posterior eyes (pe) fuse to form the optic neuropil (on), palps (pa), prostomial cirri (pc), palpal nerve (pn)

Being soft bodies, polychaetes are under-represented in the fossil record (Rouse and Pleijel, 2001). The earliest unequivocal polychaete fossils date from the mid to late Cambrian era (~520mya) and were found in the Burgess Shale formation (Conway Morris, 1979). *Burgessochaeta setigera* fossils have clear parapodia and elongate capillary chitae. More recently a new polychaete species, found in China has been characterised and shows startling similarities to modern species (Figure 5.3 below) (Liu et al., 2015).

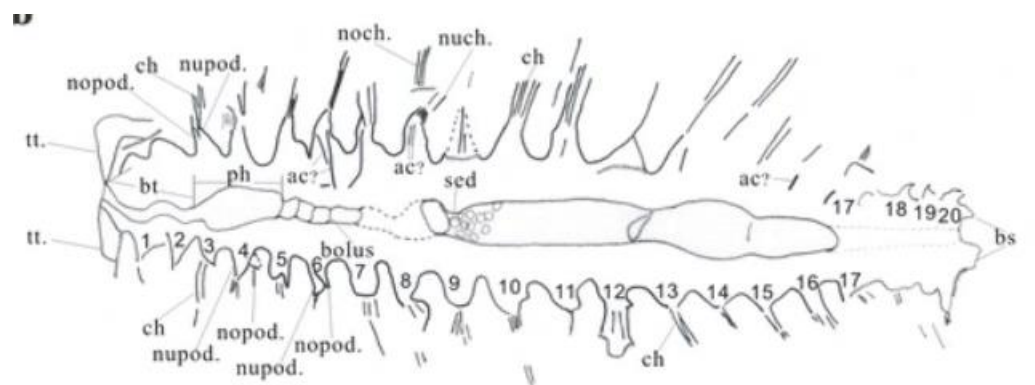


Figure 1. 12: Schematic of the Holotype of *Guanshanchaeta felicia* gen. et sp. nov. polychaete from Cambrian-era fossils found in China. Showing all characteristics of the specimen: Segments are numbered 1, 2, 3. ac acicula, bs bifid struture, bt buccal tube, ch chaetae, nopod. notopodium, nupod. neuropodium, noch. notochaetae, nuch. neurochaetae, ph pharynx, sed. sediment, tt. Tentacle (Liu et al., 2015).

Polychaetes do not fossilise well and are under-represented in the fossil record. Despite this, where fossilisation has occurred similarities in behaviour and physiology can be identified between modern day species and those from the geological past (see Figure 1.12). It is therefore conceivable that changing climatic conditions during past mass extinction events could have been exacerbated in the marine environment by some of the more subtle impact, such as the alteration in ability to identify food or predator cues. Chemical communication is the oldest form of communication and species living in marine environments are particularly reliant on it. It is therefore possible that impairment of chemical communication could have contributed to extinctions during the Permian-Triassic mass extinction, which was especially damaging to marine species. In this project, relatively minor fluctuations in pH and temperature (pH7.3 to pH8.1) were found to have a significant impact on *H. diversicolor's* ability to identify chemical cues.

1.3.5. Growth rate and Mortality

Growth rate in juvenile *H. diversicolor* has been found to range from 0.03 to 0.1mm per day (Möller, 1985, Chambers and Milne, 1975). Worms smaller than 12mm were found to have increasing growth rates with increasing size (Heip and Herman, 1979, Möller, 1985). Oocytes were found to grow faster at 5°C, with a negative growth rate at 15C for a population in the west of Sweden (Möller, 1985). Growth and regeneration in juvenile Nereididae is promoted by the hormone Nereidine which is secreted by the supraoesophageal ganglion (Lawrence and Soame, 2009). Nereidine inhibits sexual maturation, but declines in concentration with age leading to reduced growth and the onset of sexual maturation (Durchon and Porchet, 1971, Lawrence,

1996). Nereidine also promotes the uptake of the yolk protein vitellin by developing oocytes in *H. diversicolor* (Lawrence and Soame, 2009).

Reduced growth rates have been observed in a range of marine organisms exposed to elevated CO₂ (e.g. Sokolova et al., 2012, Dorey et al., 2013 and see Figure 1.11) and it has been proposed that reduced extracellular pH (exacerbated by reduced water pH) causes metabolic rate depression and lower growth rates (Michaelidis et al., 2005). However, further research is required in order to determine if extracellular pH, extracellular pCO₂ or extracellular bicarbonate are responsible (Melzner et al., 2020).

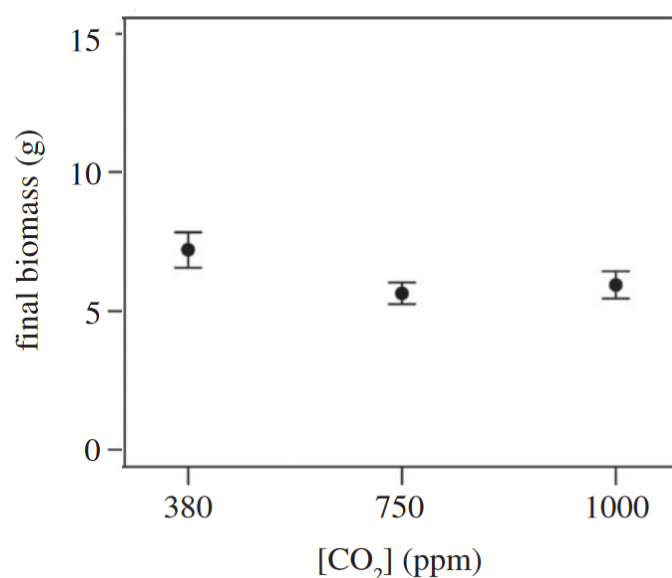


Figure 1.13: The impact of [CO₂] (ppm) on the biomass (g, mean+s.e.) of *Alitta virens* under ambient temperature conditions (Godbold and Solan, 2013).

1.3.6. Multi-stressor Effects: Temperature and Pollution

Increasing temperature is a recognised effect of climate change and this, combined with ocean acidification can cause cumulative impacts on survival, reproduction and physiological processes of marine organisms (Gunderson et al., 2016). The confounding effect of multiple stressors on organisms is something that has been highlighted over the past few years. For example, it is predicted that larvae will respond

to warming by reducing their Pelagic Larval Duration, however, ocean acidification slows larval development in some species (Dupont et al., 2010, Gazeau et al., 2013). Theoretically, combinations of stressors can have additive, antagonistic or synergistic impacts of an organism and studies have been conducted that provide examples of each of these (Gunderson et al., 2016). A meta-analysis of the literature by Przeslawski et al. (2015) indicated that synergistic effects are the most common impact of multiple-stressors.

Increasing ocean temperatures may lead to ocean hypoxia (O₂ deficiency), which can catastrophically alter ecosystems, driving mortality and altering biogeochemical cycles (Conley et al., 2009). Rising ocean temperatures creates increased stratification and reduced ventilation (due to declining upwelling and reduced mixing) (Shepherd et al., 2017). In addition, oxygen is less soluble at higher temperatures and therefore oxygenation levels in surface waters will reduce (Shepherd et al., 2017). Influxes of pollutants into the oceans via runoff, particularly in coastal areas will have a profound effect on ocean chemistry as well as marine organisms. Nutrient-rich runoff can exacerbate pH fluxes causing temporary pH extremes (Gravinese, 2017). Lower oxygen levels are also heavily influenced by eutrophication and nutrient input. The input of excess nutrients increases the rate of oxygen consumption via the decomposition of organic matter (Conley et al., 2009). Algal blooms caused by the input of excess nitrogen and phosphorous (often from anthropogenic sources such as agricultural fertilizer runoff) create anoxic and more acidic conditions leading to 'dead zones' (Ngatia et al., 2019).

Although multi-stressor studies are increasing, there remain significant gaps in the literature. Figure 1.12 highlights the focus of multi-stressor studies in the marine environment (Gunderson et al., 2016).

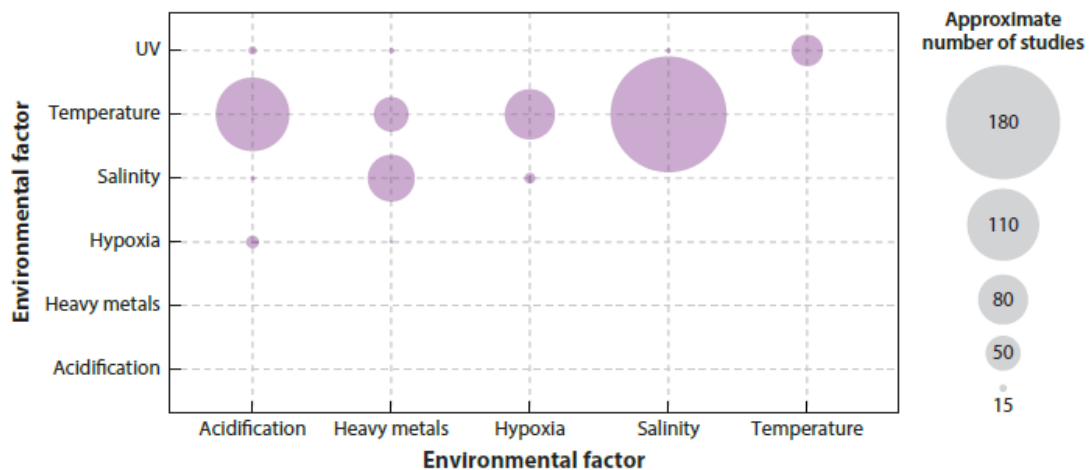


Figure 1.14: Approximate number of studies conducted on marine organisms exposed to multiple stressors from a 2015 review paper by Gunderson et al. (2016).

The presence or absence of multiple species can alter an organism's response to abiotic stressors such as temperature and pH. Evidence suggests that predictability of species response to ocean acidification and warming reduces when testing multispecies systems (Kroeker et al., 2013). While small scale experiments identify causality and the associated mechanisms for individual species, such experiments are a simplification of natural systems and fail to tackle community-level or ecosystem-level impacts of climate change (Stewart et al., 2013). Mesocosm experiments combined with modelling offers scope to investigate the more complex responses of ecosystems to the impacts of changing climates (Stewart et al., 2013). *In situ* studies in areas with naturally high levels of CO₂ (such as hydrothermal vents) have provided interesting results, however the fact that such sites are atypical along with the inability to control all variables *in situ* bring into question the validity of these results (Stewart et al., 2013). However, the vents at the Castello Aragonese on the island of Ischia, Italy have been the focus of a

wealth of studies due to the presence of future-relevant [CO₂] gradients and little evidence of the presence of toxic substances (Foo et al., 2018). At the Ischia vents, investigations of the species occurring along the pH gradient show that decreased pH is associated with a reduction in calcifying species, mirroring the trends seen at other vent systems and in laboratory studies (Foo et al., 2018). Species at this site that inhabit areas with near future conditions (mean pH 7.8) exhibit a range of physiological and ecological mechanisms for acclimatisation and adaptation to low pH, illustrating resilience of many species to elevated CO₂, including many calcifying species (Foo et al., 2018). Despite this, species assemblages are likely to become dominated by fleshy algae and smaller-bodied, generalist invertebrates as the oceans acidify to pH levels below 7.8 (Foo et al., 2018).

1.3.6. Energetic costs of climate change

Pörtner et al. (1998) investigated the energetic impact of elevated CO₂ on the marine annelid *Sipunculus nudus*. Elevated pCO₂ (to 1% CO₂ in air) led to a decrease in both intra and extracellular pH, with intracellular pH quickly returning to normal at the expense of extracellular acidosis. Extracellular space was partially compensated via the expulsion of protons to surrounding water during prolonged exposure to hypercapnia (Pörtner et al., 1998). Interestingly, it was found that O₂ consumption declined under hypercapnia, indicating metabolic depression. This, along with the increased gas partial pressure gradients was linked to an observed decrease in ventilation effort (Pörtner et al., 1998).

The cellular mechanisms responsible for ion-balance are poorly constrained for many marine invertebrates and paracellular transport across the external epithelium into extracellular fluids is not well understood (Melzner et al., 2020). Despite this, there a

small number of studies that have used fluorescent labelling to show that relatively large molecules (in the range of ~ 0.6 kDa) can enter extracellular space through paracellular transport in echinoderm larvae, mollusc larvae and corals (Stumpp et al., 2012, Tambutté et al., 2012, Ramesh et al., 2017). In heterotrophic invertebrates, pCO₂ values are highest in mitochondria, followed by intracellular fluid with extracellular fluid having the lowest pCO₂ values. Extracellular fluid has higher pCO₂ than surrounding seawater and any increase in seawater pCO₂ will lead to a subsequent increase in extracellular pCO₂. This is because relatively large concentration gradients are required in order to excrete metabolic CO₂ produced within the cells (Melzner et al., 2009). Whether equilibrium can be achieved via paracellular transport is unknown.

Compensatory mechanisms for increased internal pH include buffering via the accumulation of bicarbonate in extracellular space and active ion transport. In cephalopods, sodium pumps are primarily responsible for acid-base flux, by actively creating low Na⁺ concentrations in the cell which can then be utilised by sodium-proton exchangers to expel protons. Bicarbonate is similarly transported along an electrical gradient created by sodium pumps (Melzner et al., 2020). Acid-base transporters in other invertebrates are very poorly studied and caution should be taken when assuming homology between the mechanisms used by different taxa (Melzner et al., 2020).

A range of more long-term mechanisms to mitigate the effect of increased pCO₂ and the accompanied decrease in pH have been found. The upregulation of mRNA for Rhesus proteins, which are generally considered to act as gas channels, and an associated reduction in diffusion distance (at a cost of increased diffusive water loss) (Esbaugh et al., 2016). This upregulation, which has been empirically observed in fish, crustaceans and cephalopods, suggests plasticity allowing the maintenance of CO₂ flux when diffusion gradients are reduced (Esbaugh et al., 2016, Hu et al., 2014, Weihrauch

and O'Donnell, 2017). In mammals, the cholesterol content of membranes has been found to alter their permeability to CO₂, with higher cholesterol reducing CO₂ flux (Arias-Hidalgo et al., 2018). However, increased cholesterol is linked to increased membrane fluidity, which may limit the effectiveness of such responses. Although this mechanism has not been studied in marine organisms, it could potentially offer some resilience to increasing levels of water CO₂.

Pan et al. (2015) found that, although the sea urchin (*Strongylocentrotus purpuratus*) appeared resilient to ocean acidification, at the cellular level, protein synthesis and ion regulation accounted for the majority of energy expenditure in acidified conditions for growing larvae (84% at reduced pH, compared to 40% in control conditions).

A decrease in pH has been found to negatively affect *H. diversicolor* physiology. In individuals held at pH7.6 and pH7.3, Freitas et al. (2016) identified an increase in the activity of carbonic anhydrase which aids in the conversion of CO₂ and water to carbonic acid and bicarbonate during respiration. Additionally, lower energy reserves and higher metabolic rate (measured as electron transport system activity) were seen in individuals held at reduced pH. The elevated carbonic anhydrase activity was linked to osmoregulation capacity, while the reduced reserves and higher metabolic rate was linked to the development of defences such as antioxidant enzyme activity. The build-up of antioxidants appeared to be a successful strategy in this study because lipid peroxidation was similar for individuals in low pH (7.3) and those in the control pH (7.9).

A paper (Hayward and Gillooly, 2011) investigating the energetics of gamete production used values for wet weight of gametes collected from the literature (and

converted, where necessary using a conversion factor of 0.4 to convert grams of carbon to dry weight and then a conversion factor of 0.25g dry weight per g of wet weight). Biomass production in g/day was converted into J/day using a conversion factor of 7×10^6 J/g. This was then converted into Watts in order to allow comparison to basal metabolic rate of ectotherms at a given temperature (at 20C, metabolic rate ($W = 0.14 \times \text{mass}(\text{kg})^{0.751}$). Corrections for temperature were computed in order to assess gamete production at 20C. To do this it was assumed that production increased exponentially with temperature using the Boltzmann-Arrhenius factor ($e^{-E/kT}$). E = average activation energy of the respiratory complex (eV), k = Boltzmann's constant, T = absolute temperature (Kelvin). Hayward and Gillooly utilised methodology from Peters and Peters (1986).

Computation of external cues, such as determining the concentration of a chemical ligand, incurs an energetic cost. In addition, Landauer's principle asserts that erasure of past observations also requires energy (Mehta and Schwab, 2012). Mehta and Schwab (2012) use the Berg–Purcell strategy to calculate the energetic cost of determining ligand concentration in a simple cellular network with two components. Berg and Purcell (1977) showed that a cell is limited in its capacity to acquire environmental information by stochastic fluctuations in the occupancy of receptor protein by the ligand being detected. Assuming that a receptor binds to a ligand with a concentration-dependant rate (k_{off}) and the receptor releases the ligand at a constant rate (k_{on} (unaffected by concentration)), a cell can compute the average time a receptor is bound in a given time period (T) in order to estimate ligand concentration (Berg and Purcell, 1977). A more efficient method would be to calculate the average time a receptor is unbound in a given time period (Endres and Wingreen, 2009). In bacteria, receptor-catalysed phosphorylation of a response regulator protein is a common signalling

pathway and act as a simple model for calculation of computational cost (Mehta and Schwab, 2012). Assumptions include: membrane-bound receptors are either ‘on’ or ‘off’; Receptor binding affinity is extremely high, meaning that all ligand-bound receptors are ‘on’ and all unbound receptors are ‘off’; Receptor-binding activates a protein from inactive form X to active form X^* at a state-dependent rate (K_{2s}) where $s=on,off$; Proteins are deactivated at a constant rate K_1 , independent of state ratios. Effective selection of the time period T is based on K_1 , the inactivation rate of response regulator proteins ($T \propto K_1^{-1}$) (Mehta and Schwab, 2012). To calculate entropy production (EP), the process was formulated as a non-equilibrium Markov process, eventually producing:

Although metabolic scope for activity increases with temperature in *H. diversicolor* (Galasso HL, 2018), calculating the energetic cost of altered cue reception or biomass production in organisms as complex as polychaetes has currently not been attempted. Though difficult to calculate, each of chapters outlined in this thesis contribute to an alteration in energetic cost with changing pH and temperatures for *H. diversicolor*.

1.3.7. Bioturbation

Bioturbation (defined as the biological reworking of soils and sediments by organisms) is recognised as a form of ecosystem engineering (Meysman et al., 2006) and includes behaviours such as burrow formation and infilling (once burrow is abandoned), burrow irrigation, prey excavation, mound formation (for example by heart urchins) and sediment particle ingestion and egestion (Meysman et al., 2006). Kristensen et al. (2012) expanded this definition to include “all transport processes carried out by animals that directly or indirectly affect sediment matrices.” The overall impact of such activities is greater than the sum of their parts and the impact of bioturbation is on the scale of landscape formation (Meysman et al., 2006). Bioturbation

is a key factor in sediment transport and nutrient cycling, which in turn influence geomorphology (Boyle et al., 2014, Meysman et al., 2006). For example, bioturbation increases the retention of phosphorus in sediments (relative to carbon) and because it acts as the limiting nutrient for oxygen production this can have an impact on oxygen reservoirs (Boyle et al., 2014)

The action of bioturbation alters sediment surface topography, which, in aquatic environments, can impact flow regimes and alter resuspension and erosion (Shrivastava et al., 2021). Filter feeders impact sediment transport by ingesting particles, they also impact resuspension in the form of faecal fluid ejections (Meysman et al., 2006, Boudreau and Jorgensen, 2001). Resting eggs of many organisms are incorporated into the sediment and potentially returned to the surface through the action of burrowing organisms. These dormant eggs typically hatch in response to a stimulus such as O₂ availability and their incorporation into sediments can effectively create a ‘seed bank’, which impacts recruitment for a range of species (in particular planktonic species) (Ståhl-Delbanco and Hansson, 2002). Organisms can alter the texture of sediment; changing porosity, cohesiveness, solute diffusion and inducing spatial heterogeneity, thus creating a range of environmental niches (see Figure 1.13) (Meysman et al., 2006).

1.3.8. Evolution of Bioturbation and the Expansion of Accessible Habitat

The onset of animal burrowing and mixing sediments (bioturbation) is first (indisputably) seen in the late Ediacaran and is characterised by the transition from stratified Precambrian to the more mixed sediments of the Phanerozoic (see Figure 1.14) (Boyle et al., 2014). There is some emerging evidence that simple substrate feeders existed as early as 40-55 My before the Cambrian (Chen et al., 2004). Prior to the appearance of bioturbating organisms, benthic habitats consisted of simple, one-dimensional microbial mats which formed layers of microbe communities with

differing metabolisms (Meysman et al., 2006). These microbial mats coated the substrate surface and as such, oxygen penetration was shallow. Trace fossils of early ‘Ediacaran fauna’ suggest that they existed alongside microbial mat communities (Meysman et al., 2006).



Figure 1.15: Examples of the range of types of bioturbation and the variety organisms that perform this important service. (a) mole track (Thomomys talpoides macrotis) (b) mole track in prairie grasslands. (c) dugong (Dugong dugong) feeding on rhizomes (d) feeding pit attributed to the blue-spotted stingray (Taeniura lymma) (e) foraging blue-spotted stingray (f) the common earthworm (Lumbricus terrestris). In the marine environment, the dominant bioturbators are deposit-feeding polychaetes and burrowing crustaceans. Invertebrates have a small per capita impact, but due to their population density they are dominant from a global perspective. From Meysman et al. (2006).

The earliest bioturbators (*Planolites*) are identified ichnologically by remains of their simple, unbranching, shallow burrows or surface trails with diameters typically in the range of a few millimetres (Lipps and Signor, 2013). Pelleted traces created by ichnogenus *Neonereis* and *Torrowangea* occur slightly above these simplest burrows in the fossil record. Later, the burrows increase in complexity and size, becoming bilobed and vertical, reaching depths of a few centimetres (attributed to *Didymaulichnus* and *Skolithos*). All of these burrow forms occur in the Vendian (635 to 541Mya) (Lipps and Signor, 2013). Traces of simple arthropod scratch marks created by *Monomorphichnus* appear in the late Vendian, but only become common in younger rocks and more complex *Rusophycus* and *Cruziana* are not found until the Tommotian. The evolution of branching burrows and traces of spreite burrows are first found later in the Tommotian (Lipps and Signor, 2013).

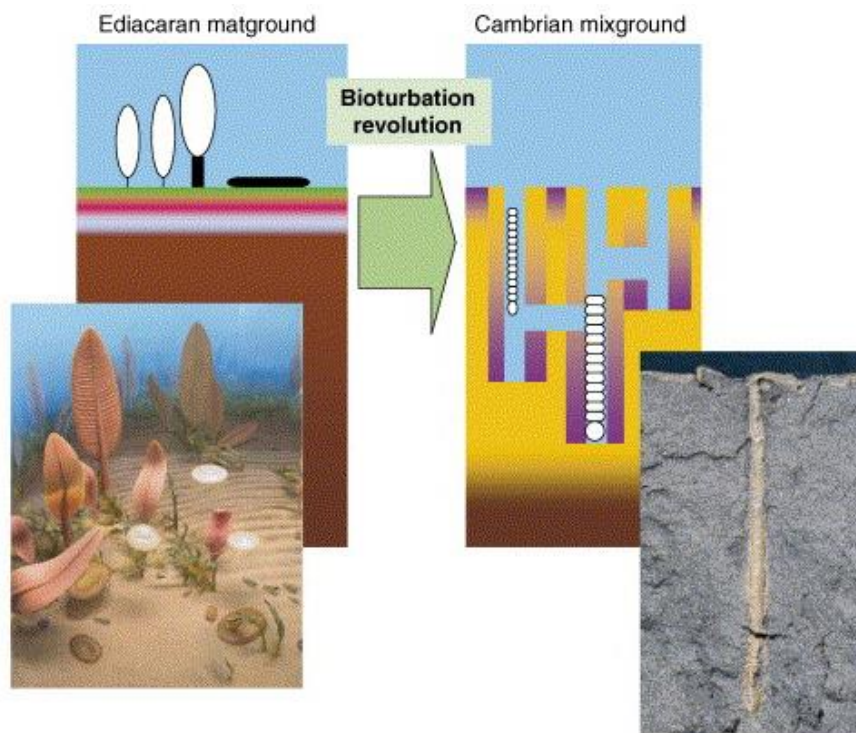


Figure 1.16: Conceptual illustration showing the transition between Ediacaran matground habitat with microbial matt covered sediments to Cambrian mixground where the sediment is mixed due to complex burrow networks. Burrow flushing

allows oxygen transportation deep into sediments. Inset photograph shows Arenicola marina with a light halo of oxidised sediment around its burrow as compared to grey background of reduced sediment. Meysman et al. (2006).

The Cambrian Explosion was characterised by rapid speciation and this is evidenced in the fossil record by increased biodiversity and population sizes. It has been hypothesised that one of the driving forces behind this explosion was the evolution of bioturbation and the associated expansion into new habitats. Not only did burrowing organisms turn an essentially two-dimensional habitat into a complex three-dimensional habitat, but they also opened up a new food source in the form of buried organic matter (Herringshaw et al., 2017). Burrowing into the sediment also provided shelter from predators, however, over time predators evolved to excavate sediments in their search for infaunal prey and these adaptations also aided the Cambrian Explosion (Herringshaw et al., 2017). The rise of bioturbation led to an increase in relative surface area available for nutrient exchange between the sediment and the water column (Boyle et al., 2014).

1.3.9. Loss of Bioturbation

Early Triassic ichnofaunas show a loss of sediment mixing by organisms. Evidence for this includes: superior preservation of epifaunal or shallow infaunal species and a distinct scarcity of deep-tier species, lack of bioturbation textures and dominance of fossil types that suggest the presence of cohesive and microbial-mat ground sediments (Hofmann et al., 2015, Twitchett et al., 2001). Bioturbation intensity is measured using an ‘ichnofabric index’ allowing rapid, semi-quantitative assessment of sedimentary rock (Droser and Bottjer, 1986). Using a combination of ichnofabric index and appearance of cohesive, microbial-mat type fossil assemblages, the collapse of benthic ecosystems can be tracked.

Loss of bioturbation during the EPME led to the loss of associated ecosystem engineer behaviours such as sediment mixing, aeration and enhanced geochemical cycling. It has been suggested that the demise of bioturbation during this period may be responsible for the levels of anoxia observed in the Early Triassic (this has previously been used as a proxy for seawater anoxia) (Hofmann et al., 2015). It is also possible that discrepancies in sulfate evaporate minerals observed in the fossil record may be due to the impact of bioturbation loss on the sulfur cycle (Canfield and Farquhar, 2009).

Ocean anoxia is viewed as a strong factor in the slow recovery of marine ecosystems following the EPME (Hallam and Wignall, 1997, Wignall and Twitchett, 1996, Moffitt et al., 2015). However, there is increasing evidence that ecosystem recovery, even that of benthic systems, occurred in areas that were believed to be inimical to life due to anoxia (Hofmann et al., 2015). Recent research from Cribb and Bottjer (2020) present trace fossil evidence that indicates that there was no loss of bioturbation ecosystem engineering behaviors after the mass extinction, including deep tier, high-impact, complex ecosystem engineering. Similarly, Feng et al. (2022) identified well established infaunal ecologic structure was in the early Smithian (251.2 to 247.2 Mya) in Chinese trace fossils. However, the impact of trophic group interactions could have delayed the recovery of nonmotile, suspension-feeding epifauna in the Early Triassic (Feng et al., 2022). The loss of bioturbating organisms and the subsequent reduction of mixing in marine sediments might have been a key influence on the delayed recovery of marine ecosystems (Hofmann et al., 2015).

1.3.10. *Hediste diversicolor*

Throughout this thesis the harbour ragworm (*Hediste diversicolor*) is used as a model bioturbating organism. *H. diversicolor* is a common burrowing polychaete worm found in intertidal and shallow estuarine environments throughout Europe and North

America (see Figure 1.15) (e.g. Scaps, 2002, Muus, 1967, Heip and Herman, 1979, Kristensen, 1984). Population density is highly variable ranging from 35 to 3700 ind.m⁻² depending on season and environmental factors such as temperature, salinity and location (Scaps, 2002). A relationship between the feeding strategy of an organism (e.g. suspension versus deposit feeders) and irrigation rate (and therefore solute exchange with surface waters) has been identified in burrowing species (Kristensen and Kostka, 2005). *H. diversicolor* use several feeding mechanisms including deposit feeding, suspension feeding and active hunting (Fauchald and Jumars, 1979, Harley, 1950). They produce mucus to stabilise their burrows and can build mucus nets outside their burrows to catch detritus, which they then consume. The burrows of *H. diversicolor* are typically either Y shaped or U shaped and the internal burrow conditions are stabilised by active irrigation by the worm (Esselink and Zwarts, 1989).

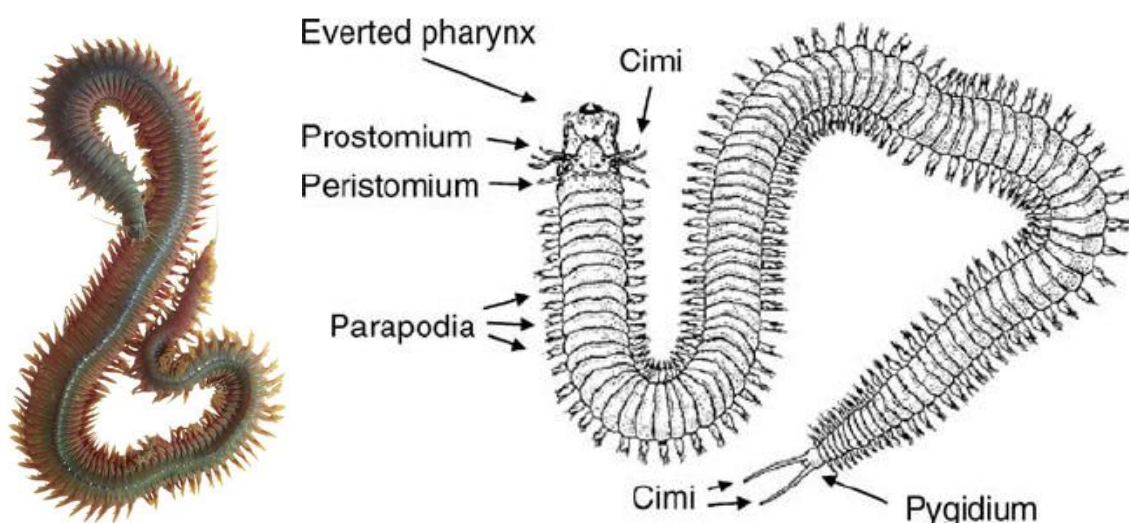


Figure 1.17: Drawing of a typical ragworm with pharynx everted and photograph of the common ragworm *Hediste diversicolor*. From Hesselberg (2007).

Their burrowing activity increases the oxic zone in the host sediment and increases meiofaunal and microbial populations in the area adjacent to burrow walls (Scaps, 2002, Fang et al., 2021). In areas where *H. diversicolor* are abundant, their

bioturbating activities likely have a crucial effect on ecosystem functioning (e.g. Godbold et al., 2011, Godbold et al., 2009, Solan et al., 2008). Solan et al. (2008) conducted a mesocosm study using three bioturbating species (*Hediste diversicolor*, *Hydrobia ulvae* and *Cerastoderma edule*) and identified *H. diversicolor* as providing the largest contribution to nutrient generation as well as having the highest bioturbation intensity. This study also identified the importance of species richness reflecting species-specific impacts on particle reworking and associated nutrient production. A further study (this time using *Hediste diversicolor*, *Hydrobia ulvae* and *Littorina littorea*) identified that species composition, rather than species richness better explained resource use and decomposition (Godbold et al., 2009). The burrowing, bio-irrigation and associated sediment re-working of *H. diversicolor* has led to their being classed as a keystone species and it has been suggested that the feeding of this species acts as a rate-limiting step in estuarine detritus processing (Moreira et al., 2006, Mermillod-Blondin et al., 2005). Additionally, migrating bird species rely on benthic invertebrates such as *H. diversicolor* as a food source, with overwintering birds consuming as much as 90% of *H. diversicolor* populations (e.g. Boates and Goss-Custard, 1992, Scheiffarth, 2001, Ens et al., 1996, Evans et al., 1979).

Hediste diversicolor are semelporous, undergoing one spawning event after which the individual dies (Möller, 1985). Co-ordination of spawning is therefore critical for the success of the species and they commence a prolonged spawning during spring (Kristensen, 1984). One of the possible impacts of increasing sea surface temperatures due to climate change is the uncoupling of photoperiod and temperature, which act in combination to stimulate spawning, larval development, gamete development and production of spawning hormone (Lawrence, 1996, Kristensen, 1984, Lawrence and Soame, 2004). Indeed, individuals held at high temperatures spawn

asynchronously (Bartels-Hardege and Zeeck, 1990). Gamete maturation is stimulated at temperatures of 6°C, with spawning occurring 4 weeks later in temperatures of around 12°C (Bartels-Hardege and Zeeck, 1990). The changing temperatures in early spring are thought to be involved in assisting synchronisation of spawning as is the semi-lunar cycle, with peaks at new and full moon (Bartels-Hardege and Zeeck, 1990). *H. diversicolor* may be particularly vulnerable to climate change due to their lack of planktonic larvae and associated reduction in dispersal distance and population mixing (Lawrence and Soame, 2004). However, they have a wide distribution and are tolerant to a variety of conditions which may alleviate some of the risk.

H. diversicolor is widely used as a bio-indicator species for assessing the impact of metal pollution, nanoparticles, pharmaceuticals and hydrocarbons (Freitas et al., 2016).

1.4. Past Mass Extinctions and the Modern Day Link

A mass extinction is defined as a geologically short time period (<2 million years) during which more than 75% of all species disappear (Jablonski, 1994). Over the past 540 million years, mass extinctions have occurred five times (see Figure 1.16) (Barnosky et al., 2011b). The causes of these mass extinctions vary, however, most extinction events are linked to climate change and associated factors such as ocean acidification and marine anoxia (Bond and Grasby, 2017, Barnosky et al., 2011b). Large scale volcanism is often cited as the cause of past climate change events due to the negative carbon isotope excursions that occur in tandem with large igneous province volcanism (Bond and Grasby, 2017, Wignall, 2001, Wignall et al., 2009). Volcanic eruptions release large volumes of gases, including CO₂ and SO₂. Although CO₂ contributes to global warming, SO₂ has the opposite effect by creating aerosols that

block the sun. However, while the cooling effect of SO₂ is short-lived because of rain out, the warming effect of CO₂ lasts much longer (Bond and Grasby, 2017).

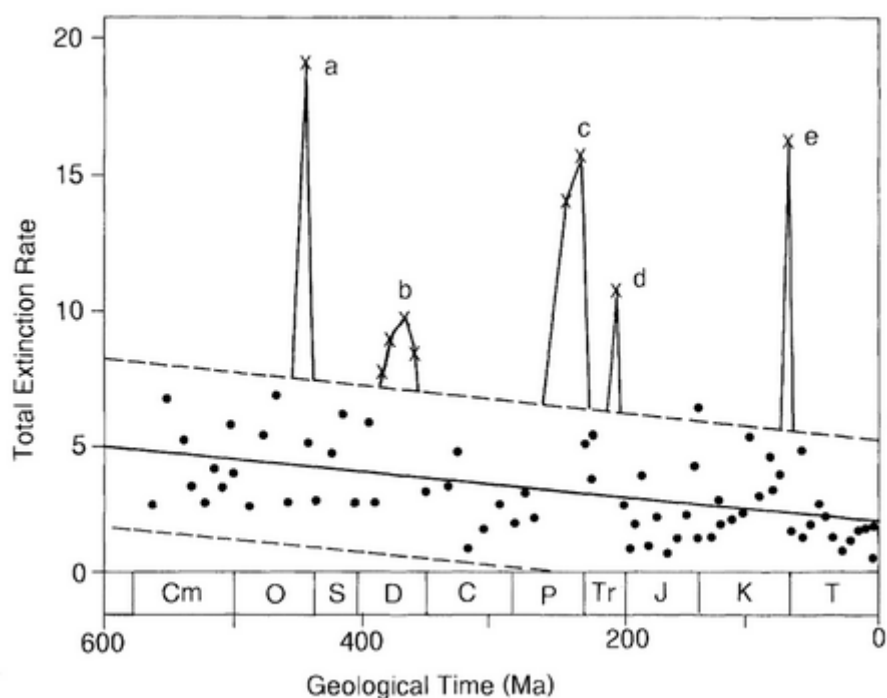


Figure 1.18: The occurrence of mass extinctions through geological time during the Phanerozoic with extinction rates given as families per million years. The five mass-extinctions can be seen clearly as peaks that stand well above background extinction levels. a) Late Ordovician, b) Late Devonian, c) End Permian, d) Late Triassic, e) Late Cretaceous. Taken from Hallam and Wignall (1997).

The most severe mass-extinction to occur was the End Permian Mass Extinction (EPME), 252 million years ago (Shen et al., 2011). More than 90% of marine species went extinct during this event (Erwin, 1994). The PTME was not confined to oceanic taxa, there was also a profound effect on terrestrial ecology. The Permian Triassic boundary was marked by a transition from diverse seed ferns to low diversity conifers and lycopsids. The ‘coal gap’ that begins in the late Permian (~250Mya) and continues to Mid Triassic (~243Mya) is indicative of the loss of peat-forming plants during this interval (Retallack et al., 1996). Variation in paleosols (fossilised soils) from Antarctica

indicate a transition to low-productivity ecosystems with high proportions of stress-tolerant opportunistic plants during the EPME (Retallack & Krull, 1999). Loss of coniferous vegetation in Europe also lead to a degraded ecosystem where lycopsids dominated for ca. 4-5My (Looy et al., 1999). Proximal kill factors such as climate change, acid rain, ocean acidification and anoxia, hypercapnia and toxic metal pollution are most commonly cited causes (Bond and Grasby, 2017). The total CO₂ release from Siberian Trap Large Igneous Province (LIP) has been estimated at 30,000 Gt (Courtilot and Renne, 2003). Anthropogenic CO₂ input to the atmosphere currently stands at about 37 Gt. This means that in around 800 years humans could have released the same mass of CO₂ into the atmosphere as 0.9 million years (My) of Siberian Traps volcanism (Courtilot and Renne, 2003, Bond and Grasby, 2017).

There is an increasing concern with regard to modern-day extinction rates (e.g. Ceballos et al., 2015, Pereira et al., 2010) and there is evidence to suggest that we are now facing a sixth mass extinction event (Ceballos et al., 2015). There is some uncertainty in estimating the background rates of extinction and speciation, particularly because most extant species have not been formally described yet (Barnosky et al., 2011b), however, this often leads to underestimation of current extinction rates and an overly optimistic outcome. Currently, the most common metric used to quantify extinction rates is extinctions per million species year (E/MSY), or the number of extinctions per million years per species (Pimm et al., 2006, Pimm et al., 1995). Using conservative assumptions and estimates of modern extinction rates Ceballos et al. (2015) computed that the average rate of loss for vertebrate species is 100 times the background rate. This corresponds to 800-1,000 years' worth of extinctions occurring in just one century (Ceballos et al., 2015).

Modern extinction rates appear to be driven by similar stressors that lead to past mass extinctions, namely, climate change and associated factors (Bond and Grasby, 2017). What is unclear is why certain extinction events are so much more severe than others, despite similar causal mechanisms. It has been suggested that biological factors, such as tolerance of certain species to reduced pH, might elucidate this and experimental setups with modern day analogues could provide insight (Bond and Grasby, 2017).

The Permian-Triassic Mass Extinction (PTME), which occurred ~252.28 million years ago (Ma), is the most severe extinction event in earth's history and profoundly altered marine ecosystems (Song et al., 2013, Shen et al., 2011). It has been linked to increased ocean temperature, acidity and anoxia and as such, it acts as a good comparison for today's biotic declines.

1.5. Permian-Triassic Mass Extinction

1.5.1. Background Information

The eruption of the Siberian Traps Large Igneous Province is hypothesised to be the underlying cause of the end Permian mass extinction (see Figure 1.17). Such an eruption is proposed to have caused large scale atmospheric changes via the release of volatiles during the degassing of sediments and lava leading to environmental perturbations and marine and terrestrial mass extinction (Wignall, 2001). A single, short-lived (1-2 My) eruption may have caused the late Permian mass extinction, however, U-Pb and Ar-Ar dating for the Siberian Traps are currently only able to conclude that magmatism occurred during or soon after mass extinction (Burgess et al., 2014).

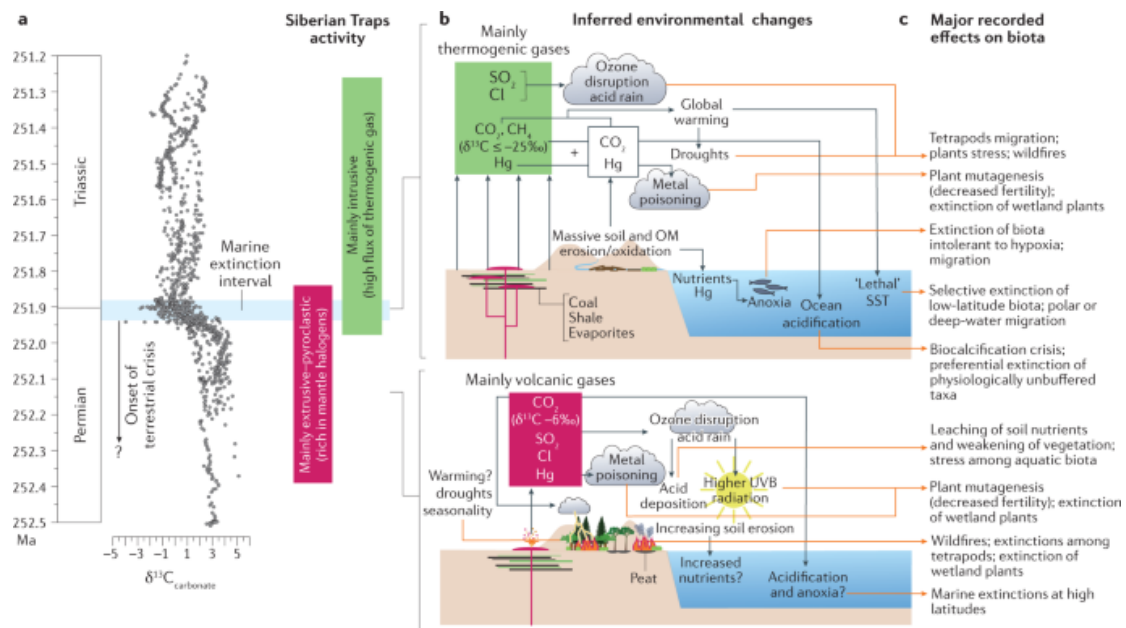


Figure 1.19: A) Changes in marine carbonate over the Permian Triassic period with the mass extinction event period shaded in blue. B) Diagrams illustrating the main environmental impacts of thermogenic (top) and volcanic (bottom) gasses during this time. C) The impact of environmental change illustrated in B on biota (Dal Corso et al., 2022).

Although the extinction itself was relatively short-lived (≈ 60 kyr) (Burgess et al., 2014), the broad impacts of the end Permian mass extinction could be seen for 5-10 Myr (Chen and Benton, 2012). Complex ecosystems were not readily identified in the fossil record until the mid-Triassic (Romano et al., 2012). This recovery period is longer and more drawn out than in any other Phanerozoic extinction. Such a short extinction period and drawn out recovery suggest that the mechanisms underlying the extinction event were rapid and severe, whereas the recovery period involved a complex combination of recovery and extinction events (Burgess et al., 2014). It has been hypothesised that this is because environmental conditions at the time may have crossed a “tipping point”, which is very difficult for ecosystems to recover from (Burgess et al., 2014).

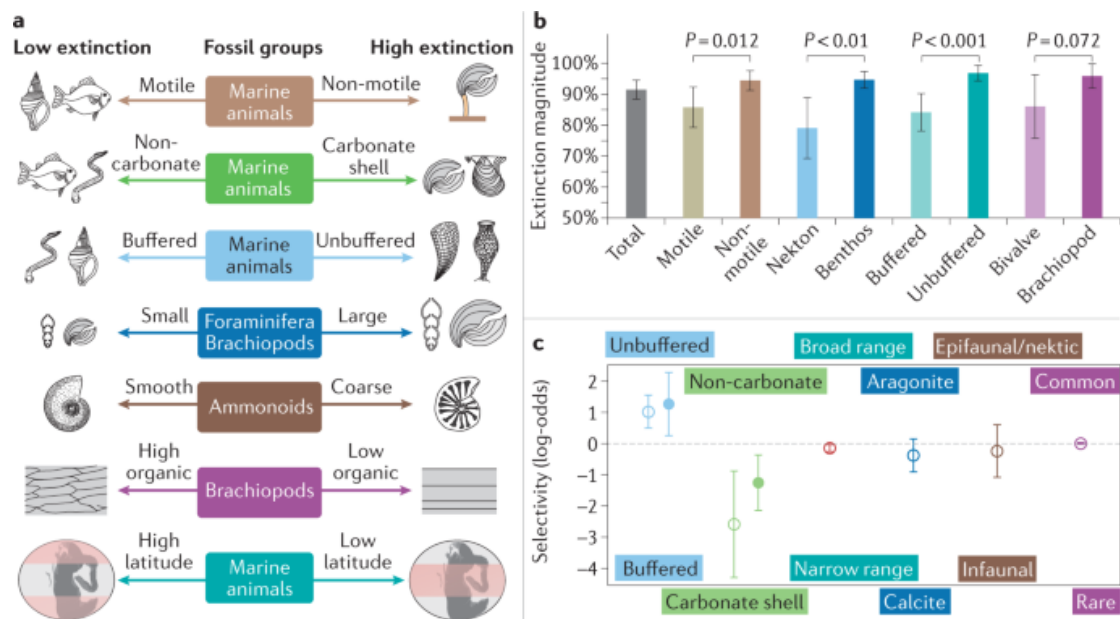


Figure 1.20: A) Vulnerability to extinction for different groups of marine organisms based on susceptibility to climate change. B) Extinction magnitude for different groups of marine organisms during the Permian Triassic mass extinction event with non-motile, benthic, unbuffered taxa as well as brachiopods suffering the highest extinction rates. C) Selectivity of groups of marine organisms to a range of conditions. From Dal Corso et al. (2022).

Ocean anoxia, acidification and high temperatures continued into the Early Triassic, and this was followed by a minor extinction event at the Smithian-Spathian boundary, hindering recovery (Sun et al., 2012, Bond and Wignall, 2010, Grasby et al., 2016). The slow recovery following the EPME is illustrated by lack of reef-building species found in the Early Triassic, a gap in coal formation and evidence for lack of nutrient upwelling (Grasby et al., 2016, Retallack et al., 1996, Flügel, 2002). The marine environment is particularly susceptible to increased $p\text{CO}_2$ (see Figure 1.18) and more than 90% of marine species became extinct at the end of the Permian (Erwin, 1994). Although a recent analysis by Stanley (2016) demonstrates that the figure for overall extinction during this event is 81% due to levels of background extinction and overlapping data from the earlier Capitanian extinction.

Global ocean anoxia, high ocean temperatures and increased $p\text{CO}_2$ (leading to ocean acidification) are thought to be some of the ‘kill mechanisms’ that contributed to this mass extinction event (Burgess et al., 2014). However, the geological record is scattered with examples of these conditions, but it is rare that they lead to mass extinctions (Burgess et al., 2014, Bond and Grasby, 2017). One reason for this could be varying availabilities of carbon sinks (such as the ocean) in different time periods, but more detailed research into the causes and timescales of mass extinction events is required in order to understand the complete mechanisms that drive them.

1.5.2. Environmental Conditions During the PTME – Based on Fossil Records

The End Permian Mass Extinction represents the most severe loss in biodiversity in the past 542 My. Research by Song et al. (2013) and Shen et al. (2016) suggests that the PTME occurred in two pulses with a ca. 200 Ky recovery period in between. The Latest Permian Extinction (LPE) is associated with high extinction rates in corals, calcareous algae, sponges, radiolarians, fusulinids and echinoderms (Song et al., 2013, Song et al., 2014). The taxa identified as having high extinction rates appear to be calcifying organisms, which are known to be particularly susceptible to changes in ocean chemistry due to the reduced availability of CO_3^{2-} ions (Gattuso and Buddemeier, 2000). The fact that these groups have low upper thermal limits also implies an increase in ocean surface water temperatures (see Figure 1.20) (Song et al., 2013).

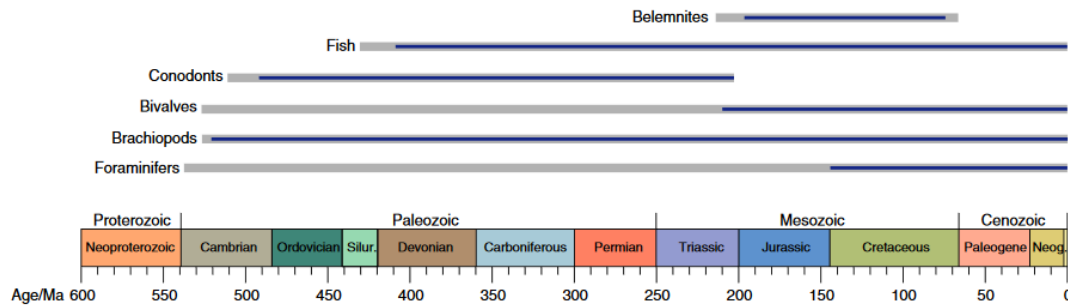


Figure 1.21: Time series of fossil groups used to reconstruct paleotemperatures. Gray lines show the temporal range of group (bivalves, brachiopods, foraminifers, and fish are extant); blue lines show stratigraphic range where each group has paleothermometry applications. Note jawless fish are not included as they are not useful for oxygen isotope paleothermometry. Taken from Bond and Sun (2021).

In the interim between the two extinction pulses thermally tolerant benthic biota diversified. The second pulse of extinction (the Earliest Triassic Extinction or ETE) coincides with the disappearance of species intolerant to a combination of high temperatures and low oxygen availability suggesting increasing anoxic conditions during this period (Song et al., 2014). In addition, nektonic dominated communities replaced benthos dominated communities suggesting an advantage to being motile and able to inhabit pelagic zones (Song et al., 2013). There is also sedimentological evidence for anoxic conditions in this time-period such as authigenic uranium enrichment, pyrite morphology, iron speciation and pyrite sulphur isotope data (Wignall and Newton, 2003, Shen et al., 2016). This combination of lethally high temperatures in shallow waters and anoxic deep waters is hypothesised to be the most deadly combination for marine biodiversity during the late Permian and early Triassic (Song et al., 2014). The existence of a ‘refuge zone’ in between lethally hot surface waters and anoxic deep waters can explain the patterns of species survival and extinction during and after the PTME (Song et al., 2014). Others have argued that

hypoxia best explains the paleo-physiology of surviving and extinct taxa through the PTME (Knoll et al., 2007).

Data from Wang et al. (2014) imply a single pulse of rapid extinction beginning just before the Permian Triassic boundary (PTB). The two-phase extinction hypothesis by Song et al. (2012) may have been flawed due to fossil preservation being influenced by lithofacies (Wang *et al.* 2014). Further, a thorough study on Permian diversity trends by Clapham et al. (2009) indicates that biodiversity gradually decreased from the Wordian (ca. 265.1 Mya) to the end Permian with little evidence for peaks in extinction rates.

Predictions of oceanic conditions during the PTME based on the physiology of species are confounded by outliers and irregularities. For example, in more acidic oceans, calcifying species (such as corals, sponges and bryozoans) should suffer great losses and this can be seen in the geological record during the EPME. However, this does not account for the losses suffered by more tolerant cephalopods and ammonoids (Song et al., 2014). In addition, those taxa that produce siliceous skeletons (such as radiolarians) would be expected to have a higher tolerance to more acidic conditions and ought to escape the PTME with relatively few losses. Interestingly, the chert gap (chert is a rock formed from silica microfossils) indicates a sudden reduction in silica producing organisms from the earliest to the mid-Triassic, pointing toward large scale extinctions of such taxa (Beauchamp and Baud, 2002). Using such predictive principles, it would be expected that burrowing infauna that are regularly exposed to hypercapnia would be more resilient to increasing CO₂ associated with climate change events (Knoll et al., 2007). Clapham and Payne (2011) found the opposite pattern with infaunal bivalves being more susceptible to extinction than their epifaunal counterparts. In

addition, evidence for burrowing activity largely disappeared during this extinction event suggesting alternative drivers of extinction.

Song et al. (2013) define ‘physiologically un-buffered’ taxa (with reference to high temperature and anoxic waters) as those with a low metabolic rate, low levels of internal circulation and high investment in CaCO_3 skeletons. This includes; brachiopods, corals, calcareous sponges, radiolarians, small foraminifera and represents the majority of Palaeozoic benthic taxa. Buffered species include bivalves, gastropods, ammonoids and trilobites (Song et al., 2013). It is possible that this is an oversimplification and that less obvious mechanisms might be at play. For example, although ammonites are considered ‘buffered’ taxa, they may be more vulnerable to high temperature, low pH and anoxia during the larval stage, potentially causing large-scale population declines.

1.5.3. Environmental Conditions in the PTME – Based on Isotope Analysis

Thanks to constantly evolving isotopic analysis techniques, we are learning more and more about the environmental conditions during mass extinction events. Not only this, but higher resolution climate data is becoming available offering us a window into climate variability over shorter timescales.

Analysis of Boron isotope data from two transects in a marine open water carbonate succession suggests that during the late PTME, ocean pH reduced rapidly (by 0.7 pH in ca. 10,000 years) (Clarkson et al., 2015). It should be noted that boron isotope records are extremely susceptible to the evolution of pore water through diagenesis and variations in boron-rich clay content (Bond and Grasby, 2017).

There is also evidence that the oceans became highly anoxic during the end Permian, although timing and scales of anoxia are under debate (Song et al., 2012,

Baresel et al., 2017). In shell carbonate, the ^{18}O to ^{16}O ratios correlate with the ratios present in the water and the calcification temperature (Spero et al., 1997). Temperatures of ocean surface waters act as a major contributor to mass extinctions and during the Latest Permian Mass Extinction (Song et al., 2014). A decrease in oxygen isotope ratios of 2‰ in the latest Permian is hypothesised to translate to an increase of 8°C in low-latitude surface waters (see Figure 1.20) (Joachimski et al., 2012). Sun et al. (2012) also analysed oxygen isotope ratios ($\delta^{18}\text{O}$) from conodonts in Nanpanjiang Basin, South China and calculated a late Smithian Thermal Maximum (~250.7Mya) of 38°C, with predicted sea surface temperatures exceeding 40°C.

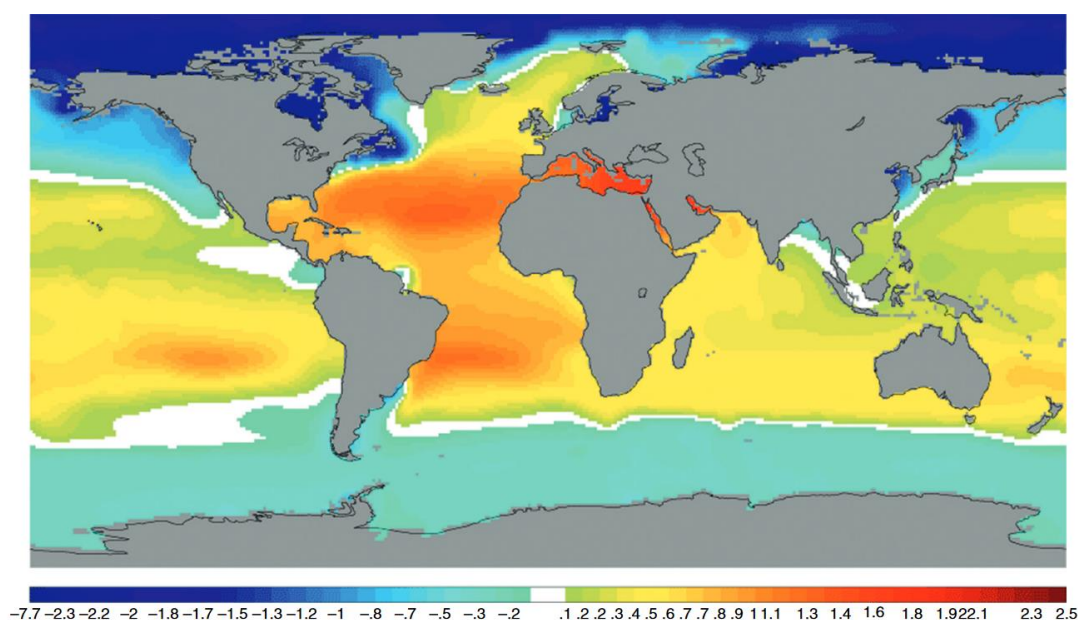


Figure 1.22: Global ocean distribution of oxygen isotope composition showing large latitudinal variation in seawater $\delta^{18}\text{O}$. $\delta^{18}\text{O}$ of seawater reflects both regional evaporation and precipitation as well as the global change in continental ice volume. In addition $\delta^{18}\text{O}$ can be used to assess paleothermometry due to differences in the energy required to break bonds in the heavier versus lighter isotopes. This leads to predictable isotope fractionation which is recorded in the shell material when it is precipitated from seawater in equilibrium and is a function of temperature. Taken from Bond and Sun (2021), originally from Schmidt (1999).

Euxinic conditions have been identified using highly-reactive iron to total iron ratios as well as pyrite-iron to highly-reactive iron in the Xiakou section, South China (Shen et al., 2016). Nutrient-limited surface waters and reduced primary productivity (based on Nitrogen isotope analysis and paleoproductivity proxies) in the Early Triassic in northwest Pangea are indicative of reduced oceanic upwelling (Grasby et al., 2016). Nutrient-rich upwelling appears to return to northwest Pangea in the Middle Triassic and coincides with increased primary productivity and reduced sea surface temperature (Grasby et al., 2016, Sun et al., 2012).

A biogeochemical proxy for increased UV-B radiation has been proposed by Fraser et al. (2014): Sporopollenin, a major part of pollen walls, alters in chemical composition in response to UV light and this offers a tool for assessment of past UV flux using preserved pollen spores (Fraser et al., 2014). This method has proved successful in a modern species grown across a range of latitudes and hence receiving a range of UV levels (Jardine et al., 2016). Although this method is still under debate, it has been proposed that, during the PTME, ozone-depleting aerosols lead to increased levels of UV-B (Beerling et al., 2007, Seddon et al., 2019). An experiment by Benca et al. (2018b) recreated a common pollen mutation found in the bisaccate gymnosperm pollen in the Permian by exposing the dwarf pine (*Pinus mugo*) to increased levels of UV-B radiation.

Extinction events are marked by widespread reductions in macroscopic biodiversity and act as drivers of major and large scale evolutionary change (Shen et al., 2011, Song et al., 2014, Song et al., 2013). Mass extinction events include the five most severe extinction events found in the geological record plus the present day extinction. The Permian-Triassic Mass Extinction (PTME), which occurred ~252.28Ma,

is the most severe extinction event in earth's history and profoundly altered marine ecosystems (Shen et al., 2011; Song et al., 2013). It has been linked to increased ocean temperature, acidity and anoxia, as such it acts as a good comparison for today's biotic declines. Many extinction events are accompanied by a negative carbon isotope ($\delta^{13}\text{C}$) excursion and during the EPME a negative shift of up to -8‰ has been reported in the literature (Bond and Grasby, 2017). Ratios of ^{13}C to ^{12}C alter with the ratio of dissolved inorganic carbon in the water and this is used as a proxy for changes in respiration and photosynthesis and therefore the amount primary productivity (Spero et al., 1997). A negative excursion of ^{13}C may also be caused by an increase in ^{13}C -depleted carbon into the atmosphere which eventually dissolves into oceans (van Breugel et al., 2007).

Based on the stabilisation of carbon isotopes, the termination of volcanism in the Siberian Traps and the recovery of scleractinian corals, full recovery after the EPME is believed to have occurred in the Mid Triassic (Petsios et al., 2017). Recent studies indicate that the rate of recovery varied locally depending on the taxonomic group, shelf environment and ecology (Petsios et al., 2017)

It is likely that there were spatial and temporal variations in climate change during the EPME with some areas suffering rapid change at certain times while others were less affected during the same period. Modern-day climate change is also occurring relatively rapidly, with some regions affected more significantly than others. The sea surface temperature increase of 8°C that has been derived from oxygen isotope ratios (Joachimski et al., 2012) would have exceeded the thermal limits of modern-day corals (Lough et al., 2018).

Rationale for Research

Today, loss of biodiversity appears to be driven by the same stressors that led to past mass extinctions, namely, climate change and associated factors (Bond and Grasby, 2017). What is unclear is why certain extinction events are so much more severe than others, despite similar causal mechanisms. It has been suggested that biological factors, such as tolerance of certain species to reduced pH, might elucidate this and experimental setups with modern day analogues could provide insight (Bond and Grasby, 2017). The use of primitive bioturbators such as polychaete worms as experimental analogues for climate change research is beneficial for several reasons. They are numerous and relatively easy to collect from the estuarine environments as well as being relatively hardy and easy to keep in a lab setting. As ecosystem engineers, they are important organisms in many marine habitats and population collapse in future climate change scenarios could drastically alter marine benthic habitats. Although not perfect analogues to species from the fossil record, they are relatively primitive and offer scope for experimental research to investigate the mechanisms behind the disappearance of bioturbation seen in previous mass extinctions while at the same time offering insight into their susceptibility to future climate change.

This project aims to investigate the more subtle impacts of climate change on a modern day hardy, benthic species, *Hediste diversicolor*. Specifically, the impact of temperature and pH on the species ability to forage and avoid predators. This will help to elucidate some of the more insidious impacts of climate change and offer insight into population level effects climate change will have on *H. diversicolor* as well as illustrate some of the driving forces behind the loss of biodiversity seen during the Permian Triassic mass extinction. Second, this project aims to investigate the impact of

climate change on burrowing. By experimentally examining the impact of pH and temperature on in-burrow oxygen dynamics I hope to shed some light on the impacts of climate change on biogeochemical cycling, macrofauna and in-burrow behaviour of these important bioturbators.

Chapter 2 aims to investigate the impact of changing pH and temperature on the ability of *H. diversicolor* to sense chemical cue molecules. Previous studies have identified natural substances, such as flounder mucous, as a predator cue, eliciting avoidance behaviour (Schaum et al., 2013). In this work we hypothesise that; 1) simple biological molecules, such as amino acids, act as chemical cues for the omnivorous benthic invertebrate *H. diversicolor*, eliciting feeding or avoidance behaviour and 2) altering the pH and temperature of surrounding water would cause chemical and/ or biological alterations such that behavioural responses change. By testing future-relevant pH and temperature conditions and comparing to average current conditions, any alteration in behaviour would indicate in a change of ability to sense cues or a change in risk/ reward dynamics.

Chapter 3 utilises cutting edge optode sensing equipment to image and investigate oxygen levels in and around *H. diversicolor* burrows. *H. diversicolor* is considered an ecosystem engineer with its bioturbation and burrowing activities disproportionately contributing to decomposition and biogeochemical cycling (Solan et al., 2008). *H. diversicolor* burrow into otherwise anoxic sediment and through their sediment reworking and irrigation activities they affect sediment oxygen levels and microbiota communities (Pischedda et al., 2012, Pischedda et al., 2008). In this chapter we hypothesise that water pH and temperature will have an effect on 1) in-burrow oxygen levels through changes in ventilation frequency and/ or oxygen consumption by *H. diversicolor* and 2) penetration depth of oxygen from the burrow wall into the

sediment through changes in in-burrow oxygen levels and/ or thickness of mucous wall lining.

Chapter 4 investigates the impact of pH and temperature on mucous production and mucous composition by *H. diversicolor*. Mucus can act as a protective coating, reducing the impacts of stressful environmental conditions. The antioxidant properties of mucous are related to carbohydrate content of its mucoproteins which act as radical species (Stabili, 2019). Previous research has linked increased mucus production to several stressors, including elevated levels of pollution (e.g. Bastidas and Garcia, 2004) and increased water temperature (Neudecker, 1981, Tal et al., 2021). We hypothesise that reduced pH and increased temperature will increase the quantity of mucous produced by *H. diversicolor* as a response to more stressful conditions. Also, that higher carbohydrate concentrations will occur in the mucous produced at lower pH and at higher temperatures, again as a defence mechanism against stressful conditions.

Combining the results of these three chapters provides novel insight to the ecological functioning of *H. diversicolor* and how future-relevant pH and temperature conditions may alter this functioning.

2.0. Chapter 2

The Future of Chemical Cues: Responses of the polychaete *Hediste diversicolor* to artificial food cues in a warm, acidic ocean.

2.1. The Future of Chemical Cues: Responses of the polychaete *Hediste diversicolor* to artificial food cues in an warm, acidic ocean.

2.1.1. Abstract

Anthropogenic climate change has altered marine, terrestrial and freshwater habitats, exposing ecosystems to conditions unprecedented over millennia. Ocean surface pH is expected to decrease by 0.33 units and ocean temperatures are projected to increase by an average of 3.7°C by the end of the century. Further, global ocean biomass is projected to decrease by up to 15.5% ($\pm 8.5\%$) by 2100. The impacts of climate change on marine organisms are species specific and vary depending on the response variable measured. Very little attention has been given to the impact of future relevant pH and temperature change on the sensory abilities of marine species, a factor that has the potential to impact a species ability to find food, avoid predators, locate habitat and identify potential mates.

The animals used in these experiments were not collected from the wild but were second and third generation worms housed in static pH and temperature conditions so no pre-acclimation was required. By using F2 and F3 generation worms the impacts of acclimation and acclimatisation were removed and inter-generational, long term impacts of pH could be assessed.

Investigations into behavioural responses to chemical cues have focused on the use of complex organic mixtures such as ‘predator conditioned water’. In such experiments it is impossible to know what the target organism is responding to or the concentrations that are required to elicit a response. There are a few studies that have utilised artificial chemical cues in order to investigate the dose-response relationship and decision making in benthic deposit feeders. By utilising known chemicals,

concentrations can be accurately controlled and the chemical changes of the cue molecule driven by water pH and temperature are identifiable.

Here behavioural response (measured as percentage time spent out of the burrow) of the harbour ragworm (*Hediste diversicolor*) to multiple synthetic chemical cues under present and future ocean pH and temperature scenarios is investigated. Dimethyl sulphide (DMS), taurine and glutathione were found to act as food cues in both present and future climate scenarios. The pH and temperature conditions affected the concentrations required to elicit a response as well as impacting the strength of the response to the cue. Such a response could be due to physiological changes in the ragworm or chemical alterations to the cue molecules in the different pH/ temperature conditions (pH8.1 and pH7.3 both at 18°C and 22°C). The pH was found to affect the response of ragworms to chemical cues that are known to alter their protonation state. This occurred across the pH conditions tested (pH7.3 and pH8.1), suggesting that the conformational change induced in these chemical cue molecules is contributing to altered response levels, potentially by reducing the binding potential between the cue molecule and the associated receptor protein.

ATP was found to act as a food cue only in pH8.1 at elevated temperatures (22°C). ATP readily hydrolyses to ADP in above pH7.4 and this combined with elevated temperatures may have been creating high enough proportions of ADP to act as a food cue and cause the behavioural response observed in this condition.

Urea caused a significant reduction in response compared to the control only at pH8.1, 18°C, suggesting that it is acting as a predator cue. Chondroitin sulphate caused a non-significant reduction in response at 18°C, but a significant positive response at

22°C. The structure of chondroitin sulphate is relatively stable across a broad pH and temperature range, suggesting that the variation in activity is physiologically driven.

The results presented here suggest that the ability of *H. diversicolor* to respond appropriately to food and predator cues is impacted by pH and temperature. Higher concentrations of cue are required at reduced pH for DMS, taurine and GSH at low pH, however, this may be mitigated in mixtures of cues. Higher temperatures are generally associated with higher levels of activity, which may be linked to increased metabolic stress causing higher foraging drive. Response to predator cues is altered at different temperatures and pH. All of which has the potential to effect survival in future ocean conditions.

2.1.2. Introduction

Chemical communication is the oldest form of communication, with evidence suggesting it dates back to primordial protists (Kittredge et al., 1974). Today chemical cues are common in the marine environment and are utilised by a myriad of organisms to signal a range of processes. From sensing predators (e.g. Schaum et al., 2013) to initiating reproduction (e.g. Snell et al., 2006) chemical signalling is important for the survival of many species. Schaum et al. (2013) found that the polychaete *Hediste diversicolor* significantly reduced their distance, frequency and duration of burrow emergences in the presence of flounder (*Platichthys flesus*) mucus, suggesting chemosensory mechanisms leading to an anti-predator response. Polychaetes also respond to chemical cues created by food, such as an injured amphipod, by increasing their feeding response (Ferner and Jumars, 1999). Low molecular weight compounds (such as amino acids), including glycine (evidence from Kolkovski et al., 1997, Velez et al., 2007) and proline (Ferner and Jumars, 1999, Velez et al., 2007) have been shown to increase feeding behaviour, although Ferner and Jumars (1999) found that glycine

significantly reduced feeding in two polychaete species. Numerous amino acids, including phenylalanine, glutathione and methionine have also been found to elicit feeding behaviour in polychaetes (Mangum and Cox, 1971, Ferner and Jumars, 1999). Ferner and Jumars (1999) found that complex organic mixtures generate the strongest feeding responses in spionid polychaetes and several amino acids had a depressant effect or no effect at all. This variability may be linked to individual variation, species tested or experimental design. Responses may vary in species with alternative feeding mechanisms.

Much work has been dedicated to investigating the responses of aquatic organisms to general, non-specific cues such as predator conditioned water or fish mucus (Dudman and de Wit, 2021, Schaum et al., 2013, Dijk et al., 2016, Abreu et al., 2016). While the results of these experiments are interesting, they are inherently limited because the chemical cue is not known. This means that cue concentration cannot be controlled and restricts the conclusions that can be drawn from behavioural responses. It also prevents any conclusions on the chemistry involved in cue detection such as whether alterations in chemical conditions (such as pH) interfere with the signalling molecules.

The experiments conducted in this chapter investigated whether a range of chemicals could act as a synthetic food or predator warning cue, as has been noted in other groups (e.g. fish (Mathuru et al., 2012) and crustaceans (Rittschof and Cohen, 2004)). It was expected that predator cues would lead to a reduction in out of burrow activity and food cues would encourage out-of-burrow and feeding behaviour.

H. diversicolor is omnivorous and has numerous feeding strategies including hunting species smaller than itself, scavenging, deposit feeding from the sediment

surface and filter feeding (Barnes, 1994). It is able to actively hunt for food, leaving its burrow entirely, or it can collect detritus using mucus 'nets' and drawing sediment into the net by creating a current with undulating body movements (Barnes, 1994). *H. diversicolor* use several feeding mechanisms including deposit feeding, suspension feeding and active hunting (Fauchald and Jumars, 1979, Harley, 1950). Their ability to actively hunt and consume other organisms, as well as their broad, generalist diet, makes them an ideal study species for testing responses to chemical food cues. They are a common and widespread species and are important ecosystem engineers providing large scale bioturbation in intertidal sediments (Braeckman et al., 2014). Bioturbators have important effects on their habitat, including; redistribution of organic matter; stimulation of biogeochemical cycles leading to increased nutrient flux and oxygenation of sediments (Braeckman et al., 2014). Because of their large population size *H. diversicolor*, and other common bioturbating species likely have a significant impact on European estuarine habitats (Braeckman et al., 2014).

Ocean acidification and warming

In 2011, the concentrations of greenhouse gases (CO₂, CH₄ and N₂O) exceeded records from ice cores spanning the past 800,000 years. Rising levels of atmospheric CO₂ since pre-industrial times has had a corresponding impact on ocean pCO₂ causing a decrease in pH of 0.1 and a further decrease of up to 0.33 by 2100 is predicted (IPCC, 2013b, Pörtner et al., 2022, Hoegh-Guldberg and Bruno, 2010). Ocean pH typically ranges from 7.7 to 8.2 with the highest pH occurring in the summer at high latitude shallow waters and the lowest pH in very deep waters (Brewer Peter et al., 1995). Based on IPCC (2013b) predictions this will decrease to a range of 7.28 to 7.7 by the end of

the 21st century. By 2300 it is estimated that ocean pH will be as low as 7.38 (Hartin et al., 2016).

The impact ocean acidification will have on chemical ecology is a rapidly expanding subject. Some calcifying organisms will suffer due to the increased solubility of calcium carbonate minerals at lower pH creating a CaCO₃ deficit (Widdicombe and Spicer, 2008), with others able to acclimate to long term CO₂ perturbations (e.g. Form and Riebesell, 2012). The impact of reduced pH on chemical signalling has been studied much less, in part because of our lack of knowledge of the molecules responsible for chemical signalling. Roggatz et al. (2016) found that reduced pH led to protonation of peptides which are responsible for chemical signalling in the shore crab *Carcinus maenas*. This altered the molecular charge and impacted receptor binding, reducing normal behavioural responses to these chemical cues. In future oceans protonated versions of signalling peptides will become more commonplace (Roggatz et al., 2016).

The ocean has absorbed more than 90% of additional energy added to the climate system between 1971 and 2010 and surface temperatures increased by 0.11°C per decade over this period (Bindoff et al., 2019). Global mean surface temperatures are predicted to continue to increase to the end of the 21st century (2081–2100) relative to 1986–2005, with RCP8.5 indicating an increase in the range of 2.6°C to 4.8°C. Bhuiyan (2021) found that the impact of increased temperature exacerbated the negative behavioural effects of reduced pH, with slower burrowing in *H. diversicolor*. However, feeding rate was affected by pH but not temperature in this species. Godbold and Solan (2013) found that the polychaete *Alitta virens* created deeper burrows in summer months, but when exposed to future relevant temperature (+4°C above natural mean or 14.36 (± 0.12°C)) conditions the overall burrow depth was shallower.

Although they are considered to be pollution tolerant (Gillet et al., 2008), the impact of reduced pH and increased temperature due to ocean acidification may have more subtle impacts on this species. Interference with chemical signalling such as predator detection and larval settlement cues could reduce survival rate dramatically.

The intention of this study was to investigate the response of the harbour ragworm (*H. diversicolor*) to varying concentrations of artificial cues: dimethyl sulphide (DMS), adenosine triphosphate (ATP), glutathione (GSH), taurine, chondroitin sulphate, and urea. These chemicals have been found to induce avoidance or feeding responses in other marine organisms (Rittschof and Cohen, 2004, Mathuru et al., 2012, Mangum and Cox, 1971, Ferner and Jumars, 1999). Additionally, the impact of reduced pH and increased temperature on these behavioural responses was examined to draw conclusions on the impact these factors are having on the response to signalling molecules.

2.1.3. Method

Worm collection and housing

Approximately 800 worms were collected from Hessle Foreshore, East Yorkshire (53°42'52.94"N, 00°27'11.2"W). Worms (*H. diversicolor*) were collected at low tide by digging up with a spade. Mature (green coloured) worms were not collected. The Humber Estuary is one of the largest estuaries in the UK, draining more than 20% of total English land surface area (Tappin et al., 2011). Major tributaries flowing into the estuary include the Rivers Hull, Trent, Ouse, Wharfe, Aire, and Don. The Humber Estuary European Marine Site is comprised of the marine components of the Humber Estuary Special Area for Conservation, Special Protected Area and Ramsar site (Tappin et al., 2011). The entire Humber Estuary (37,000Ha) were designated as a Site of Special Scientific Interest and the estuary supports nationally important numbers of

wintering waterfowl and waders. Intertidal mudflats and sandflats are one of several interest features of the site (Winn et al., 2003, Lonsdale et al., 2022). The collection site at Hessle Foreshore is easily accessible mudflat habitat, locally known for presence of high densities of *H. diversicolor*. Although the Humber Estuary is home to a range of polluting industries and has one of the UK's biggest constellations of oil refining industries (Eke et al., 2021) the majority of dredging occurs down estuary of the Hessle Foreshore collection site (Lonsdale, 2013). Data from the 2008 to 2010 Environment Agency sampling exercise indicated that metal, organotin, PCB and PAH concentrations within Humber Estuary sediments are typically below Cefas action level 2, and the Hessle Foreshore collection site showed no pollutants above Cefas action level 1 (Lonsdale, 2013). On site measurements of pore-water pH (using Hanna HI-991301 handheld probe) and water temperature were taken. Sediment samples were taken for contaminant analysis and particle size distribution analysis. Worms were separated from the sediment by gently filtering with saline water and placed in one of two 'culture tanks'. The conditions in the culture tanks mimicked the natural environment as closely as possible. The water temperature was kept at 18°C, water pH was based on the measurements taken at the collection site (pH 8.1). Daylight (12h light, 12h dark simulated with standard LED lighting) and moon light cycles (simulated with a 6W UV LED lamp) were simulated using artificial lighting systems. The tanks contained salinity appropriate rinsed sand and diluted natural seawater (18‰). Water pH was controlled using JBL ProFlora pH control units. CO₂ was bubbled through the water to reduce the pH in each tank to a pre-set level. Worms were left to acclimate for one week and fed three times per week on fish flakes. After this time the pH in one of the culture tanks was reduced gradually over the period of one week. After one week the tanks were set at pH 8.1 and 7.3. Worms remained in these conditions and

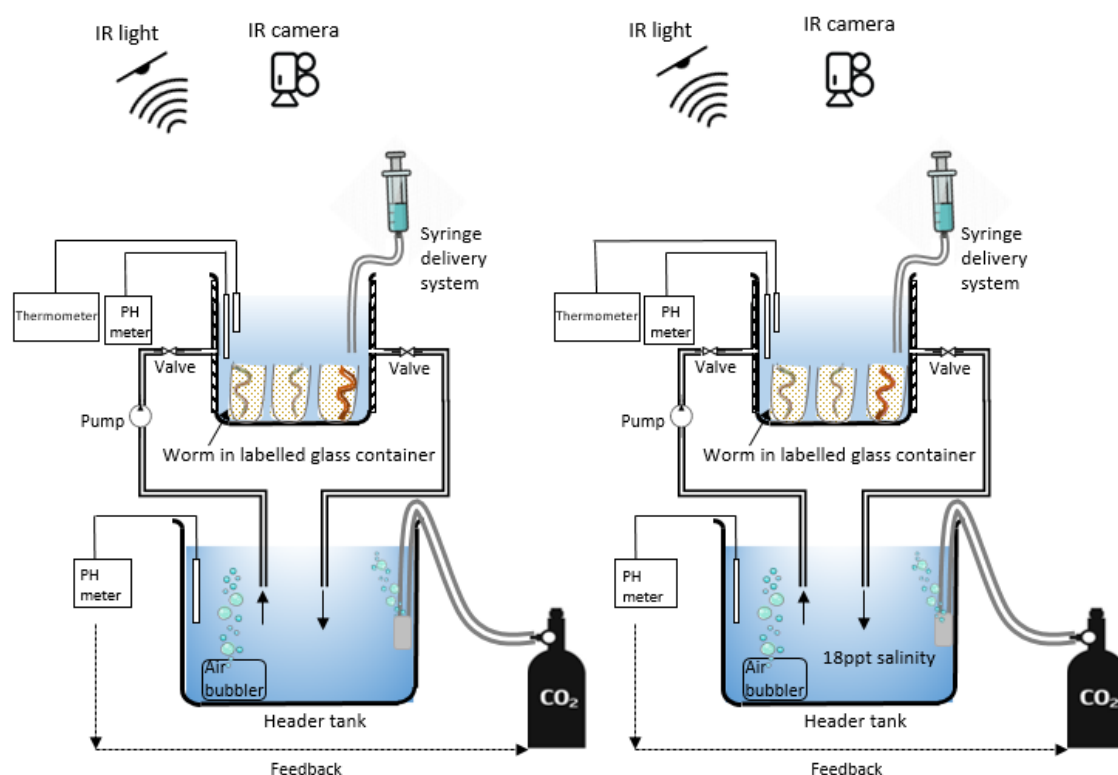
reproduced within the tanks. The animals used in these experiments were not collected from the wild but were second and third generation worms housed in static pH and temperature conditions so no pre-acclimation was required. By using F2 and F3 generation worms the impacts of acclimation and acclimatisation were removed and inter-generational, long term impacts of pH could be assessed. The temperature that worms were kept in (18°C) is representative of UK summer temperatures and the constant temperature prevented large scale maturation events. Temperature was controlled using an Airco air conditioning system which controlled room temperature. High temperature conditions (22°C) was controlled using a Hygger 300W aquarium heater. During maturation worms divert energy resources into gamete development prior to spawning and this has the potential to affect behaviour, growth and metabolism (Hardege, pers. comm, March 2021).

The pH of the water used was based on current average ocean pH (8.1) and predictions of ocean pH in 2100 based on IPCC RCP8.5 scenarios (pH 7.3) (IPCC, 2013b, Hartin et al., 2016). RCP8.5 is a high emission scenario and was chosen to test response to more extreme pH change. Additionally, estuarine waters undergo complexities such as fresh water and nutrient input, therefore the impacts of climate change are more difficult to predict. However, increased rates of algal blooms in estuarine habitats are predicted to increase hypoxic, acidic conditions and the more extreme climate scenarios were chosen to represent this (Bindoff et al., 2019). Similarly, temperature conditions used (18°C and 22 °C) were based on UK summer water temperatures (18°C) and IPCC predictions of an increase in average surface temperatures of 4.8 °C.

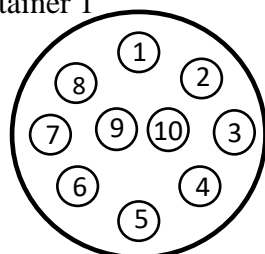
Protocol – Bioassays

Figure 2.1 shows the bioassay set up. Bioassays were set up with 20 worms tested in each. Water pH and temperature was controlled. Salinity and oxygen levels were kept constant via water cycling. At the entrance to each worm burrow and dose of chemical cue was added and the behaviour of the worms was monitored via CCTV recording. The assays were completed in the dark under infrared (IR) light because *H. diversicolor* are nocturnal and therefore are more active at night (Last, 2003). The pH in each header tank was maintained using a JBL ProFlora pH control units, with CO₂ bubbled through the water in order to reduce the pH. Worms were assayed in the same pH conditions that they were raised in i.e. worms from the pH7.3 culture tank were assayed in pH7.3. Experiments took place in a temperature controlled room set at 18 °C, with an aquarium heater used to produce the 22 °C condition. Twenty similar size, immature worms were selected from the culture tank (after 24 hours starvation), and added to the assay containers as shown in Figure 2.1 (ten in each side of the system). They were given one hour to acclimate and create a burrow with water cycling on in order to prevent the build-up of metabolites or reduction in pH. Wet weight of worms were taken by blotting individuals dry and weighing to ± 0.0001 using Mettler College scales. Glass containers were capped with mesh to prevent escape prior to the assays. The same twenty worms were used for all concentrations tested. Worms were replaced when a new pH/ temperature condition was tested.

A.



B. Container 1



Water salinity 18‰

Container 2

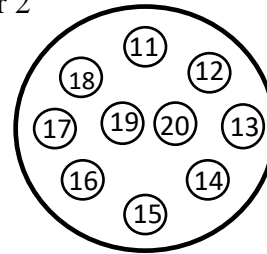


Figure 2. 1: A. Bioassay setup— Ten worms were added to each assay container. They were given one hour to create a burrow with water cycling on. Worms were pre-weighed prior to the assays. Each worm was in an individual glass container to allow individual monitoring and containers were capped with mesh to prevent escape. Each container had its own syringe to allow accurate cue delivery. Before adding the chemical cue, mesh was removed to allow a clear line of sight for recording. Assays were conducted 1 hour after ‘sunset’, when the lights were turned off. B. Numerical layout of the test tubes in the assay container to allow individual monitoring of worms.

Following the one hour burrowing a chemical food or predator cue (dissolved in 18% Artificial Seawater) at a set concentration (ranging from 1×10^{-9} to 1×10^{-2} M) was added to each glass container simultaneously using a syringe dosing system. 18% salinity Artificial Seawater was used as a control and was added using the same method. Chemical cues were added from the lowest concentration (1×10^{-9} M) to the highest concentration (1×10^{-2} M), with a tenfold increase in concentration between each addition. At each concentration, worm behaviour was monitored for thirty minutes using infrared cameras connected to a computer. Activity tracking software (Loligo Lolitrack Activity Tracker V1) was used to analyse the footage for worm activity, defined as any time that a worm emerges from their burrow. The water pH and temperature were monitored throughout the assay using fixed JBL probes.

Statistical analysis

After testing for normality with a Shapiro-Wilk's test and homogeneity of variance with a Levene's test, for each of the chemical cues, a robust factorial repeated measures ANOVA was computed in R using the WRS2 package (Mair and Wilcox, 2020). The WRS2 package provides an implementation of a robust heteroscedastic repeated measurement ANOVA based on the trimmed means. This investigated the overall affects of pH, temperature and cue concentration on the response variable (percentage active time). To test the impact of cue concentration on the response variable compared to the control (an equal volume of 18‰ artificial seawater), a Dunn's multiple comparison test with Bonferroni correction was used. Finally, to investigate the correlation of chemical dose-response at each of the separate pH/temperature conditions tested the open source software Dr Fit (Di Veroli et al., 2015) was used to fit multiphasic curves to the data. Once a curve was fitted, EC_{10} was calculated to allow comparison of the chemical cue concentration required to elicit 10% active time (when compared to the control).

2.1.4. Results

Sediment samples taken from the collection site at Hessle Foreshore were analysed for contaminants and particle size distribution. The sediment was found to be ‘very fine sandy very coarse silt’ and contaminant metals were found to be lower than the national average with the highest levels consisting of aluminium (50,410.12ppm), potassium (19696.13ppm), and iron (43,111.17ppm).

Response of ragworms to each chemical cue was tested for the same range of concentrations. Activity was measured as the percentage of time worms spent out of their burrow and this was considered a feeding response. All cues were tested at four environmental conditions with the exception of ATP due to loss of the bioassay video recordings for the pH7.3, 22°C condition.

DIMETHYL SULPHIDE (DMS)

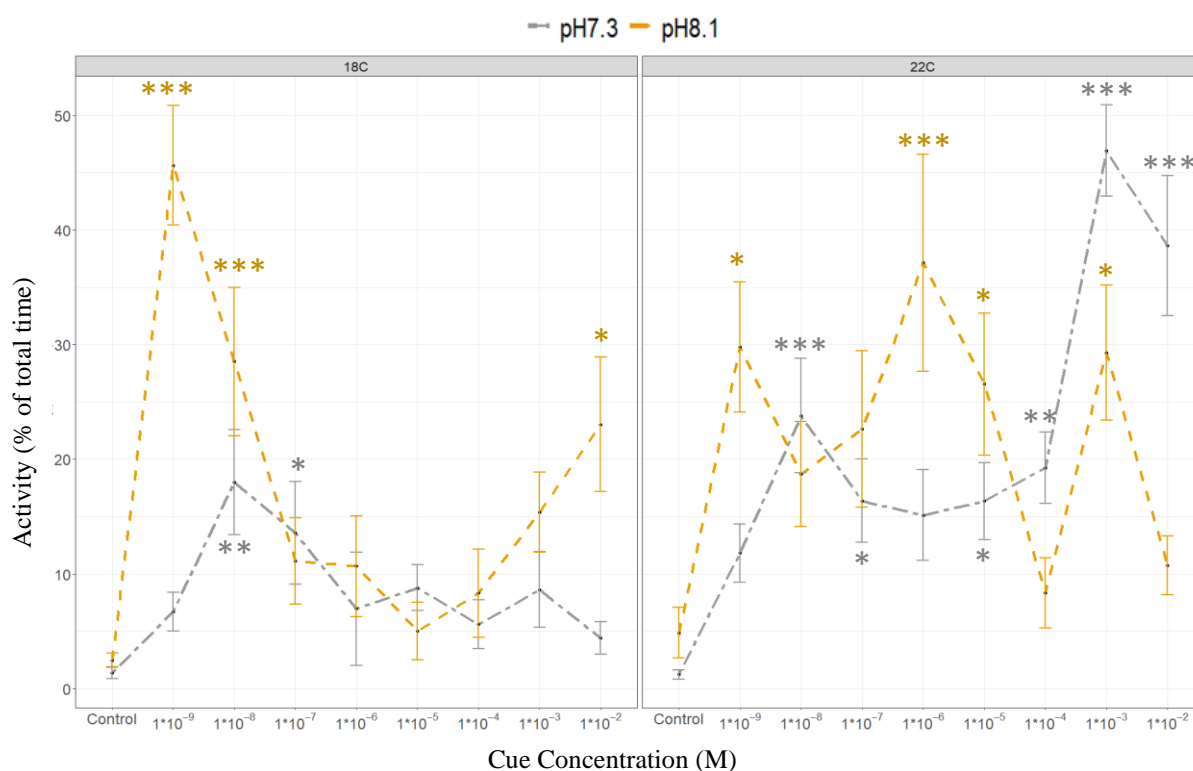


Figure 2. 2: Response of ragworms (*Hediste diversicolor*) to the chemical food cue dimethyl sulphide. Activity was measured as the percentage of time spent out of the burrow during a

30 minute recording, $n=20$ for each condition. Response was tested in four pH/ temperature conditions, namely pH 8.1, 18°C; pH8.1, 22°C; pH7.3, 18°C; pH7.3, 22°C. Cue concentrations ranging from $1 \times 10^{-2} \text{M}$ to $1 \times 10^{-9} \text{M}$ were tested at ten times dilution between concentrations. A control was tested with the addition of water alone. Points show the group mean and bars show standard error. Significance stars show those points that are significantly different to the control (Signif. codes: *** = $p < 0.001$, ** = $p < 0.01$, * = $p < 0.05$)

Figure 2.2 illustrates the dose-response chart of the percentage time worms spent out of their burrows (percentage active time) in a range of pH/ temperature conditions. *H. diversicolor* responded significantly to DMS in all pH/ temperature conditions tested compared to the control (see significance stars on Figure 2.2 and full statistics in table S2.2 to S2.5 in Supplementary Materials). A significant difference in activity compared to the control was found: At pH8.1, 18°C at concentrations of $1 \times 10^{-2} \text{M}$ ($p=0.01$), $1 \times 10^{-8} \text{M}$ ($p < 0.001$), $1 \times 10^{-9} \text{M}$ ($p < 0.001$); at pH8.1, 22°C at concentrations of $1 \times 10^{-3} \text{M}$ ($p=0.02$), $1 \times 10^{-5} \text{M}$ ($p=0.04$), $1 \times 10^{-6} \text{M}$ ($p < 0.001$), $1 \times 10^{-9} \text{M}$ ($p=0.01$); at pH7.3, 18°C at concentrations of $1 \times 10^{-7} \text{M}$ ($p=0.04$), $1 \times 10^{-8} \text{M}$ ($p=0.02$). The concentrations that the worms responded significantly to differed depending on water pH/temperature. Across all four conditions there is an apparent increase in activity levels at very low concentrations of DMS (in the range of $1 \times 10^{-9} \text{M}$ to $1 \times 10^{-6} \text{M}$) when compared to the control. At 18°C the activity levels are reduced at pH7.3 when compared to pH 8.1 at the lowest concentration ($1 \times 10^{-9} \text{M}$). Above this concentration activity levels are similar between the two different pH conditions, with a second divergence at the highest concentration ($1 \times 10^{-2} \text{M}$) where once again, activity levels are much higher at pH 8.1 compared to pH7.3.

Dose -response curves were fitted to each of the response lines in Figure 2.2 (see supplementary materials) and the concentration of cue that elicited 10% activity compared to the control (EC_{10}) was computed for each of these curves. Table 2.1 below shows the results

of this analysis. The EC₁₀ cue concentration was lowest in pH8.1, 18°C and highest in pH7.3, 18°C.

Table 2. 1: The concentration of cue that elicited 10% activity compared to the control level (EC₁₀) was calculated to allow comparison of cue response between the pH/ temperature conditions tested.

Condition	EC₁₀ (M)
pH8.1, 18°C	1.26x10 ⁻¹⁰
pH8.1, 22°C	1.87x10 ⁻¹⁰
pH7.3, 18°C	9.46x10 ⁻⁹
pH7.3, 22°C	1.42x10 ⁻⁹

A robust factorial repeated measures two-way ANOVA indicated that temperature had a statistically significant impact on the response variable, activity ($F=29.49$, $p<0.001$) whereas pH did not have a statistically significant effect ($F=0.08$, $p=0.78$). A statistically significant interaction effect of pH and temperature on activity was found ($F=7.36$, $p=0.007$).

ADENOSINE TRIPHOSPHATE (ATP)

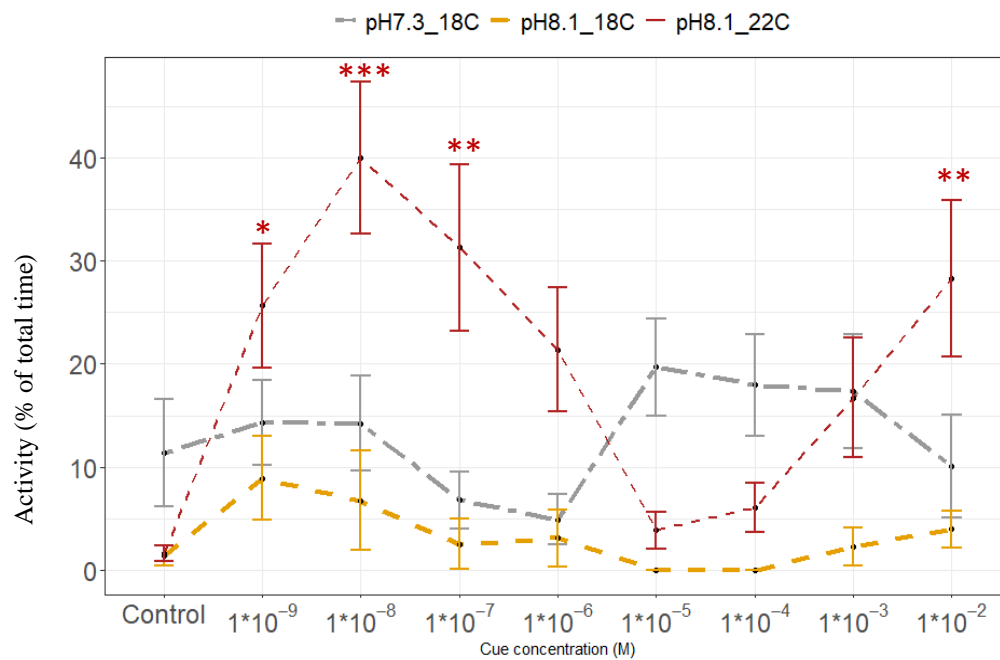


Figure 2. 3: Response of ragworms (*Hediste diversicolor*) to the chemical food cue ATP.

Activity was measured as the percentage of time spent out of the burrow during a 30 minute recording, $n=20$ for each condition. Response was tested in three pH/ temperature conditions, namely pH 8.1, 18°C; pH8.1, 22°C; pH7.3, 18°C. Cue concentrations ranging from $1 \times 10^{-2} \text{M}$ to $1 \times 10^{-9} \text{M}$ were tested at ten times dilution between concentrations. A control was tested with the addition of water alone. Points show the group mean and bars show standard error. Significance stars show those points that are significantly different to the control (Signif. codes: *** = $p < 0.001$, ** = $p < 0.01$, * = $p < 0.05$)

Figure 2.3 illustrates the dose-response chart of the percentage time worms spent out of their burrows (percentage active time) in a range of pH/ temperature conditions. *H. diversicolor* responded significantly to ATP only at pH8.1, 22°C compared to the control at four of the concentrations tested (see significance stars on Figure 2.3 and full statistics in table S2.6 to S2.8 in Supplementary Materials). A significant difference in activity compared to the control was found: At pH8.1, 22°C at concentrations of $1 \times 10^{-2} \text{M}$ ($p=0.005$), $1 \times 10^{-7} \text{M}$

($p=0.002$), $1 \times 10^8 \text{M}$ ($p < 0.001$) and $1 \times 10^{-9} \text{M}$ ($p=0.01$). The worms did not respond significantly to ATP at pH 8.1, 18°C or pH 7.3, 18°C compared to the control response level.

Dose -response curves were fitted to each of the response lines in Figure 2.3 (see supplementary materials) and EC_{10} was computed for each of these curves. Table 2 below shows the results of this analysis. The EC_{10} cue concentration could not be computed for pH 8.1, 18°C due to the poor correlation between concentration and activity. EC_{10} was lowest in pH 8.1, 22°C and highest in pH 7.3, 18°C .

Table 2. 2: The concentration of cue that elicited 10% activity compared to the control level (EC_{10}) was calculated to allow comparison of cue response between the pH/ temperature conditions tested.

Condition	EC_{10} (M)
pH 8.1, 18°C	/
pH 8.1, 22°C	1.27×10^{-10}
pH 7.3, 18°C	2.96×10^{-6}

A robust factorial repeated measures two-way ANOVA indicated that the pH/ temperature interaction had a statistically significant impact on the response variable, activity ($p=0.001$). The individual effect of pH was not significant ($p=0.35$) but temperature did have a significant effect on activity ($p=0.005$).

TAURINE

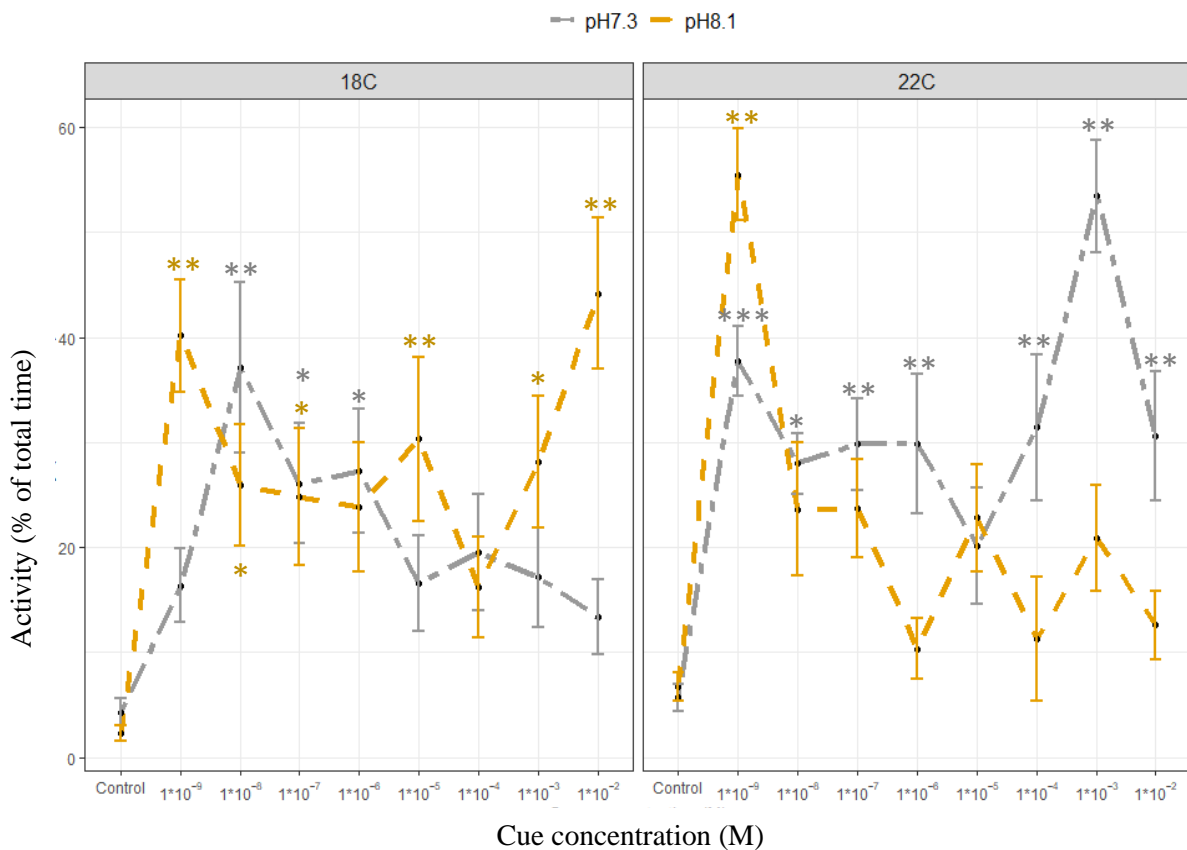


Figure 2. 4: Response of ragworms (*Hediste diversicolor*) to the chemical food cue taurine. Activity was measured as the percentage of time spent out of the burrow during a 30 minute recording, $n=20$ for each condition. Response was tested in three pH/ temperature conditions, namely pH 8.1, 18°C; pH8.1, 22°C; pH7.3, 18°C; pH7.3, 22°C. Cue concentrations ranging from 1×10^{-2} M to 1×10^{-9} M was tested at ten times dilution between concentrations. A control was tested with the addition of water alone. Points show the group mean and bars show standard error. Points show the group mean and bars show standard error. Significance stars show those points that are significantly different to the control (Significant. codes: *** = $p < 0.001$, ** = $p < 0.01$, * = $p < 0.05$)

Figure 2.4 illustrates the dose-response chart of the percentage time worms spent out of their burrows (percentage active time) in a range of pH/ temperature conditions. *H. diversicolor* responded significantly to taurine compared to the control in all four pH/

temperature conditions tested (see significance stars on Figure 2.4 and full statistics in table S2.10 to S2.13 in Supplementary Materials). A significant difference in activity compared to the control was found: At pH8.1, 18°C, at concentrations of $1 \times 10^{-2} \text{M}$ ($p < 0.001$), $1 \times 10^{-3} \text{M}$ ($p = 0.02$), $1 \times 10^{-5} \text{M}$ ($p = 0.006$), $1 \times 10^{-7} \text{M}$ ($p = 0.04$), $1 \times 10^{-8} \text{M}$ ($p = 0.03$), $1 \times 10^{-9} \text{M}$ ($p < 0.001$); at pH8.1, 22°C, at concentrations of $1 \times 10^{-9} \text{M}$ ($p < 0.001$); at pH7.3, 18°C, at concentrations of $1 \times 10^{-6} \text{M}$ ($p = 0.01$), $1 \times 10^{-7} \text{M}$ ($p = 0.02$), $1 \times 10^{-8} \text{M}$ ($p < 0.001$); at pH7.3, 22°C, at concentrations of $1 \times 10^{-2} \text{M}$ ($p = 0.004$), $1 \times 10^{-3} \text{M}$ ($p < 0.001$), 1×10^{-4} ($p = 0.001$), 1×10^{-6} ($p = 0.004$), $1 \times 10^{-7} \text{M}$ ($p = 0.003$), $1 \times 10^{-8} \text{M}$ ($p = 0.01$) and $1 \times 10^{-9} \text{M}$ ($p < 0.001$). The concentrations that the worms responded significantly to differed depending on water pH/ temperature. The worms had the strongest response (measured in terms of activity, or percent active time) at the lowest cue concentrations tested ($1 \times 10^{-9} \text{M}$ and $1 \times 10^{-8} \text{M}$). A strong secondary peak in response was observed at the highest concentrations tested ($1 \times 10^{-3} \text{M}$ and $1 \times 10^{-2} \text{M}$) only in pH8.1, 18°C and pH7.3, 22°C.

Dose -response curves were fitted to each of the response lines in Figure 2.4 (see supplementary materials) and EC_{10} was computed for each of these curves. Table 1.3 below shows the results of this analysis. The EC_{10} cue concentration was lowest in pH8.1, 22°C with only marginally higher EC_{10} concentration in pH8.1, 18°C. The EC_{10} was slightly higher for pH7.3 at both 18°C and 22°C.

Table 2. 3: The concentration of cue that elicited 10% activity compared to the control level (EC_{10}) was calculated to allow comparison of cue response between the pH/ temperature conditions tested.

Condition	EC_{10} (M)
pH8.1, 18°C	1.2×10^{-10}
pH8.1, 22°C	1.07×10^{-10}

pH7.3, 18°C	3.29×10^{-10}
pH7.3, 22°C	5.49×10^{-10}

A robust factorial repeated measures two-way ANOVA indicated that pH had a statistically significant impact on the response variable, activity ($F=4.3$, $p=0.039$) whereas temperature did not have a statistically significant effect ($F=3.4$, $p=0.066$). A statistically significant interaction effect of pH and temperature on activity was found ($F=32.5$, $p<0.0001$).

GLUTATHIONE (GSH)

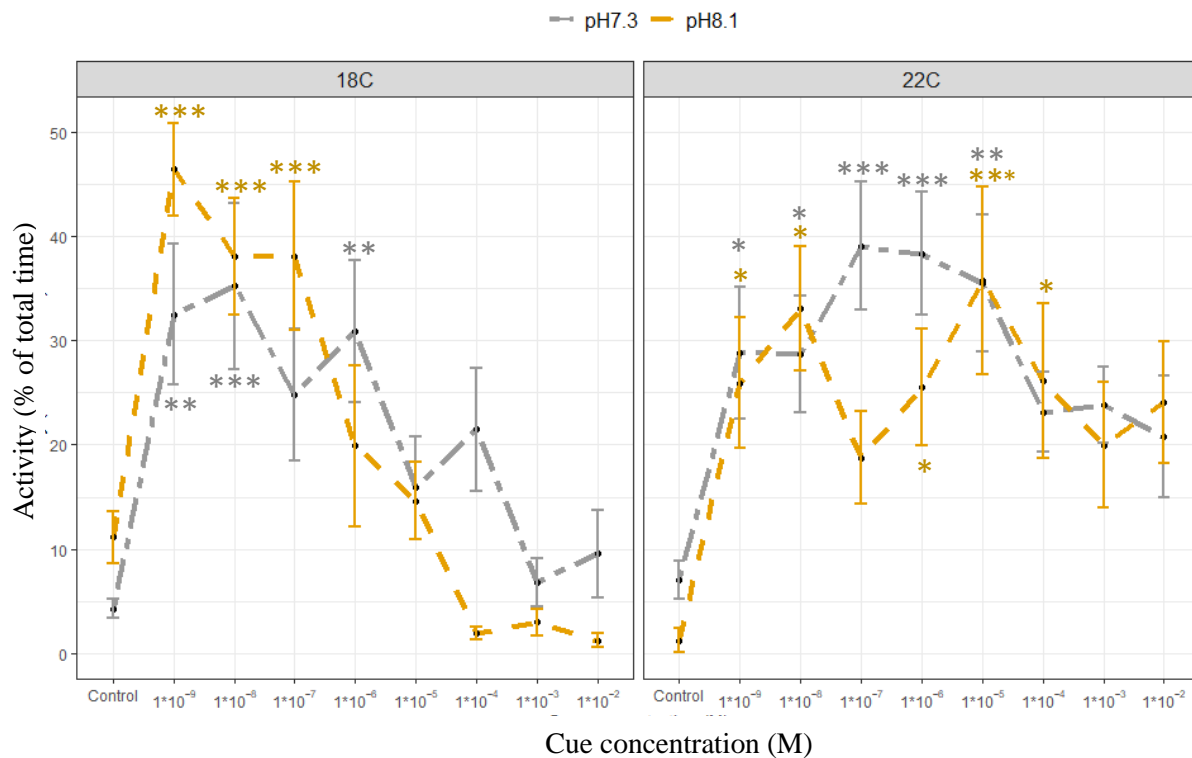


Figure 2. 5: Response of ragworms (Hediste diversicolor) to the chemical food cue GSH. Activity was measured as the percentage of time spent out of the burrow during a 30 minute recording, n=20 for each condition. Response was tested in three pH/ temperature conditions, namely pH 8.1, 18°C; pH8.1, 22°C; pH7.3, 18°C; pH7.3, 22°C. Cue concentrations ranging from 1×10^{-2} M to 1×10^{-9} M was tested at ten times dilution between concentrations. A control was tested with the addition of water alone. Points show the group mean and bars

show standard error. Significance stars show those points that are significantly different to the control (Signif. codes: *** = $p < 0.001$, ** = $p < 0.01$, * = $p < 0.05$)

Figure 2.5 illustrates the dose-response chart of the percentage time worms spent out of their burrows (percentage active time) in a range of pH/ temperature conditions. *H. diversicolor* responded significantly to GSH compared to the control in all four pH/ temperature conditions tested (see significance stars on Figure 2.5 and full statistics in table S2.15 to S2.18 in Supplementary Materials). A significant difference in activity compared to the control was found: At pH8.1, 18°C, at concentrations of 1×10^{-7} M ($p < 0.001$), 1×10^{-8} M ($p < 0.001$) and 1×10^{-9} M ($p < 0.001$); at pH8.1, 22°C, at concentrations of 1×10^{-4} M ($p = 0.03$), 1×10^{-5} M ($p < 0.001$), 1×10^{-6} M ($p = 0.03$), 1×10^{-8} M ($p = 0.002$), 1×10^{-9} M ($p = 0.03$); at pH7.3, 18°C, at concentrations of 1×10^{-6} M ($p = 0.006$), 1×10^{-8} M ($p < 0.001$) and 1×10^{-9} M ($p = 0.003$); at pH7.3, 22°C, at concentration of 1×10^{-5} M ($p = 0.002$), 1×10^{-6} M ($p < 0.001$), 1×10^{-7} M ($p < 0.001$), 1×10^{-8} M ($p = 0.03$) and 1×10^{-9} M ($p = 0.03$). The cue concentration range that the worms responded significantly to was similar in all four pH/ temperature conditions. The worms had the strongest response (measured in terms of activity, or percent active time) at the lowest cue concentrations tested (1×10^{-9} M and 1×10^{-8} M) with the exception of pH7.3, 22°C which peaked at 1×10^{-7} M. At 18°C activity levels dropped strongly at high cue concentrations (1×10^{-4} M and higher) but this reduction was not as pronounced at 22°C.

Dose -response curves were fitted to each of the response lines in Figure 2.5 (see supplementary materials) EC_{10} was computed for each of these curves. Table 2.4 below shows the results of this analysis. The EC_{10} cue concentration was lowest in pH8.1, 18°C with higher EC_{10} concentration in all other pH/ temperature conditions tested.

Table 2. 4: The concentration of cue that elicited 10% activity compared to the control level (EC_{10}) was calculated to allow comparison of cue response between the pH/ temperature conditions tested.

Condition	EC_{10} (M)
pH8.1, 18°C	7.57×10^{-12}
pH8.1, 22°C	2.28×10^{-10}
pH7.3, 18°C	1.98×10^{-10}
pH7.3, 22°C	3.65×10^{-10}

A robust factorial repeated measures two-way ANOVA indicated that pH had a statistically significant impact on the response variable, activity ($F=4.4$, $p=0.037$) as did temperature ($F=12.5$, $p=0.0005$). No statistically significant interaction effect of pH and temperature on activity was found ($F=2.8$, $p=0.095$).

CHONDROITIN SULPHATE

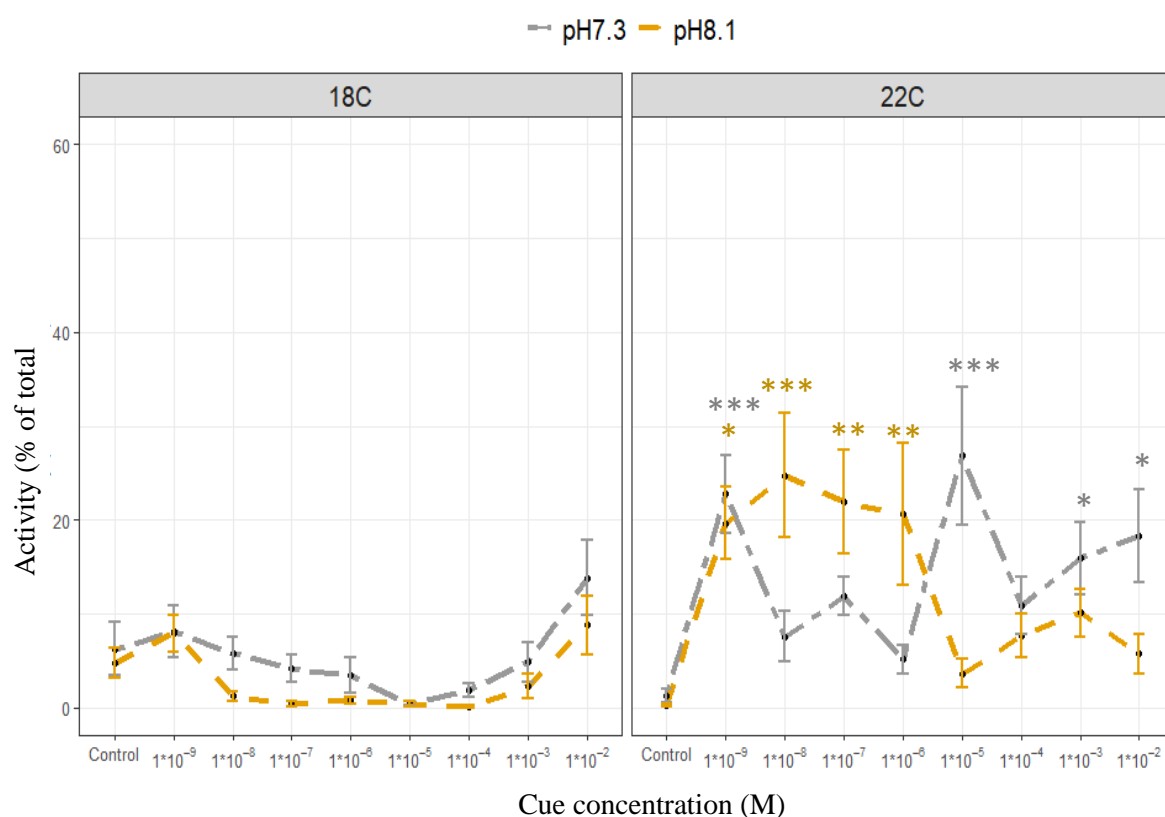


Figure 2.6: Response of ragworms (*Hediste diversicolor*) to the chemical cue chondroitin sulphate. Activity was measured as the percentage of time spent out of the burrow during a 30 minute recording, $n=20$ for each condition. Response was tested in four pH/ temperature conditions, namely pH 8.1, 18°C; pH 8.1, 22°C; pH 7.3, 18°C; pH 7.3, 22°C. Cue concentrations ranging from $1 \times 10^{-2} \text{ M}$ to $1 \times 10^{-9} \text{ M}$ was tested at ten times dilution between concentrations. A control was tested with the addition of water alone. Points show the group mean and bars show standard error. Points show the group mean and bars show standard error. Significance stars show those points that are significantly different to the control (Signif. codes: *** = $p < 0.001$, ** = $p < 0.01$, * = $p < 0.05$)

Figure 2.6 illustrates the dose-response chart of the percentage time worms spent out of their burrows (percentage active time) in a range of pH/ temperature conditions. At 18°C *Hediste diversicolor* showed a non-significant reduction in activity compared to the control for concentrations between 1×10^{-8} to $1 \times 10^{-4} \text{ M}$. This was true for both pH 8.1 and pH 7.3 at 18°C. At 22°C a significant increase in activity was observed (see significance stars on Figure 2.6

and full statistics in table S2.25 to S2.28 in Supplementary Materials). A significant difference in activity compared to the control was found: At pH8.1, 22°C, at concentrations of 1×10^{-6} M ($p=0.007$), 1×10^{-7} M ($p=0.003$), 1×10^{-8} M ($p<0.001$) and 1×10^{-9} M ($p=0.01$); at pH7.3, 22°C, at concentration of 1×10^{-2} M ($p=0.01$), 1×10^{-3} M ($p=0.05$), 1×10^{-5} M ($p<0.001$), 1×10^{-9} M ($p<0.001$).

Dose -response curves were fitted to each of the response lines in Figure 2.6 (see supplementary materials) and the concentration of cue that elicited 10% activity (EC_{10}) was computed for each of these curves. Table 2.5 below shows the results of this analysis. The EC_{10} could not be calculated for pH8.1, 18°C due to the low response elicited by chondroitin sulphate. The EC_{10} concentrations were similar for both pH levels tested at 22°C, with much higher EC_{10} found at pH7.3, 18°C.

Table 2. 5: The concentration of cue that elicited 10% activity compared to the control level (EC_{10}) was calculated to allow comparison of cue response between the pH/ temperature conditions tested. Due to lack of response in pH8.1, 18°C, EC_{10} could not be calculated and EC_5 was calculated instead.

Condition	EC_{10} (M)
pH8.1, 18°C	/
pH8.1, 22°C	6.56×10^{-10}
pH7.3, 18°C	3.97×10^{-3}
pH7.3, 22°C	1.33×10^{-10}

A robust factorial repeated measures two way ANOVA indicated that pH had a statistically significant impact on the response variable, activity ($F= 3.9$, $p=0.0497$) as did temperature ($F=40.6$, $p<0.001$). No statistically significant interaction effect of pH and temperature on activity was found ($F=0.3$, $p=0.595$).

UREA

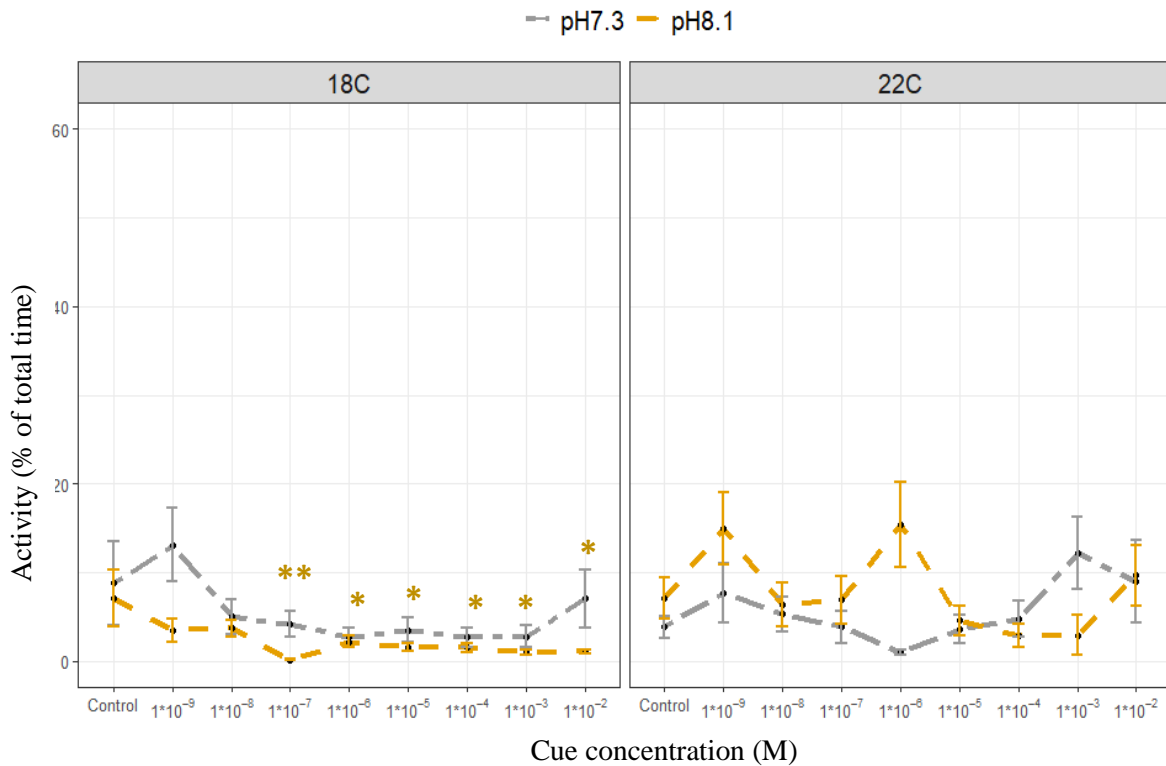


Figure 2. 7: Response of ragworms (*Hediste diversicolor*) to the chemical cue urea. Activity was measured as the percentage of time spent out of the burrow during a 30 minute recording, $n=20$ for each condition. Response was tested in four pH/ temperature conditions, namely pH 8.1, 18°C; pH8.1, 22°C; pH7.3, 18°C; pH7.3, 22°C. Cue concentrations ranging from 1×10^{-2} M to 1×10^{-9} M was tested at ten times dilution between concentrations. A control was tested with the addition of water alone. Points show the group mean and bars show standard error. Points show the group mean and bars show standard error. Significance stars show those points that are significantly different to the control (Signif. codes: *** = $p < 0.001$, ** = $p < 0.01$, * = $p < 0.05$)

Figure 2.7 illustrates the dose-response chart of the percentage time worms spent out of their burrows (percentage active time) in a range of pH/ temperature conditions. At pH8.1, 18°C *H. diversicolor* showed a significant reduction in activity compared to the control for concentrations between 1×10^{-7} to 1×10^{-2} M. At pH7.3, 18°C, although activity levels were lower than the control at most concentrations, the reduction was non-significant. At 22°C, no

significant difference between control activity levels and activity levels after the addition of urea at either pH8.1 or pH7.3 (see significance stars on Figure 2.7 and full statistics in table S2.21 to S2.24 in Supplementary Materials). A significant difference in activity compared to the control was found: At pH8.1, 18°C, at concentrations of $1 \times 10^{-2} \text{M}$ ($p=0.005$), $1 \times 10^{-3} \text{M}$ ($p=0.004$), $1 \times 10^{-4} \text{M}$ ($p=0.01$), $1 \times 10^{-5} \text{M}$ ($p=0.01$), $1 \times 10^{-6} \text{M}$ ($p=0.04$), $1 \times 10^{-7} \text{M}$ ($p<0.001$).

Dose -response curves were fitted to each of the response lines in Figure 2.7 (see supplementary materials) and the concentration of cue that elicited 10% activity (EC_{10}) was computed for each of these curves. Table 2.6 below shows the results of this analysis. Due to the low and variable level of response, dose response curves could only be fitted to for pH7.3, 22°C. EC_{10} could not be calculated for pH8.1, 18°C, pH7.3, 18°C or pH8.1, 22°C due to the low response elicited by urea.

Table 2. 6: The concentration of cue that elicited 10% activity compared to the control level (EC_{10}) was calculated to allow comparison of cue response between the pH/ temperature conditions tested.

Condition	EC_{10} (M)
pH8.1, 18°C	/
pH8.1, 22°C	/
pH7.3, 18°C	/
pH7.3, 22°C	0.00415

A robust factorial repeated measures two-way ANOVA indicated that pH did not have a statistically significant impact on the response variable, activity ($p=0.19$) nor did temperature ($p=0.089$). However, a statistically significant interaction effect of pH and temperature on activity was found ($p=0.022$).

2.1.5. Discussion

Chemical food cues

DMS, ATP, GSH and taurine all appear to act as a food-cues to *H. diversicolor*, eliciting significantly increased activity levels compared to the control at a range of concentrations. Although response varied across the conditions tested, all of these chemical food cues elicited a significant response at the lowest concentration tested ($1 \times 10^{-9} \text{M}$) in some conditions. pH 8.1, 18°C (except for ATP) and pH8.1, 22°C were the conditions that elicited a significant response at the lowest concentration across all chemical food cues tested, suggesting that these are favourable environmental conditions for *H. diversicolor* to sense and respond to these chemicals. The EC_{10} concentrations varied by several orders of magnitude depending on the chemical cue and condition. Notably, GSH had very low EC_{10} concentrations, particularly at pH8.1, 18°C ($\text{EC}_{10} = 7.57 \times 10^{-12}$).

It is possible that the response levels observed at such low concentrations are linked to the experimental setup. The assays were run in artificial seawater made up with purified water creating an artificially clean environment with few other chemical signals (Crane et al., 2022). This potentially acted to allow the ragworms being tested to sense the cue at a lower concentration than expected. The food cues tested show an initial peak in response at the lowest concentrations followed by a drop off in activity levels as concentrations increase (typically in the range of 1×10^{-5} to $1 \times 10^{-4} \text{M}$ but this varies depending on the cue and condition tested). This may be due to the higher concentrations overwhelming the animal's sensory system causing them to respond at a lower rate, as has been observed in *Caenorhabditis elegans* (Colbert and Bargmann, 1995, Ardiel and Rankin, 2010). The drop off in activity could also be due to negative learning by the animals, whereby the response to the cue elicits no reward leading to a reduced level of further response to the cue. Evans (1969) identified rapid habituation to changes in illumination, shadowing, noise and touch in *H. diversicolor* with reduced responses

observed after as few as two shadowing stimulants (shadowing was conducted every 30 seconds) and continued diminishing response to the maximum of 40 stimulants. Several of the food cues tested (DMS, ATP and taurine) showed a secondary increase in activity levels at very high concentrations of cue (in the range of $1 \times 10^{-3} \text{M}$ to $1 \times 10^{-2} \text{M}$). These are higher concentrations than would be expected in nature and may be causing a secondary reaction due to stress. Previous studies have found that Nereid worms are 18 times more likely to abandon their burrows or ‘surface’ (partially exit the burrow) in response to hypoxia stress compared to tubificid-like worms and small spionid-like worms (Sturdivant et al., 2012). A similar ‘surfacing’ behaviour could be occurring in response to high concentrations of cue.

The water pH had a significant impact on the percent active time for taurine and GSH. Reduced pH has been found to impair the ability of *H. diversicolor* to find a food cue (Feugere et al., 2021) as well as reduce feeding behaviour (Bhuiyan, 2021). Water pH is known to impact the conformation state of some amino acids, shifting them between protonated and unprotonated states (Vila-Viçosa et al., 2013, El Ibrahimy et al., 2019). This molecular level alteration has been found to impact the ability of organisms to sense chemical cues (Roggatz et al., 2016) and the results of this study indicate a similar mechanism occurring in *H. diversicolor* for the amino acids taurine and GSH.

Temperature had a significant impact on the percent active time for DMS ($p < 0.001$), ATP and GSH. Increased temperature has been linked to slower regeneration rate in *H. diversicolor* (Bhuiyan, 2021) but not specifically linked to varied response to food cues. Reef fish (*Pomacentrus chrysurus*) have been found to take greater risks in response to food at higher temperatures (Lienart et al., 2014) and a similar mechanism could be driving the disparity in response seen in some of the chemical cues at higher temperature (in particular for ATP).

The pH/ temperature interaction had a significant impact on the percent active time for DMS, ATP and taurine. Temperature has been found to exacerbate the negative impacts of pH on survival and burrowing in *H. diversicolor* (Bhuiyan et al, 2021) and has been linked to reduced regeneration. The negative effects associated with reduced pH and increased temperature on survival could drive the reduced activity observed at higher temperatures and lower pH in this study.

Although this experiment is focussed on the impacts of pH and temperature on behavioural responses in *H. diversicolor*, additional anthropogenically induced impacts, such as heavy metal pollutants, could exacerbate negative effects driven by climate change. The worms used in this experiment were bred and housed in clean conditions, however, sediment analysis from the initial collection site identified above national average levels aluminium (50,410.12ppm), potassium (19696.13ppm), and iron (43,111.17ppm). Exposure to a range of pollutants, including cadmium and copper and pharmaceutical compounds including paracetamol as well as emerging contaminants such as micro and nano-plastics and graphene oxide nanosheets have all been found to reduce burrowing behaviour in *H. diversicolor* (Molledo et al., 2019, Pedro et al., 2022, Bonnard et al., 2009, Nogueira and Nunes, 2021, Silva et al., 2020, Pires et al., 2022). Other physiological effects of pollutant exposure include increased mucus production, reduced regenerative capacity, altered antioxidant status and biochemical damage (Pires et al., 2022) Work on the combined effects of pollutants and acidification and/ or temperature on *H. diversicolor* have had mixed results with some finding no evidence of exacerbating impacts of these multiple stressors on physiology (when worms were exposed to Hg in reduced pH conditions) (e.g. Freitas et al., 2017) and others identifying increased oxidative stress in reduced pH conditions (when worms were exposed to carbon nanoparticles) (De Marchi et al., 2019). Benthic invertebrates may be at increased risk of

exposure to pollutants due to accumulation in sediments and the impacts of pollutants combined with climate-driven stressors on behaviour is currently under-studied.

Chemical predator cues

Due to the low activity levels observed during the control, it was difficult to prove that statistically significant reductions in activity were observed in response to the presence the chemical predator cues tested. However, the data supports the conclusion that urea acts as a predator-cue to *H. diversicolor*, eliciting significantly reduced activity levels compared to the control at a range of concentrations. At 22°C, the response to urea was variable with higher activity levels compared to 18°C, but no significant difference compared to the control. Chondroitin sulphate caused a reduction in percent active time compared to the control at 18°C, although this reduction was not significant. At 22°C the opposite response was observed, with several concentrations eliciting a significant positive response. This response change between 18°C and 22°C is concerning if chondroitin sulphate acts as a predator cue and suggests that *H. diversicolor* either cannot detect the cue or interpret it differently at higher temperatures even though urea is stable across this range of temperatures.

Due to low response levels, EC₁₀ could not be calculated for all the conditions tested. The EC₁₀ for urea (0.00415) could only be calculated for pH7.3, 22°C, where an increase in activity was observed at very high cue concentrations. This increase in activity might be a stress response to concentrations higher than would be experienced in nature. Chondroitin sulphate EC₁₀ values were calculated for the higher temperature conditions (pH7.3, 22°C and pH8.1, 22°C) and were similar for both of these conditions (1.33×10^{-10} M and 6.56×10^{-10} M respectively). In these two conditions chondroitin sulphate appears to act as a food cue or possibly stressor. At lower temperatures (pH7.3, 22°C and pH8.1, 22°C) EC₁₀ could only be

calculated for pH7.3 (0.00397M) because response levels were very low, suggesting that chondroitin sulphate might be acting as a predator cue. Similarly to urea, the calculation of an EC₁₀ value for pH7.3, 18°C was possible due to an increase in activity which was observed at very high cue concentrations. This increase in activity might be a stress response to concentrations higher than would be found in nature.

For urea, a robust factorial repeated measures two-way ANOVA indicated that pH did not have a statistically significant impact on the response variable, activity nor did temperature. However, a statistically significant interaction effect of pH and temperature on activity was found. As stated before temperature has been found to exacerbate the negative impacts of pH on survival and burrowing in *H. diversicolor* (Bhuiyan et al, 2021) and has been linked to reduced regeneration. The negative effects associated with reduced pH and increased temperature could drive the variation in activity observed in different pH/temperature conditions by driving complex risk/ response decisions in *H. diversicolor*.

In contrast, chondroitin sulphate showed that pH had a statistically significant impact on the response variable, activity as well as temperature. However, no statistically significant interaction effect of pH and temperature on activity was found. Reduced pH has been found to impair the ability of *H. diversicolor* to find a food cue (Feugere et al., 2021) as well as reduce feeding behaviour (Bhuiyan, 2021). This could explain the impact of reduced pH on activity. The structure of chondroitin sulphate is relatively stable across a broad pH and temperature range (pH6 to 11, pKa ~ 2.7 and 10 to 90°C) (Profant et al., 2019) suggesting that the variation in activity is physiologically driven.

DMS

Is it a food cue and at what concentrations?

DMS is an attractant cue in the marine environment, with organisms from reef fish larvae to procellariiform seabirds responding positively to it (Nevitt et al., 1995, Foretich et al., 2017) and is known to be emitted by marine phytoplankton (Dani and Loreto, 2017). However, to the author's knowledge, this is the first time it has been presented as a food cue in *H. diversicolor*. DMS is acting as a food cue, drawing worms out of their burrows with significantly higher activity than the control for a range of concentrations in all conditions tested (see Figure 2.2). A significant response occurred at very low cue concentrations (1×10^{-9} and 1×10^{-8} M) in all pH/ temperature conditions tested suggesting high sensitivity to this cue. The rapidly changing, high flow estuarine habitats that *H. diversicolor* are adapted to means that sensing food cues quickly and at low concentrations would be advantageous (Powers and Kittinger, 2002, Lunt and Smee, 2015). DMS is present in ocean surface waters at concentrations around 2.35×10^{-9} M (global, annual average), depending on geographical location and seasonality (Hulswar et al., 2021). The ability to sense DMS at the low concentrations tested here would therefore be environmentally viable in fast flowing estuarine environments where dilution occurs rapidly. In addition, the experimental setup used artificial seawater made up with purified water creating an artificially clean environment with few other chemical signals, which may lead to an enhanced response to low concentrations.

The impact of pH and temperature

A robust factorial repeated measures ANOVA was run to test for the effects of pH and temperature on activity (see supplementary material for full analysis). Temperature had a statistically significant impact on the response variable, activity ($p < 0.001$) whereas pH did not

have a statistically significant effect ($p=0.78$). A statistically significant interaction effect of pH and temperature on activity was found ($p=0.007$). The EC_{10} values for each pH/ temperature condition tested indicates high sensitivity to DMS in pH8.1, 18°C and pH 8.1, 22°C conditions (EC_{10} $1.26 \times 10^{-10}M$ and $1.87 \times 10^{-10}M$ respectively). The EC_{10} values for pH7.3, 22°C was a factor of ten higher ($1.42 \times 10^{-9}M$ respectively) suggesting that a higher concentration of DMS is required to elicit a response in these conditions. This reduced response could be caused by lower feeding rate and impaired ability to find food cues in low pH that have been observed in previous studies (Bhuiyan, 2021, Feugere et al., 2021).

Despite this variation in EC_{10} a robust factorial ANOVA indicated the pH alone did not have a significant impact on percent active time ($p=0.78$) but temperature did ($p<0.001$), as did the interaction between pH and temperature ($p=0.007$).

Lower response rates were seen at 22°C for the lowest concentration tested ($1 \times 10^{-9}M$) at pH8.1, however, this is compensated somewhat by a more sustained response, with higher activity levels observed at $1 \times 10^{-7}M$ and $1 \times 10^{-6}M$ at this condition. At pH 7.3 temperature seems to have the opposite effect with significantly increased levels of response activity at concentrations ranging from 1×10^{-5} to $1 \times 10^{-2}M$. This could either be linked to a stress response at higher temperatures than the worms have been raised in, a greater response to food cues in more energetically costly conditions or worms more able to sense this molecule across a greater range of concentrations at higher temperatures. Goldenberg et al. (2018) identified increased rates of risk taking and more foraging time in elevated temperatures in a mesocosm experiment which could explain the increased response at pH7.3, 22°C.

Temperature has been found to exacerbate the effects of pH on reduced feeding rate, reduced survival and reduced regeneration in *H. diversicolor* (Bhuiyan, 2021, Bhuiyan et al., 2021b), so the significant interaction found here may be driven by reduced feeding rates and

increased stress in warmer, more acidic conditions. Porteus et al. (2018) suggest that receptor proteins of European sea bass (*Dicentrarchus labrax*) were impaired in high CO₂ environments leading to lower food and predator detection and a similar mechanism could be contributing to the pH/ temperature differences observed in this experiment. DMS has been found to diffuse out of solution, into the atmosphere, at a faster rate in reduced pH (Six et al., 2013) which may be a contributing factor to the reduced response levels observed in this experiment at pH7.3 as the concentration may reduce over the 30 min experiment. Temperature, however, has been linked to higher diffusivity of DMS in solution which may be contributing to the sustained response observed at 22°C (Galí and Simó, 2015)

ATP

Is it a food cue and at what concentrations?

ATP is thought to be a reliable indicator of the presence of live or freshly dead animals and is used as a food cue by several crustacean and fish species (Kamio and Derby, 2017, Wakisaka et al., 2017). However, to the author's knowledge, this is the first time it has been presented as a food cue in *H. diversicolor*. Unfortunately data for pH7.3, 22°C were unusable. ATP appears to act as a food cue only in pH8.1, 22°C, drawing worms out of their burrows with significantly higher activity than the control for a range of concentrations (see Figure 2.3). A significant response occurred at very low cue concentrations (1×10^{-9} and 1×10^{-7} M) in this condition, suggesting high sensitivity in this condition. As already stated the rapidly changing, high flow estuarine habitats that *H. diversicolor* are adapted to means that sensing food cues quickly and at low concentrations would be advantageous, regardless of what cue is present (Powers and Kittinger, 2002, Lunt and Smee, 2015). However, in all other conditions (pH8.1, 18 °C and pH7.3, 18 °C), ATP could not be considered a food cue, with response to all concentrations not significantly different to the control response.

The impact of pH and temperature

Overall ATP appears to be acting as a food cue only at pH8.1, 22 °C with significantly increased activity peaking at a concentration of 1×10^{-8} M. In this condition a secondary peak in activity was observed at 1×10^{-2} M. This is a higher concentration than would be expected in nature and may be causing a secondary reaction due to stress.

A robust factorial repeated measures two-way ANOVA was run to test for the effects of pH and temperature on activity (see supplementary material for full analysis). Temperature had a statistically significant impact on the response variable, activity ($p=0.001$) whereas pH did not have a statistically significant effect ($p=0.35$). A statistically significant interaction effect of pH and temperature on activity was found ($p=0.005$). The EC_{10} values for each pH/temperature condition tested indicates high sensitivity to ATP at pH8.1, 22°C ($EC_{10} = 1.27 \times 10^{-10}$ M). The EC_{10} value for pH7.3, 18°C could not be calculated due to low and variable response across the concentrations tested. The EC_{10} for pH7.3, 18°C ($EC_{10} = 2.96 \times 10^{-6}$ M) is several factors larger than for pH8.1, 22°C indicating that a much higher concentration of ATP is required to elicit a response in these conditions and even at this concentration, response was not significantly different from the control level. Goldenberg et al. (2018) identified increased rates of risk taking and more foraging time in elevated temperatures in a mesocosm experiment which could explain the increased response at pH8.1, 22°C. In addition, metabolic scope for activity increases with temperature in *H. diversicolor* (Galasso HL, 2018) which could drive an increase in non-cue related activity at 22°C. There is some evidence that ATP diffuses more readily at higher temperatures (Hubley et al., 1996), which may facilitate chemoreception, however, the stark difference between worm response at 18 and 22°C suggests a physiological effect may be occurring at higher temperatures.

Although pH did not have a statistically significant impact on response, the interaction between pH and temperature did have a significant effect. ATP hydrolyses in aqueous solutions above pH7.4 (Simão et al., 2013), meaning the structures being detected by worms in pH8.1 may be the hydrolysed form (ADP). This combined with the increase in temperature may be driving a shift to ADP (Levy et al., 1962) at sufficient concentrations to elicit the significant positive response observed at pH8.1, 22°C.

TAURINE

Is it a food cue and at what concentrations?

Dissolved free amino acids are common food cues in marine environments (Kamio and Derby, 2017, Kamio et al., 2021) and taurine has been documented as a chemical cue in other polychaete species (Ferner and Jumars, 1999). Taurine is acting as a food cue, drawing worms out of their burrows with significantly higher activity than the control for a range of concentrations in all conditions tested (see Figure 2.4). A significant response occurred at very low cue concentrations (1×10^{-9} or 1×10^{-8} M) in all pH/ temperature conditions tested suggesting high sensitivity to this cue. The rapidly changing, high flow estuarine habitats that *H. diversicolor* are adapted to means that sensing food cues quickly and at low concentrations would be advantageous (Powers and Kittinger, 2002, Lunt and Smee, 2015). Taurine is present in ocean waters at concentrations ranging from around 2×10^{-10} M to 1.57×10^{-8} M, depending on depth, geographical location and seasonality (Clifford et al., 2017). The ability to sense taurine at low concentrations would therefore be a viable adaptation in fast flowing estuarine environments where dilution occurs rapidly. In addition, the experimental setup used artificial seawater made up with purified water creating an artificially clean environment with few other chemical signals, which may lead to an enhanced response to low concentrations. A secondary

increase in activity levels was observed at very high concentrations of cue (in the range of $1 \times 10^{-3} \text{M}$ to $1 \times 10^{-2} \text{M}$) in pH8.1, 18°C and pH7.3, 22°C. These are higher concentrations than would be expected in nature and may be causing a secondary reaction due to stress.

The impact of pH and temperature

A robust factorial repeated measures two-way ANOVA was run to test for the effects of pH and temperature on activity (see supplementary material for full analysis). Temperature did not have a statistically significant impact on the response variable, activity ($p=0.066$) whereas pH did have a statistically significant effect ($p=0.039$). A statistically significant interaction effect of pH and temperature on activity was found ($p<0.0001$). The EC_{10} values for each pH/ temperature condition tested indicates high sensitivity to taurine across all conditions, with slightly lower concentrations required to elicit EC_{10} response in pH8.1, 18°C and pH8.1, 22°C ($EC_{10} = 1.2 \times 10^{-10} \text{M}$ and $1.07 \times 10^{-10} \text{M}$ respectively, compared to $3.29 \times 10^{-10} \text{M}$ and $5.49 \times 10^{-10} \text{M}$ for pH7.3, 18°C and pH7.3 22°C). This reduced response could be caused by lower feeding rate and impaired ability to find food cues in low pH that have been observed in previous studies (Bhuiyan, 2021, Feugere et al., 2021).

The results show that response rate varies significantly between pH 7.3 and pH 8.1 with lower response rates at pH7.3 at the lowest concentrations ($1 \times 10^{-9} \text{M}$) and peak activity occurring at higher concentrations compared to pH8.1 (first peak at $1 \times 10^{-9} \text{M}$ at pH8.1, 18C compared to $1 \times 10^{-8} \text{M}$ at pH7.3, 18C) as well as higher EC_{10} values at pH7.3 . The protonation state of taurine is known to be pH sensitive and the change from zwitterion form to the deprotonated form occurs across the pH range tested in this experiment (see Figure 8). At pH7.3 the population of zwitterions is much higher than at pH8.1, when the deprotonated form becomes more abundant. The change in overall charge along with the associated alteration in

conformation of the molecule in the zwitterion form may inhibit signal reception at the receptor binding site (Roggatz et al., 2016).

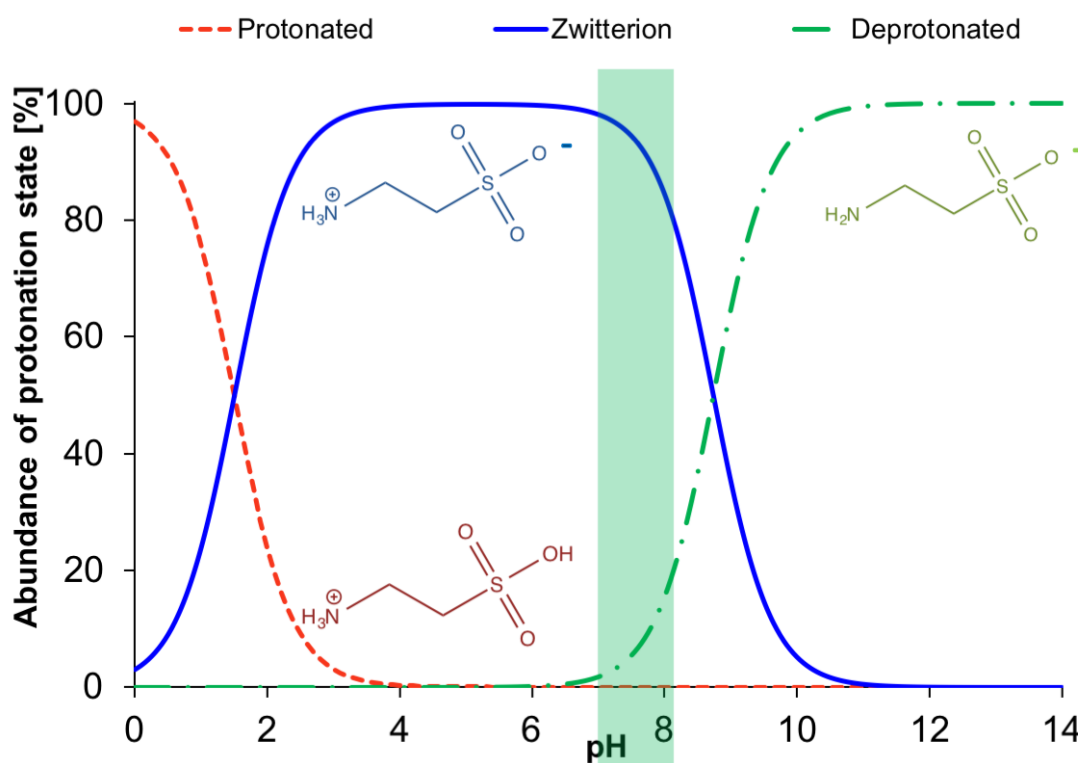


Figure 2. 8: Relative abundance of individual protonation states of taurine along with the percentage change across the pH scale. Proportions are shown for protonation states present between pH 0 and 14. The green shaded area indicates the pH range tested in this study; from pH 8.1 to pH 7.3.

GSH

To the author's knowledge, this is the first time it has been presented as a food cue in *H. diversicolor*. GSH is acting as a food cue, drawing worms out of their burrows with significantly higher activity than the control for a range of concentrations in all conditions tested (see Figure 2.5). A significant response occurred at very low cue concentrations (1×10^{-9} or 1×10^{-8} M) in all pH/ temperature conditions tested suggesting high sensitivity to this cue. The rapidly changing, high flow estuarine habitats that *H. diversicolor* are adapted to means that sensing food cues quickly and at low concentrations would be advantageous (Powers and

Kittinger, 2002, Lunt and Smee, 2015). The experimental setup used artificial seawater made up with purified water creating an artificially clean environment with few other chemical signals, which may lead to an enhanced response to low concentrations. GSH concentrations are low in the marine environment (2×10^{-10} to 8×10^{-10} M depending on geographical location, depth and seasonality) and it has been hypothesised that rapid degradation to more stable γ -Glu-Cys occurs outside the cell (Dupont et al., 2006). For GSH to be present in its non-degraded form would suggest the presence of damaged tissue in close proximity. This could explain the low EC_{10} values observed for GSH.

The impact of pH and temperature

A robust factorial repeated measures two-way ANOVA was run to test for the effects of pH and temperature on activity (see supplementary material for full analysis). Temperature had a statistically significant impact on the response variable, activity ($p=0.0005$) as did pH ($p=0.037$). However, no statistically significant interaction effect of pH and temperature on activity was found ($p=0.095$). The EC_{10} values for each pH/ temperature condition tested indicates high sensitivity to taurine across all conditions, with lower concentrations required to elicit EC_{10} response in pH8.1, 18°C ($EC_{10} = 7.57 \times 10^{-12}$ M). The EC_{10} values in all other conditions were two factors of ten higher, suggesting that higher concentrations of GSH were required to elicit the same response in these conditions. This reduced response could be caused by lower feeding rate and impaired ability to find food cues in low pH that have been observed in previous studies (Bhuiyan, 2021, Feugere et al., 2021).

The results show that response rate varies significantly between pH 7.3 and pH 8.1 with lower response rates at pH7.3 at the lowest concentrations (1×10^{-9} M) and peak activity occurring at higher concentrations compared to pH8.1 (first peak at 1×10^{-9} M at pH8.1, 18C

compared to $1 \times 10^{-7} \text{M}$ at pH 7.3, 22°C) as well as higher EC_{10} values at pH 7.3. The protonation state of GSH is known to be pH sensitive and the change from protonated form to the deprotonated form begins to occur across the pH range tested in this experiment (see Figure 2.9). At pH 7.3 the proportion of Cys-SH molecules is higher than at pH 8.1, when the Gly-NH₂ form becomes more abundant. The change in overall charge along with the associated alteration in conformation of the molecule in the deprotonated form may inhibit signal reception at the receptor binding site leading to increased response (Roggatz et al., 2016).

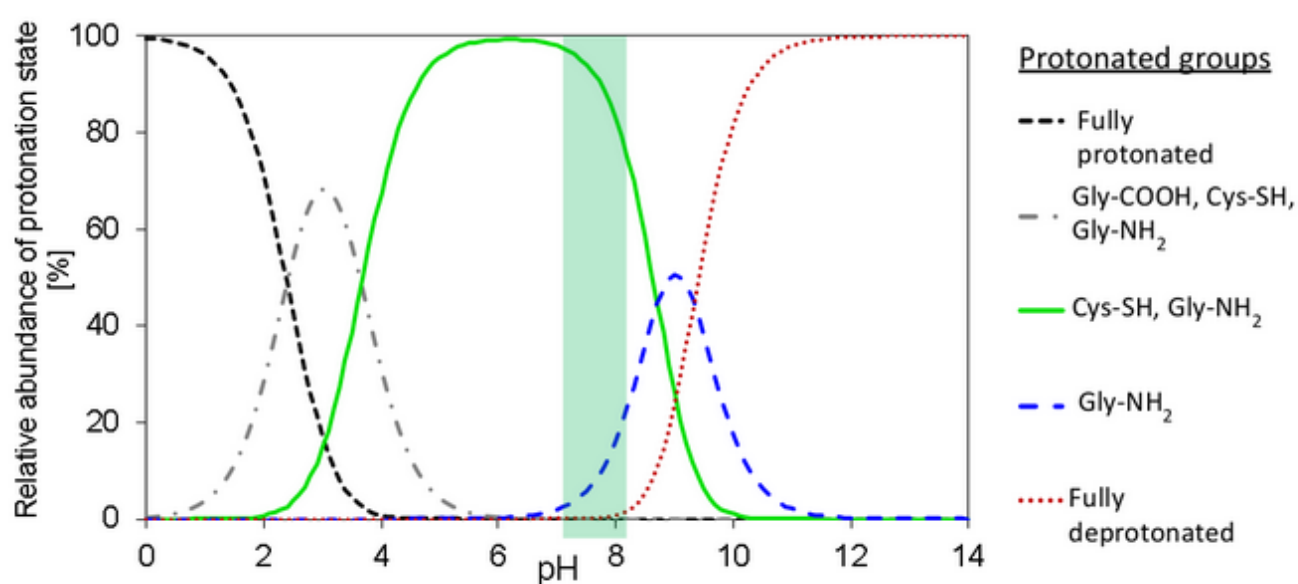


Figure 2. 9: Relative abundance of individual protonation states of GSH along with the percentage change across the pH scale. Proportions are shown for protonation states present between pH 0 and 14. The green shaded area indicates the pH range tested in this study; from pH 8.1 to pH 7.3.

CHONDROITIN SULPHATE

Chondroitin sulphate is a glycosaminoglycan (GAG) and has been identified as eliciting a predator avoidance response in several aquatic species, primarily in fish (Mathuru et al., 2012, Faulkner et al., 2017, Farnsley et al., 2016, Bajwa, 2020). Chondroitin sulphate is thought to be present in the mucus of some fish, and is released from damaged club cells of prey fish

species (Rittschof and Cohen, 2004) making it a good candidate as a predator cue. Interestingly, at 18 °C ragworms appear to respond to this cue as a predator cue, with reduced levels of activity when compared to the control (Figure 2.6). However, at 22 °C, this trend appears to reverse with significantly higher levels of activity at all cue concentrations compared to the control. The pH appears to have little effect. The results also indicate that climate change will have an impact on the ability of *H. diversicolor* to sense and respond appropriately to food and predator cues with the potential to impact survival in this keystone species.

The EC₁₀ concentrations were similar for both pH levels tested at 22°C (EC₁₀ = 6.56x10⁻¹⁰ and 1.33x10⁻¹⁰M for pH8.1, 22°C and pH7.3, 22°C respectively), when chondroitin sulphate appears to be acting as a food cue. A much higher EC₁₀ found at pH7.3, 18°C (0.00397M) reflecting the extreme concentrations required to elicit a response in this condition. A robust factorial repeated measures two-way ANOVA indicated that pH had a statistically significant impact on the response variable, activity (p=0.0497) as did temperature (p<0.001). No statistically significant interaction effect of pH and temperature on activity was found (p=0.595). Reduced pH has been found to impair the ability of *Hediste diversicolor* to find a food cue (Feugere et al., 2021) as well as reduce feeding behaviour (Bhuiyan, 2021). This could explain the impact of reduced pH on activity. Metabolic scope for activity increases with temperature in *H. diversicolor* (Galasso HL, 2018) which could drive an increase in non-cue related activity at 22°C. The structure of chondroitin sulphate is relatively stable across a broad pH and temperature range (pH6 to 11, pKa ~ 2.7 and 10 to 90°C) (Profant et al., 2019) suggesting that the variation in activity is physiologically driven.

UREA

Urea has been identified as a predator cue in several aquatic species (Brown et al., 2012, Dallas et al., 2010). In this study urea has been found to act as a predator cue, reducing the time worms spent out of their burrows with significantly lower activity than the control for a range

of concentrations but only in pH8.1, 18°C (see Figure 2.7) which correspond to current environmental conditions. A significant response occurred at cue concentrations ranging from 1×10^{-7} to 1×10^{-2} M) this condition. The EC_{10} for urea (0.00415) could only be calculated for pH7.3, 22°C, where an increase in activity was observed at very high cue concentrations. This increase in activity might be a stress response to concentrations higher than would be expected in nature. Low levels of activity were observed across all conditions tested, with slightly more variable results at warmer temperatures. Metabolic scope for activity increases with temperature in *H. diversicolor* (Galasso HL, 2018) could drive an increase in non-cue related activity at 22°C, although no significant difference between the controls was observed. Urea protonates readily at reduced pH and this change in overall charge along with the associated alteration in conformation of the molecule may inhibit signal reception at the receptor binding site leading to altered response at pH7.3.

2.1.6. Conclusion

This is the first time that GSH and DMS have been observed as acting as a food cue for *H. diversicolor*. This is also the first time that urea has been observed acting as a predator cue. In addition, this is the first time worms have been observed with varied, and in some cases opposite, response to chemical cues over a range of pH conditions. This is in spite of the worms tested being adapted to specific pH and temperature, having been bred and raised in these conditions. The results indicate a concerning change in behavioural response to food and predator cues in low pH/ high temperature conditions. Climate change is likely to drive further reductions in ocean pH and increases in temperature over the next century and, in estuarine environments, this will lead to more time these extremes will be experienced. *H. diversicolor* is regularly exposed to fluctuating pH and temperatures and was considered well adapted to tolerate these conditions. The results of this study indicate that, although tolerant to these fluctuations, the ability of this species to function effectively is reduced. This could have

population level impacts on this keystone species as exposure to pH and temperature extremes becomes more frequent and normalised.

Limitations

The chemicals used in this chapter have never previously been tested as food/ predator cues for *H. diversicolor* and were selected based on known chemical cues from other marine invertebrates as well as their likely dispersal properties. A wide range of concentrations were tested because it was not known whether the worms would respond to these chemicals or at what concentrations they would respond. Other experiments on marine invertebrates have typically identified behavioural responses to chemical cues at concentrations between 1×10^{-8} and 1×10^{-6} M (Chivers and Smith, 1998, Crane et al., 2022, Ferner and Jumars, 1999, Kamio et al., 2021, Breithaupt, 2011), therefore a range that encompassed these concentrations was selected. However, given that the results in this chapter often showed a significant behavioural response of *H. diversicolor* to the chemical cues at the lowest concentration tested (1×10^{-9} M), it would have been useful to test a range of lower concentrations in order to identify a lower threshold concentration.

The experimental setup accounted for as many potential variables as possible (maintaining light levels, temperature, pH, oxygen levels, salinity and using water cycling to remove metabolites) and utilised a custom made dosing device to inject the same volume of chemical cue to each worm at the same time. There were, however, some limitations associated with the set up. In order to run the range of concentrations tested in each condition on the same individuals, the concentrations were added from lowest (control) to highest concentration (1×10^{-2} M) in each test. Each concentration was ten times higher than the previous addition. This was to remove the problem of adding a high concentration followed by a lower

concentration to the same system which would cause contamination issues. There is a risk that using the same order each time may have introduced bias into the results.

Finally, the majority of food cues showed an initial peak in activity followed by a reduction in activity as cue concentration increased. There is a possibility that this was due to negative learning by the worms. To investigate this further it would be interesting to run a series of experiments that tested the response of the same individuals to chemical cues with increasing delays between addition of cue.

3.0. Chapter 3

Acid Reflux: How Temperature and pH Alter Oxygen
Dynamics in Bioturbated Sediments.

3.2. Acid Reflux: How Temperature and pH Alter Oxygen Dynamics in Bioturbated Sediments.

3.2.1. Abstract

Climate scenarios predict an increase in ocean surface temperatures by up to 4.8°C by 2100, as well as an associated decline of water oxygen levels and, the ocean pH is predicted to decrease by further 0.32 pH units. Reduced pH has been linked to increased oxygen demand in marine organisms, in part due to the extra cost of internal ion balance homeostasis. In an ocean with lower oxygen levels which induces higher biological oxygen demands, organisms will need to acclimate or migrate in order to maximise their survival rate. Burrowing organisms, traditionally believed to be somewhat protected from climate change, are often considered ecosystem engineers due to their capacity to mix large amounts of sediment. In this study oxygen planar optodes were used to investigate the impact of water temperature and water pH on in-burrow oxygen levels and oxygen penetration depth using the polychaete harbour ragworm *Hediste diversicolor*. The animals used in these experiments were not collected from the wild but were second and third generation worms housed in static pH and temperature conditions so no pre-acclimation was required. By using F2 and F3 generation worms the impacts of acclimation and acclimatisation were removed and inter-generational, long term impacts of pH could be assessed.

A factorial design was used to analyse the independent and combined effects of pH (pH8.3, 7.7 and 7.3) and temperature (18 and 22 °C) on in-burrow oxygen levels as well as the depth of oxygen penetration into the sediment from the burrow walls. In-burrow oxygen levels were highly variable over a 12-hour period, with some burrows being vacated for short periods leading to a rapid decline in O₂ levels. Even when burrows were uninhabited, in-burrow oxygen levels remained above those of the surrounding anoxic sediment. Warmer temperatures (22°C) led to slightly higher Oxygen ratios, possibly linked to increased O₂ requirements by *H.*

diversicolor in these conditions which trigger an increased ventilation effort. At pH 7.3 and pH 8.1 the Oxygen ratio was reduced suggesting lower ventilation effort and/or reduced oxygen demand by the worms. Oxygen penetration depth into surrounding sediments reduced with declining pH and temperatures. These results indicate that future climate conditions may cause an increase in sediment oxic zone, which in turn may cause alterations in aerobic respiration and organic matter breakdown in marine sediments.

3.2.2. Introduction

Bioturbation is an ecosystem engineering process (Meysman et al., 2006) that profoundly effects biogeochemical cycling (e.g. Kristensen, 2005, Kristensen and Kostka, 2005), redistribution of compounds such as nutrients, organic matter, oxygen and toxic metabolites (e.g. Aller, 1994, Hedman et al., 2011) as well as trace element cycling, microbial community composition (Kristensen and Kostka, 2005), sediment aeration and decomposition of organic material (Canfield and Farquhar, 2009). Common species of benthic macrofauna that actively rework sediment and irrigate burrows play an important role in ecosystem functioning and should be given attention when considering the conservation of marine areas (Braeckman et al., 2014). The presence of infaunal burrows increases the water-sediment interface allowing additional solute exchange and creating micro-habitats for micro-fauna (Kristensen, 1985). Molecular diffusion and water flow, including bioturbator driven flow, drives oxygen transport into the sediments (Huettel and Gust, 1992). Increasing the oxic layer in sediments allows an increase in the proportion of aerobic respiration. There is some evidence that the breakdown of organic matter occurs faster in oxic conditions (Kristensen et al., 1995), suggesting that the presence of burrows may increase this process in benthic sediments. The radiation of marine invertebrates during the Cambrian is largely attributed to the evolution of burrowing organisms and the creation of new ecospace (Bottjer et al., 2000, Solan and Herringshaw, 2008). During past mass extinctions, the loss of burrowers has led to the

preservation of unbioturbated, laminated sediments in the aftermath. Additionally, metrics such as burrow size and depth (recorded by trace fossils) are used as a measure of environmental stress during post-extinction recovery periods (Twitchett et al., 2001, Twitchett and Barras, 2004).

H. diversicolor is a burrowing polychaete worm found in intertidal and shallow estuarine environments throughout Europe and North America (e.g. Scaps, 2002, Muus, 1967, Heip and Herman, 1979, Kristensen, 1984). Population density is highly variable ranging from 35 to 3700 individuals/m² for adult worms depending on season and environmental factors such as temperature, salinity and location (Scaps, 2002). A relationship between the feeding strategy of an organism (e.g. suspension versus deposit feeders) and irrigation rate (and therefore solute exchange with surface waters) has been identified in burrowing species (Kristensen and Kostka, 2005). *H. diversicolor* use several feeding mechanisms including deposit feeding, suspension feeding and active hunting (Fauchald and Jumars, 1979, Harley, 1950). They produce mucus to stabilise their burrows and can build mucus nets outside their burrows to catch detritus, which they then consume. The burrows of *H. diversicolor* are typically either Y-shaped or U-shaped and the internal burrow conditions are stabilised by active irrigation (Esselink and Zwarts, 1989).

The bioturbating activities of *H. diversicolor* have a crucial effect on ecosystem functioning. The burrowing, biorrigation, and associated sediment reworking of *H. diversicolor* has led to their classification as a keystone species. It has been suggested that its feeding activity acts as a rate-limiting step in estuarine detritus processing (Moreira et al., 2006, Mermillod-Blondin et al., 2005). Anything that impacts on their ability to burrow and irrigate sediment could have complex effects on estuarine environments, limiting the processing of organic matter and reducing aerobic respiration in the sediment.

The ocean has absorbed more than 90% of additional energy added in to the climate system between 1971 and 2010 leading to surface temperatures increasing by 0.11°C per decade over this period (IPCC, 2014; (Hoegh-Guldberg, 2014). Global mean surface temperatures are predicted to continue to increase by the end of the 21st century (2081–2100) relative to 1986–2005, with the IPCC’s ‘business-as-usual’ scenario (RCP8.5) predicting an increase in the range of 2.6°C to 4.8°C. Elevated temperatures has been found to reduce chaetiger regeneration, enhance metabolic capacity, reduce survival and induce oxidative stress in ragworms. In addition, when increased temperatures were combined with reduced pH, these effects were intensified (Bhuiyan et al., 2021b). Ectotherms such as *H. diversicolor* are likely to respond to increasing temperatures with an associated increase in oxygen demand (Pörtner, 2001). The full effects on marine benthic invertebrates are poorly constrained, in part due to their ‘hardy’ nature and high tolerance to stress. However, as ecosystem engineers, any alterations in the behaviour or survival of burrowers such as *H. diversicolor* has the potential to meaningfully effect ecosystems (Ducrottoy et al., 2019, Hiddink et al., 2015).

Ocean pH has declined on average by 0.1 units since the beginning of the industrial revolution as it absorbed approximately one third of anthropogenically released CO₂ (Orr et al., 2005, Steckbauer et al., 2015). A global decrease of up to 0.32 pH units is predicted by 2100 (IPCC, 2014). The associated alteration in carbonate chemistry is expected to have a negative impact on vulnerable calcifying organisms and this is where research effort tends to be focused (Kleypas and Langdon, 2006, Feely et al., 2004, Doney et al., 2009). The effects of reduced pH have been found to vary significantly between species with some organisms able to create more favourable pH conditions in the diffusive boundary layer around their surface. Other mitigation factors include more efficient ion exchange, build-up of antioxidants, buffering and CO₂ transport systems (Fabry et al., 2008, Ries, 2011, Freitas et al., 2016). Harsher conditions will have implications on the physiology of all multicellular marine

organisms. Maintenance of acid-base balance between extracellular body fluids (such as haemolymph or blood) and intracellular fluids will be affected by increased water pH (Pörtner and Farrell, 2008). Typically, in lower marine invertebrates, bicarbonate ions are used to neutralise acidosis of extracellular fluids associated with reduced water pH (Pörtner and Farrell, 2008, Pörtner et al., 2004). Additional mechanisms of acid-base balance include: metabolic consumption of protons and the active transport of ions that are equivalent to protons out of cells (Michaelidis et al., 2005). Increased concentration of protons can further influence key metabolites and interfere with some enzymatic reactions if the substrates involved differ due to protonation (Pörtner and Bock, 2000). In addition, reduced water pH has been linked to reduced metabolic rate and increased ammonia excretion in a number of species (Michaelidis et al., 2005, Langenbuch and Pörtner, 2002). Different organisms employ different types of metabolic response based on length of exposure to stressors (Strader et al., 2020). The upregulation of genes involved in lipid metabolism is observed in many experiments involving long-term pCO₂ stress response in a variety of taxa (Strader et al., 2020). All of these mechanisms are associated with energetic costs, diverting resources from growth and reproduction (Pörtner and Bock, 2000).

Lower pH and higher temperatures associated with climate change may lead to an increased oxygen demand by *H. diversicolor* (Pörtner and Bock, 2000, Pörtner, 2001) as well as lower availability of oxygen (Conley et al., 2009). Such potential negative consequences on ecosystems resulting from climate change-induced altered bioturbation pinpoints the need to understand the effects of pH and temperature upon the behaviour of *H. diversicolor*.

Although calcifying organisms appear to be disproportionately affected by reduced pH, changes in the global oceans will impact all marine organisms (e.g. Hendriks et al., 2010). *Hediste diversicolor* is a keystone species in estuarine environments and any impact climate change has on these organisms may have ecosystem wide impacts. We evaluate the potential

effects of water pH and temperature on *H. diversicolor* burrowing behaviour using 2D planar oxygen optode imaging.

3.2.3. Methods

Experimental design – sampling and animal care

Approximately 800 adult specimens of *Hediste diversicolor* were collected from Hessle Foreshore on the Humber Estuary in East Yorkshire, UK (53°42'52.94"N, 00°27'11.2"W) on 25th October 2018 by shovel sampling. The water temperature was recorded as 13.4°C, water salinity was 12‰ and water pH was 8.16 (using Hanna HI-991301 handheld probe). Worms were then transported to the University of Hull where they were removed from the natural sediment and placed in three tanks containing washed coral sand (4 cm depth) and 18‰ salinity ($\pm 1\%$) water, which was constantly aerated with an air stone. The climate was controlled at 18°C, 12 hours light, 12 hours dark with natural moonlight cycles mimicked using a UV light. The animals used in these experiments were not those collected from the wild but were second and third generation worms housed in static pH and temperature conditions so no pre-acclimation was required prior to experimentation. By using F2 and F3 generation worms the impacts of acclimation and acclimatisation were removed and inter-generational, long term impacts of pH could be assessed.

Initially animals were acclimated to pH 8.1 for one week, after which time the pH was reduced gradually in two of the tanks by bubbling CO₂ through the water. After fourteen days the tanks were set at pH 8.1 (± 0.0081), pH 7.7 (± 0.0075) and pH 7.3 (± 0.0055). An air pump was used to maintain oxygen levels in the tanks and an 'AllPondSolutions' aquarium filter with activated carbon filter element (600 L per hour flow) maintained water clarity (see Figure 3.1). The pH was recorded daily (supplementary materials). The pH of the water was controlled using JBL ProFlora pH control units, which constantly monitored pH and triggered CO₂

bubbling if the pH reached 0.05 pH units above the specified level. (IPCC, 2013b). Worms were held in a temperature controlled room at 18°C.

Several reproduction events occurred over the duration of this experiment across all three tanks. The worms used in the experiments described in this paper were randomly selected from F2 and F3 generation. The animals used in these experiments were not collected from the wild but were second and third generation worms housed in static pH and temperature conditions so no pre-acclimation was required. By using F2 and F3 generation worms the impacts of acclimation and acclimatisation were removed and inter-generational, long term impacts of pH could be assessed.

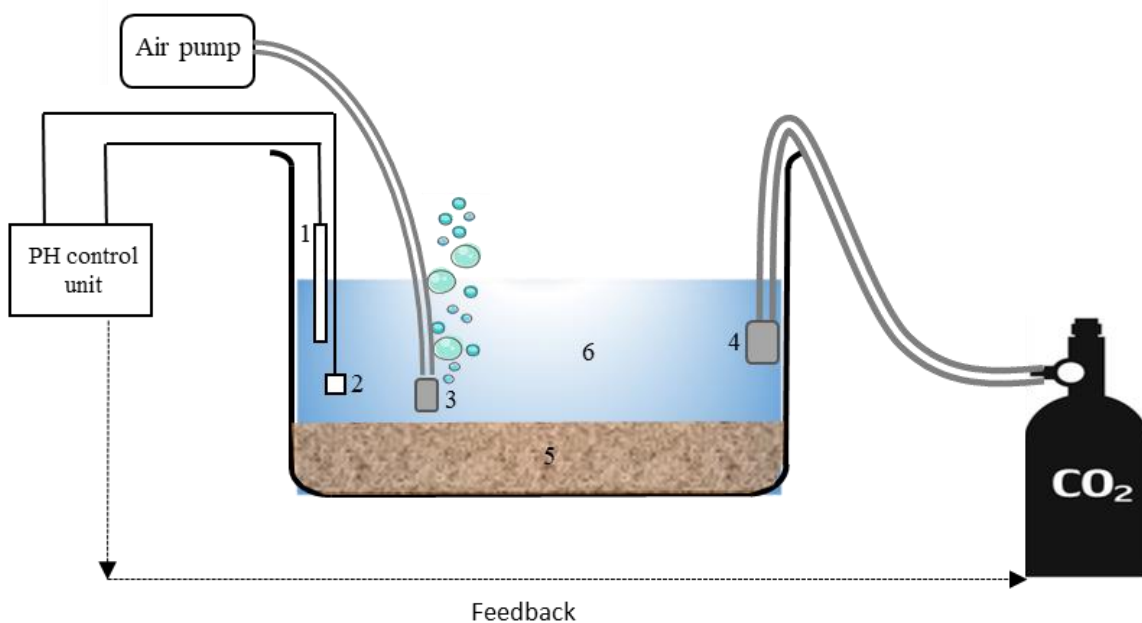


Figure 3. 1: Schematic diagram of pH control system used to house Hediste diversicolor. JBL ProFlora control units were used to automatically adjust the pH of the water by triggering the release of CO₂ if the water pH rose by 0.05 pH units above the set level. A pH probe (1) and temperature probe (2) were used to feed information to the pH control unit. An air pump and air stone (3) bubbled air through the water to maintain oxygen levels. A second air stone (4) was used to bubble the CO₂ from a tank. 4cm depth of washed 3mm coral sand (5) was used as sediment. Tanks were filled with 18‰ salinity ($\pm 1\%$) water diluted with

purified water (6). All tanks were housed in a climate-controlled room in order to maintain constant temperature, daily light/ dark cycles and monthly moon cycles.

Experimental design – test conditions

Six environmental conditions were tested (Figure 3.2): pH8.1/ 18°C, pH8.1/ 22 °C, pH7.7/18 °C, pH7.7/ 22 °C, pH7.3/18 °C and pH7.3/ 22 °C. The pH conditions were chosen based on: current average ocean pH (8.1); pH conditions predicted by 2100 based on the IPCC RCP8.5 climate model (pH 7.7) (IPCC, 2013b) and a more extreme condition of pH 7.3 likely to be found in future estuaries given a predicted decline of 0.32 pH units by 2100 based on the same climate model (IPCC, 2013b). Worms were raised in a temperature controlled room held at 18°C which is representative of UK summer temperatures. Using a constant temperature prevented large scale maturation events. The warmer temperature condition (22°C) was maintained using an aquarium heater and was based on RCP8.5 IPCC climate predictions of an increase in surface temperatures of between 2.6°C and 4.8°C.

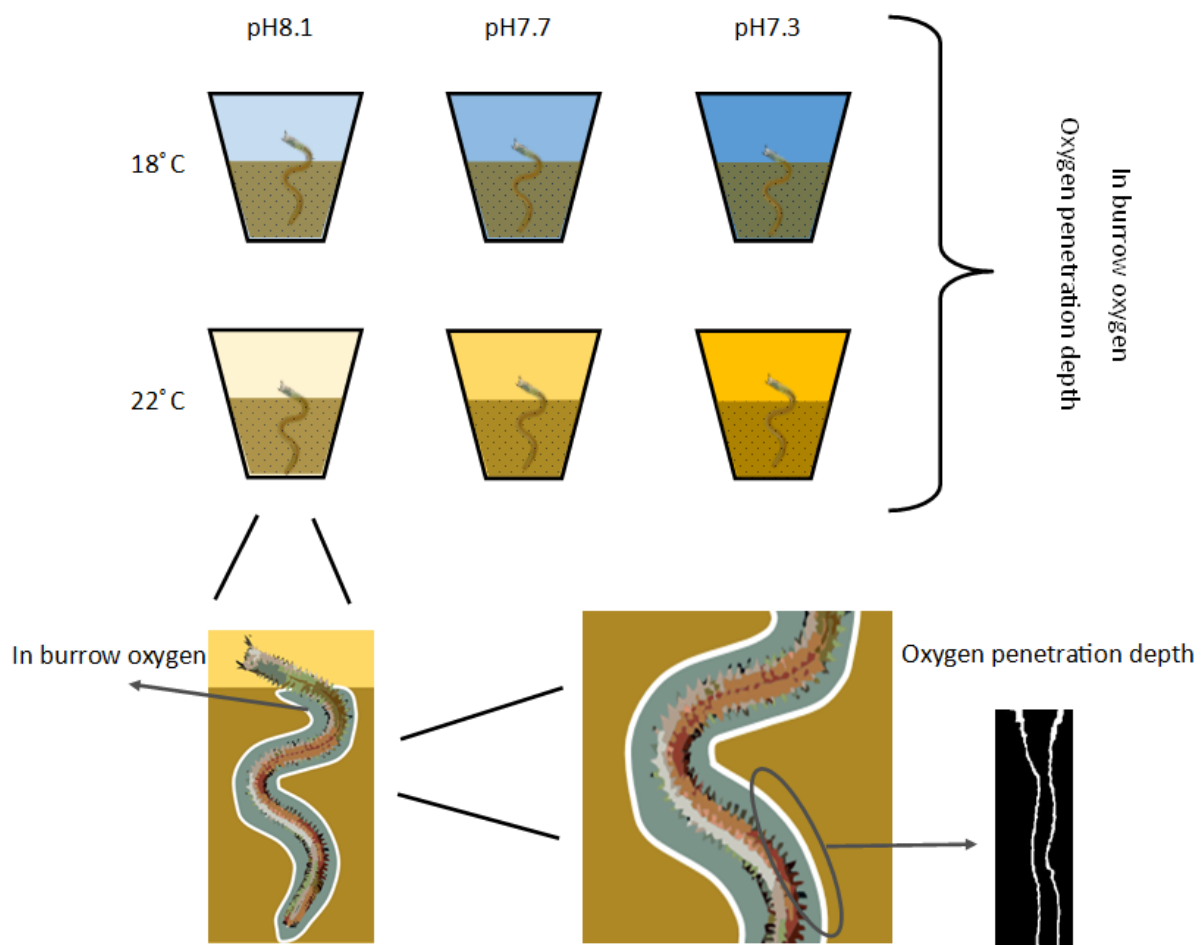


Figure 3. 2: Schematic illustrating the six pH/temperature conditions used in this study. In each condition burrows were analysed for in-burrow oxygen levels and oxygen penetration depth.

Experimental design - optode foil set up

A PreSens VisiSens™ fluorescent sensor foil and detector unit were used in combination with VisiSens AnalytiCal software to acquire two-dimensional maps recording the O₂ concentration in contact with the sensor foil (see Larsen et al., 2011, for a description of optode imaging).

Optical oxygen sensing is underpinned by the reversible reaction of oxygen molecules with a fluorescent dye layer on the foil. Light is then used to excite the electrons of a

fluorophore molecule, which releases a quantum of luminescence light when it returns to its ground state and this light is affected by the presence of oxygen. The presence of oxygen at the excited fluorophore molecule reduces the intensity and/or the duration of luminescence (Franke, 2005). Optical filters are used to separate the excitation light, which is typically blue or green light, from the emitted light, which is typically red. A modified version of the Stern-Volmer equation (Carraway et al., 1991) is used to calibrate images taken with a detector unit. PreSens provide O₂ sensor foils capable of providing accurate ($\pm 0.1\%$ air saturation at 100% air saturation and $\pm 0.02\%$ air saturation at 0% air saturation) oxygen concentrations at temperature ranges of 5-45°C.

A two-point calibration was used for the oxygen sensor foils, which were calibrated in the experimental setup shown in Figure 3.3. Anoxic sediment was used for the 0% oxygen calibration (C_0) and air saturated water was used to provide the data for the second calibration point (C_1). VisiSens AnalytiCal software was used to calculate the calibration curve and apply this data to the images taken during each experiment. Calibration was done for each set of images taken due to the sensitivity of the foils to changes in experimental setup.

The experimental setup for the sensor foils is shown in Figure 3.3. Natural sediment, which was sieved to 250 μm in order to remove macrofauna and added to a slim glass tank (8 cm x 20 cm x 25 cm) to a depth of 12 cm with the sensor foil attached to the largest outer face of the tank. Marine CentreTM artificial seawater (18‰ ($\pm 1\%$)) was added to the tank and to a second header tank (45 litre capacity). The water was cycled from the header tank to the experimental tank and back using two adjustable mini water pumps, which were combined with float switches to prevent overflow. The water in the header tank was bubbled with air and the pH was set by bubbling CO₂ through the water and controlled using a JBL pH control unit. Alkalinity and salinity were monitored daily throughout the experiment and before and after image acquisition.

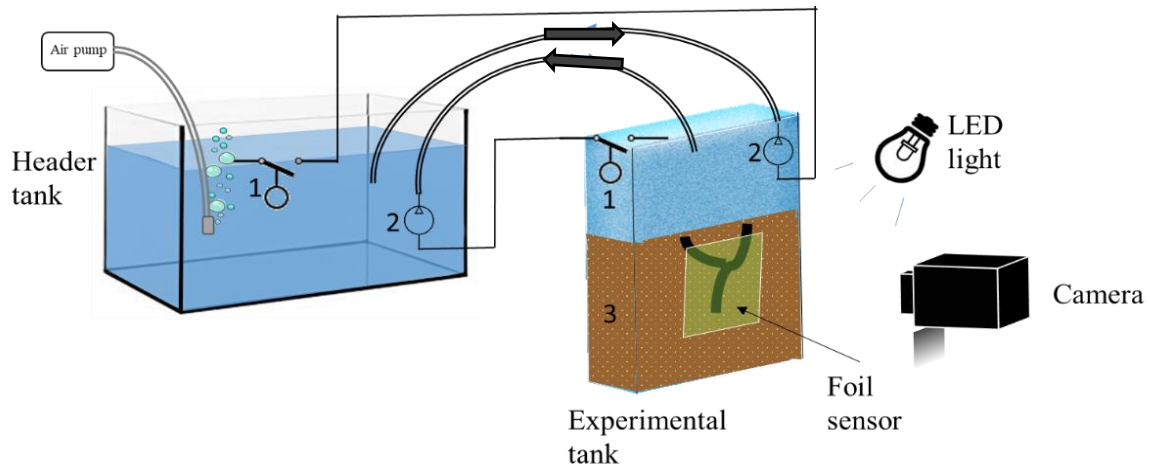


Figure 3. 3: Schematic diagram of the setup for optode sensor foil experiments. The header tank (45cm x 25cm x 25cm) contained seawater which was pH adjusted with a JBL ProFlora control unit, which bubbled CO₂ to reduce water pH. The experimental tank (25cm x 8cm x 25cm) contained natural, filtered sediment (3) and 18‰ (±1‰) seawater. Float switches (1) were used to prevent overflow and mini water pumps (2) were used to circulate the water between the header tank and the experimental tank.

Three worms were added every 24 hours until a burrow was formed adjacent to the sensor foil. Some of the burrows analysed had adjoining secondary burrows that were variously oxygenated. These adjoining burrows were ignored, with only the main (deepest) burrow being analysed. In each instance between six and fifteen worms were added to the experimental tank before an adjacent burrow was formed. This corresponds to equivalent densities of between 30 and 75 individuals per m². Although increasing the density of individuals present in the sediment has been found to increase sediment permeability for densities ranging from 1000 individuals per m² to 9000 individuals per m² (Meadows and Tait, 1989), the density range in this experiment is not thought to impact permeability. Once a burrow was created next to the optode foil, image acquisition began at the next 'dusk' period and ran throughout dark hours.

Burrow O₂

The experimental setup is shown in Figure 3.3. Worms were added to the experimental tank three at a time until a worm burrowed adjacent to the foil. Using the VisiSens camera and AnalytiCal software one image taken every three minutes for a period of 12 hours in the dark. Due to the difficulty in collecting 12 hour long time series, only one repeat for each pH/temperature condition was obtained.

Average burrow O₂ was calculated using VisiSens AnalytiCal software by selection of a region of interest. In order to gain an accurate depiction of in-burrow oxygen levels, a series of 20 images (covering a one hour period) were selected during which time the burrows were actively being utilised by a worm. This effect could be seen by consistently elevated O₂ level (average in-burrow oxygen > 10% air saturation for the entire series). By removing periods where the burrow was inactive, we were able to reduce the impact of low oxygen levels that occur when a burrow is not being irrigated. In order to mitigate the effects of varying O₂ levels in the overlying water, an ‘Oxygen ratio’ was calculated by dividing the average oxygen level in the burrow by the average oxygen level in the water overlying the burrow entrance (Oxygen ratio = in-burrow oxygen / overlying water oxygen) (simplified from Pischedda *et al.*, 2008).

O₂ Penetration Depth

In order to compute oxygen penetration depth, defined as the distance from the sediment surface to the point where oxygen levels reach 0% air saturation, a custom Matlab script was created (see Supplementary Materiel) to process images based on the RGB (red, green blue) levels at the sediment-water interface and at 0% O₂. Average distance between the sediment surface contour and the 0% O₂ contour was calculated in pixels. The number of pixels was converted to mm using a scaling factor which was obtained by measuring the number of pixels in 10mm for each image.

Using inhabited burrows (where $O_2 < 20\%$ air saturation) a series of three consecutive images were selected for penetration depth analysis based on the quality of the burrow image and the oxygen levels within the burrow (higher in-burrow oxygen levels were selected). The average penetration of oxygen into the sediment surrounding burrow walls was calculated and averaged over the 3 images. Between 6 and 8 repeats were acquired for each of the six pH/temperature regimes.

When using planar optode sensors to measure oxygen around cylindrical burrows a small increase in the penetration depth is incurred due to the removal of sediment at the optode sensor, which replaced sediment that would consume oxygen (Murphy and Reidenbach, 2016, Glud, 2008).

In order to accurately detect oxygen penetration depth, an image analysis was conducted using a custom Python script (see Supplementary Materials for script). Initially images were cropped to a section of the burrow. Cropping was selected based on the quality of the image and, where possible, a section approximately half way down the burrow was used. A Gaussian filter was applied to all images to reduce noise. Contours were drawn based on the colour at the sediment/ burrow interface and the colour at 0 % air saturation of oxygen. A dilation and erosion function was applied to fill in any gaps in the contour line. A mask was then applied to the image and the oxygen penetration depth (in pixels) was computed by counting the number of white pixels (which represent oxygen penetration depth) in each image row.

Data screening

Due to the complexity of the experimental setup and difficulty in getting a worm to burrow directly adjacent to the planar optode foil as well as worms frequently leaving their burrows, there was a limited number of successful image acquisition runs. In order to make the most of

the successful acquisition runs burrow images were selected based on best available sequences: 1) in burrow O₂ levels (continually above 10% air saturation for the oxygen gradient measurements and above 20% air saturation for the O₂ penetration depth measurements). This ensured that the burrows were inhabited. 2) Images were taken every 3 minutes and a time-series of 20 successive images (equating to one hour) were selected for oxygen gradient measurements. For oxygen penetration depth measurements a series of 3 successive images (equating to 9 minutes elapsed time) were selected. Screening out burrow images with low oxygen levels removed the issue of analysing uninhabited burrows. A higher minimum oxygen level was used for the oxygen penetration measurements so as to identify penetration depth in actively ventilated inlet burrows.

Statistical Analysis

A Shapiro-Wilks test for normality of data along with a Levene's test for homogeneity of variance was conducted for average burrow oxygen level and oxygen penetration depth (see Supplementary Material). Due to deviations from normal distribution in both the in-burrow oxygen levels data, a robust two-way anova with trimmed means (0.2) was used to compare the means of each pH/ temperature condition followed by a post hoc test using the `mcp2atm` function from the WSM package in R (Mair & Wilcox, 2020). A generalised linear model was used to compare the mean oxygen penetration depth in the six different pH, temperature conditions tested. Burrow width was included in the model in order to test for any confounding effects of this variable. The `lme4` package in R was utilised for this model (Bates *et al.*, 2015)

3.2.4. Results

Oxygen optodes were used to investigate varying oxygen dynamics in the burrows of *Hediste diversicolor* housed in different climatic conditions. Average oxygen levels along with depth of oxygen penetration into the surrounding sediment within burrows were compared for a range of pH-temperature conditions.

Burrow oxygen levels

The depth and shape of burrow varied slightly (minimum vertical depth 45mm in pH 8.1, temperature 18°C, maximum vertical depth 48mm in pH 7.3, temperature 22°C), as did the in-burrow behaviour, with some worms appearing to spend periods outside of the burrow (see Figure 3.4). Worms were weighed prior to being added to the experimental tank (pH 8.1 mean = 0.189g, SD = 0.061; pH 7.3 mean = 0.204g, SD = 0.0751). Figure 3.4 illustrates some of the structural and depth differences between the burrows analysed. Some burrows had adjoining secondary burrows that connected to the sediment surface.

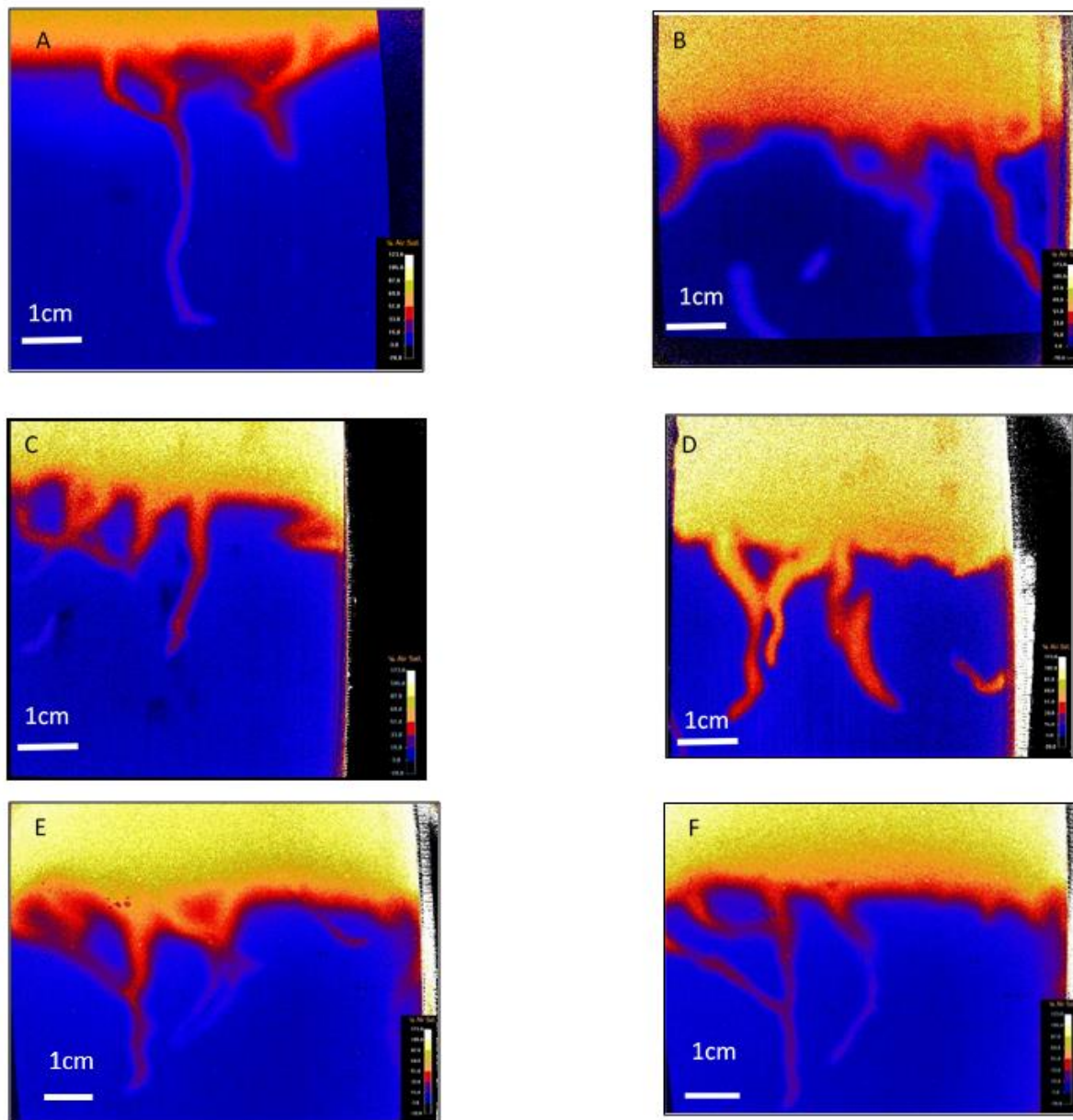


Figure 3. 4: Example images of the burrows used for analysis. A) pH 8.1, temperature 18°C, 45mm vertical depth. B) pH 8.1, temperature 22°C, 47mm vertical depth. C) pH 7.7, temperature 18°C 48mm vertical depth. D) pH 7.7, temperature 22°C, 48mm vertical depth. E) pH 7.3, temperature 18°C 46mm vertical depth. F) pH 7.3, temperature 22°C, 48mm vertical depth.

12 hour O₂ time series

In-burrow oxygen level over the 12 hour sample period was calculated for the six pH/ temperature regimes and by selecting a region of interest the average oxygen level over time could be plotted (Figure 2.5).

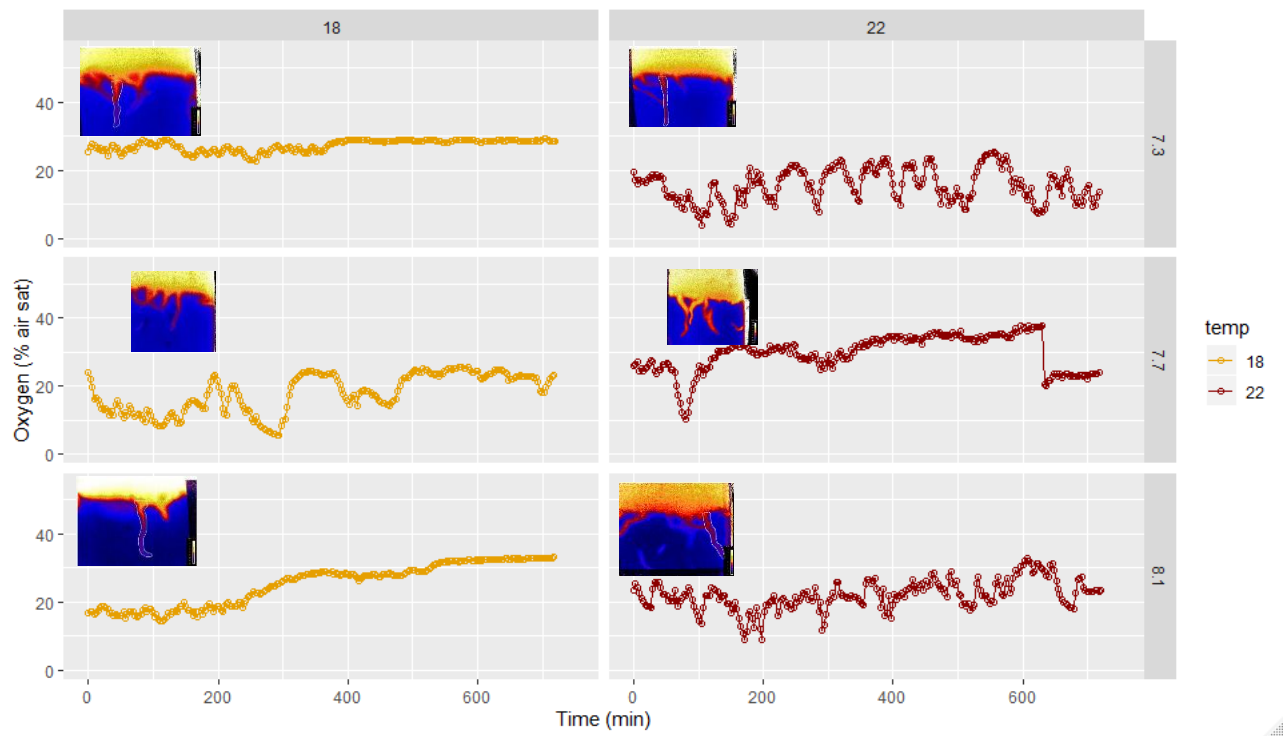


Figure 3. 5: Time series of the in-burrow O₂ fluctuations over a 12-hour image acquisition period for each pH/ temperature regime (n=1 for each regime). Inset on each graph is an image of the burrow with the burrow border drawn in white.

Due to difficulty in collecting twelve hour time series, in each pH/ temperature regime only one burrow was analysed and the data in Figure 3.5 is presented as qualitative. With the exception of pH 7.7, in-burrow O₂ appears to fluctuate less in the cooler temperature regimes (18°C). The pH 7.3, low temperature (18°C) regime has the lowest levels of in-burrow oxygen fluctuation over the 12 hour period, whereas the pH 7.3, high temperature (22°C) showed very high regular fluctuations. A similar pattern is seen at pH 8.1, with very low fluctuations at 18°C

and high fluctuations at 22C. The impact of pH is less clear with little link between pH and oxygen fluctuation.

Oxygen Ratio

Oxygen ratio was calculated using the ratio between the oxygen levels in the burrow and the oxygen levels in the overlying water. This compensates for any variation in oxygen levels in the overlying water across the different regimes.

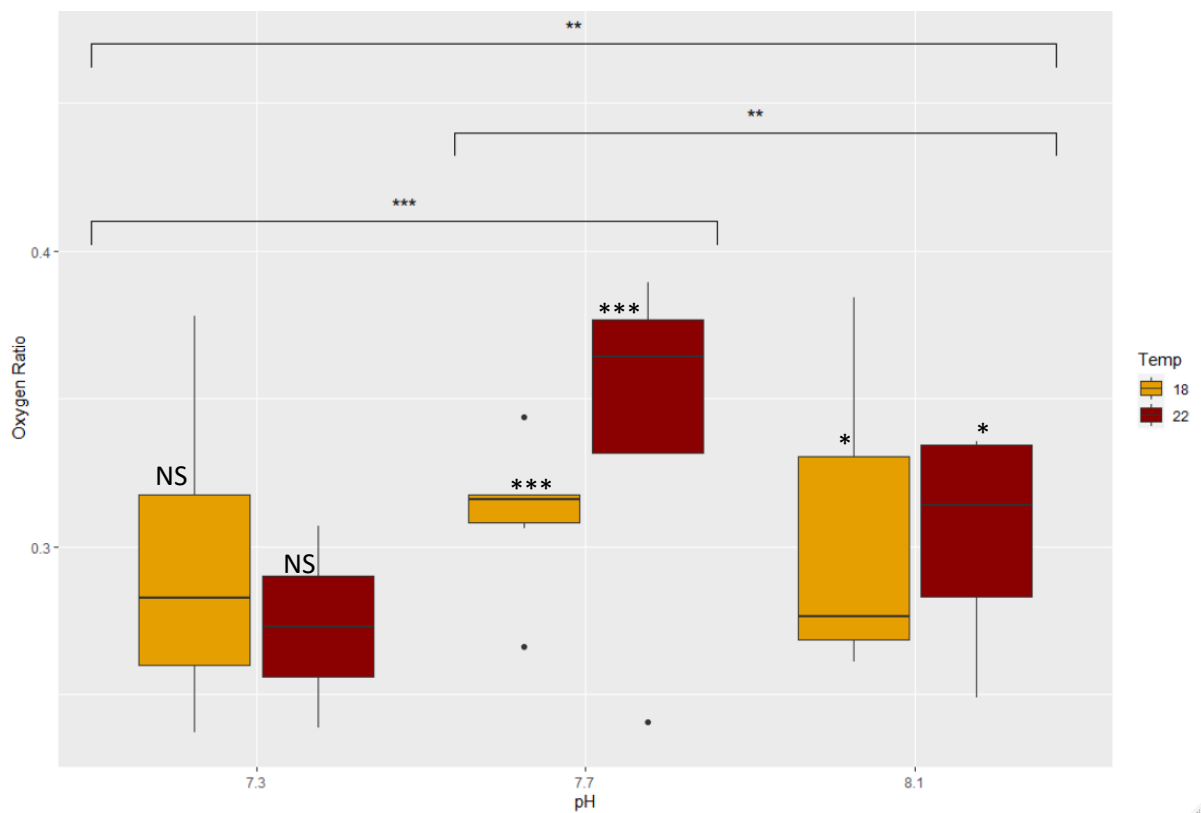


Figure 3.6: Boxplot comparing the burrow O₂ ratio across the six pH and temperature regimes. O₂ ratio was calculated using the ratio between in-burrow oxygen and overlying water oxygen levels. Lower ratios indicate a higher difference between oxygen in the burrow and the oxygen in the overlying water. Black circles indicate outliers. N=5 for each pH/ temperature condition. A significant difference was found between each pH regime (robust factorial anova with trimmed mean (0.2), $p=0.001$) but not between temperature regimes ($p=0.147$). The interaction effect (temperature~pH was significant ($p=0.004$), therefore an mcp2atm post-hoc test was run to investigate independent effects (Mair and Wilcox, 2020) ($p=0.002$ for pH 7.7

vs. pH 8.1, $p=0.004$ for pH 7.3 vs. pH 8.1, $p=0.0001$ for pH 7.3 vs pH 7.7 as well as a significant difference between the two temperatures at pH 7.7 ($p = 0.0009$) and pH 8.1 ($p=0.04$) but not at pH 7.3 ($p=0.4$)). Significance levels; $p<0.05$ (), $p<0.01$ (**), $p<0.001$ (***)*.

The highest Oxygen ratio is at pH 7.7, 22°C, which, along with pH 7.7, 18°C are significantly higher than in any other conditions. In addition, pH 7.3 and 8.1 are also associated with lower oxygen ratios. Significant differences were found between all pH conditions using robust factorial anova with trimmed mean ($p=0.002$ for pH 7.7 vs. pH 8.1, $p=0.004$ for pH 7.3 vs. pH 8.1, $p=0.0001$ for pH 7.3 vs. pH 7.7). Additionally, a significant interaction effect was found between temperature and pH ($p=0.004$). Post hoc tests using the `mcp2atm` function in R (Mair & Wilcox, 2020) show a significant difference between the two temperatures at pH 7.7 ($p = 0.0009$) and pH 8.1 ($p=0.04$) but not at pH 7.3 ($p=0.4$). The graph appears bell shaped for both temperature and pH, with a peak in oxygen ratio at pH 7.7.

Oxygen penetration depth

Using inhabited burrows (where $O_2 < 20\%$ air saturation) a series of three consecutive images were selected for penetration depth analysis based on the quality of the burrow image and the oxygen levels within the burrow (higher in-burrow oxygen levels were selected). The average penetration of oxygen into the sediment surrounding burrow walls was calculated and averaged over the 3 image (9 min) recording period.

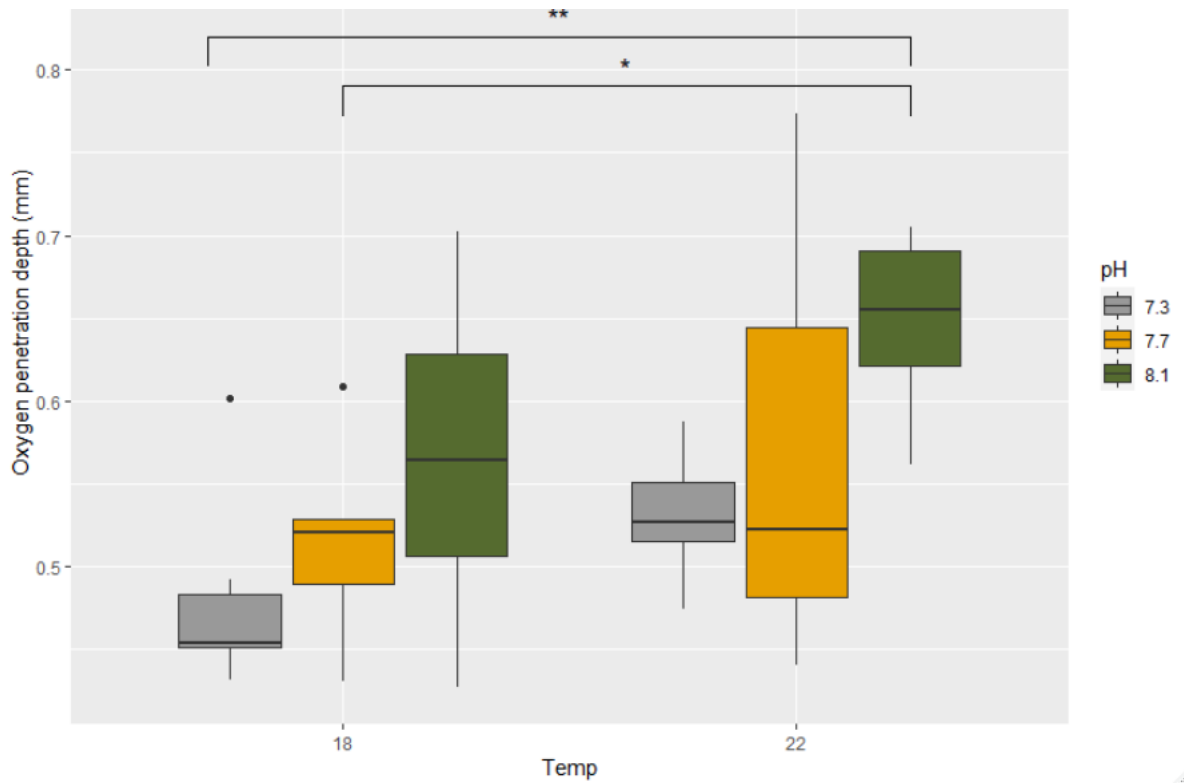


Figure 3. 7: Boxplot comparing the average O₂ penetration depth (mm) into the sediment surrounding burrow walls across the six pH and temperature regimes. Black dots indicate outliers. A significant difference was found for temperature ($p=0.015$) and pH ($p=0.004$) but no significance was found for the pH: temperature interaction ($p=0.58$), based on ANOVA with trimmed mean (0.2) using the WSM package in R. Significance levels; $p<0.05$ (*), $p<0.01$ (**), $p<0.001$ (***)).

The oxygen penetration depth varies with temperatures ($p=0.015$ between 18 and 22°C) as well as with pH ($p=0.004$) based on ANOVA with trimmed mean (0.2) using the WSM package in R. No significance was found for the interaction between pH and temperature.

Burrow width analysis

A Matlab script was used to measure the width of each burrow used in oxygen penetration depth analysis in order to check for any relationship. Figure 3.8 shows a plot of the relationship between the burrow width and oxygen penetration depth, no correlation was found (Spearman's Rank = 0.098, p -value = 0.2603).

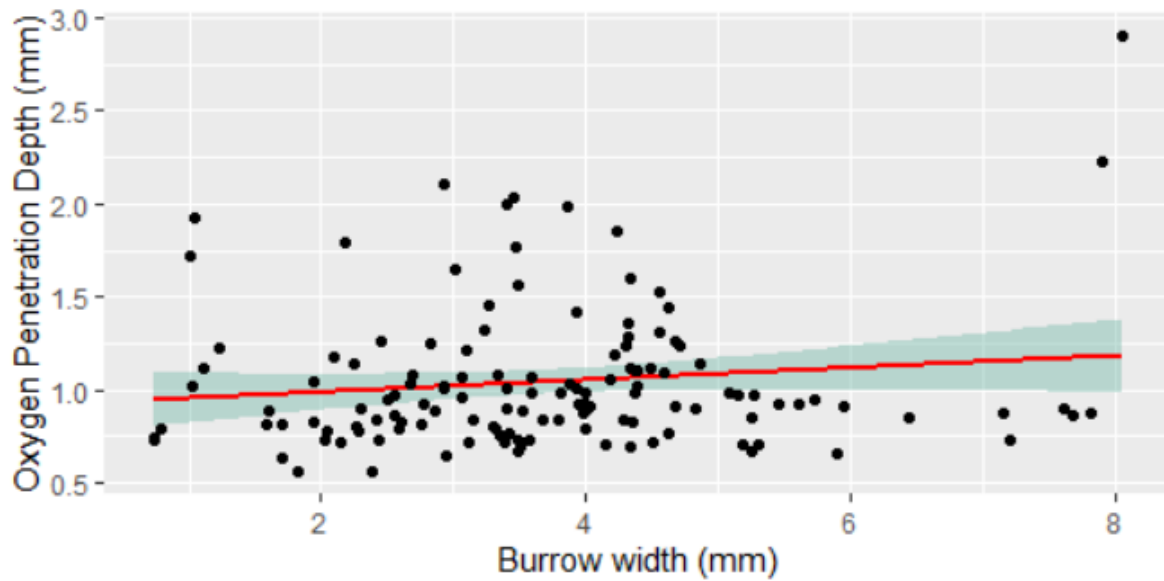


Figure 3. 8: Scatter graph comparing the average width of each burrow with oxygen penetration depth into the sediment surrounding the burrow. No correlation was found (Spearman's Rank = 0.098, p -value = 0.2603).

3.2.5. Discussion

Estuarine environments are highly fluctuating environments with daily and seasonal pH, temperature and salinity cycles. Environment Agency data collected at New Holland in the Humber Estuary between 1991 and 2005 show daily fluctuations of 0.56 pH units between low and high tide (pH 7.77 to pH 8.26) and seasonal fluctuations of 1.54 pH units (pH 7.0 to pH 8.54), as well as seasonal temperature fluctuations of 19.5°C (3°C to 22.5°C). The pH and temperature conditions used in this study are therefore not outside of present-day extreme conditions and these extremes will likely get worse with climate change. The animals used in these experiments were not collected from the wild but were second and third generation worms housed in static pH and temperature conditions so no pre-acclimation was required. The temperature that worms were kept in (18°C) is representative of UK summer temperatures and the constant temperature prevented large scale maturation events. During maturation worms divert energy resources into gamete development prior to spawning and this has the potential to effect behaviour, growth and metabolism (Hardege, pers. comm, March 2021).

Comparing Average Burrow O₂ Timelines

Relatively constant in-burrow oxygen levels are interpreted as the burrow being continuously inhabited and frequent ventilation behaviour occurring. Conversely, fluctuations in oxygen levels suggest that the burrow may be empty for periods, potentially while feeding behaviour occurs or alternate burrow structures are being formed. Lower in-burrow fluctuations in cooler temperatures suggests that worms are consistently inhabiting and frequently ventilating their burrows in these conditions. However, the pH 7.7/18°C regime shows slightly higher oxygen fluctuations over the 12-hour period, suggesting that the worm engaged in other behaviours such as burrow building or feeding during this period (Figure 3.5). *H. diversicolor* were collected from the Humber Estuary where average pH is 7.69 and average annual temperature is 11.3°C (based on Environment Agency data from 1996 to 2005). It is possible that this slight increase in oxygen fluctuation is linked to the fact that pH7.7/ 18°C is the condition closest to those that the *H. diversicolor* are adapted to. However, the link between higher temperature and increased burrow oxygen fluctuations could be linked to higher oxygen demand (due to increased metabolic rate) at these temperatures causing an associated increase in feeding behaviour in order to compensate for increased energy use by the worms.

A previous study of oxygen levels in *H. diversicolor* burrows has found similar rates of oxygen fluctuation (at the scale of minutes when burrow is inhabited) (Pischedda et al., 2008). Other studies have used water flow out of burrows to monitor oxygen levels and ventilation rates and have identified cycles of active and resting phases lasting approximately 10 minutes and 5 minutes respectively (Kristensen, 1981). This study was unable to clearly identify specific ventilation patterns, in part due to the time lag between images (3 minutes). There was also a high degree of variability between ventilation patterns between the conditions and further repeats would be needed to establish a baseline pattern and allow quantitative comparisons to other conditions.

Oxygen fluctuation in sediments has been linked to switches between the type of bacterial metabolism occurring, which in turn influences geochemical cycling and burial of organic matter (Hansen and Kristensen, 1998). Furthermore, organic matter degradation in oxic conditions has been found to occur up to ten times faster than in anoxic conditions (Kristensen, 2000), therefore the more stable oxygen profiles identified at lower temperatures may be beneficial for organic matter cycling.

Due to the logistical and technical difficulties in collecting 12 hour time series, only one repeat was acquired per pH/ temperature condition. This data is therefore anecdotal and more data is needed before any significance can be drawn. Where only one burrow opening was seen (in most of the burrows analysed) the direction of flow during ventilation is not known. Therefore oxygen analysis could be effected depending on whether the intake or exhaust opening was analysed. Pischedda et al. (2008) found a difference of 6.8 $\mu\text{mol/L O}_2$ concentration in the intake compared to exhaust openings. Although it was assumed that during periods of low in-burrow oxygen, worms were exhibiting foraging or burrow building activities, it would be necessary to identify these behaviours with visual observations.

Comparing Burrow O_2 Gradients

Lower Oxygen ratios indicate a large variation between the oxygen levels in the overlying water and those within the burrow. This is interpreted as low ventilation effort and/or high oxygen consumption by the worms. Low Oxygen ratio could also be indicative of temporary burrow abandonment, which rapidly leads to a large difference between the high oxygen levels in the overlying water and low oxygen levels within the burrow. This was compensated for by selecting one-hour time series with active burrows (average in-burrow oxygen > 10% air saturation). Conversely, high Oxygen ratios are indicative of high ventilation effort and/or low oxygen demand.

There was a significant difference between the two temperatures at pH 7.7 ($p = 0.0009$) and pH 8.1 ($p=0.04$) with lower temperatures were associated slightly with lower Oxygen ratios (therefore likely lower ventilation effort). However, this was somewhat confounded by the impact of pH, which appears to reduce Oxygen ratio at the lowest and highest pH (7.3 and 8.1). Figure 3.5 illustrates that temporary burrow abandonment at 18°C was relatively low and oxygen levels were maintained relatively consistently. It is possible that oxygen demands by the worm are lower at cooler temperatures and therefore maintenance of high oxygen levels within the burrow was less critical. Increased metabolic rate by the worms at elevated temperatures (e.g. Freitas et al. (2016) and associated increase in oxygen demand may have induced this increased ventilation effort.

Oxygen ratios are lower at pH 7.3 and 8.1, suggesting that ventilation effort is reduced at these pH conditions and/or that worms are rapidly absorbing available O₂. Freitas et al. (2016) found an increase in metabolic capacity in *H. diversicolor* exposed to reduced pH, therefore the low ratio seen at pH 7.3 may be linked to an associated increase in O₂ demand at this condition. Interestingly, at pH 7.7, Oxygen ratios appear to be elevated irrespective of temperature (pH 7.7 vs. pH 8.2: $p=0.004$, pH 7.7 vs. pH 7.3: $p<0.0001$). This pH condition is the closest to the average pH in the Humber Estuary (pH 7.69, based on Environment Agency data). Worms may therefore be best adapted to this pH (despite all worms being F2/3 generation, raised in the pH condition they were tested in) and therefore have lower metabolic requirements and an associated reduced O₂ consumption at this condition, which would help explain the higher oxygen ratios.

Hediste diversicolor are resistant to the effects of reduced O₂ and employ a range of behavioural (e.g. increased ventilation frequency) and physiological (e.g. optimisation of O₂ extraction from the water and switching to anaerobiosis) mechanisms (Kristensen, 1983, Schöttler, 1979). The increased ventilation effort at elevated temperature regimes found in this

study may be a behavioural response to lower oxygen solubility at higher temperatures. Alternatively, reduced O₂ solubility at high temperatures may lead to worms employing temporary anaerobiosis, therefore reducing oxygen consumption leading to higher oxygen levels within the burrow and an associated increase in Oxygen ratio.

The burrows of *H. diversicolor* are typically U or Y shaped with one opening used as an inlet and one as an exhaust opening during ventilation (Pischedda et al., 2012). The burrow images collected during these experiments were 2-dimensional and relied on worms creating burrows adjacent to the planar optode. Although several of the burrow images showed multiple openings to the surface, some burrow images only had one opening, likely because the secondary openings were not adjacent to the planer optode. Where multiple burrow openings were imaged, the dominant (and therefore, likely the inlet) stem was analysed. The dominant stem was identified by the clarity of the image (driven by oxygen levels) and was usually a vertical burrow leading from the sediment surface directly down into the sediment. Although attempts were made to analyse inlet burrows, oxygen levels around inlet openings are higher than those of exhaust opening and this could have had an impact on the oxygen levels measured in this experiment. Burrow formation also tended to be more complex than the standard U or Y shape expected, with multiple surface openings, often extending from a dominant stem (see figure 3.4 for examples), further confounding efforts to identify inlet and exhaust opening.

Comparing Oxygen penetration

Although highly variable, there is an apparent increase in O₂ penetration depth with increasing temperature ($p=0.015$) as well as an increase in penetration depth with increasing pH ($p=0.004$). The increased oxygen penetration depth found at higher temperatures (see Figure 3.6; 18°C and 22°C) could be explained by the higher ventilation effort drawing more oxygen into the burrow.

The lower O₂ penetration depths seen at reduced pH may be linked to higher oxygen demand by the worms in these lower pH conditions (e.g. Freitas et al. (2016), diverting oxygen away from the sediment. Alternatively, the mucus that is produced by *H. diversicolor* to line burrow walls and provide structural stability of burrows (Meadows et al., 1990, Meadows and Tait, 1989), has an additional function to act as an antioxidant defence to protect the worm from reactive oxygen species (present in the sediment due to UV radiation and bacterial/ fungal activity) which occur more frequently at low pH (Moraes et al., 2006, Bhuiyan et al., 2021b). Additional mucus may be produced as a protection mechanism when worms are exposed to reduced pH conditions and this additional mucus may act to prevent oxygen diffusion into the sediment, subsequently reducing penetration depth. Furthermore, penetration depth may be impacted by varied biofilm growth lining the burrow walls. Respiration of burrow microbes along with the burrower organism quickly deplete oxygen in stagnant burrow water (Murphy and Reidenbach, 2016) and more established burrow microbes would likely reduce the amount of O₂ available for diffusion into surrounding sediments. It is possible that low pH/ low temperature conditions may favour the establishment of burrow microbes and lead to reduced oxygen penetration depth.

Timmermann et al. (2006) reports that 49% of oxygen pumped into the lugworm *Arenicola marina* burrows was consumed by the worm, with 23% was lost to diffusive mediated transport to the burrow wall. If penetration depth across the burrow wall is increased at higher pH and higher temperatures, these percentages may alter.

Oxygen penetration depth into the sediments has been linked to proximity to the burrow entrance as well as oxygen concentrations in the burrow lumen (Pischedda et al., 2008, Timmermann et al., 2006). Although Pischedda et al. (2008) measured oxygen penetration depths of between 1.67mm and 3.27mm, dependant on the proximity to the burrow entrance, Timmermann et al. (2006) measured a penetration depth of 0.7mm in *Arenicola marina*

burrows, which is more similar to the readings in this study. A more recent study on the clam worm *Alitta succinea* determined that irrigation of the burrow results in oscillations in oxygen flux across the burrow wall (Murphy and Reidenbach, 2016). The same study found that increased temperature resulted in increased irrigation frequency by the worm and a corresponding increase in volumetric flow rate and oxygen flux across the burrow wall, although, time averaged oxygen flux did not change with temperature nor did sediment penetration of oxygen (Murphy and Reidenbach, 2016). This study found an overall increase in Oxygen ratio, suggesting elevated ventilation effort at higher temperatures (22°C) which may also help to explain the larger oxygen penetration depths identified in higher temperatures.

Limitations

The complexity of the experimental setup used in this chapter meant that it was very time consuming to collect sufficient data for analysis. Technical issues along with interruptions due to covid lockdown limited the scope of this experiment. Given more time, this method could be used to investigate a range of in-burrow measurements such as ventilation rate and frequency as well as the impact of burrow density on sediment oxygen levels. Similar setups can also be used to measure pH and dissolved CO₂ concentrations which could potentially be used to investigate the impact of multiple stressors on respiration in a mesocosm or to tease apart the effects of pH, CO₂ and alkalinity on burrowing marine invertebrates.

As mentioned previously, where only one burrow opening was seen (in most of the burrows analysed) oxygen analysis could be affected depending on whether the intake or exhaust opening was analysed. Other potentially confounding variables include; the width of the burrow and size of worm ventilating it; the age of the burrow which could potentially impact hydrodynamics due to increased complexity (although all worms were given at least 24 hours to create a burrow) (Davey, 1994); the age of the burrow and its associated effect on presence

of bacterial communities (Marinelli et al., 2002). Natural variations in the pH, salinity, temperature and oxygen levels in estuarine systems are likely to make in-burrow oxygen dynamics highly variable depending on daily and seasonal fluctuations, however this is outside of the scope of this study. Future work should aim to incorporate a more natural set of conditions and include diurnal variations in biogeochemical conditions.

Further research is required to investigate the link between ventilation frequency, ventilation intensity (pumping rate) and associated Oxygen ratios in order to gain a better understanding of the mechanisms involved.

4.0. Chapter 4

Mucus production in future climatic conditions

4.1. Mucus production in future climatic conditions

4.1.1. Abstract

Due to their population density and burrowing activities *Hediste diversicolor* is considered a keystone specie in estuarine sediments. *H. diversicolor* line their burrows with mucus and produce mucus nets on the sediment surface to trap food. Mucus may also play a role in isolating invertebrates from surrounding environmental conditions and as such have a protective function in stressful conditions. Mucopolysaccharides (mucus) produced by many marine invertebrates can act as a source of organic carbon to microbiota and *H. diversicolor* mucus has been found to affect microbial communities involved in nitrogen cycling. CO₂ emissions into the atmosphere dissolve into the ocean and are driving a reduction in ocean pH. By the end of the century some scenarios predict that ocean pH will reduce from today's pH8.1 to pH7.3 and average temperatures may increase by more than 4°C. This study investigates whether water pH and temperature have an impact on the quantity and carbohydrate levels in the mucus produced by *H. diversicolor* with a view to examine the impacts of future marine conditions based on these climate change scenarios. No significant difference in dry mass of mucus was observed between pH8.1 and pH7.3 or between 18°C and 22°C, suggesting that *H. diversicolor* may be robust to these conditions. However, carbohydrate content was significantly lower in mucus produced at lower pH and higher temperatures. This may be due to the energetic costs associated with producing carbohydrates in more stressful environmental conditions. The results of this study suggest that future climatic conditions will be associated with reduced carbohydrate content in the mucus of *H. diversicolor*. Invertebrate mucus has been linked to sediment microbiota and sediment carbohydrate content has been positively associated with nitrification rates. Both microbial community composition and nitrogen cycling could be affected in future climate scenarios.

4.1.2. Introduction

Increasing carbon dioxide levels in the atmosphere dissolves into surface oceans altering ocean chemistry and driving pH decline (e.g. Doney et al., 2009, Raven et al., 2005). Coupled with this are increasing ocean temperatures driven by increasing greenhouse gasses and associated atmospheric warming (e.g. Laffoley and Baxter, 2016). The IPCC report that average surface ocean pH has declined by 0.1pH units since pre-industrial times and average ocean temperatures have increased by 0.11°C per decade between 1971 and 2010 the same period (IPCC, 2013b). Furthermore, by 2100 pH are predicted to decline by up to 0.32pH units and temperatures increase by up to 4.8°C (RCP8.59, IPCC, 2013b). Burrowing marine invertebrates are traditionally believed to be relatively tolerant of changing climatic conditions due to the buffering effect of living in sediments and exposure to naturally fluctuating conditions such as estuarine environments (Freitas et al., 2016). Despite this some studies have found that reduced water pH: Reduces feeding rate, slows chaetiger regeneration and induces oxidative stress in *Hediste diversicolor* (Bhuiyan et al., 2021a); reduces fertilization success in *Pomatoceros lamarckii* (Lewis et al., 2013); reduces survival rate, burrowing activity and glycogen content in *Nereis virens* (Batten and Bamber, 1996). The effect of increasing temperature may act synergistically with pH for some behavioural or physiological impacts in some species (e.g. reduced chaetiger regeneration and increased mortality in low pH (pH 7.0) and high temperature (25°C) conditions when compared to low pH and low temperature (15°C) in *H. diversicolor* (Bhuiyan et al., 2021a). Other research on the polychaete *Alitta virens* found that the impacts of pH and temperature are not detectable in the short-term, but affect growth, bioturbation and bioirrigation behaviour and in turn nutrient generation over longer term (542 days) (Godbold and Solan, 2013). Godbold et al. (2011), Godbold and Solan (2013) also highlight that seasonal temperature and photoperiod variation could either exacerbate or buffer these long-term climatic effects.

As a keystone species (Moreira et al., 2006, Mermillod-Blondin et al., 2005) burrowing *Hediste diversicolor* provides a service to microbes and meiofauna by providing additional oxygenated habitat at the sediment-water interface. Banta et al. (1999) found that the presence of *H. diversicolor* in sandy sediment stimulated O₂ uptake and CO₂ release by 80 to 90% indicating an increase in benthic metabolism by the worms and associated microbial activity. Increasing oxygenation of the sediment alters the pace of nutrient and organic matter cycling and the feeding activities of this species acts as a rate-limiting step in estuarine detritus processing (Moreira et al., 2006, Mermillod-Blondin et al., 2005).

Mucus secreted by *Hediste diversicolor* is used to line burrow walls, providing stability to the burrow networks they create. Mucus may also act as an antioxidant defence against reactive oxygen species (Moraes et al., 2006). In addition, mucus nets are produced in order to catch falling particles for later ingestion. An inadvertent attribute of this mucus is the binding together of sediment particles, leading to an increased shear strength and improved sediment stability (Meadows et al., 1990, Meadows and Tait, 1989). Lateral compaction of sediment induced by the creation of burrows is also believed to increase shear strength of sediments (Fernandes et al., 2006). However, the mechanical reworking of sediment by bioturbating organisms creates a fluid surface layer that is easily re-suspended (Rhoads and Young, 1970), permeability is found to increase with *H. diversicolor* density (Meadows and Tait, 1989) and some results show that sedimentation is reduced when natural densities of *H. diversicolor* are present (Meadows et al., 1990).

The presence of invertebrate mucus compounds in benthic sediments provides habitat for microbial fauna which can have a profound effect on biogeochemical cycling within the sediment (Dale *et al.* 2019). Although these interactions are poorly understood Dale (2019b) found that presence of *H. diversicolor* mucus enhances sediment nitrification rates by enhancing nitrifying microbial groups. Indeed, it has been proposed that invertebrate

polysaccharide groups in benthic sediments ought to be considered as a distinct functional trait when assessing invertebrate contributions to sediment ecosystem function (Dale, 2019b). Therefore any impact on the presence of mucus in marine sediments could have a serious ecosystem wide effect.

This experiment aims to investigate variability in the quantity and total carbohydrate content of mucus produced by *H. diversicolor* in four pH/ temperature regimes. The worms were tested at pH 8.1, which is representative of current average oceanic conditions and pH 7.3 which is representative of conditions that will be common in 2100 (Bindoff et al., 2019). Temperature conditions were chosen based on current summer temperatures (18°C) and temperatures likely to be experienced regularly by the end of the century (22°C) (Collins M., 2019). Impacts on the quantity and quality of mucus produced by *H. diversicolor* could have a profound impact on estuarine habitats, impacting sediment stickiness as well as the micro and macro fauna that depend on the mucus for habitat or sustenance (Kristensen, 2005). Previous research has linked increased mucus production to several stressors, including elevated levels of pollution (e.g. Bastidas and Garcia, 2004) and increased water temperature (Neudecker, 1981, Tal et al., 2021). We hypothesise that reduced pH and increased temperature will increase the quantity of mucous produced by *H. diversicolor* as a response to more stressful conditions. Also, that higher carbohydrate concentrations will occur in the mucous produced at lower pH and at higher temperatures, again as a defence mechanism against stressful conditions.

4.1.3. Method

Worm collection and housing

Approximately 800 *Hediste diversicolor* were collected from Hessle Foreshore on the Humber Estuary in East Yorkshire, UK (53°42'52.94"N, 00°27'11.2"W) on 25th October 2018 by shovel sampling. Worms were then transported to the University of Hull where they were removed from the natural sediment and placed in three tanks containing washed coral sand

(4cm depth) and 18‰ salinity ($\pm 1‰$) water, which was aerated with an air stone. The climate was controlled at 18°C, 12 hours light, 12 hours dark with natural moonlight cycles mimicked using a UV light.

Initially the water pH was set at 8.1 for a period of one week, after which time the pH was reduced in two of the tanks by bubbling CO₂ through the water. After fourteen days the tanks were set at pH 8.1 and pH 7.3 (the pH control units were accurate to a standard error of ± 0.0081 , ± 0.0075 and ± 0.0055 for the pH 8.1, 7.7 and 7.3 tanks respectively based on daily recordings of pH. See supplementary materials for data). The pH of the water was controlled using JBL ProFlora pH control units, which constantly monitored pH and triggered CO₂ bubbling if the pH reached 0.05 pH units above the specified level. The pH conditions were chosen based on: current average ocean pH (8.1); pH conditions expected by 2100 based on the IPCC RCP8.5 climate model (pH 7.7) (IPCC, 2013b) and a more extreme condition likely to be found in future estuaries given a predicted decline of 0.32 pH units by 2100 based on the same climate model (IPCC, 2013b). The temperature that worms were kept in (18°C) is representative of UK summer temperatures and the constant temperature prevented large scale maturation events. The warmer temperature condition used (22°C) was based on RCP8.59 IPCC climate predictions of an increase in surface temperatures between 2.6°C and 4.8°C.

An air pump was used to maintain oxygen levels in the tanks and an 'AllPondSolutions' aquarium filter with activated carbon filter element (600l per hour flow) maintained water clarity. Several reproduction events occurred over the duration of this experiment across all three tanks. The animals used in these experiments were not those collected from the wild but were second and third generation worms housed in static pH and temperature conditions so no pre-acclimation was required prior to experimentation. By using F2 and F3 generation worms the impacts of acclimation and acclimatisation were removed and inter-generational, long term impacts of pH could be assessed.

Mucus collection method

30 worms (*Hediste diversicolor*) were selected from each culture tank (pH8.1, 18°C and pH7.3, 18°C) culture tank. These worms were blotted dry on a paper towel and weighed on weighing scales (Mettler, accurate to ± 0.0001 g) in order to acquire a wet weight. These worms were then split into 6 groups of 5 worms and placed in one of 18 glass basins (190mm diameter) containing 1.5L of 18% artificial seawater (TropicMarin). A folded piece of black polypropylene sheet (300mm x 300mm) was added to each basin and completely submerged. Polypropylene is a non-leaching plastic and therefore removes the impact of leachate chemicals. This provided a place for the worms to hide in and acted as a surface onto which mucus was secreted. This also prevented the worms from cannibalising one another by creating separate spaces for the worms to inhabit. An air pump and airstone were used to maintain oxygen levels in the water and salinity was tested daily and adjusted when necessary. The pH was maintained using a JBL pH control unit which bubbled CO₂ through the water when the pH drifted +0.05 pH units above the desired level. Due to the small volume of water in each basin additional control valves were used to slow the release of CO₂ and prevent pH 'overshoot'. Temperature control was achieved either by placing the basins in a temperature controlled room (18°C) or by placing the basins in a water bath that was warmed to 22°C (temperature in the basin was found to warm up to 22 °C after 4 hours in the water bath). These methods were used to create 3 basins for each of the 4 pH/ temperature condition (pH 8.1, 18 °C; pH 8.1, 22°C; pH7.3, 18°C; pH7.3, 22°C). Worms remained in the basins for 96 hours after which time the polypropylene sheet was removed and a plastic razorblade used to scrape the mucus and residual artificial seawater into pools which were collected in syringes. This process was repeated with the glass basin once the majority of the artificial seawater was drained. The samples were then transferred from the syringes into appropriate lengths of Biotech Cellulose Ester Dialysis Membrane (3.1ml/cm, Spectra/Por

Biotech CE Trail Kit, MWCO: 100-500 D) which were sealed off as both ends using plastic clips. The samples in the dialysis membrane were then suspended in 2.5L ultrapure water with a magnetic stirrer running for 3 days, with the ultrapure water being replaced after 2 hours, 4 hours, 12 hours, 36 hours and 60 hours. This process removed the salt from the samples. After dialysis the samples were transferred to glass jars and frozen at -20°C until further analysis could be done. Samples were freeze dried overnight in a VirTis SP Scientific lyophiliser and the dried samples were weight using Mettler scales, accurate to $\pm 0.0001\text{g}$.

Chemical analysis

A modified Dubois assay was used to measure carbohydrate concentrations in the mucus samples collected (Dubois et al., 1956). A standard glucose curve was made by weighing out known amounts of glucose and mixing with corresponding volumes of distilled water in a volumetric flask.

The chemicals used for this method were analytical grade. Phenol 5% solution, analytical grade concentrated sulphuric acid (min assay 98% BDH 102761C). 5ml of the glucose standard samples were decanted into a test tube and 0.5 ml of 5% phenol solution followed immediately by 2.5 ml of concentrated sulphuric acid were added directly onto the solution surface and solution was vortexed for 10 seconds. These solutions were left for 35 minutes to develop after which time they were decanted into cuvettes and the absorbencies (spectrophotometer) at 485 nm were measured three times per sample. Distilled water and assay reagents are used to form a zero baseline. Three curves were made and the average used to calculate the linear regression used to convert the absorbance into glucose equivalents. Data was plotted as absorbance against glucose to make standard curve.

Total carbohydrate fraction

Freeze dried mucus samples were weighed and 1ml distilled water added. This was vortexed and then centrifuged at 2500 rpm for 15 minutes. 0.5ml of the supernatant was decanted into a boiling tube. A blank was made by adding 1ml of distilled water to a boiling tube. 0.5 ml of 5% phenol solution followed immediately by 2.5 ml of concentrated sulphuric acid were directly onto the solution surface and this solution was vortexed for 10 seconds. Samples were left for 35 minutes for the colour to develop. Supernatant was decanted into cuvettes and measure absorbencies (spectrophotometer) at 485 nm. Distilled water and assay reagents are used to form a zero baseline. The absorbance value is converted to concentration (μg glucose equivalents ml^{-1}) by using a standard curve. The resulting value multiplied by the proportion of total extraction solution volume to the volume used for the assay (e.g. if 400 μl of sample is taken from a total volume of extraction solution of 600 μl this value will be 1.5). This value is then divided by the dry weight of the sample to obtain the amount of carbohydrate expressed as mass of glucose equivalents per mass of dry sediment (μg mg^{-1}).

Statistical analysis

A Shapiro-Wilks test for normality of data along with a Levene's test for homogeneity of variance was conducted for both mucous produced per gram of tissue and carbohydrate concentration. A two way factorial ANOVA was then computed for both of these variables to test for significant difference between different pH/ temperature conditions. The impact of total biomass of worms in each test condition was plotted against the dry mass of mucous they produced to identify any relationship between these variables and a Loess smoothing function was used to produce a line of best fit.

Carbohydrate analysis

A glucose standard curve was created using the colorimetric absorbance values at 485nm for known concentrations of glucose (see Figure 4.2)



Figure 4. 1: Glucose calibration curve (dissolved in distilled water) measured at 490 nm according to protocol. . Each calibration point represents the average of 3 technical replicates. The blue line represents linear fit of the measured points calculated by the least squares method. The linear regression equation ($y = ax + b$) represents calibration equation slope (α) and intercept (β). The R^2 coefficient was calculated by the least squares method.

Total carbohydrates in each mucus sample was investigated using colorimetric analysis. Measured concentration was calculated using the equation from the calibration curve (Figure 4.3). Carbohydrates in each sample solution were then calculated using Formula 1:

$$\text{Carbohydrates concentration } [\mu\text{g ml}^{-1}] = \text{measured concentration} \times \frac{\text{volume of 2.5\% phenol } (\mu\text{l})}{\text{volume of sample } (\mu\text{l})}$$

4.1.4. Results

Mucus production under different climatic conditions was investigated with four pH/ temperature regimes tested. Mucus production (from weighed, freeze dried samples) per gram of worm biomass was calculated and Figure 4.2 shows the variation in production.

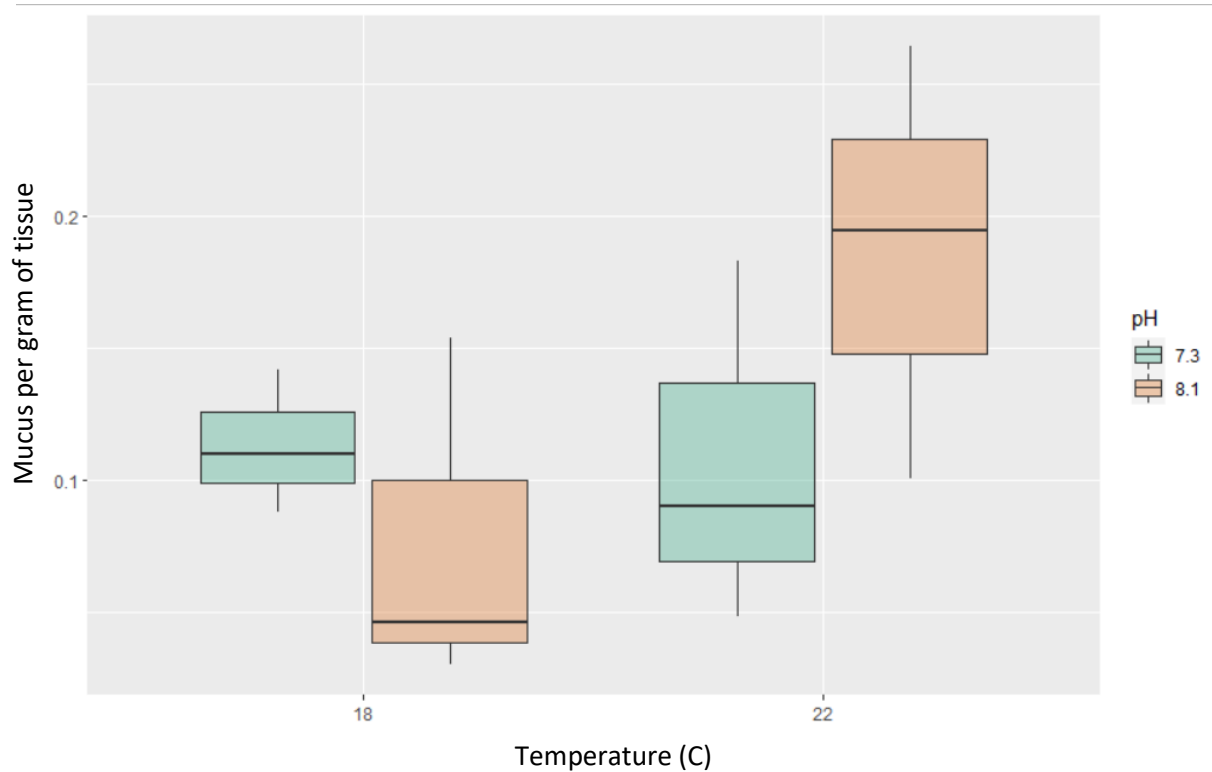


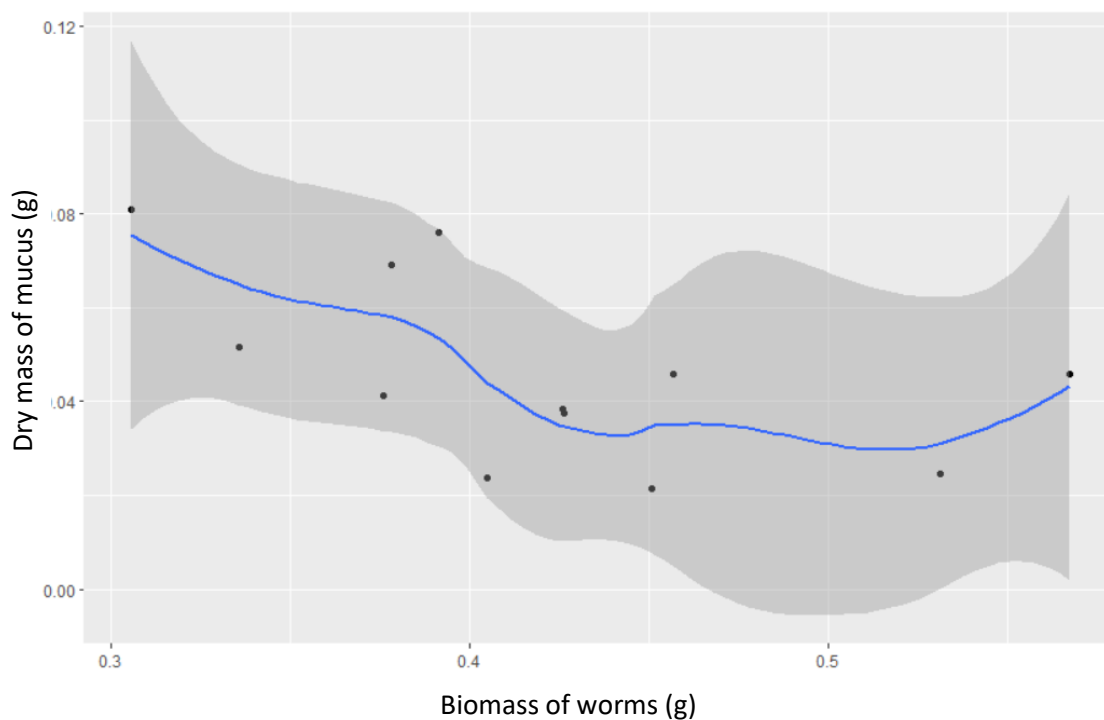
Figure 4. 2: Bar plot illustrating the mean (\pm standard deviation) mucus production per gram of biomass by the harbour ragworm *Hediste diversicolor* at different pH/ temperature conditions. For each condition $n=3$.

A Shapiro-Wilk's normality test indicated that data was normally distributed ($W = 0.95169$, $p\text{-value} = 0.6618$) and Levene's test indicated homogeneity of variance ($F \text{ value} = 2.591$, $p = 0.1385$). A two way factorial ANOVA was computed to test for significant differences in mucus production per gram of biomass in the different conditions. No significant difference was observed in mucus production per gram of biomass for pH, temperature or pH:temperature interaction (see Table 4.1 below)

*Table 4. 1: Results of a two way factorial ANOVA testing for differences in mucus production by the harbour ragworm *Hediste diversicolor* in different pH/ temperature conditions. No significant differences were observed.*

	Df	Sum Sq	Mean Sq	F value	Pr(>F)
pH	1	0.003969	0.003969	1.044	0.337
Temp	1	0.009776	0.009776	2.571	0.148
pH:Temp	1	0.005567	0.005567	1.464	0.261
Residuals	8	0.030418	0.003802		

Biomass was measured by adding the wet weight of each of the five worms added to each sample (see Table 4.2). This was plotted against the freeze dried mucus mass to investigate the effect of biomass on mucus production.



*Figure 4. 3: : Loess smoothing function (blue line) showing the relationship between dry mass of mucus produced and biomass of worms (*Hediste diversicolor*) and 95% confidence intervals (grey shading).*

Table 4. 2: Total biomass of the five worms used in each of the pH/ temperature conditions tested

Condition	Biomass (g)	Standard deviation
pH8.1, 18C	0.42	0.08
pH8.1, 22C	0.38	0.06
pH7.3, 18C	0.46	0.08
pH7.3, 22C	0.42	0.03

Interestingly, lower biomass corresponds with higher levels of mucus production (Figure 4.3). Carbohydrate concentration in the freeze dried sample was then calculated in ug/mg by dividing the concentration by the mass of the initial freeze dried sample. Figure 4.4 shows the variation in carbohydrate content in the mucus samples collected from *H. diversicolor* in the different pH/ temperatures tested.

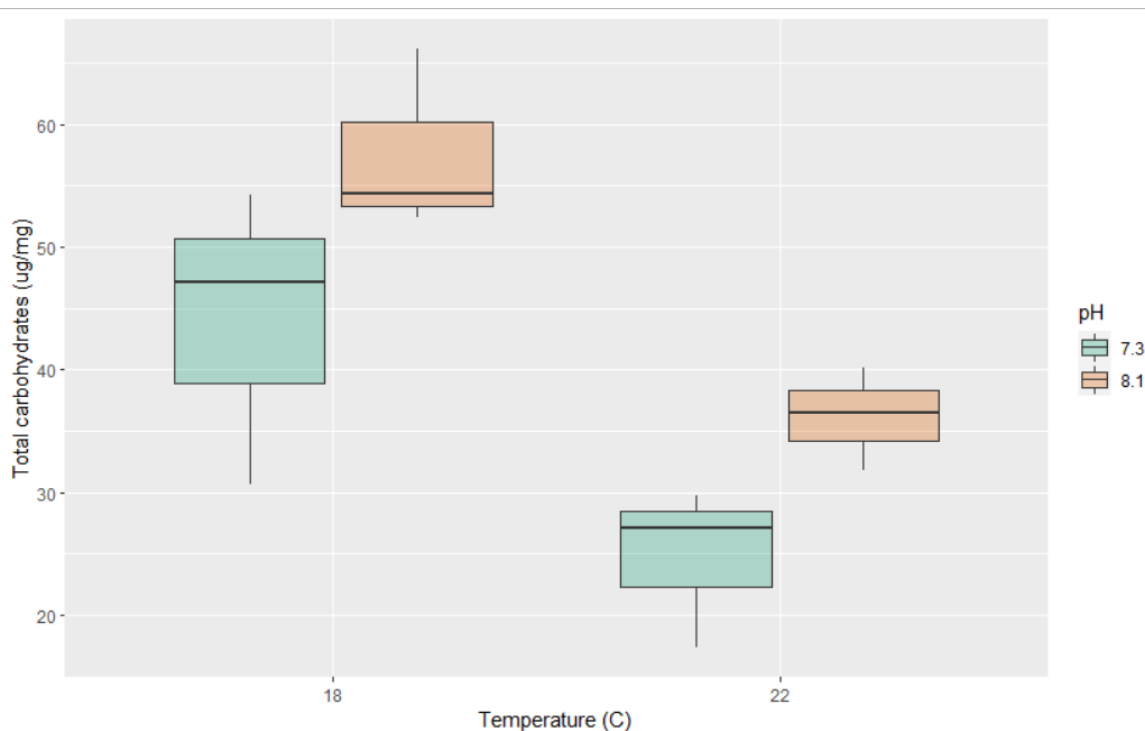


Figure 4. 4: Boxplot illustrating the carbohydrate content in mucus samples produced by the harbour ragworm *Hediste diversicolor* at different pH/ temperature conditions. For each condition $n=3$.

A Shapiro-Wilk's normality test indicated that data was normally distributed ($W = 0.96368$, $p\text{-value} = 0.8347$) and Levene's test indicated homogeneity of variance ($F\text{ value} = 0.1747$, $p\text{ value} = 0.6848$). A two way factorial ANOVA was computed to test for significant differences in mucus carbohydrate in the different conditions. Total carbohydrate content of mucus was found to differ significantly between pH7.3 and pH8.1. In addition total carbohydrate content varied significantly between 18°C and 22°C. No significant interaction between pH:temperature was found (see Table 4.3 below).

*Table 4. 3: : Results of a two way factorial ANOVA testing for differences in carbohydrate content of mucus produced by the harbour ragworm *Hediste diversicolor* in different pH/temperature conditions. Significance codes: 0 = '***', 0.001 = '**', 0.01 = '*',*

	Df	Sum Sq	Mean Sq	F value	Pr (>F)	
pH	1	469.4	469.4	7.155	0.02815	*
Temp	1	1242.9	1242.9	18.944	0.00244	**
pH:Temp	1	3.7	3.7	0.056	0.81836	
Residuals	8	524.9	65.6			

4.1.5. Discussion

Experimental conditions were based on future relevant pH and temperature conditions, compared to present day conditions. The experiment was designed to test whether these future-relevant conditions triggered physiological defence mechanisms, in the form of altered mucous production, in *H. diversicolor*, as has been identified with exposure to pollutants (e.g. Pires et al., 2022). The production of excess mucous would not only impact the fitness and survival of the worms themselves, but, thanks to their high population densities (Scaps, 2002) could impact sediment stability, oxygen penetration into sediments, microbial communities and organic matter cycling (Kristensen et al., 2013, Dale et al., 2019).

Mucus typically consists of an entanglement of proteins and polysaccharides that form a gel which is usually in the region of 95% water (Stabili, 2019). Marine invertebrate mucus has a range of functions, from reducing drag to enhancing adhesion and reducing sedimentation (Stabili, 2019). In addition, marine invertebrate mucus serves as a microhabitat, providing food and stability for a range of microbial fauna (Stabili, 2019). Experiments using coral mucus found elevated oxygen use in seawater containing coral mucus samples compared to seawater alone suggesting significant microbial activity (Coles and Strathmann, 1973). These bacteria may act as a carrier for energy, creating a food chain converting mucus compounds into organic matter (Coles and Strathmann, 1973). Mucus can also act as a pathogen deterrent and, notably, coral mucus has been found to demonstrate high antimicrobial activity (Shnit-Orland and Kushmaro, 2009). Communities of microorganisms that colonise mucus may act together to provide a variety of anti-microbial and protective properties (Stabili, 2019). An additional function of some microbes that inhabit coral mucus may be to provide nitrogen and phosphorous that the zooxanthellae cannot produce (Anthony and Fabricius, 2000). Infaunal polychaete species such as *H. diversicolor* are likely to use mucus secretions as a protective mechanism against pollutants and reactive oxygen species (Moraes et al., 2006). Further, the antioxidant properties of mucus are related to carbohydrate content of its mucoproteins which act as radical species (Stabili, 2019). *H. diversicolor* have been found to produce more mucous when exposed to certain pollutants including, graphene oxide, metals and pharmaceuticals (Pires et al., 2022, Mouneyrac et al., 2003, Gomes et al., 2019). This is thought to be a defence mechanism, with the mucous acting to bind harmful particles to prevent direct contact with the body (Pires et al., 2022).

Mucus quantity

Although no significant increase in mucus production was observed in this experiment either at elevated temperatures (22°C) or reduced pH (pH7.3), there was a non-significant increase in mean mucus mass (freeze dried sample) at pH8.1, 22°C. At pH7.3 mucus production is remarkably consistent between 18°C and 22°C, whereas at pH8.1 there is more variation in mucus production between 18°C and 22°C. Previous research has linked increased mucus production to several stressors, including elevated levels of pollution (e.g. Bastidas and Garcia, 2004) and increased water temperature (Neudecker, 1981, Tal et al., 2021). Mucus has been hypothesised to isolate the animal from the environment in stressful conditions and act as an ionoregulator (Davies and Hawkins, 1998). The results of this experiment indicate that *H. diversicolor* is robust to a range of future climatic conditions with some indication that high pH and high temperature increases mucus production. Producing mucus is energetically costly (up to 70% of consumed energy), therefore its functionality as a buffer from stressful environmental conditions may be only a short term solution (Davies and Hawkins, 1998). This may partially explain why neither pH or temperature had a significant impact on mucus production. There was also no significant impact of the pH: temperature interaction suggesting that reduced pH and elevated temperatures combined are not causing the worms to produce more mucus.

Biomass

Biomass was measured by adding the wet weight of each of the five worms added to each sample. This was plotted against the freeze dried mucus mass to investigate the effect of biomass on mucus production. Interestingly, lower biomass corresponds with higher levels of mucus production (Figure 2.2). This could be due to increased sensitivity of smaller individuals to environmental change causing an increase in production of protective mucus. Experiments

on the polychaete *Laeonereis acuta* using hepatoma cell lines exposed to H₂O₂, found that: mucus co-exposure significantly lowered DNA damage induced by H₂O₂; reactive oxygen species production was significantly reduced when cells were exposed simultaneously with mucus samples compared to H₂O₂ alone (Moraes et al., 2006).

Total carbohydrates

In this study total carbohydrate content of mucus was found to differ significantly between pH7.3 and pH8.1 with significantly lower carbohydrate content at pH 7.3. In addition total carbohydrate content varied significantly between 18°C and 22°C, with significantly lower carbohydrate content at 22°C. The interaction between pH:temperature did not have a significant effect on mucus carbohydrate content. The results do appear to show that low temperature (18°C) and high pH (pH8.1) is associated with increased carbohydrate content suggesting that the worms expended more energy on mucous production in these conditions. These conditions are not typically considered stressful for the worms used in these experiments, with the original worms collected from Hessel Foreshore, where mean summer water temperature is 18°C and pH based on present day average ocean pH of 8.1pH units (IPCC, 2013a). The lower levels of carbohydrate in the mucous of those worms held at pH7.3, 22°C could be linked to lack energy reserves limiting production. Indeed, Freitas et al. (2016) tested physiological responses of *H. diversicolor* to ocean acidification and found that individuals under low pH (7.6 and 7.3) presented higher carbonic anhydrase (CA) activity, lower energy reserves (protein and glycogen content) and higher metabolic rate (measured as electron transport system activity). The increase on CA activity was associated to organisms osmoregulation capacity while the increased metabolic rate and decrease on energy reserves was associated to the polychaetes capacity to develop defence mechanisms (e.g. antioxidant defences such as mucous). This lack of energy reserve and reduced capacity to produce defence mechanisms could partially explain the low

carbohydrate content of mucous produced at pH7.3. Elevated temperature has been found to exacerbate the negative physiological effects caused by acidification in *H. diversicolor*, including regeneration rate (Bhuiyan et al., 2021b). A similar interaction could be occurring in this experiment, with pH and temperature impacting the physiology of the worms in such a way that they are less able to produce carbohydrate-rich mucous.

The DuBois method used here to measure total carbohydrates detects nearly all carbohydrate classes (mono-, di-, oligo-, and polysaccharides) (Nielsen, 2017). Mucins, which are the glycoprotein that give mucus its elasticity and viscosity will be measured in the DuBois assay (Masuko et al., 2005). The basic structure of mucins are fairly highly conserved in metazoans and consists of a 200-500kDa protein core surrounded by oligosaccharide side chains.

Bansil and Turner (2006) found carbohydrate content in mucus to be around 80%. Stabili et al. (2014) found that the mucus of the polychaete *Myxicola infundibulum* consists of 95% water and a dry weight containing 2.1% protein, 0.2% carbohydrate, 3% lipid and 57% inorganic materials. The mucus of several polychaete species has been found to be composed of between 2 and 8% carbohydrates (Stabili, 2019). In this experiment, carbohydrate content was found to be in the range of 1.7 to 5.4% of the total freeze dried sample suggesting the presence of large amounts of other material. This remaining material is likely to contain a mixture of protein, lipids and inorganic material (Stabili, 2019).

Bacterial abundance has been correlated with sediment carbohydrate concentrations which in turn is correlated with mucus presence (Dale et al., 2019). Dale (2019b) found a 67% increase in bacterial abundance in mucus treated sediment compared to sediment alone. In addition, the same study found that increased carbohydrate concentration in sediments were positively correlated with ammonia-oxidising bacteria (AOB) and archaea (AOA) as well as

the AOB:AOA ratio, along with concomitant increases in nitrification rates. Nitrogen cycling in estuarine sediments consists of a network of microbially mediated biogeochemical processes which may be impacted by the presence of mucus secretions from burrowing invertebrates (Dale et al., 2019). Dale et al. (2019) found that the addition of mucopolysaccharides from *H. diversicolor* to sediments led to a more abundant and distinct microbial community as well as bacterial and archaeal ammonia oxidisers, accompanied by an increase in nitrite and nitrate. *H. diversicolor* mucus was therefore linked to enhanced sediment nitrification rates via stimulation and feeding of nitrifying microbial groups.

In this experiment, both pH and temperature had a significant impact on the total carbohydrate content of mucus ($p=0.029$ and 0.002 respectively) with higher pH and lower temperatures associated with increased carbohydrate content. Lower pH and higher temperatures are becoming more common in the marine environment and the conditions tested here are likely to be common-place in estuarine habitats by the end of the century (Bindoff et al., 2019). Producing mucus is energetically costly and reduced carbohydrate content observed at lower pH and higher temperatures may be an energy saving mechanism in conditions that could be more energetically costly. In addition, although mucus is thought to function as protection from environmental conditions, it is possible that this is a short term strategy and the exposure times used in this experiment reduced the effectiveness of this tactic.

The reduced carbohydrate concentrations in the mucus of *H. diversicolor* at these future conditions could have an associated impact on microbial communities, potentially reducing the presence of nitrifying microbial groups and nitrification rates. Due to the high density of naturally occurring populations of *H. diversicolor* (up to 1150 individuals per m^2 (Duport et al., 2006)) this reduction in carbohydrate content could have an ecosystem level impact in estuarine habitats. In addition, Dale et al. (2019) suggest that *H. diversicolor* mucus excretions could exceed $15 \text{ g m}^{-2} \text{ day}^{-1}$ and contribute $0.34 \text{ g C m}^{-2} \text{ day}^{-1}$ and $0.05 \text{ g N m}^{-2} \text{ day}^{-1}$ to

sediments. A reduction in the quality of this mucus contribution could significantly effect sediment habitats, changing microbial fauna and altering nutrient cycling.

The presence of *H. diversicolor* mucus potentially alters cohesion in muddy sediments and can have an effect on sediment fluxes and bedform development (Malarkey et al., 2015, Hope et al., 2020, Kristensen et al., 2013, Tolhurst et al., 2002, Parsons et al., 2016). Biologically cohesive extracellular polymeric substances (EPS) are typically considered to be generated by microorganisms (e.g. Hope et al., 2020), however, the presence of mucus-stabilised burrows is thought to impact the biodiversity and quantity of EPS producing microorganisms (Dale et al., 2019). Previous studies have found that the presence of *H. diversicolor* causes a decrease in the free-stream erosion threshold and an increase in erosion rate (Kristensen et al., 2013). This is largely due to their feeding activities diminishing the surface stabilizing effect of extracellular polymeric substances (EPS). However, the impact of altered carbohydrate production with pH and temperature may have an impact on the EPS producing microfauna that colonise *H. diversicolor* mucus. This could have an impact on sediment stickiness in future pH (7.3) and temperature (22°C) conditions but more research into this effect is needed.

Limitations and future work

Due to time and equipment constraints this experiment, although informative, had a limited number of repeats with only three technical replicates per condition tested. Despite this, statistically significant differences were identified between the carbohydrate concentration in mucous produced at different conditions. Each replicate contained five worms and a 300x 300mm polypropylene sheet was used as a medium for mucous adherence. Five worms were used in each replicate to reduce issues with cannibalisation, however, in hindsight, this was not a problem and therefore more worms could have been used. The addition of more

worms in each replicate, along with a larger polypropylene sheet could have increased the mucous yield which would have allowed for additional analysis (such as protein concentration) and would have improved ease and accuracy of dry mass measurements.

H. diversicolor mucus has been linked to enhanced sediment nitrification rates via stimulation and feeding of nitrifying microbial groups. However, there is scarce information in the literature as to the impacts of quantity and carbohydrate concentrations in invertebrate mucous and how these might affect biochemical cycling. Further investigation into the link between invertebrate mucus production and nutrient cycling in a range of pH and temperature conditions would help to unpick the impacts climate change might have of benthic ecosystems. Analysis of the additional constituent components of *H. diversicolor* mucus and how they relate to environmental conditions would also be informative and might provide insight into the quality of mucus produced in stressful conditions. Additionally, mucus production and composition in more extreme pH and temperature conditions as well as over an extended period of exposure would allow more robust quantification of variations associated with climate change.

5.0. Conclusion

5.1. Chemical Communication and Environmental Change

This is the first time that GSH and DMS have been observed as acting as a food cue for *H. diversicolor*. This is also the first time that urea has been observed acting as a predator cue. In addition, this is the first time worms have been observed with varied, and in some cases opposite, response to chemical cues over a range of pH conditions. This is in spite of the worms tested being adapted to specific pH and temperatures, having been bred and raised in these conditions. These results indicate a concerning change in behavioural response to food and predator cues in low pH/ high temperature conditions. Conceivably, alterations in the ability to sense and respond appropriately to food and predator cues could reduce survival rates and significantly reduce fitness. Climate change is likely to drive further reductions in ocean pH and increases in temperature over the next century and, in estuarine environments, this will lead to longer periods in which these extremes will be experienced. *H. diversicolor* is regularly exposed to fluctuating pH and temperatures and was considered well adapted to tolerate these conditions (Budd, 2008). The results of this study indicate that, although tolerant to these fluctuations, the ability of this species to function effectively is reduced. This could have population level impacts on this keystone species as exposure to pH and temperature extremes becomes more frequent and normalised.

Here we tested several food and predator cues, but similar impacts may occur for any chemical cue, for example reproductive chemical cues. *H. diversicolor* are dioicous and semelparous, spawning only once in a lifetime (Budd, 2008). The worms spawn synchronously in spring, with timing thought to be triggered by a combination of increasing temperatures, lunar cycle and pheromones. Pheromones are of particular use in the final stages of reproduction for co-ordinating processes such as mate location and the synchronization of

gamete release and spawning at the population level (Budd, 2008). Currently the chemical properties of *H. diversicolor* pheromones are unknown and the impacts of climate change on their functionality unclear. However, given the results of chapter 2, the impacts of pH and temperature have the potential to affect chemical sensing across all life stages with serious implications for a broad range of life history traits, including reproduction.

Behavioural response to changing ocean conditions has the potential to mitigate some of the negative impacts, for example, mobile species migrating to more hospitable regions or increasing ventilation activity to compensate for reduced pO₂. However, some behavioural changes are driven by shifts in body chemistry and are therefore less of an adaptation to changing conditions and more of an involuntary consequence. Adaptation and acclimation to environmental change has the potential to offset some of the negative consequences of climate change, particularly in short-lived, rapidly reproducing species such as *H. diversicolor* (Gibbin et al., 2017). However, the experiments in this thesis all used animals that are second and third generation, bred and raised in their respective environmental test conditions. Despite this, the consequences of pH and temperature were still measurable in nearly all experiments conducted, suggesting that adaptation was limited.

Chemical signalling is the oldest form of communication and is pervasive across living organisms; from single celled bacteria to complex species such as humans (Hardege, 1999). Information transfer between invertebrates in the marine environment heavily relies on chemical communication (Hardege, 1999). Hearing, vision and mechanoreceptors also contribute to varying degrees. For example, in turbid estuarine environments visibility is low and therefore less useful as a means of communication. Marine animals rely on chemical cues to survive, using chemical sensing to detect food, predators/prey, conspecifics, habitat, mediate social interaction and stimulate spawning, (e.g. Poulin et al., 2018, Abreu et al., 2016, Breithaupt, 2011, Kicklighter et al., 2011, Schaum et al., 2013, Sutrisno et al., 2014, Hardege,

1999). Altered response to chemical signals driven by changing environmental conditions has the potential to impair the ability of marine organisms to perform all of these functions. For prey species, rapid detection of predators is crucial in order to initiate a predator avoidance response and escape capture. Predator kairomones, disturbance cues released by stressed prey (Ferrari et al., 2010), and alarm cues released by injured conspecifics (Ferrari et al., 2010) are all used to detect danger. Ferrari et al. (2010) argues that early predator detection by prey is subject to greater evolutionary pressure compared to prey detection by predators because the outcome is more severe for a prey species (the ‘lunch versus life’ concept). Therefore, it is particularly concerning that, urea, the predator cue identified in chapter 2, was found to elicit non-significant behavioural responses in higher temperatures and at reduced pH (see Figure 2.7, chapter 2). In addition, it is similarly concerning that chondroitin sulphate elicited a non-significant avoidance response at 18°C, yeast acted as a food cue at 22°C, eliciting feeding behaviour.

Even with decades of research, it has proved difficult to identify any specific molecular compounds involved in the recognition of environmental information (Chivers and Smith, 1998, Roggatz et al., 2016, Poulin et al., 2018). A successful chemical cue needs to travel to the receiver via diffusion or be transported by currents. It also has to be specifically targeted and elicit a specific reaction by the receiver (Hardege, 1999). Additionally, an organism must be able to respond to low threshold concentrations so as to reduce the energetic cost of synthesising pheromones and increase ability to quickly react to cues (Hardege, 1999). These requirements allow researchers to narrow their search and has led to speculation as to the types of molecules that are likely to fit these requirements. In aquatic environments, small lipophilic molecules have limited interaction with polar water molecules, allowing them to be transported further (Hardege, 1999). Small peptides have also been proposed as a candidate cue type due to their small size and associated rapid dispersal, numerous forms (allowing for a range of

bouquets) and chemical stability (Rittschof, 1990). Despite the specificity required, it is probable that certain molecules act heterospecifically as chemical cues, with some cues mediating opposing behaviours in different species (e.g. Rittschof, 1990). Hardege et al. (1998) used electrophysiological and behavioural assays to show that coelomic fluid stimulates the receptors of 10 different Nereid species, indicating that overlap of cues does indeed occur. Uric acid, nereithione and GSH was found to explain some of this heterospecificity (Hardege et al., 1997). Here we confirm that GSH and DMS elicit significant feeding responses in *H. diversicolor* and that urea elicits significant avoidance response (only in pH8.1, 18°C). Further work investigating behavioural and electrophysiological responses to combinations of chemical cues would be beneficial for identifying: 1) responses to more ‘natural’ cues, which are likely to be combinations of molecules and 2) whether the impact of multiple molecules offset the negative impacts on response caused by changing pH and temperatures.

Nereidid worms have long been used as model organisms to investigate response to chemical cues. They have relatively simple anatomical organisation, are common and easy to collect, culture well in the laboratory and manipulation of their life cycle is possible via photoperiod/ temperature and artificial moonlight (Hardege, 1999). However, the impacts of ocean acidification have been found to be quite species-specific and it would be useful to run similar behavioural experiment to those conducted in chapter 2 on other polychaetes. This would help build understanding of how universal these cues are and whether other species will be similarly impacted.

One mechanism driving behavioural change in marine organisms is caused by the protonation of signalling peptides driven by more acidic conditions (Roggatz et al., 2016). Ocean acidification will create conditions that allow protonation of amino-acid containing signalling peptides with a pK_a similar the pH of seawater. Protonation of peptides will alter their charge and in doing so may also modify their structure. Such alterations can affect the

ability of an organism to receive and understand the signalling peptide (Roggatz et al., 2016). Roggatz et al. (2016) demonstrated this empirically using signalling peptides used by *Carcinus maenus* to mediate egg ventilation behaviour. At reduced pH it was found that around 10 times the amount of signalling peptide was required to initiate egg ventilation due to protonation of the signalling peptide interfering with reception by the animal (Roggatz et al., 2016). Here we identified that urea, taurine and GSH change their protonation state over the pH range tested (see figure 2.8 and 2.9 in chapter 2), potentially accounting for some of the differences in behavioural response observed. Other chemicals tested undergo different chemical changes, such as ATP, which hydrolysis in aqueous solutions above pH7.4. However, the structure of chondroitin sulphate is relatively stable across a broad pH and temperature range (pH6 to 11, pKa ~ 2.7 and 10 to 90°C) (Profant et al., 2019) suggesting that the variation in activity is physiologically driven. It is possible that a complex interplay between chemical and physiological change is driving the differences in behavioural response observed across the pH and temperature conditions tested and more work will need to be done to unpick this.

5.2. Burrow Oxygen and Environmental Change

This is the first time that the impacts of both temperature and pH have been linked to oxygen levels in burrows and surrounding sediments. Warmer temperatures (22°C) led to slightly higher Oxygen ratios, possibly linked to increased O₂ requirements by *H. diversicolor* in these conditions triggering an increased ventilation effort. At pH 7.3 and pH 8.1 Oxygen ratio was reduced suggesting lower ventilation effort and/or reduced oxygen demand by the worm. Oxygen penetration depth into surrounding sediments reduced with declining pH and declining temperatures. In chapter 4, mucus carbohydrate concentrations were found to be lower at reduced pH, and in chapter 3 lower pH was linked to lower penetration of oxygen. This would suggest that low carbohydrate concentrations at the burrow wall are associated with

a reduction in penetration depth. However, higher temperatures were also strongly associated with lower mucus carbohydrate concentrations and these same reduced temperatures were linked to significantly higher oxygen penetration depths in chapter 3. Increased carbohydrate levels have been linked to the increased microbial colonisation of the carb rich mucus(Dale, 2019a). The composition of microbes is also related to pH and temperature conditions and the interplay between microbial communities colonising the mucous and their oxygen demand may partially explain the changes in oxygen penetration depth.

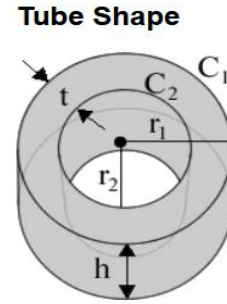
These results indicate that future pH conditions may cause a decrease in sediment oxic zone, which in turn may cause alterations in aerobic respiration and organic matter breakdown in marine sediments. Lower pH and higher temperatures both led to reduced oxygen penetration depth into the sediment, which may cause an increase in sediment oxic zone in these conditions, with associated alterations in aerobic respiration and organic matter breakdown in marine sediments. Water temperature regulates oxygen and carbonate solubility with warmer temperatures causing reduced oxygen solubility. Despite this, oxygen penetration depth was higher at warmer temperatures suggesting that additional ventilation effort or reduced oxygen consumption by the worms might be occurring.

Alterations in oxygen penetration depth across different pH and temperature conditions have the potential to radically change the volume of oxic sediment in estuarine habitats. Here we found the highest penetration depth occurring in pH8.1, 22°C (median 0.6658mm) and the lowest in pH7.3, 18°C (median 0.4685mm). This represents a 29.6% change on oxygen penetration depth. Based on average burrow width for a medium worm of 2.2mm and average burrow length of 160mm (Davey, 1994) and using the formula below, the volume of the oxic zone around an average burrow can be calculated.

$V1 = \pi r_1^2 h$ for the volume enclosed by C1

$V2 = \pi r_2^2 h$ for the volume enclosed by C2

$C1 - C2 = \text{volume of tube wall}$



Using this formula the oxic zone around an average burrow in pH8.1, 22°C is 959.09mm³ compared to 628.42mm³ in pH7.2, 18°C. Taking this further, average *H. diversicolor* population density in suitable estuarine habitats is 1150 adult individuals per m² (Duport et al., 2006). Assuming one burrow per individual the oxic zone around burrows in pH8.1, 22°C would be 1,102,953.96mm³ per square meter compared to 722,683mm³ in pH7.3, 18°C, a 34.48% reduction in oxic zone. Changing pH and temperature conditions have clearly have the potential to meaningfully alter the volume of oxic habitat available in estuaries, which will have knock on effects on nutrient and organic matter cycling as well as microbial communities in sediments (Damashek and Francis, 2018).

As keystone species (Moreira et al., 2006, Mermillod-Blondin et al., 2005) burrowing *Hediste diversicolor* provides a service to microbes and meiofauna by providing additional oxygenated habitat at the sediment-water interface. Banta et al. (1999) found that the presence of *H. diversicolor* in sandy sediment stimulated O₂ uptake and CO₂ release by 80 to 90% indicating an increase in benthic metabolism by the worms and associated microbial activity. Increasing oxygenation of the sediment alters the pace of nutrient and organic matter cycling and the feeding activities of this species acts as a rate-limiting step in estuarine detritus processing (Moreira et al., 2006, Mermillod-Blondin et al., 2005). The transformation of carbon and nitrogen substances along with sediment-water interface fluxes are important drivers of biogeochemical cycling.

Plankton dynamics are largely responsible for the rate of deposition of organic matter on marine sediments. However, biodeposition, biological resuspension and infaunal particle mixing contribute to net incorporation into sediments (Christensen et al., 2000, Graf and Rosenberg, 1997). Burrowing organisms are known to encourage microbially mediated decomposition processes in marine sediments (Andersen and Kristensen, 1991, Marinelli and Boudreau, 1996). Burrow creation essentially extends the sediment-water interface and irrigation enhances solute fluxes and creates steeper solute gradients (Martin and Banta, 1992, Aller, 1994b, Fenchel, 1996, Reichardt, 1988). The remineralisation and release of inorganic nitrogen from marine sediments benefits primary producers (Andersen and Kristensen, 1991). Biogeochemical cycling in estuarine habitats is complex and dependant on a range of locally specific factors such as riverine input, tidal factors and sediment type (Martin, 2009). However, the importance of burrowing organisms is generally agreed, even if the exact mechanisms are not fully understood. Changes in the volume of oxic zone surrounding *H. diversicolor* burrows, as identified here, could have a range of complex effects on ecosystem functioning. Potentially altering microbially mediated decomposition processes and limiting chemical cycles, such as the nitrogen cycle which would have knock on effect on primary producers that rely on the release of inorganic nitrogen from marine sediments.

The presence of burrowing organisms can increase anaerobic sulphate reduction 3 to 5 times by drawing additional electron acceptors (sulphate) deeper into the sediment. Denitrification is similarly enhanced, with Nereid burrows contributing an estimated 50 to 80% of bulk sediment denitrification (Andersen and Kristensen, 1991). Burrow ventilation is thought to cause an influx of sulphate and nitrate electron acceptors and an outflow of reduced sulphide and ammonium (Andersen and Kristensen, 1991) and it has been estimated that polychaetes such as *H. diversicolor* ventilate at a rate of 10-20 ml water g⁻¹ hr⁻¹ (Kristensen, 1988). Recent work by Dale (2019) has found that the polysaccharide secretions of burrowing

invertebrates can stimulate nitrification and denitrification processes, enhancing the nitrogen cycle. However, Banta et al. (1999) argues that the presence of burrowing organisms increases solute flux and thereby inhibits anaerobic decomposition with lower sulphate reduction rates seen in experimental setups containing *H. diversicolor* or *Arenicola marina*. Increased water temperature, (which was found to be associated with increased oxygen penetration in chapter 3) also affects important microbial processes such as nitrogen fixation and denitrification in estuaries (Lomas et al., 2002).

Periodic ventilation of burrows by benthic invertebrates creates oscillating redox conditions, providing episodic exposure to oxygen, which have been shown to result in more complete (and sometimes more rapid) breakdown of organic matter than constant conditions (Aller, 1994b). Estuarine environments are highly fluctuating environments with daily and seasonal pH, temperature and salinity cycles. Environment Agency data collected at New Holland in the Humber Estuary between 1991 and 2005 show daily fluctuations of 0.56 pH units between low and high tide (pH 7.77 to pH 8.26) and seasonal fluctuations of 1.54 pH units (pH 7.0 to pH 8.54), as well as seasonal temperature fluctuations of 19.5°C (3°C to 22.5°C). The pH and temperature conditions used in this study are therefore not outside of present-day extreme conditions and these extremes will likely get more exaggerated with climate change.

Here we calculated a 34.48% reduction in oxic zone depending on pH and temperature conditions. Although estuarine environments fluctuate naturally, climate change will generally lead to reduced average pH and in estuaries lower pH extremes (Bindoff et al., 2019). Chapter 3 identified a significant reduction in oxygen penetration depth between pH 8.1 and pH 7.3. If a similar reduction occurs as pH declines further with ocean acidification in the coming decades the oxic zone around burrow walls could decrease even more.

5.3. Mucous Production and Environmental Change

In this study the mass of mucous produced (per gram of worm biomass) did not vary significantly with pH or temperature. Total carbohydrate content of mucus was found to differ significantly between pH7.3 and pH8.1 with significantly lower carbohydrate content at pH 7.3. In addition, total carbohydrate content varied significantly between 18°C and 22°C, with significantly lower carbohydrate content at 22°C. The interaction between pH:temperature did not have a significant effect on mucus carbohydrate content. The results do appear to show that low temperature (18°C) and high pH (pH8.1) are associated with increased carbohydrate content suggesting that the worms expended more energy on mucous production in these conditions. These conditions are not typically considered stressful for the worms used in these experiments, with the original animals collected from Hessel Foreshore, where mean summer water temperature is 18°C and pH equivalent to present day average ocean pH of 8.1pH units (IPCC, 2013a). The lower levels of carbohydrate in the mucous of those worms held at pH7.3, 22°C could be linked to lack energy reserves limiting production. Based on the results found here, future pH and temperature conditions will lead to a reduced level of carbohydrates in the mucous produced by *H. diversicolor* and therefore lower carbohydrate levels in the sediment. This will have a knock on effect on the microbial communities that are able to colonise *H. diversicolor* burrows reducing the resources they have available to consume (Michaud et al., 2010).

Recent work by Dale (2019) has found that the polysaccharide secretions of burrowing invertebrates can stimulate nitrification and denitrification processes, enhancing the nitrogen cycle. However, Banta et al. (1999) argues that the presence of burrowing organisms increases solute flux and thereby inhibits anaerobic decomposition with lower sulphate reduction rates seen in experimental setups containing *H. diversicolor* or *Arenicola marina*. It is plausible that future environmental conditions and their impact on mucous carbohydrate levels will have a

knock on effect on nitrate cycles, reducing nitrification and denitrification processes. The reduced carbohydrate concentrations in the mucus of *H. diversicolor* at these future conditions could also have an associated impact on microbial communities, potentially reducing the presence of nitrifying microbial groups and further reducing nitrification rates. Due to the high density of naturally occurring populations of *H. diversicolor* (up to 1150 individuals per m² (Duport et al., 2006)) this reduction in carbohydrate content could have an ecosystem level impact in estuarine habitats. In addition, Dale et al. (2019) suggest that *H. diversicolor* mucus excretions could exceed 15 g m⁻² day⁻¹ and contribute 0.34 g C m⁻² day⁻¹ and 0.05 g N m⁻² day⁻¹ to sediments. A reduction in the quality of this mucus contribution could significantly effect sediment habitats, changing microbial fauna and altering nutrient cycling.

Marine invertebrate mucus has a range of functions, from reducing drag to enhancing adhesion and reducing sedimentation (Stabili, 2019). In addition, marine invertebrate mucus serves as a microhabitat, providing food and stability for a range of microbial fauna (Stabili, 2019). Experiments using coral mucus found elevated oxygen use in seawater containing coral mucus samples compared to seawater alone suggesting significant microbial activity (Coles and Strathmann, 1973). These bacteria may act as a carrier for energy, creating a food chain converting mucus compounds into organic matter (Coles and Strathmann, 1973). Mucus may also act as a protective coating, reducing the impacts of stressful environmental conditions. Infaunal polychaete species such as *H. diversicolor* are likely to use mucus secretions as a protective mechanism against pollutants and reactive oxygen species. Further, the antioxidant properties of mucus are related to carbohydrate content of its mucoproteins which act as radical species (Stabili, 2019). Previous research has linked increased mucus production to several stressors, including elevated levels of pollution (e.g. Bastidas and Garcia, 2004) and increased water temperature (Neudecker, 1981, Tal et al., 2021). Producing mucus is energetically costly, therefore its functionality as a buffer from stressful environmental conditions may be only a

short term solution (Davies and Hawkins, 1998). The mucous produced in lower pH and at higher temperatures contained lower total carbohydrate levels, which could impact the functionality of the mucous. In particular, lower carbohydrate levels could reduce the protective nature of the mucous which could exacerbate immunological impairment driven by more acidic conditions (Cuvillier-Hot et al., 2018).

Increased PCO₂, driving a reduction in ocean pH along with increasing temperatures in marine environments impacts organisms in a number of ways. Mobile species tend to move pole-wards to avoid increasing temperatures, however, reduced pH is more difficult to avoid. *H. diversicolor* may be particularly vulnerable to climate change due their lack of planktonic larvae and associated reduction in dispersal distance and population mixing (Lawrence and Soame, 2004). However, this is likely mitigated somewhat by their wide distribution and tolerance to a variety of conditions. In addition, climate migrants looking for more hospitable environments may be inhibited by the lack of connectivity of isotherms, effectively stranding organisms in a pocket of habitable conditions (Burrows et al., 2014). Adaptation and acclimation to environmental change has the potential to offset some of the negative consequences of climate change, particularly in short-lived, rapidly reproducing species such as *H. diversicolor* (Gibbin et al., 2017). However, the experiments in this thesis all used animals that are second and third generation, bred and raised in their respective environmental test conditions. Despite this, the consequences of pH and temperature were still measurable in nearly all experiments conducted, suggesting that adaptation was limited.

5.4. Climate change and polychaetes

Rapid climate change has been observed numerous times throughout geological history and appears to come hand-in-hand with declining biodiversity. In the ocean it is typically calcifying organisms that suffer the heaviest losses however loss of hardy, benthic invertebrates has been observed during mass extinctions. Figure 5.4 below uses data from the Paleo-biology

database to illustrate fluctuations in the number of polychaete genera throughout the Phanerozoic.

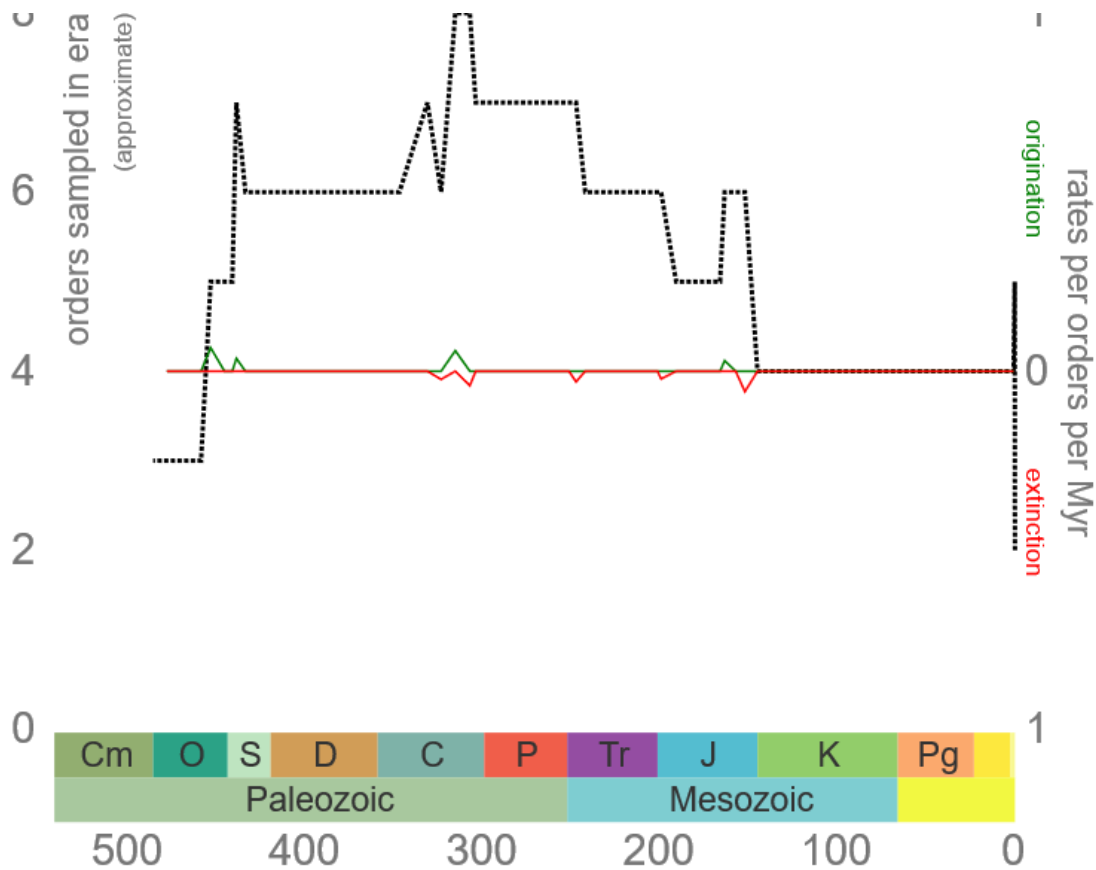


Figure 5. 1: Number of occurrences of the class polychaeta throughout the Phanerozoic based on fossil records. Cm = Cambrian, O = Ordovician, S = Silurian, D = Devonian, C= Carboniferous, P= Permian, T= Triassic, J = Jurassic, K = Cretaceous Pg = Paleogene, (Paleobiology Database, 2019) Range through diversity (dotted line) shows each taxon as present from its first occurrence to its last occurrence, whether or not it was ever found in the fossil record in the intervening intervals. Origination and extinction rates (green and red lines) are estimated here using the "per-capita rate" method of (Foote, 2000)

The results of this project provide evidence that the impacts of climate change will lead to increasing energetic costs with the potential to drive population declines in *H. diversicolor*. Similar mechanisms may have contributed to the extreme declines observed during past mass extinctions. The Permian-Triassic mass extinction was associated with similar levels of pH and temperature change as those predicted for the end of this century. In this research we have found evidence that the primitive sensory systems of polychaete worms are impaired by changing pH and temperatures making them less able to respond appropriately to chemical cues. In addition, increased mucus carbohydrate levels were produced at lower temperatures and higher pH which is associated with increased microbial colonisation and increased rates of nutrient cycling. Reduced pH and higher temperatures observed during the Permian-Triassic were associated with microbial mudflats, with little infaunal or burrowing activity. Declining polychaete samples in the fossil record correspond with periods of climatic change (see Figure 5.1) suggesting that they are susceptible to changing environmental conditions.

Future work

There is a paucity of research into the impacts of multiple stressors as well as the interaction between multiple species in stressful conditions. More research is needed to investigate the physiological responses of different taxa to future ocean conditions and elucidate the impacts these responses might have on survival and community ecology in the marine environment. It would be interesting to conduct a meta-analysis of the literature comparing the variability of abiotic conditions (pH, temperature etc.) to the breeding behaviour of species in that habitat. One particularly interesting avenue for such analysis lies in determining whether it is more likely for species in variable, estuarine environments to be broadcast spawners (potentially exposing their gametes to harsh conditions), egg brooders (environmental variation can be somewhat mediated) or external bearers of young.

Supplementary materials - Chapter 2

SUPPLEMENTARY MATERIALS – CHEMICAL CUES

DMS

Shapiro-Wilk test for normality

Data tested for normality using a Shapiro-Wilk test in R and found to be non-normal ($W = 0.75659$, $p\text{-value} < 2.2e-16$)

Levene's test for homogeneity of variance

Data tested for homogeneity of variance using a Levene's test in R and found to have heteroscedastic variance ($DF=8$, $F\text{-value} 8.7088$, $p 2.18e-11$)

Robust factorial repeated measures ANOVA

Table S2. 1: Results of robust factorial repeated measures ANOVA using WRS2 package in R

	value	df1	df2	p.value
temp	29.4925	1	190.8966	0
ph	0.0799	1	167.7703	0.7778
temp:ph	7.3607	1	167.7703	0.0074

Dunn's test

In order to compare the control response of ragworms (*Hediste diversicolor*) to their response at various concentrations of the chemical cue a non-parametric Dunn's multiple comparison test was run. The full results are shown below. Signif. codes: 0 '***' 0.001 '**' 0.01 '*' 0.05 '.' 0.1 ' ' 1

Table S2. 2: : Results of nonparametric multiple comparison Dunn's test for pH8.1, 18C

		Estimate	Std. Error	t value	Pr(> t)	
1x10 ⁻²	Control	18.559	5.833	3.182	0.0118	*
1x10 ⁻³	Control	11.649	5.833	1.997	0.2378	
1x10 ⁻⁴	Control	5.286	5.833	0.906	0.9278	
1x10 ⁻⁵	Control	2.31	5.833	0.396	0.9996	
1x10 ⁻⁶	Control	7.395	5.833	1.268	0.7146	
1x10 ⁻⁷	Control	7.797	5.833	1.337	0.6638	
1x10 ⁻⁸	Control	23.628	5.833	4.051	<0.001	***
1x10 ⁻⁹	Control	39.633	5.833	6.794	<0.001	***

Table S2. 3:: Results of nonparametric multiple comparison Dunn's test for pH8.1, 22C

		Estimate	Std. Error	t value	Pr(> t)	
1x10 ⁻²	Control	5.888	7.946	0.741	0.9754	
1x10 ⁻³	Control	24.436	7.946	3.075	0.0164	*
1x10 ⁻⁴	Control	3.498	7.946	0.44	0.9992	
1x10 ⁻⁵	Control	21.702	7.946	2.731	0.0437	*
1x10 ⁻⁶	Control	32.283	7.946	4.063	<0.001	***
1x10 ⁻⁷	Control	17.786	7.946	2.238	0.1447	
1x10 ⁻⁸	Control	13.85	7.946	1.743	0.3752	
1x10 ⁻⁹	Control	24.909	7.946	3.135	0.0138	*

Table S2. 4: Results of nonparametric multiple comparison Dunn's test for pH7.3, 18C

		Estimate	Std. Error	t value	Pr(> t)	
1x10 ⁻²	Control	3.058	4.475	0.683	0.9847	
1x10 ⁻³	Control	7.276	4.475	1.626	0.45177	
1x10 ⁻⁴	Control	4.26	4.475	0.952	0.90858	
1x10 ⁻⁵	Control	7.433	4.475	1.661	0.42792	
1x10 ⁻⁶	Control	5.595	4.475	1.25	0.72732	
1x10 ⁻⁷	Control	12.234	4.475	2.734	0.04337	*
1x10 ⁻⁸	Control	16.646	4.475	3.72	0.00205	**
1x10 ⁻⁹	Control	5.341	4.475	1.193	0.76767	

Table S2. 5: Results of nonparametric multiple comparison Dunn's test for pH7.3, 22C

		Estimate	Std. Error	t value	Pr(> t)	
1x10 ⁻²	Control	37.416	5.475	6.834	< 0.001	***
1x10 ⁻³	Control	45.718	5.475	8.35	< 0.001	***
1x10 ⁻⁴	Control	18.032	5.475	3.293	0.00825	**
1x10 ⁻⁵	Control	15.119	5.475	2.761	0.04024	*
1x10 ⁻⁶	Control	13.914	5.475	2.541	0.07129	.
1x10 ⁻⁷	Control	15.161	5.475	2.769	0.03934	*
1x10 ⁻⁸	Control	22.584	5.475	4.125	< 0.001	***
1x10 ⁻⁹	Control	10.598	5.475	1.936	0.26707	

Curve fitting

In order to analyse the dose-response relationship between cue concentration and activity in each pH/ temperature condition Dr Fit (Di Veroli et al., 2015) was used to fit mono or multiphasic curves. The fitted curves and associated parameters are detailed below.

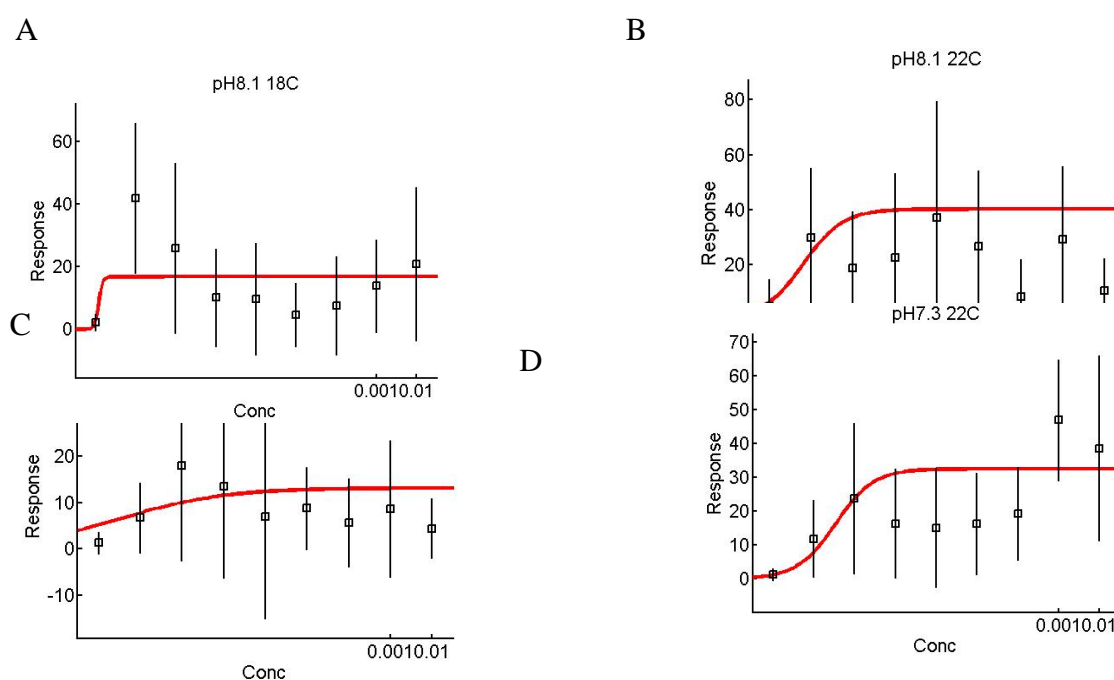


Figure S2. 1: Dose response fitted curves for response of *Hediste diversicolor* to DMS A) pH8.1, 18C, goodness of fit = 0.001. B) pH8.1, 22C, goodness of fit <0.0001. C) pH7.3, 18C, goodness of fit <0.0001. D) pH7.2, 22C, goodness of fit <0.0001.

ATP

Shapiro-Wilk test for normality

Data tested for normality using a Shapiro-Wilk test in R and found to be non-normal ($W = 0.61668$, $p\text{-value} < 2.2e-16$)

Levene's test for homogeneity of variance

Data tested for homogeneity of variance using a Levene's test in R and found to have heteroscedastic variance ($DF=8$, $F\text{-value}=2.7$, $p=0.006$)

Dunn's test

In order to compare the control response of ragworms (*Hediste diversicolor*) to their response at various concentrations of the chemical cue a non-parametric Dunn's multiple comparison test was run. The full results are shown below. Signif. codes: 0 '***' 0.001 '**' 0.01 '*' 0.05 '.' 0.1 ' ' 1

Table S2. 6: Results of nonparametric multiple comparison Dunn's test for pH8.1, 18C

		Estimate	Std. Error	t value	Pr(> t)	
1x10 ⁻²	Control	2.5449	3.6732	0.693	0.983	
1x10 ⁻³	Control	0.8448	3.6732	0.23	1	
1x10 ⁻⁴	Control	-1.3707	3.6732	-0.373	1	
1x10 ⁻⁵	Control	-1.3877	3.6732	-0.378	1	
1x10 ⁻⁶	Control	1.6777	3.6732	0.457	0.999	
1x10 ⁻⁷	Control	1.1068	3.6732	0.301	1	
1x10 ⁻⁸	Control	5.3496	3.6732	1.456	0.574	
1x10 ⁻⁹	Control	7.5177	3.6732	2.047	0.216	

Table S2. 7: Results of nonparametric multiple comparison Dunn's test for pH8.1, 22C

		Estimate	Std. Error	t value	Pr(> t)	
1x10 ⁻²	Control	26.785	7.712	3.473	0.00459	**
1x10 ⁻³	Control	16.112	7.712	2.089	0.19831	
1x10 ⁻⁴	Control	4.885	7.712	0.633	0.9904	
1x10 ⁻⁵	Control	2.377	7.712	0.308	0.99994	
1x10 ⁻⁶	Control	20.541	7.712	2.663	0.05218	.
1x10 ⁻⁷	Control	28.854	7.712	3.741	0.00179	**
1x10 ⁻⁸	Control	37.121	7.712	4.813	< 0.001	***
1x10 ⁻⁹	Control	24.322	7.712	3.154	0.01292	*

Table S2. 8: Results of nonparametric multiple comparison Dunn's test for pH7.3, 18C

		Estimate	Std. Error	t value	Pr(> t)
1x10 ⁻²	Control	-1.331	6.311	-0.211	1
1x10 ⁻³	Control	5.976	6.311	0.947	0.911
1x10 ⁻⁴	Control	5.799	6.311	0.919	0.923
1x10 ⁻⁵	Control	8.299	6.311	1.315	0.68
1x10 ⁻⁶	Control	-6.471	6.311	-1.025	0.872
1x10 ⁻⁷	Control	-4.596	6.311	-0.728	0.978
1x10 ⁻⁸	Control	2.862	6.311	0.453	0.999
1x10 ⁻⁹	Control	2.93	6.311	0.464	0.999

Curve fitting

In order to analyse the dose-response relationship between cue concentration and activity in each pH/ temperature condition Dr Fit (Di Veroli et al., 2015) was used to fit mono or multiphasic curves. The fitted curves and associated parameters are detailed below.

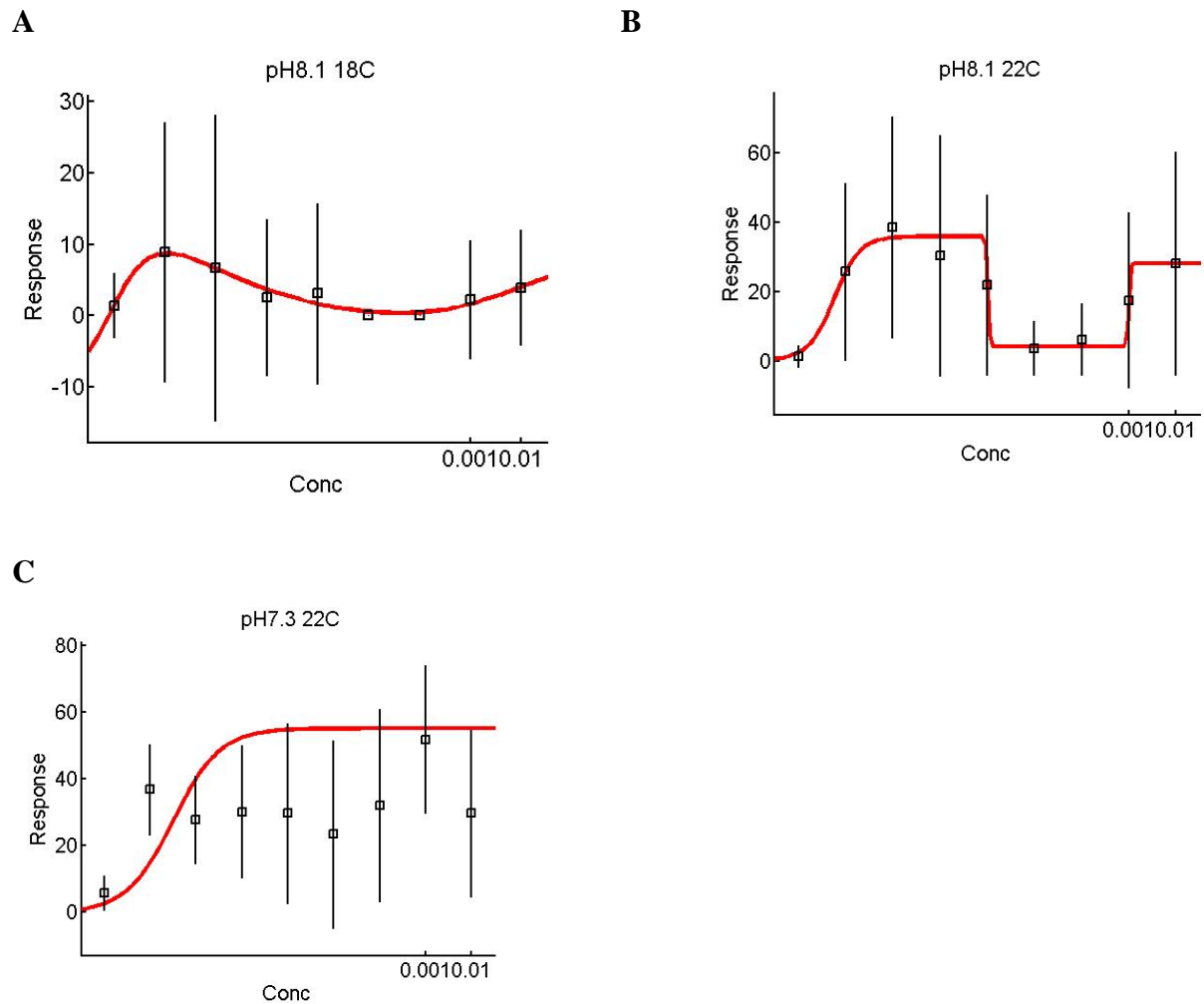


Figure S2. 2: Dose response fitted curves for response of *Hediste diversicolor* to ATP A) pH 8.1, 18C, goodness of fit = 0.001. B) pH 8.1, 22C, goodness of fit <0.0001. C) pH 7.3, 18C, goodness of fit =0.003.

TAURINE

Shapiro-Wilk test for normality

Data tested for normality using a Shapiro-Wilk test in R and found to be non-normal ($W = 0.8518$, $p\text{-value} < 2.2e-16$)

Levene's test for homogeneity of variance

Data tested for homogeneity of variance using a Levene's test in R and found to have heteroscedastic variance (DF=8, F-value, $p = 1.46e-9$)

Robust factorial repeated measures ANOVA

Table S2. 9: Results of robust factorial repeated measures ANOVA using WRS2 package in R

	value	df1	df2	p.value
temp	3.4161	1	212.5985	0.066
ph	4.3354	1	211.6463	0.0385
temp:ph	32.4544	1	211.6463	0.000

Dunn's test

In order to compare the control response of ragworms (*Hediste diversicolor*) to their response at various concentrations of the chemical cue a non-parametric Dunn's multiple comparison test was run. The full results are shown below. Signif. codes: 0 '***' 0.001 '**' 0.01 '*' 0.05 '.' 0.1 ' ' 1

Table S2. 10: Results of nonparametric multiple comparison Dunn's test for pH8.1, 18C

		Estimate	Std. Error	t value	Pr(> t)	
1X10 ⁻²	Control	39.799	8.229	4.837	< 0.001	***
1X10 ⁻³	Control	24.985	8.229	3.036	0.01864	*
1X10 ⁻⁴	Control	13.857	8.229	1.684	0.41282	
1X10 ⁻⁵	Control	27.989	8.229	3.401	0.00587	**
1X10 ⁻⁶	Control	21.509	8.229	2.614	0.05929	.
1X10 ⁻⁷	Control	22.505	8.229	2.735	0.04322	*
1X10 ⁻⁸	Control	23.569	8.229	2.864	0.0304	*
1X10 ⁻⁹	Control	37.801	8.229	4.594	< 0.001	***

Table S2. 11: Results of nonparametric multiple comparison Dunn's test for pH8.1, 22C

		Estimate	Std. Error	t value	Pr(> t)	
1X10 ⁻²	Control	6.098	6.13	0.995	0.8882	
1X10 ⁻³	Control	14.415	6.13	2.352	0.1122	
1X10 ⁻⁴	Control	3.688	6.13	0.602	0.9931	
1X10 ⁻⁵	Control	14.218	6.13	2.319	0.1208	
1X10 ⁻⁶	Control	3.347	6.13	0.546	0.9963	
1X10 ⁻⁷	Control	15.557	6.13	2.538	0.0717	.

1X10 ⁻⁸	Control	15.08	6.13	2.46	0.0871	.
1X10 ⁻⁹	Control	46.017	6.13	7.507	<0.001	***

Table S2. 12: Results of nonparametric multiple comparison Dunn's test for pH7.3, 18C

		Estimate	Std. Error	t value	Pr(> t)	
1X10 ⁻²	Control	8.358	6.752	1.238	0.7364	
1X10 ⁻³	Control	12.014	6.752	1.779	0.3528	
1X10 ⁻⁴	Control	15.248	6.752	2.258	0.1385	
1X10 ⁻⁵	Control	12.437	6.752	1.842	0.3169	
1X10 ⁻⁶	Control	21.452	6.752	3.177	0.0121	*
1X10 ⁻⁷	Control	20.53	6.752	3.041	0.0182	*
1X10 ⁻⁸	Control	35.654	6.752	5.28	<0.001	***
1X10 ⁻⁹	Control	12.202	6.752	1.807	0.3365	

Table S2. 13: Results of nonparametric multiple comparison Dunn's test for pH7.3, 22C

		Estimate	Std. Error	t value	Pr(> t)	
1X10 ⁻²	Control	24.012	6.865	3.498	0.00422	**
1X10 ⁻³	Control	46.162	6.865	6.724	< 0.001	***
1X10 ⁻⁴	Control	26.434	6.865	3.85	0.00126	**
1X10 ⁻⁵	Control	17.747	6.865	2.585	0.06383	.
1X10 ⁻⁶	Control	24.007	6.865	3.497	0.00423	**
1X10 ⁻⁷	Control	24.49	6.865	3.567	0.00333	**
1X10 ⁻⁸	Control	22.145	6.865	3.226	0.01035	*
1X10 ⁻⁹	Control	31.176	6.865	4.541	< 0.001	***

Curve fitting

In order to analyse the dose-response relationship between cue concentration and activity in each pH/ temperature condition Dr Fit (Di Veroli et al., 2015) was used to fit mono or multiphasic curves. The fitted curves and associated parameters are detailed below.

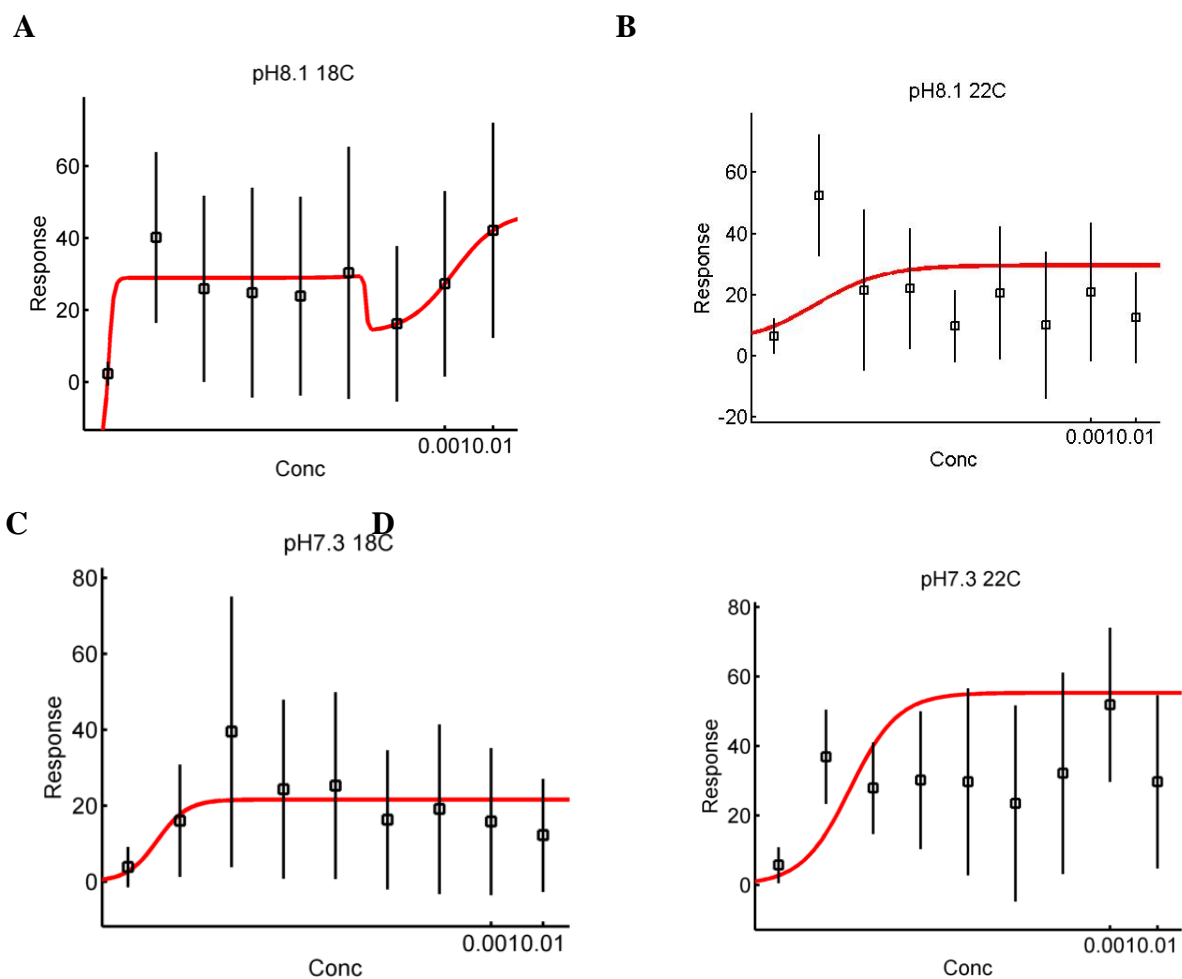


Figure S2. 3: Dose response fitted curves for response of *Hediste diversicolor* to taurine A) pH8.1, 18C, goodness of fit < 0.0001 . B) pH8.1, 22C, goodness of fit < 0.0001 . C) pH7.3, 18C, goodness of fit < 0.0001 . D) pH7.2, 22C, goodness of fit < 0.0001 .

GSH

Shapiro-Wilk test for normality

Data tested for normality using a Shapiro-Wilk test in R and found to be non-normal ($W = 0.80975$, $p\text{-value} < 2.2e-16$)

Levene's test for homogeneity of variance

Data tested for homogeneity of variance using a Levene's test in R and found to have heteroscedastic variance ($DF=8$, $F\text{-value} 9.3985$, $p = 2.18e-12$).

Robust factorial repeated measures ANOVA

Table S2. 14: Results of robust factorial repeated measures ANOVA using WRS2 package in R

Table					
S2.13:	value	df1	df2	p.value	
temp	12.5039	1	212.519	0.0005	
ph	4.4011	1	200.4508	0.0372	
temp:ph	2.817	1	200.4508	0.0948	

Dunn's test

In order to compare the control response of ragworms (*Hediste diversicolor*) to their response at various concentrations of the chemical cue a non-parametric Dunn's multiple comparison test was run. The full results are shown below. Signif. codes: 0 '***' 0.001 '**' 0.01 '*' 0.05 '.' 0.1 ' ' 1

Table S2. 15: Results of nonparametric multiple comparison Dunn's test for pH8.1, 18C

		Estimate	Std. Error	t value	Pr(> t)	
1X10 ⁻²	Control	-9.905	6.408	-1.546	0.508	
1X10 ⁻³	Control	-8.168	6.408	-1.275	0.71	
1X10 ⁻⁴	Control	-9.22	6.408	-1.439	0.587	
1X10 ⁻⁵	Control	3.494	6.408	0.545	0.996	
1X10 ⁻⁶	Control	8.774	6.408	1.369	0.639	
1X10 ⁻⁷	Control	27.024	6.408	4.217	<0.001	***
1X10 ⁻⁸	Control	26.986	6.408	4.211	<0.001	***
1X10 ⁻⁹	Control	35.362	6.408	5.518	<0.001	***

Table S2. 16: Results of nonparametric multiple comparison Dunn's test for pH8.1, 22C

		Estimate	Std. Error	t value	Pr(> t)	
1X10 ⁻²	Control	22.899	8.619	2.657	0.05314	.
1X10 ⁻³	Control	18.81	8.619	2.182	0.1631	

1X10 ⁻⁴	Control	24.986	8.619	2.899	0.02751	*
1X10 ⁻⁵	Control	34.589	8.619	4.013	< 0.001	***
1X10 ⁻⁶	Control	24.335	8.619	2.823	0.03386	*
1X10 ⁻⁷	Control	17.592	8.619	2.041	0.21807	
1X10 ⁻⁸	Control	31.904	8.619	3.701	0.00219	**
1X10 ⁻⁹	Control	24.75	8.619	2.871	0.02949	*

Table S2. 17Results of nonparametric multiple comparison Dunn's test for pH7.3, 18C

		Estimate	Std. Error	t value	Pr(> t)	
1X10 ⁻²	Control	5.278	7.884	0.67	0.98648	
1X10 ⁻³	Control	2.565	7.884	0.325	0.99991	
1X10 ⁻⁴	Control	17.23	7.884	2.185	0.1621	
1X10 ⁻⁵	Control	11.651	7.884	1.478	0.5579	
1X10 ⁻⁶	Control	26.656	7.884	3.381	0.00632	**
1X10 ⁻⁷	Control	20.56	7.884	2.608	0.06014	.
1X10 ⁻⁸	Control	30.996	7.884	3.931	< 0.001	***
1X10 ⁻⁹	Control	28.286	7.884	3.588	0.00311	**

Table S2. 18: Results of nonparametric multiple comparison Dunn's test for pH7.3, 22C

		Estimate	Std. Error	t value	Pr(> t)	
1X10 ⁻²	Control	13.791	7.505	1.838	0.3192	
1X10 ⁻³	Control	16.843	7.505	2.244	0.14279	
1X10 ⁻⁴	Control	16.138	7.505	2.15	0.17477	
1X10 ⁻⁵	Control	28.544	7.505	3.803	0.00151	**
1X10 ⁻⁶	Control	31.347	7.505	4.177	< 0.001	***
1X10 ⁻⁷	Control	32.101	7.505	4.278	< 0.001	***
1X10 ⁻⁸	Control	21.731	7.505	2.896	0.02767	*
1X10 ⁻⁹	Control	21.772	7.505	2.901	0.02714	*

Curve fitting

In order to analyse the dose-response relationship between cue concentration and activity in each pH/ temperature condition Dr Fit (Di Veroli et al., 2015) was used to fit mono or multiphasic curves. The fitted curves and associated parameters are detailed below.

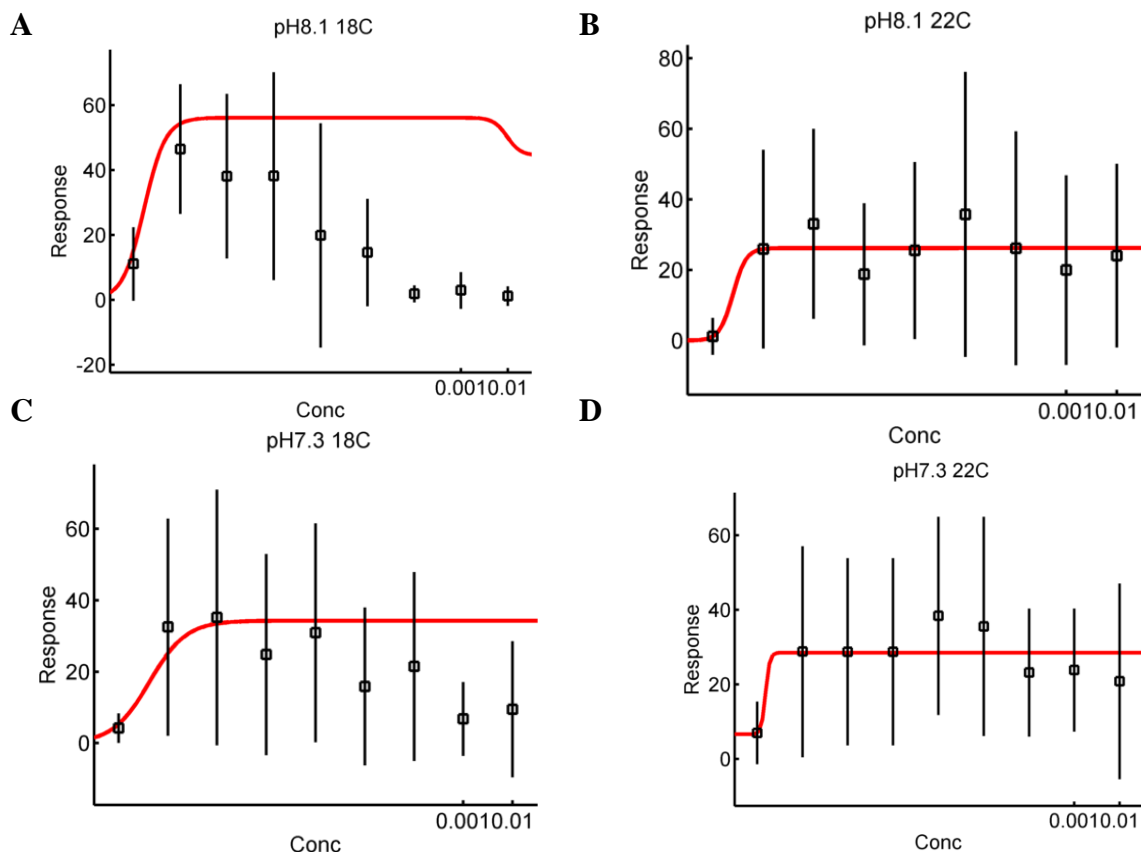


Figure S2. 4: Dose response fitted curves for response of *Hediste diversicolor* to GSH A) pH8.1, 18C, goodness of fit < 0.0001. B) pH8.1, 22C, goodness of fit < 0.0001. C) pH7.3, 18C, goodness of fit < 0.0001. D) pH7.2, 22C, goodness of fit = 0.0017.

UREA

Shapiro-Wilk test for normality

Data tested for normality using a Shapiro-Wilk test in R and found to be non-normal ($W = 0.53314$, $p\text{-value} < 2.2e-16$)

Levene's test for homogeneity of variance

Data tested for homogeneity of variance using a Levene's test in R and found to have heteroscedastic variance ($DF=8$, $F\text{-value} 2.8773$, $p = 0.0037$).

Robust factorial repeated measures ANOVA

Table S2. 19: Results of robust factorial repeated measures ANOVA using WRS2 package in R

	value	df1	df2	p.value
temp	2.9209	1	168.724	0.0893
ph	1.7043	1	168.2996	0.1935
temp:ph	5.3545	1	168.2996	0.0219

Dunn's test

In order to compare the control response of ragworms (*Hediste diversicolor*) to their response at various concentrations of the chemical cue a non-parametric Dunn's multiple comparison test was run. The full results are shown below. Signif. codes: 0 '***' 0.001 '**' 0.01 '*' 0.05 '.' 0.1 ' ' 1

Table S2. 20: Results of nonparametric multiple comparison Dunn's test for pH8.1, 18C

		Estimate	Std. Error	t value	Pr(> t)	
1x10 ⁻²	Control	-6.017	1.733	-3.472	0.00457	**
1x10 ⁻³	Control	-6.137	1.733	-3.541	0.0037	**
1x10 ⁻⁴	Control	-5.583	1.733	-3.221	0.01044	*
1x10 ⁻⁵	Control	-5.502	1.733	-3.174	0.01207	*
1x10 ⁻⁶	Control	-4.871	1.733	-2.81	0.03525	*
1X10 ⁻⁷	Control	-6.931	1.733	-3.999	< 0.001	***
1X10 ⁻⁸	Control	-3.364	1.733	-1.941	0.26464	
1X10 ⁻⁹	Control	-3.603	1.733	-2.079	0.20221	

Table S2. 21: Results of nonparametric multiple comparison Dunn's test for pH8.1, 22C

		Estimate	Std. Error	t value	Pr(> t)
1x10 ⁻²	Control	2.5217	4.2242	0.597	0.993
1x10 ⁻³	Control	-4.2424	4.2242	-1.004	0.883
1x10 ⁻⁴	Control	-4.2799	4.2242	-1.013	0.879
1x10 ⁻⁵	Control	-2.5661	4.2242	-0.607	0.993
1x10 ⁻⁶	Control	8.2314	4.2242	1.949	0.261
1X10 ⁻⁷	Control	-0.2566	4.2242	-0.061	1

1X10 ⁻⁸	Control	-0.7719	4.2242	-0.183	1
1X10 ⁻⁹	Control	7.795	4.2242	1.845	0.315

Table S2. 22: Results of nonparametric multiple comparison Dunn's test for pH7.3, 18C

		Estimate	Std. Error	t value	Pr(> t)
1x10 ⁻²	Control	-1.771	3.669	-0.483	0.998
1x10 ⁻³	Control	-6.029	3.669	-1.643	0.44
1x10 ⁻⁴	Control	-6.133	3.669	-1.671	0.421
1x10 ⁻⁵	Control	-5.306	3.669	-1.446	0.582
1x10 ⁻⁶	Control	-6.124	3.669	-1.669	0.423
1X10 ⁻⁷	Control	-4.61	3.669	-1.256	0.723
1X10 ⁻⁸	Control	-3.806	3.669	-1.037	0.866
1X10 ⁻⁹	Control	4.336	3.669	1.182	0.776

Table S2. 23: Results of nonparametric multiple comparison Dunn's test for pH7.3, 22C

		Estimate	Std. Error	t value	Pr(> t)
1x10 ⁻²	Control	5.12521	3.80124	1.348	0.655
1x10 ⁻³	Control	8.37671	3.80124	2.204	0.156
1x10 ⁻⁴	Control	0.93189	3.80124	0.245	1
1x10 ⁻⁵	Control	-0.20796	3.80124	-0.055	1
1x10 ⁻⁶	Control	-2.87687	3.80124	-0.757	0.972
1X10 ⁻⁷	Control	0.01628	3.80124	0.004	1
1X10 ⁻⁸	Control	1.47443	3.80124	0.388	1
1X10 ⁻⁹	Control	3.83493	3.80124	1.009	0.881

Curve fitting

Where possible, in order to analyse the dose-response relationship between cue concentration and activity in each pH/ temperature condition Dr Fit (Di Veroli et al., 2015) was used to fit mono or multiphasic curves. The fitted curves and associated parameters are detailed below.

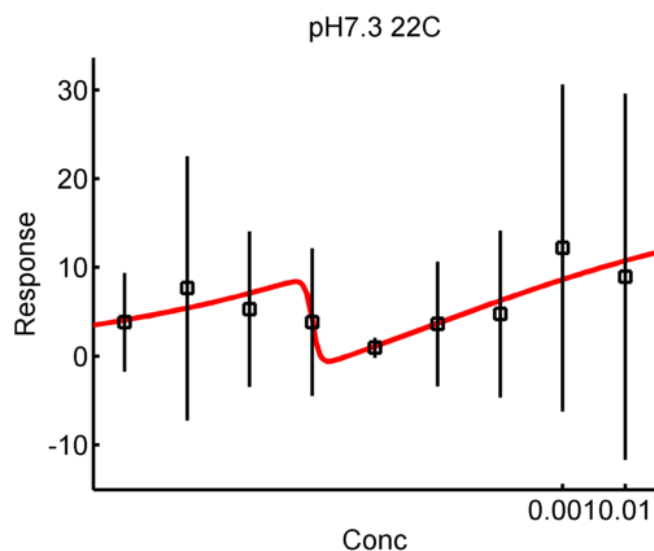


Figure S2. 5: Dose response fitted curves for response of *Hediste diversicolor* to urea at pH7.2, 22C, goodness of fit , 0.0001.

CHONDROITIN SULPHATE

Shapiro-Wilk test for normality

Data tested for normality using a Shapiro-Wilk test in R and found to be non-normal (W = 0.60296, p-value < 2.2e-16)

Levene's test for homogeneity of variance

Data tested for homogeneity of variance using a Levene's test in R and found to have heteroscedastic variance (DF=8, F-value= 2.7015 , p = 0.006204).

Robust factorial repeated measures ANOVA

Table S2. 24: Results of robust factorial repeated measures ANOVA using WRS2 package in R

	value	df1	df2	p.value
temp	40.6797	1	126.5472	0
ph	3.9268	1	124.0392	0.0497
temp:ph	0.2839	1	124.0392	0.5951

Dunn's test

In order to compare the control response of ragworms (*Hediste diversicolor*) to their response at various concentrations of the chemical cue a non-parametric Dunn's multiple comparison test was run. The full results are shown below. Signif. codes: 0 '***' 0.001 '**' 0.01 '*' 0.05 '.' 0.1 ' ' 1

Table S2. 25: Results of nonparametric multiple comparison Dunn's test for pH8.1, 18C

		Estimate	Std. Error	t value	Pr(> t)
1x10 ⁻²	Control	4.01	2.014	1.991	0.241
1x10 ⁻³	Control	-2.44	2.014	-1.211	0.755
1x10 ⁻⁴	Control	-4.67	2.014	-2.318	0.121
1x10 ⁻⁵	Control	-4.401	2.014	-2.185	0.162
1x10 ⁻⁶	Control	-3.986	2.014	-1.979	0.246
1x10 ⁻⁷	Control	-4.364	2.014	-2.166	0.169
1x10 ⁻⁸	Control	-3.58	2.014	-1.777	0.354
1x10 ⁻⁹	Control	3.114	2.014	1.546	0.508

Table S2. 26: Results of nonparametric multiple comparison Dunn's test for pH8.1, 22C

		Estimate	Std. Error	t value	Pr(> t)	
1x10 ⁻²	Control	5.465	6.058	0.902	0.92938	
1x10 ⁻³	Control	9.827	6.058	1.622	0.45424	
1x10 ⁻⁴	Control	7.432	6.058	1.227	0.74429	
1x10 ⁻⁵	Control	3.373	6.058	0.557	0.99582	
1x10 ⁻⁶	Control	20.356	6.058	3.36	0.00667	**
1x10 ⁻⁷	Control	21.688	6.058	3.58	0.00322	**
1x10 ⁻⁸	Control	24.454	6.058	4.037	< 0.001	***
1x10 ⁻⁹	Control	19.365	6.058	3.197	0.01143	*

Table S2. 27: Results of nonparametric multiple comparison Dunn's test for pH7.3, 18C

		Estimate	Std.Error	t value	Pr(> t)
1x10 ⁻²	Control	7.5382	3.175	2.374	0.107
1x10 ⁻³	Control	-1.3808	3.175	-0.435	0.999
1x10 ⁻⁴	Control	-4.4108	3.175	-1.389	0.624
1x10 ⁻⁵	Control	-5.8454	3.175	-1.841	0.317
1x10 ⁻⁶	Control	-2.7634	3.175	-0.87	0.941
1x10 ⁻⁷	Control	-2.1459	3.175	-0.676	0.986
1x10 ⁻⁸	Control	-0.5234	3.175	-0.165	1
1x10 ⁻⁹	Control	1.8529	3.175	0.584	0.994

Table S2. 28: Results of nonparametric multiple comparison Dunn's test for pH7.3, 22C

		Estimate	Std. Error	t value	Pr(> t)	
1x10 ⁻²	Control	17.087	5.468	3.125	0.0141	*
1x10 ⁻³	Control	14.694	5.468	2.687	0.049	*
1x10 ⁻⁴	Control	9.649	5.468	1.765	0.3621	
1x10 ⁻⁵	Control	25.6	5.468	4.682	<0.001	***
1x10 ⁻⁶	Control	3.911	5.468	0.715	0.9799	
1x10 ⁻⁷	Control	10.713	5.468	1.959	0.2553	
1x10 ⁻⁸	Control	6.364	5.468	1.164	0.7877	
1x10 ⁻⁹	Control	21.502	5.468	3.933	<0.001	***

Curve fitting

Where possible, in order to analyse the dose-response relationship between cue concentration and activity in each pH/ temperature condition Dr Fit (Di Veroli et al., 2015) was used to fit mono or multiphasic curves. The fitted curves and associated parameters are detailed below.

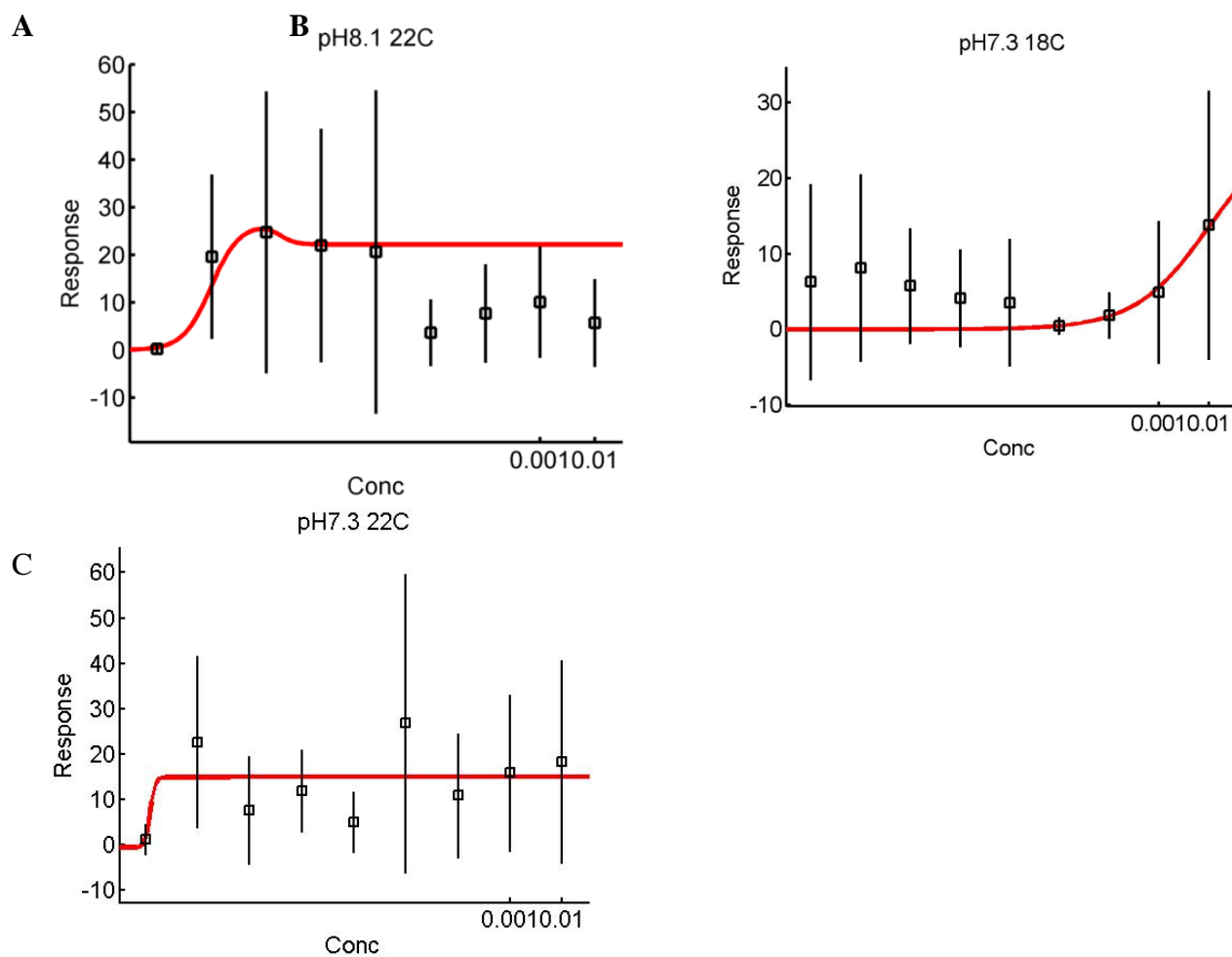


Figure S2. 6: Dose response fitted curves for response of *Hediste diversicolor* to chondroitin sulphate A) pH8.1, 22C, goodness of fit < 0.0001. B) pH7.3, 18C, goodness of fit = 0.0059. C) pH7.3, 22C, goodness of fit = 0.0029.

Supplementary Materials – Chapter 3

Supplementary Material – In-burrow oxygen

Average water oxygen levels

Table S3. 1: Average oxygen level in the water above the analysed burrow. Computed using a region of interest in the VisiSens AnalytiCal.

pH	Temperature (Celsius)	Average water oxygen (% air sat)
8.1	18	71.63 (SD = 9.11)
8.1	22	65.56 (SD = 7.71)
7.7	18	68.22 (SD = 11.29)
7.7	22	73.95 (SD = 9.52)
7.3	18	78.95 (SD = 5.14)
7.3	22	78.56 (SD = 3.26)

Monitoring data for pH, salinity and temperature of culture tanks

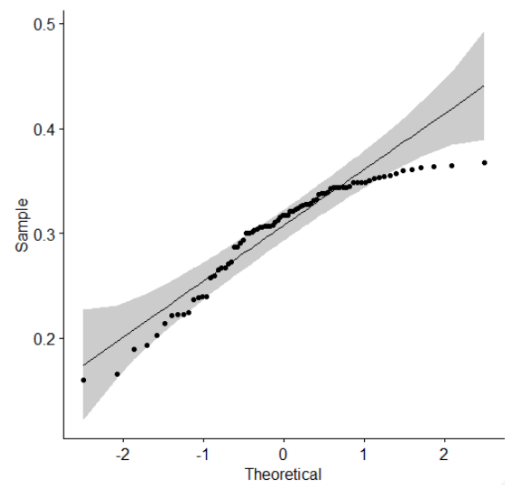
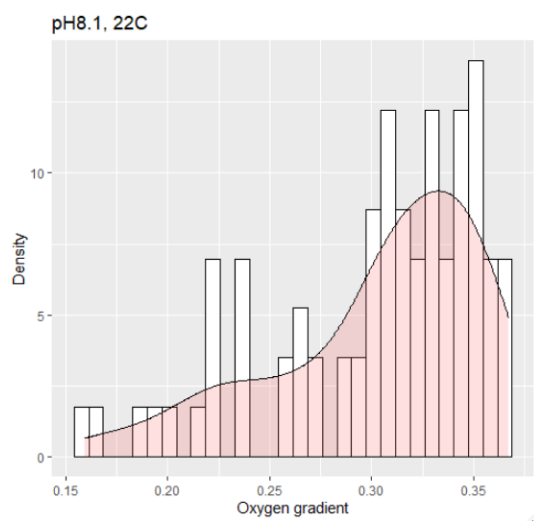
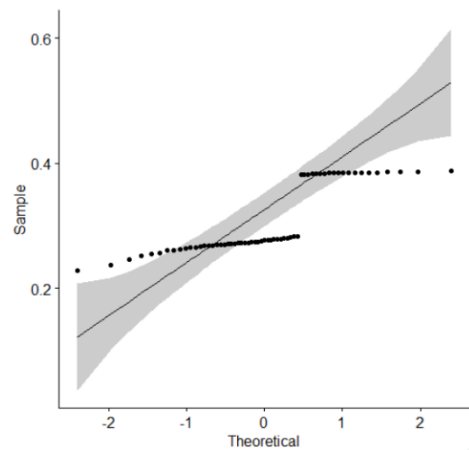
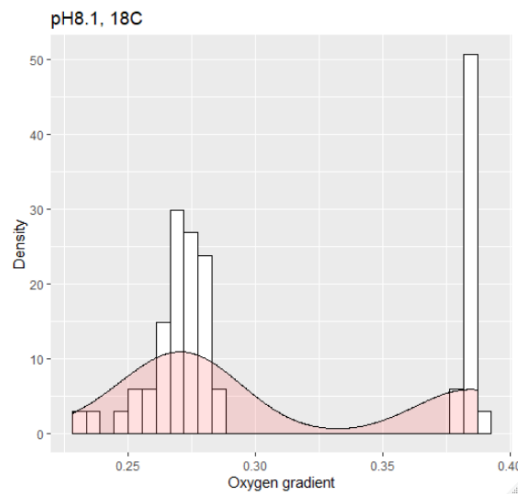
Table S3. 2: Monitoring of temperature, pH and salinity in worm culture tanks was done three times per week when possible. The data is shown below and was used to calculate variation (standard error) in these variables.

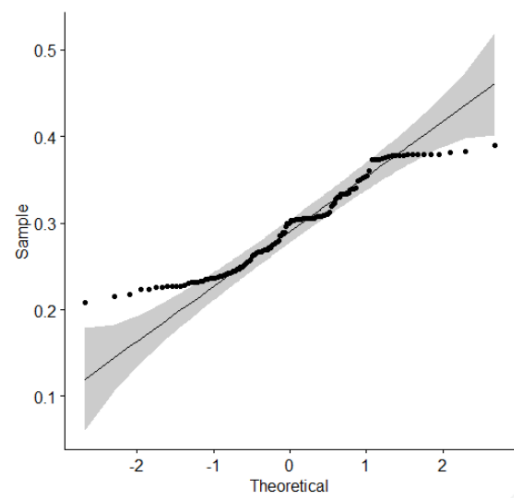
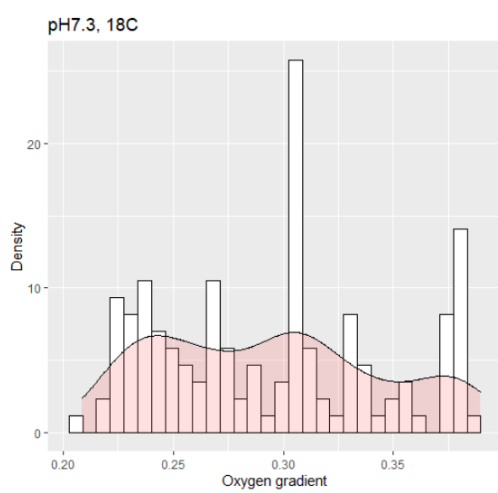
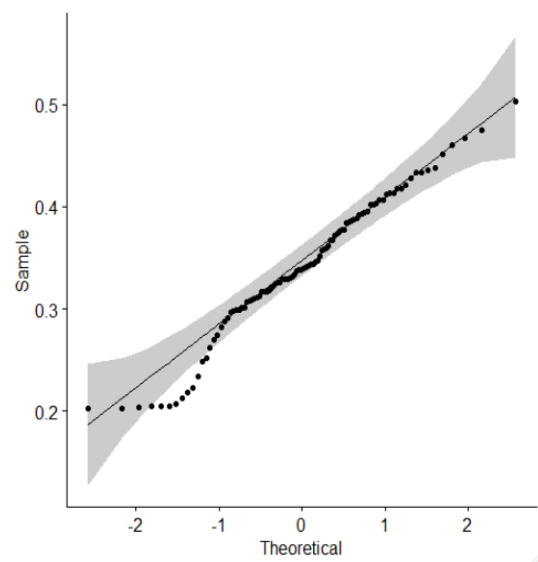
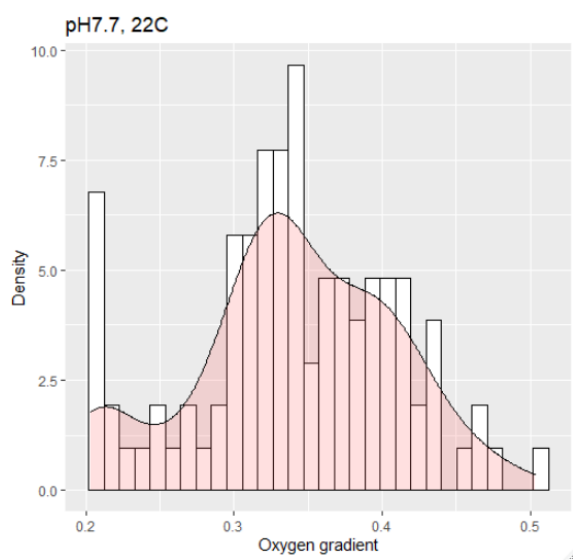
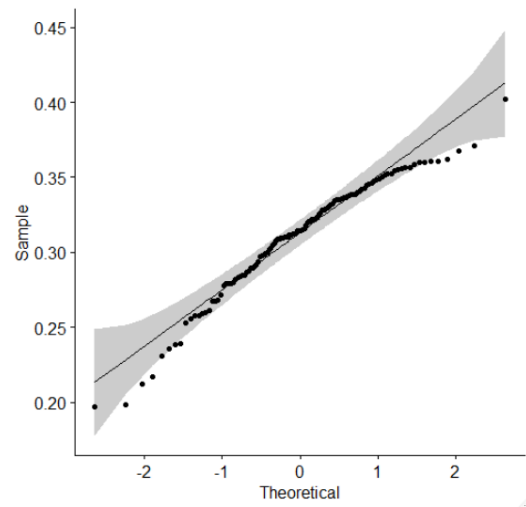
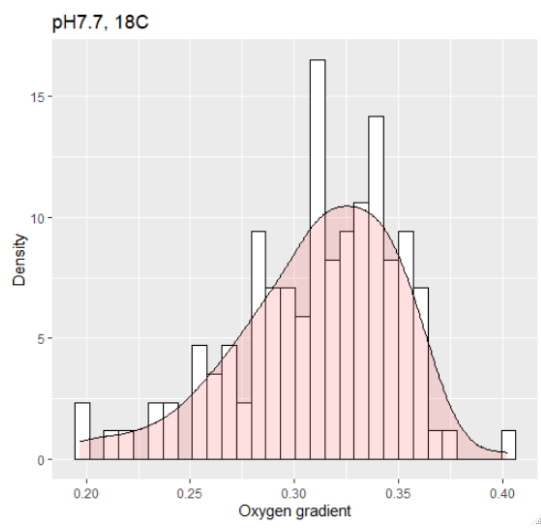
Date	Temp	8.1		7.7		7.3	
		pH	Salinity	pH	Salinity	pH	Salinity
01/07/2020	17	8.14	21	7.66	22	7.28	21
03/07/2020	18	8.03	18	7.67	18	7.31	18
07/07/2020	18	8.16	18	7.66	18	7.26	18
08/07/2020	18	8.09	17	7.7	18	7.29	17
09/07/2020	18	8.1	19	7.72	20	7.32	20
11/07/2020	18	8.11	19	7.69	18	7.27	19
13/07/2020	18	8.01	20	7.67	18	7.35	18
14/07/2020	18	7.92	18	7.6	18	7.31	18
13/07/2020	18	8.03	18	7.62	18	7.28	19
14/07/2020	18	8.13	19	7.54	18	7.28	18

16/07/2020	18	8.11	19	7.55	18	7.32	18
17/07/2020	18	8.04	20	7.71	18	7.24	19
22/07/2020	18	8.14	17	7.65	19	7.25	20
24/07/2020	18	8.01	18	7.62	17	7.35	17
25/07/2020	18	8.11	18	7.72	17	7.3	17
26/07/2020	18	8.02	18	7.7	17	7.3	18
27/07/2020	18	8.09	18	7.71	17	7.29	18
29/07/2020	18	8.10	18	7.73	17	7.29	18
31/07/2020	18	8.11	18	7.75	17	7.30	18
01/08/2020	18	8.00	18	7.64	18	7.22	18
02/08/2020	18	8.12	18	7.64	18	7.3	18
03/08/2020	18	8.06	18	7.69	18	7.23	18
04/08/2020	18	8.02	18	7.61	18	7.22	18
05/08/2020	18	8.04	18	7.67	18	7.3	18
07/08/2020	18	8.10	17	7.68	19	7.29	19
08/08/2020	18	8.13	18	7.73	19	7.23	19
09/08/2020	18	8.12	18	7.69	18	7.34	17
10/08/2020	18	8.08	18	7.75	18	7.34	17
11/08/2020	18	8.11	18	7.65	18	7.3	18
13/08/2020	18	8.10	18	7.63	18	7.26	18
14/08/2020	18	8.00	19	7.72	18	7.29	18
20/08/2020	18	8.12	18	7.64	18	7.31	18
21/08/2020	18	8.09	18	7.68	18	7.3	18
22/08/2020	18	8.10	18	7.68	18	7.34	18
24/08/2020	18	8.03	18	7.70	18	7.35	18
25/08/2020	18	8.01	18	7.61	18	7.31	18
26/08/2020	18	8.14	18	7.66	18	7.24	18
27/08/2020	18	8.10	18	7.69	18	7.29	18
28/08/2020	18	8.04	18	7.74	18	7.26	18
29/08/2020	18	8.01	18	7.61	18	7.28	18
30/08/2020	18	8.09	18	7.65	18	7.33	18

31/08/2020	18	8.15	18	7.71	18	7.33	18
mean		8.076405	18.19841	7.670032	18.06984	7.291639	18.13307
SD		0.053287	0.753886	0.049256	0.840521	0.035814	0.816554
SE		0.008124	0.114934	0.007509	0.128142	0.00546	0.124488

Assessing normality of data for O₂ Ratio Groups





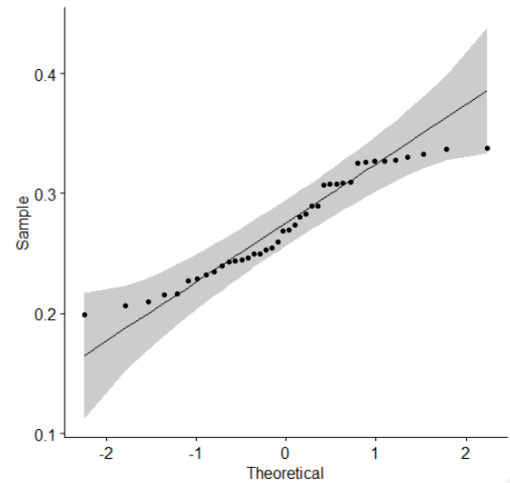
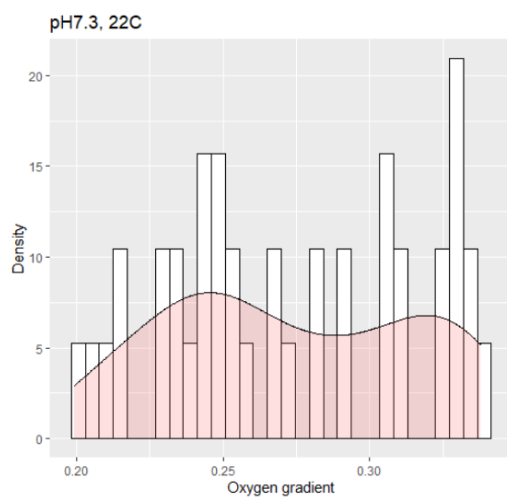


Figure S3. 1: Histograms and QQ plots for assessment of normality on Oxygen Ratio for each of the conditions tested.

Data for oxygen ratio were tested for normality using a Shapiro-Wilk test. Data were found to significantly deviate from a normal distribution for all pH/ temperature groups ($p < 0.05$, see Supplementary Table 2).

Table S3. 3: : Results of Shapiro-Wilk's test of normality for the oxygen ratio variable generated in R (centre= median) for each pH/ temperature group. All groups are significantly non-normal.

pH	Temperature	W	P value
8.1	18	0.7357029	3.775829e-09
8.1	22	0.8959771	8.270375e-06
7.7	18	0.9613549	1.627841e-03
7.7	22	0.9755389	5.946258e-02
7.3	18	0.9406025	1.414013e-05
7.3	22	0.9344617	2.257920e-02

Table S3. 4: Results of Shapiro-Wilk's test of normality for the oxygen ratio variable generated in R (centre= median) for all data. The data does not conforms to a normal distribution ($p < 0.05$).

dat\$O2_Grad	W = 0.99401	p-value = 0.03231
--------------	-------------	-------------------

A Levene's test for homogeneity of variance indicated that variance was not homogenous for the oxygen ratio variable (see Supplementary Table 3).

Table S3. 5: Results of Levene's test for homogeneity of variance (centre=median) for O2 ratio variable.

Df	F value	Pr(>F)
5	5.5632	5.24e-05 ***

A robust independent factorial ANOVA test with trimmed means (0.2) was therefore used to test for differences between independent treatments (different individuals were used in each test condition) using the WRS2 package and t2way function (see Supplementary Table 4). The ANOVA test result was followed by a multiple comparison post hoc test using the mcp2atm function in R (Mair and Wilcox, 2020).

Table S3. 6: Results of robust independent factorial ANOVA test with trimmed means (0.2) using the WRS2 package and t2way function for oxygen ratio variable.

	value	P.value
Temperature	2.1307	0.147
pH	52.5829	0.001
Temperature ~ pH	12.0291	0.004

The impact of temperature on O₂ Ratio was not significant (p=0.147) but the impact of pH on O₂ ratio is significant (p=0.001). The interaction between pH and temperature was significant (p=0.004) meaning the relationship between pH and oxygen ratio is dependent upon temperature. Because of this interaction, a post-hoc test was run.

Python script for oxygen penetration depth

```
import cv2
import numpy as np
import os
import sys
import glob
from PIL import Image
from scipy import ndimage
```



```

os.sys.path
import matplotlib.pyplot as plt
from scipy import misc
from pathlib import Path
from os import listdir
from os.path import isfile, join
import pandas as pd
from os.path import abspath

#####SET PATHS#####

image_path = 'E:/BOX BACKUP/ OxygenFoil/Individual burrows for penetration
analysis/pH7.3_18C*.jpg'
FILE_FORMAT = ".jpg"

#Batch processing many images:
imgs= glob.glob('E:/BOX BACKUP/OxygenFoil/Individual burrows for penetration
analysis/pH7.3_18C/*.jpg' )
print('Found files:', )
print(imgs)

#####BLUR#####

#Save images in new folder
folder_blur = 'E:/BOX BACKUP/ OxygenFoil/Individual burrows for penetration
analysis/blurred'
if not os.path.exists(folder_blur):
    os.makedirs(folder_blur)

```

```

#GaussianBlur
i=0

for img in imgs:
    blur = cv2.imread(img, cv2.IMREAD_UNCHANGED) # import
    dst = cv2.GaussianBlur(blur,(7,7),0) # blur (Gaussian)
    cv2.imwrite('/BOX BACKUP/BestRevengeIs/OxygenFoil/Individual burrows for
penetration analysis/blurred/image%04i.jpg' %i, dst)
    i += 1

#####CREATE MASK AND BINARYSE IMAGES#####

folder_mask = 'E:/BOX BACKUP/ OxygenFoil/Individual burrows for penetration
analysis/Mask'
if not os.path.exists(folder_mask):
    os.makedirs(folder_mask)

#- Initial Setting --
#folder = 'E:/BOX BACKUP/ OxygenFoil/Individual burrows for penetration
analysis/blurred/'
#Set new file path for blurred imgs
BLURRED_PATH = glob.glob('E:/BOX BACKUP/ OxygenFoil/Individual burrows for
penetration analysis/blurred/*.jpg' )
FILE_FORMAT = ".jpg"
print('Found files, blurred_path:', )
print(BLURRED_PATH)

# color threshold
red_low = np.array([60 , 2, 70] )
red_high = np.array([190, 65, 195])
blue_low = np.array([20 , 10 , 59])
blue_high = np.array([136 ,40 , 135])

```

```

#-----BGR codes for use with CV2
def batchprocessor(Img):

    i=0
    for img in BLURRED_PATH:

        blur = cv2.imread(img, cv2.IMREAD_UNCHANGED)
        img=np.array(Image.open(img))

        #blur_denoise = cv2.fastNlMeansDenoisingColored(img, None, 3, 7, 11)

        #Set colour limits for red and blue detection
        red_mask = cv2.inRange(blur, red_low, red_high)
        blue_mask = cv2.inRange(blur, blue_low, blue_high)

        #Fill in the burrow
        red_closing = red_mask
        blue_closing = blue_mask
        kernel = np.ones((5,5),np.uint8) #erosion to minimise noise
        red_closing = cv2.morphologyEx(red_closing,cv2.MORPH_OPEN,kernel)
        blue_closing = cv2.morphologyEx(blue_closing,cv2.MORPH_OPEN,kernel)

        mask = cv2.bitwise_or(red_mask, blue_mask)

        se1 = cv2.getStructuringElement(cv2.MORPH_RECT, (5,5))
        se2 = cv2.getStructuringElement(cv2.MORPH_RECT, (2,2))
        mask_close = cv2.morphologyEx(mask, cv2.MORPH_CLOSE, se1)
        mask_open = cv2.morphologyEx(mask_close, cv2.MORPH_OPEN, se2)

        #mask_processed = np.dstack([mask, mask, mask]) / 255
        #out = img * mask
        #kernel2 = cv2.getStructuringElement(cv2.MORPH_RECT, (2,2))
        #erosion = cv2.erode(mask, kernel2, iterations=1)

```

```

#kernel3 = cv2.getStructuringElement(cv2.MORPH_RECT, (3,3))
#dilate = cv2.dilate(erosion, kernel3, iterations=1)

target = cv2.bitwise_and(blur, blur, mask = mask_open)
#target_denoise = cv2.fastNlMeansDenoisingColored(target, None, 3, 7, 11)
edges = cv2.Canny(target,100,200)

cv2.imshow("mask", mask)
cv2.imshow("processed", mask_open)
cv2.imshow("edge", edges)
cv2.waitKey(0)
cv2.destroyAllWindows()

cv2.imwrite('E:/BOX BACKUP/BestRevengeIs/OxygenFoil/Individual burrows for
penetration analysis/Mask/mask%04i.jpg' %i, mask_open)
i += 1

#cv2.imwrite('Mask/mask'+ str(uuid.uuid4()) + FILE_FORMAT, mask)
#cv2.imwrite(IMAGE_PATH[0:-
len(FILE_FORMAT)]+"_mask"+FILE_FORMAT,mask)

print(batchprocessor(BLURRED_PATH))

#####SCAN FOR WHITE PIXEL
THICKNESS#####

#- Initial Setting --

image_path=('E:/BOX BACKUP/BestRevengeIs/OxygenFoil/Individual burrows for
penetration analysis/Mask/')

def average_depth_in_total(image_path):

    img = np.array(Image.open(image_path).convert('L'))

    im_bool = img > 1 # Binarise

    boundary_list = [] # list for the location of boundaries

```

```

width_list = [] # list for the width of the barrow at each point

for i in range(len(im_bool)):

    row_temp = im_bool[i]

    flag = False # current state of pixel

    for j,val in enumerate(row_temp):

        if val != flag: # detect boundary (whether current state of pixel is the same as the
next pixel's state or not)

            flag = val # change the state

            if val == False: # if the boundary is the one from inside of a burrow to the
outside of a burrow

                width = j-boundary_list[-1][1]+1 # calc the width

                width_list.append(width)

                boundary_list.append([i,j])

    average = np.average(np.array(width_list))

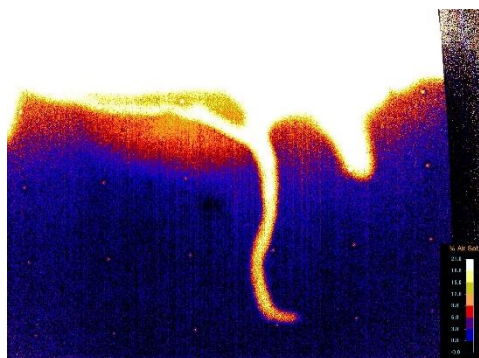
    return average

for img in listdir(image_path):

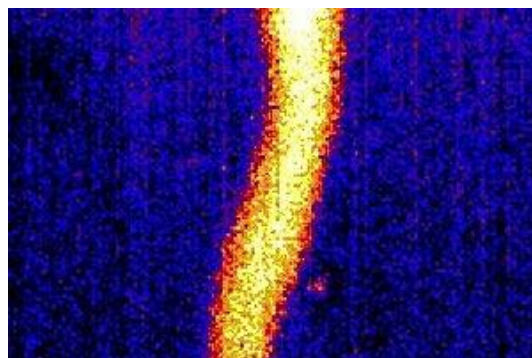
    print( average_depth_in_total(image_path + img))

```

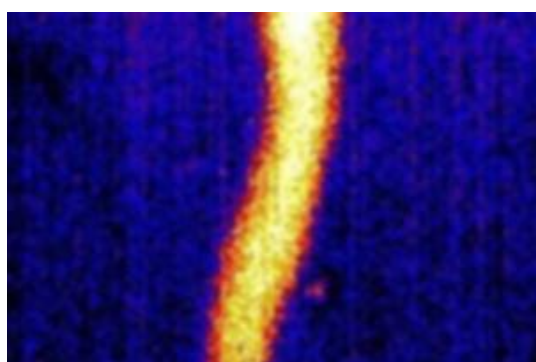
Example output images from Python script



Original



Crop



Gaussian smoothing

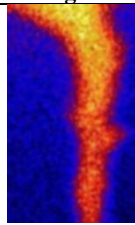

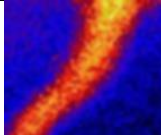

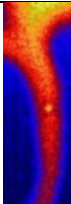

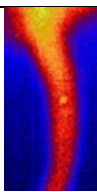



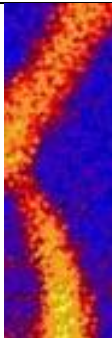

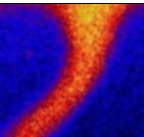

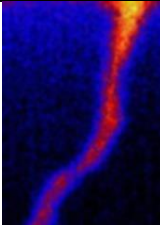
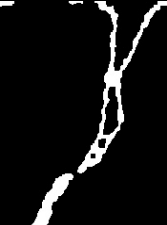
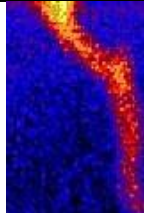

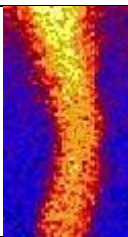

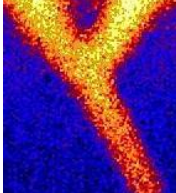

Mask for BGR colour range

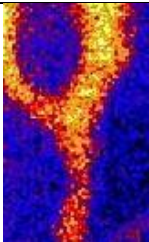

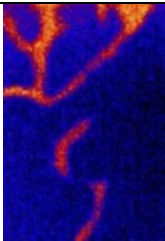

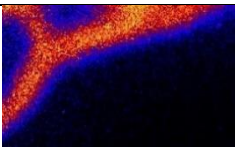

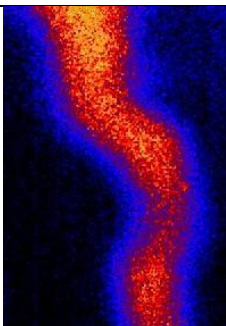
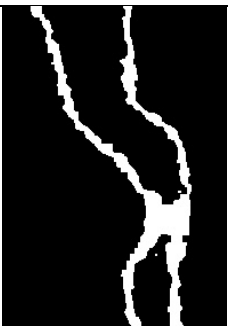
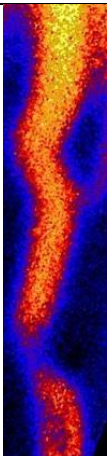

Figure S3. 2: Output images from various stages of the Python image analysis script used to compute oxygen penetration depth into the sediment.

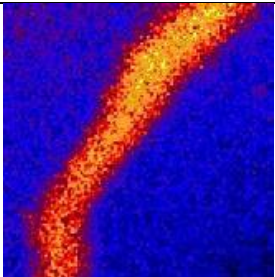

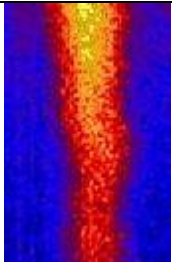

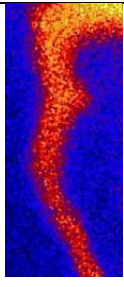

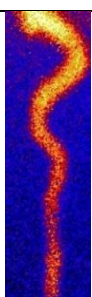

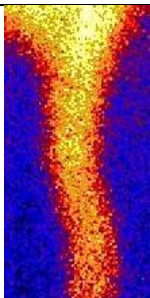

Images used

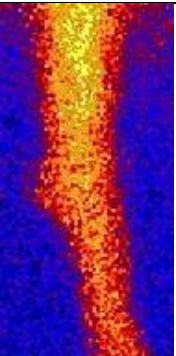

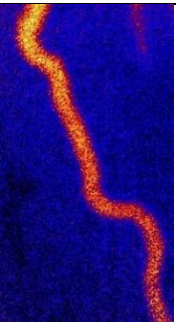
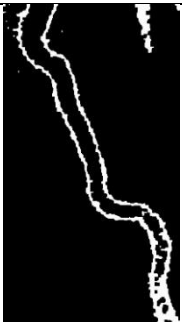
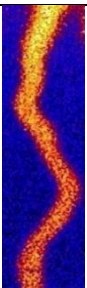

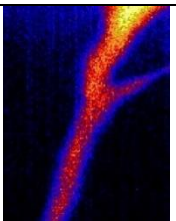

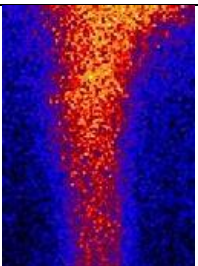
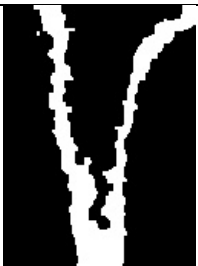
Table S3. 7: Table showing one of three representative images used for each burrow repeat in O₂ penetration depth calculation along with the corresponding 'Mask' image after processing for set RGB colour thresholds in Python. The Mask images were then used to *quantify O₂ penetration depth by counting the number of white pixels in each row and averaging.*

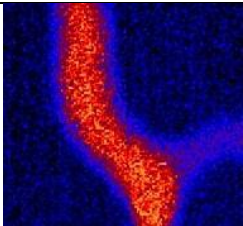
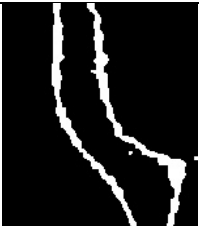
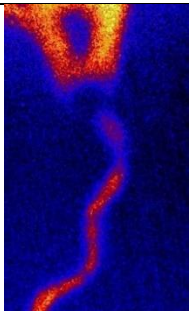

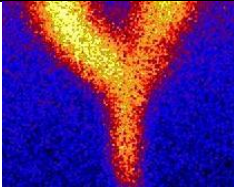

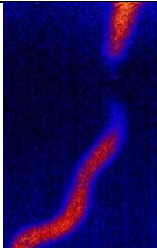

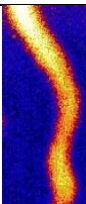

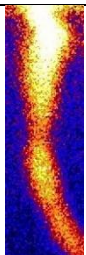

Filename	Original	Mask
pH8.1_18C_10_10_19_1_crop.jpg		
pH8.1_18C_10_10_19_2_crop.jpg		
pH8.1_18C_10_10_19_3_crop.jpg		
pH8.1_18C_10_10_19_burrow2_1_crop.jpg		
pH8.1_18C_10_10_19_burrow2_2_crop.jpg		
pH8.1_18C_10_10_19_burrow2_3.jpg		
pH8.1_18C_13_08_19_1_crop.jpg		
pH8.1_18C_13_08_19_2_crop.jpg		
pH8.1_18C_13_08_19_3_crop.jpg		
pH8.1_18C_14_08_19_1_crop.jpg		
pH8.1_18C_14_08_19_2_crop.jpg		
pH8.1_18C_14_08_19_3_crop.jpg		

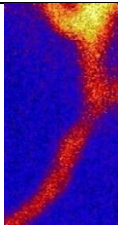

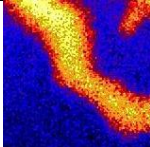

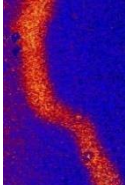

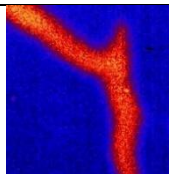

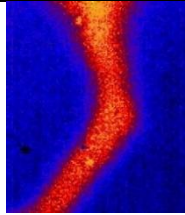

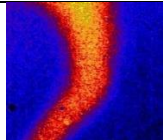

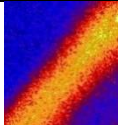

pH8.1_18C_19_11_20_1_crop.jpg		
pH8.1_18C_19_11_20_2_crop.jpg		
pH8.1_18C_19_11_20_3_crop.jpg		
pH8.1_18C_29_08_19_1_crop.jpg		
pH8.1_18C_29_08_19_2_crop.jpg		
pH8.1_18C_29_08_19_3_crop.jpg		
pH8.1_18C_30_08_20_1_crop.jpg		
pH8.1_18C_30_08_20_2_crop.jpg		
pH8.1_18C_30_08_20_3_crop.jpg		
pH8.1_22C_12_10_20_1_crop.jpg		
pH8.1_22C_12_10_20_2_crop.jpg		
pH8.1_22C_12_10_20_3_crop.jpg		
pH8.1_22C_14_11_20_1_crop.jpg		
pH8.1_22C_14_11_20_2_crop.jpg		
pH8.1_22C_14_11_20_3_crop.jpg		
pH8.1_22C_15_11_20_1_crop.jpg		
pH8.1_22C_15_11_20_2_crop.jpg		
pH8.1_22C_15_11_20_3_crop.jpg		



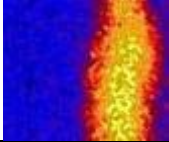

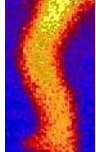

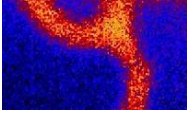

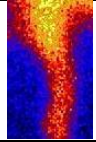

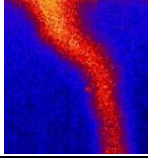

pH8.1_22C_24_10_20_1_crop.jpg		
pH8.1_22C_24_10_20_2_crop.jpg		
pH8.1_22C_24_10_20_3_crop.jpg		
pH8.1_22C_26_10_20_1_crop.jpg		
pH8.1_22C_26_10_20_2_crop.jpg		
pH8.1_22C_26_10_20_3_crop.jpg		
pH8.1_22C_31_08_19_1_crop.jpg		
pH8.1_22C_31_08_19_2_crop.jpg		
pH8.1_22C_31_08_19_3_crop.jpg		
pH8.1_22C_31_08_19_burrow2_1_crop.jpg		
pH8.1_22C_31_08_19_burrow2_2_crop.jpg		
pH8.1_22C_31_08_19_burrow2_3_crop.jpg		
pH8.1_22C_12_10_20_1_crop.jpg		

pH7.7_18C_05_03_20_1_crop.jpg		
pH7.7_18C_05_03_20_2_crop.jpg		
pH7.7_18C_05_03_20_3_crop.jpg		
pH7.7_18C_08_08_20_1_crop.jpg		
pH7.7_18C_08_08_20_2_crop.jpg		
pH7.7_18C_08_08_20_3_crop.jpg		
pH7.7_18C_12_03_20_1_crop.jpg		
pH7.7_18C_12_03_20_2_crop.jpg		
pH7.7_18C_12_03_20_3_crop.jpg		
pH7.7_18C_18_03_20_1_crop.jpg		
pH7.7_18C_18_03_20_2_crop.jpg		
pH7.7_18C_18_03_20_3_crop.jpg		
pH7.7_18C_18_03_20_burrow2_1_crop.jpg		
H7.7_18C_18_03_20_burrow2_2_crop.jpg		
pH7.7_18C_18_03_20_burrow2_3.jpg		

pH7.7_18C_18_03_20_burrow3_1.jpg		
pH7.7_18C_18_03_20_burrow3_2.jpg		
pH7.7_18C_18_03_20_burrow3_3.jpg		
pH7.7_18C_19_03_20_1_crop.jpg		
pH7.7_18C_19_03_20_2_crop.jpg		
pH7.7_18C_19_03_20_3_crop.jpg		
pH7.7_18C_19_03_20_burrow2_1_crop.jpg		
pH7.7_18C_19_03_20_burrow2_2.jpg		
pH7.7_18C_19_03_20_burrow2_3.jpg		
pH7.7_18C_26_03_20_1.jpg		
pH7.7_18C_26_03_20_2.jpg		
pH7.7_18C_26_03_20_3.jpg		
pH7.7_22C_01_11_19_1_crop.jpg		
pH7.7_22C_01_11_19_2_crop.jpg		
pH7.7_22C_01_11_19_3_crop.jpg		

pH7.7_22C_01_11_19_burrow2_2_crop.jpg		
pH7.7_22C_01_11_19_burrow2_3_crop.jpg		
pH7.7_22C_01_11_19_burrow2_1_crop.jpg		
pH7.7_22C_13_11_19_1_crop.jpg		
pH7.7_22C_13_11_19_2_crop.jpg		
pH7.7_22C_13_11_19_3_crop.jpg		
pH7.7_22C_14_10_19_1.jpg		
pH7.7_22C_14_10_19_2_crop.jpg		
pH7.7_22C_14_10_19_3_crop.jpg		
pH7.7_22C_18_11_19_1_crop.jpg		
pH7.7_22C_18_11_19_2_crop.jpg		
pH7.7_22C_18_11_19_3_crop.jpg		
pH7.7_22C_20_12_19_1_crop.jpg		
pH7.7_22C_20_12_19_2_crop.jpg		
pH7.7_22C_20_12_19_3_crop.jpg		
pH7.7_22C_20_12_19_burrow2_1_crop.jpg		

pH7.7_22C_20_12_19_burrow2_2_crop.jpg		
pH7.7_22C_20_12_19_burrow2_3_crop.jpg		
		
pH7.7_22C_26_11_19_1_crop.jpg		
pH7.7_22C_26_11_19_2_crop.jpg		
pH7.7_22C_26_11_19_3_crop.jpg		
		
pH7.3_18C_05_02_21_2_crop.jpg		
pH7.3_18C_05_02_21_3_crop.jpg		
pH7.3_18C_05_02_21_crop.jpg		
		
pH7.3_18C_19_08_19_2_crop.jpg		
pH7.3_18C_19_08_19_3_crop.jpg		
pH7.3_18C_19_08_19_crop.jpg		
		
pH7.3_18C_27_08_19_1_crop.jpg		
pH7.3_18C_27_08_19_2_crop.jpg		
pH7.3_18C_27_08_19_3_crop.jpg		
		
pH7.3_18C_27_08_19_burrow2_2_crop.jpg		
pH7.3_18C_27_08_19_burrow2_3_crop.jpg		
pH7.3_18C_27_08_19_burrow2_crop.jpg		
		
pH7.3_18C_28_08_19_1_crop.jpg		
pH7.3_18C_28_08_19_2_crop.jpg		
pH7.3_18C_28_08_19_3_crop.jpg		
		
pH7.3_18C_28_08_19_burrow2_1_crop.jpg		
pH7.3_18C_28_08_19_burrow2_2_crop.jpg		
pH7.3_18C_28_08_19_burrow2_3_crop.jpg		

pH7.3_22C_12_02_21_1_crop.jpg		
pH7.3_22C_12_02_21_2_crop.jpg		
pH7.3_22C_12_02_21_3_crop.jpg		
pH7.3_22C_16_02_21_1_crop.jpg		
pH7.3_22C_16_02_21_2_crop.jpg		
pH7.3_22C_16_02_21_3_crop.jpg		
pH7.3_22C_16_02_21_burrow2_1_crop.jpg		
pH7.3_22C_16_02_21_burrow2_2_crop.jpg		
pH7.3_22C_16_02_21_burrow2_3_crop.jpg		
pH7.3_22C_17_08_20_1_crop.jpg		
pH7.3_22C_17_08_20_2_crop.jpg		
pH7.3_22C_17_08_20_3_crop.jpg		
pH7.3_22C_20_08_20_1_crop.jpg		
pH7.3_22C_20_08_20_2_crop.jpg		
pH7.3_22C_20_08_20_3_crop.jpg		
pH7.3_22C_25_08_19_burrow2_1_crop.jpg		
pH7.3_22C_25_08_19_burrow2_2_crop.jpg		
H7.3_22C_25_08_19_burrow2_3_crop.jpg		

O₂ penetration depth data

Table S3. 8: O₂ penetration depth (in mm) used in analysis

	ID	pH	temp	pen_depth
1	2	8.1	18	0.6419432

	ID	pH	temp	pen_depth
2	3	8.1	18	0.6153724
3	4	8.1	18	0.5639371

	ID	pH	temp	pen_depth
4	5	8.1	18	0.4269875
5	7	8.1	18	0.5590882
6	8	8.1	18	0.4533599
7	9	8.1	18	0.7024296
8	11	8.1	22	0.7049352
9	12	8.1	22	0.6855600
10	13	8.1	22	0.5615688
11	14	8.1	22	0.6554302
12	15	8.1	22	0.6950692
13	16	8.1	22	0.6438990
14	17	8.1	22	0.5993976
15	19	7.7	18	0.4309839

	ID	pH	temp	pen_depth
16	20	7.7	18	0.5286791
17	21	7.7	18	0.4918721
18	22	7.7	18	0.5236727
19	23	7.7	18	0.5286096
20	24	7.7	18	0.5210222
21	25	7.7	18	0.6090721
22	26	7.7	18	0.4423287
23	28	7.7	18	0.4893749
24	29	7.7	22	0.7737281
25	30	7.7	22	0.4892923
26	32	7.7	22	0.6246210
27	33	7.7	22	0.4581061

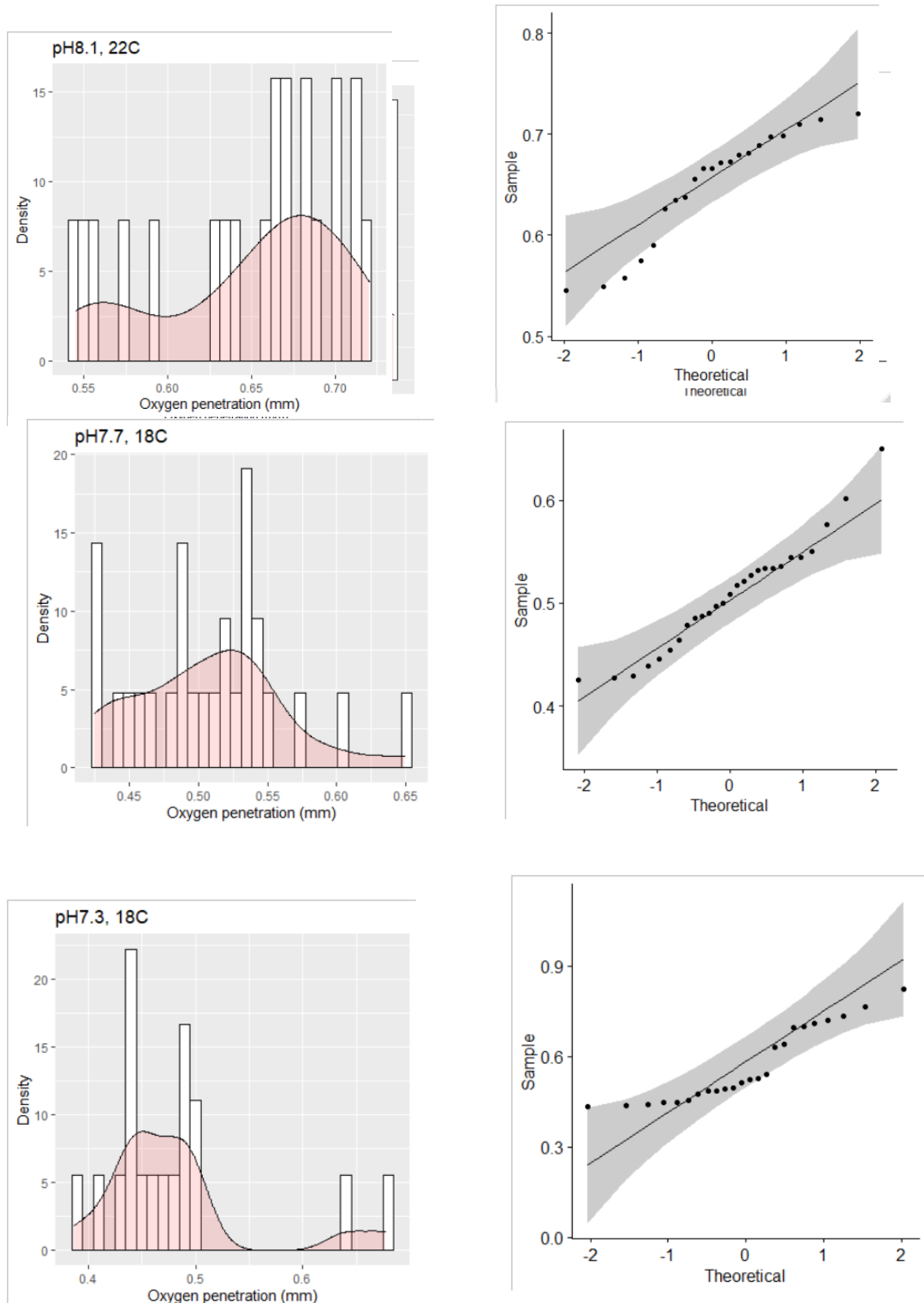
	ID	pH	temp	pen_depth
28	34	7.7	22	0.5476019
29	35	7.7	22	0.4407908
30	36	7.7	22	0.4969191
31	38	7.7	22	0.7044101
32	39	7.3	18	0.4925046
33	40	7.3	18	0.6019366
34	41	7.3	18	0.4507561
35	42	7.3	18	0.4538844
36	43	7.3	18	0.4533932
37	44	7.3	18	0.4317075
38	45	7.3	22	0.5593430
39	46	7.3	22	0.5267499

	ID	pH	temp	pen_depth
40	47	7.3	22	0.5263065
41	48	7.3	22	0.5878429
42	50	7.3	22	0.5122182
43	52	7.3	22	0.4746611

Showing 26 to 43 of 43 entries, 4 total
c

Assessing normality of data – O₂ penetration depth

Histograms and QQ plots for O₂ penetration depth, all groups. If all points fall within the boundary line suggesting normally distributed residuals in the data.



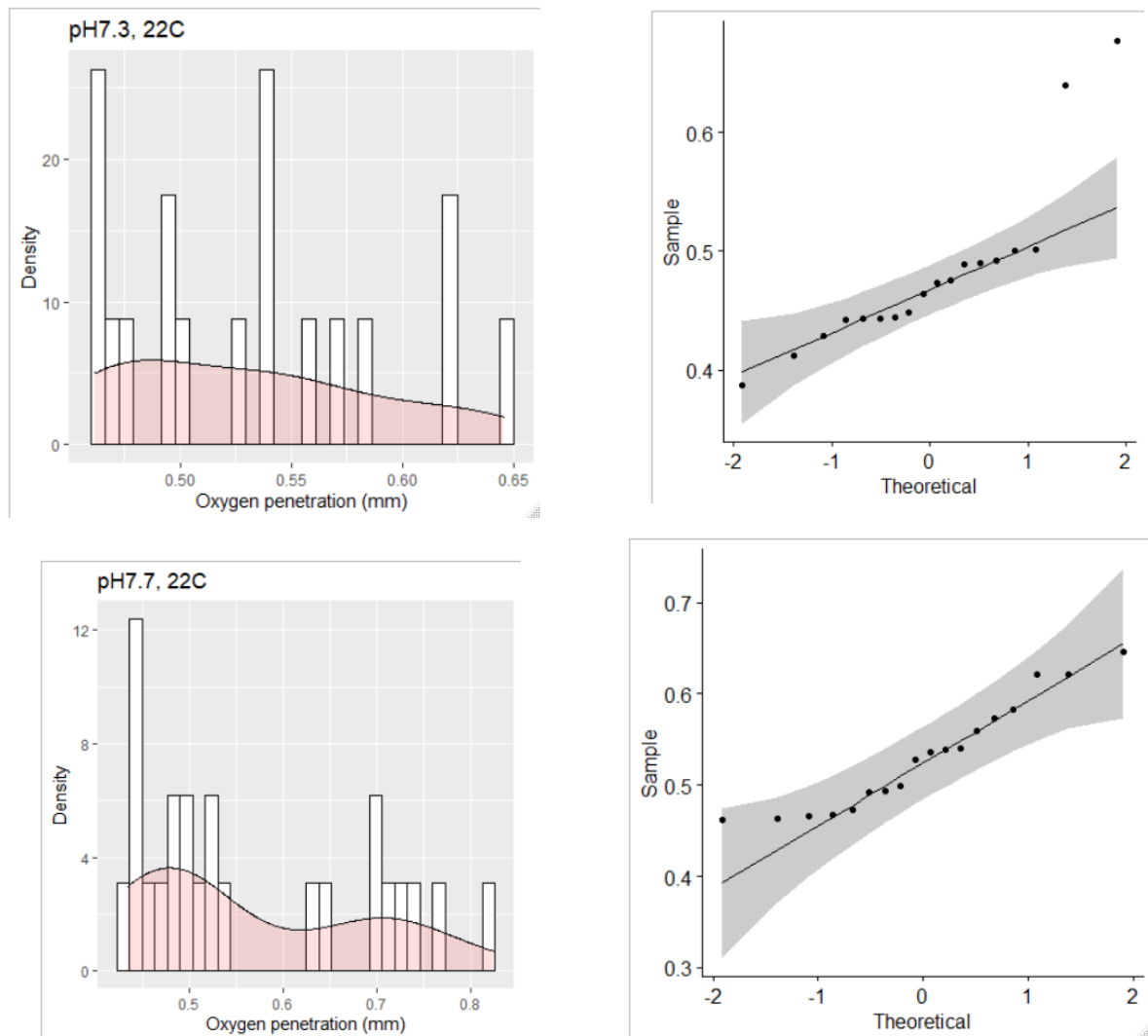


Figure S3. 3: Histograms and QQ plots for assessment of normality on Oxygen penetration depth

Shapiro-Wilks test for Normality

Table S3. 9: Results of Shapiro-Wilk's test of normality generated in R (centre= median) for each pH/ temperature group for O₂ penetration depth. The pH7.2/ 18C regime was significantly non-normal.

	pH	temp	W	P.value
1:	8.1	18	0.9516510	0.74470149
2:	8.1	22	0.9205006	0.47329135
3:	7.7	18	0.9239312	0.42577748
4:	7.7	22	0.8994004	0.28538635
5:	7.3	18	0.7496744	0.01977461
6:	7.3	22	0.9739226	0.91767138

Shapiro-Wilk's test for Normality of data (O₂ penetration depth) by pH and temperature groups. One of the groups are non-normally distributed (pH7.3, 18C, highlighted).

Levene's test

Levene's test for homogeneity of variance (O₂ penetration depth). The result is non-significant ($p > 0.05$) indicating that variance is homogenous.

	Df	F value	Pr(>F)
group	5	1.9247	0.1136
	37		

Data appears normally distributed in the QQ plot Levene's test indicates homogeneity of variance. However, the Shapiro-Wilk test indicates that the data for one of the groups (pH7.7, 18C) are non-normal, therefore a robust two-way factorial ANOVA with trimmed means (0.2) will be used as this statistic is resistant to the effects of non-normal distributions and outliers. Using the t2way function from the WRS2 package to compute the ANOVA (Mayes et al., 2009).

References

- ABREU, M. S., GIACOMINI, A. C. V., GUSSO, D., KOAKOSKI, G., OLIVEIRA, T. A., MARQUEZE, A., BARRETO, R. E. & BARCELLOS, L. J. G. 2016. Behavioral responses of zebrafish depend on the type of threatening chemical cues. *Journal of Comparative Physiology A*, 202, 895-901.
- ALLER, R. C. 1994. Bioturbation and remineralization of sedimentary organic matter: effects of redox oscillation. *Chemical Geology*, 114, 331-345.
- ANTHONY, K. R. & FABRICIUS, K. E. 2000. Shifting roles of heterotrophy and autotrophy in coral energetics under varying turbidity. *Journal of experimental marine biology and ecology*, 252, 221-253.
- ARDIEL, E. L. & RANKIN, C. H. 2010. An elegant mind: learning and memory in *Caenorhabditis elegans*. *Learning & memory*, 17, 191-201.
- ASHUR, M. M., JOHNSTON, N. K. & DIXSON, D. L. 2017. Impacts of ocean acidification on sensory function in marine organisms. *Integrative and comparative biology*, 57, 63-80.
- BAJWA, J. 2020. Chondroitin Sulphate Acts as an Alarm Cue in Zebrafish. *Student Research Proceedings*, 5.
- BANSIL, R. & TURNER, B. S. 2006. Mucin structure, aggregation, physiological functions and biomedical applications. *Current opinion in colloid & interface science*, 11, 164-170.
- BANTA, G. T., HOLMER, M., JENSEN, M. H. & KRISTENSEN, E. 1999. Effects of two polychaete worms, *Nereis diversicolor* and *Arenicola marina*, on aerobic and anaerobic decomposition in a sandy marine sediment. *Aquatic microbial ecology*, 19, 189-204.
- BARESEL, B., BUCHER, H., BAGHERPOUR, B., BROSE, M., GUODUN, K. & SCHALTEGGER, U. 2017. Timing of global regression and microbial bloom linked with the Permian-Triassic boundary mass extinction: implications for driving mechanisms. *Scientific Reports*, 7, 43630.
- BARNES, R. S. 1994. *The brackish-water fauna of northwestern Europe*, Cambridge University Press.
- BARNOSKY, A. D., MATZKE, N., TOMIYA, S., WOGAN, G. O., SWARTZ, B., QUENTAL, T. B., MARSHALL, C., MCGUIRE, J. L., LINDSEY, E. L. & MAGUIRE, K. C. 2011a. Has the Earth's sixth mass extinction already arrived? *Nature*, 471, 51.
- BARNOSKY, A. D., MATZKE, N., TOMIYA, S., WOGAN, G. O. U., SWARTZ, B., QUENTAL, T. B., MARSHALL, C., MCGUIRE, J. L., LINDSEY, E. L., MAGUIRE, K. C., MERSEY, B. & FERRER, E. A. 2011b. Has the Earth's sixth mass extinction already arrived? *Nature*, 471, 51.
- BARTELS-HARDEGE, H. & ZEECK, E. 1990. Reproductive behaviour of *Nereis diversicolor* (Annelida: Polychaeta). *Marine Biology*, 106, 409-412.
- BASS, S., ALDRIDGE, J., MCCAVE, I. & VINCENT, C. 2002. Phase relationships between fine sediment suspensions and tidal currents in coastal seas. *Journal of Geophysical Research*, 107.
- BASTIDAS, C. & GARCIA, E. 2004. Sublethal effects of mercury and its distribution in the coral *Porites astreoides*. *Marine Ecology Progress Series*, 267, 133-143.
- BATES, N. R., ASTOR, Y. M., CHURCH, M. J., CURRIE, K. I. M., DORE, J. E., GONZ, X., LEZ, D., X, VILA, M., LORENZONI, L., MULLER-KARGER, F., OLAFSSON, J. O. N. & SANTANA-CASIANO, J. M. 2014. A Time-Series View of Changing Surface Ocean Chemistry Due to Ocean Uptake of Anthropogenic CO₂ and Ocean Acidification. *Oceanography*, 27, 126-141.
- BATTEN, S. & BAMBER, R. 1996. The effects of acidified seawater on the polychaete *Nereis virens* Sars, 1835. *Marine pollution bulletin*, 32, 283-287.

- BEAUCHAMP, B. & BAUD, A. 2002. Growth and demise of Permian biogenic chert along northwest Pangea: evidence for end-Permian collapse of thermohaline circulation. *Palaeogeography, Palaeoclimatology, Palaeoecology*, 184, 37-63.
- BEERLING, D. J., HARFOOT, M., LOMAX, B. & PYLE, J. A. 2007. The stability of the stratospheric ozone layer during the end-Permian eruption of the Siberian Traps. *Philosophical Transactions of the Royal Society A: Mathematical, Physical and Engineering Sciences*, 365, 1843-1866.
- BEESELEY, P., ROSS, G. & GLASBY, C. 2000. Fauna of Australia, Volume 4A: Polychaetes and Allies. *Melbourne, Australia: CSIRO Publishing*, 465p.
- BENCA, J. P., DUIJNSTEE, I. A. & LOOY, C. V. 2018a. UV-B-induced forest sterility: Implications of ozone shield failure in Earth's largest extinction. *Science advances*, 4, e1700618.
- BENCA, J. P., DUIJNSTEE, I. A. P. & LOOY, C. V. 2018b. UV-B-induced forest sterility: Implications of ozone shield failure in Earth's largest extinction. *Science Advances*, 4.
- BHUIYAN, K. A., RODRÍGUEZ, B. M., PIRES, A., RIBA, I., DELLVALS, Á., FREITAS, R. & CONRADI, M. 2021a. Experimental evidence of uncertain future of the keystone ragworm *Hediste diversicolor* (O.F. Müller, 1776) under climate change conditions. *Science of The Total Environment*, 750, 142031.
- BHUIYAN, K. A., RODRÍGUEZ, B. M., PIRES, A., RIBA, I., DELLVALS, Á., FREITAS, R. & CONRADI, M. 2021b. Experimental evidence of uncertain future of the keystone ragworm *Hediste diversicolor* (OF Müller, 1776) under climate change conditions. *Science of The Total Environment*, 750, 142031.
- BHUIYAN, M. K. A. 2021. *Impacts of ocean acidification and other (global change) stressors on marine invertebrates*. Universidad de Cádiz.
- BINDOFF, N. L., CHEUNG, W. W., KAIRO, J. G., ARISTEGUI, J., GUINDER, V. A., HALLBERG, R., HILMI, N. J. M., JIAO, N., KARIM, M. S. & LEVIN, L. 2019. Changing ocean, marine ecosystems, and dependent communities. *IPCC special report on the ocean and cryosphere in a changing climate*, 477-587.
- BOATES, J. S. & GOSS-CUSTARD, J. D. 1992. Foraging behaviour of oystercatchers *Haematopus ostralegus* specializing on different species of prey. *Canadian Journal of Zoology*, 70, 2398-2404.
- BOND, D. P. & SUN, Y. 2021. Global Warming and Mass Extinctions Associated With Large Igneous Province Volcanism. *Large Igneous Provinces: A Driver of Global Environmental and Biotic Changes*, 83-102.
- BOND, D. P. G. & GRASBY, S. E. 2017. On the causes of mass extinctions. *Palaeogeography, Palaeoclimatology, Palaeoecology*, 478, 3-29.
- BOND, D. P. G. & WIGNALL, P. B. 2010. Pyrite framboid study of marine Permian-Triassic boundary sections: A complex anoxic event and its relationship to contemporaneous mass extinction. *GSA Bulletin*, 122, 1265-1279.
- BONNARD, M., ROMÉO, M. & AMIARD-TRIQUET, C. 2009. Effects of Copper on the Burrowing Behavior of Estuarine and Coastal Invertebrates, the Polychaete *Nereis diversicolor* and the Bivalve *Scrobicularia plana*. *Human and Ecological Risk Assessment: An International Journal*, 15, 11-26.
- BOTTJER, D. J., HAGADORN, J. W. & DORNBOS, S. Q. 2000. The Cambrian substrate revolution. *GSA today*, 10, 1-7.
- BOUDREAU, B. P. & JORGENSEN, B. B. 2001. *The Benthic Boundary Layer*, Oxford University Press.
- BOYLE, R. A., DAHL, T. W., DALE, A. W., SHIELDS-ZHOU, G. A., ZHU, M., BRASIER, M. D., CANFIELD, D. E. & LENTON, T. M. 2014. Stabilization of the coupled oxygen and phosphorus cycles by the evolution of bioturbation. *Nature Geoscience*, 7, 671.

- BRAECKMAN, U., RABAUT, M., VANAVERBEKE, J., DEGRAER, S. & VINCX, M. 2014. Protecting the Commons: the use of Subtidal Ecosystem Engineers in Marine Management. *Aquatic Conservation: Marine and Freshwater Ecosystems*, 24, 275-286.
- BREITHAUPT, T. T., MARTIN 2011. Chemical communication in crustaceans. In: BREITHAUPT, T. & THIEL, M. (eds.). New York :: Springer.
- BREWER PETER, G., GLOVER DAVID, M., GOYET, C. & SHAFER DEBORAH, K. 1995. The pH of the North Atlantic Ocean: Improvements to the global model for sound absorption in seawater. *Journal of Geophysical Research: Oceans*, 100, 8761-8776.
- BROWN, A. C. 2001. Surfing in the sandy-beach whelk *Bullia digitalis* (Dillwyn) AU - Brown, A.C. *African Zoology*, 36, 121-127.
- BROWN, G. E., JACKSON, C. D., MALKA, P. H., JACQUES, É. & COUTURIER, M.-A. 2012. Disturbance cues in freshwater prey fishes: Does urea function as an 'early warning cue' in juvenile convict cichlids and rainbow trout? *Current Zoology*, 58, 250-259.
- BUDD, G. 2008. *Hediste diversicolor*. Ragworm.
- BURGESS, S. D., BOWRING, S. & SHEN, S.-Z. 2014. High-precision timeline for Earth's most severe extinction. *Proceedings of the National Academy of Sciences*, 111, 3316-3321.
- BURROWS, M. T., SCHOEMAN, D. S., RICHARDSON, A. J., MOLINOS, J. G., HOFFMANN, A., BUCKLEY, L. B., MOORE, P. J., BROWN, C. J., BRUNO, J. F., DUARTE, C. M., HALPERN, B. S., HOEGH-GULDBERG, O., KAPPEL, C. V., KIESSLING, W., O'CONNOR, M. I., PANDOLFI, J. M., PARMESAN, C., SYDEMAN, W. J., FERRIER, S., WILLIAMS, K. J. & POLOCZANSKA, E. S. 2014. Geographical limits to species-range shifts are suggested by climate velocity. *Nature*, 507, 492-495.
- CANFIELD, D. E. & FARQUHAR, J. 2009. Animal evolution, bioturbation, and the sulfate concentration of the oceans. *Proceedings of the National Academy of Sciences*, 106, 8123-8127.
- CARRAWAY, E., DEMAS, J. & DEGRAFF, B. 1991. Photophysics and oxygen quenching of transition-metal complexes on fumed silica. *Langmuir*, 7, 2991-2998.
- CEBALLOS, G., EHRLICH, P. R., BARNOSKY, A. D., GARCÍA, A., PRINGLE, R. M. & PALMER, T. M. 2015. Accelerated modern human-induced species losses: Entering the sixth mass extinction. *Science Advances*, 1, e1400253.
- CEBALLOS, G., EHRLICH, P. R. & DIRZO, R. 2017. Biological annihilation via the ongoing sixth mass extinction signaled by vertebrate population losses and declines. *Proceedings of the National Academy of Sciences*, 114, E6089-E6096.
- CHAMBERS, M. & MILNE, H. 1975. Life cycle and production of *Nereis diversicolor* OF Müller in the Ythan Estuary, Scotland. *Estuarine and Coastal Marine Science*, 3, 133-144.
- CHEN, J.-Y., BOTTJER, D., OLIVERI, P., DORNBOS, S., GAO, F., RUFFINS, S., CHI, H., LI, C.-W. & H DAVIDSON, E. 2004. *Small bilaterian fossils from 40 to 55 million years before the Cambrian*.
- CHEN, Z.-Q. & BENTON, M. 2012. *The timing and pattern of biotic recovery following the end-Permian mass extinction*.
- CHIVERS, D. P., MCCORMICK, M. I., NILSSON, G. E., MUNDAY, P. L., WATSON, S. A., MEEKAN, M. G., MITCHELL, M. D., CORKILL, K. C. & FERRARI, M. C. 2014. Impaired learning of predators and lower prey survival under elevated CO₂: a consequence of neurotransmitter interference. *Global change biology*, 20, 515-522.
- CHIVERS, D. P. & SMITH, R. J. F. 1998. Chemical alarm signalling in aquatic predator-prey systems: A review and prospectus. *coscience*, 5, 338-352.
- CLAPHAM, M. E., SHEN, S. & BOTTJER, D. J. 2009. The double mass extinction revisited: reassessing the severity, selectivity, and causes of the end-Guadalupian biotic crisis (Late Permian). *Paleobiology*, 35, 32-50.

- CLARKSON, M. O., KASEMANN, S. A., WOOD, R. A., LENTON, T. M., DAINES, S. J., RICHOSZ, S., OHNEMUELLER, F., MEIXNER, A., POULTON, S. W. & TIPPER, E. T. 2015. Ocean acidification and the Permo-Triassic mass extinction. *Science*, 348, 229-232.
- CLEMENTS, J. 2016. *Influence of sediment acidification on the burrowing behaviour, post-settlement dispersal, and recruitment of juvenile soft-shell clams (Mya arenaria L.)*.
- CLEMENTS, J. C. & DARROW, E. S. 2018. Eating in an acidifying ocean: a quantitative review of elevated CO₂ effects on the feeding rates of calcifying marine invertebrates. *Hydrobiologia*, 820, 1-21.
- CLIFFORD, E. L., HANSELL, D. A., VARELA, M. M., NIETO-CID, M., HERNDL, G. J. & SINTES, E. 2017. Crustacean zooplankton release copious amounts of dissolved organic matter as taurine in the ocean. *Limnology and Oceanography*, 62, 2745-2758.
- COHEN, A. L. & HOLCOMB, M. 2009. Why corals care about ocean acidification: uncovering the mechanism. *Oceanography*, 22, 118-127.
- COHEN, J. H. & FORWARD JR, R. B. 2003. Ctenophore kairomones and modified aminosugar disaccharides alter the shadow response in a larval crab. *Journal of Plankton Research*, 25, 203-213.
- COLBERT, H. A. & BARGMANN, C. I. 1995. Odorant-specific adaptation pathways generate olfactory plasticity in *C. elegans*. *Neuron*, 14, 803-812.
- COLES, S. L. & STRATHMANN, R. 1973. Observations on coral mucus "flocs" and their potential trophic significance 1. *Limnology and Oceanography*, 18, 673-678.
- COLLINS M., M. S., L. BOUWER, S.-M. CHEONG, T. FRÖLICHER, H. JACOT DES COMBES, M. KOLL ROXY, I. LOSADA, K. MCINNES, B. RATTER, E. RIVERA-ARRIAGA, R.D. SUSANTO, D. SWINGEDOUW, AND L. TIBIG 2019. Extremes, Abrupt Changes and Managing Risk. *IPCC Special Report on the Ocean and Cryosphere in a Changing Climate* [H.-O. Pörtner, D.C. Roberts, V. Masson-Delmotte, P. Zhai, M. Tignor, E. Poloczanska, K. Mintenbeck, A. Alegría, M. Nicolai, A. Okem, J. Petzold, B. Rama, N.M. Weyer (eds.)].
- CONLEY, D. J., CARSTENSEN, J., VAQUER-SUNYER, R. & DUARTE, C. M. 2009. Ecosystem thresholds with hypoxia. *Eutrophication in coastal ecosystems*. Springer.
- CONWAY MORRIS, S. 1979. Middle Cambrian polychaetes from the Burgess shale of British Columbia. *Philosophical Transactions of the Royal Society of London. B, Biological Sciences*, 285, 227-274.
- CORNWALL, C. E., HEPBURN, C. D., MCGRAW, C. M., CURRIE, K. I., PILDITCH, C. A., HUNTER, K. A., BOYD, P. W. & HURD, C. L. 2013. Diurnal fluctuations in seawater pH influence the response of a calcifying macroalga to ocean acidification. *Proceedings of the Royal Society B: Biological Sciences*, 280, 20132201.
- COURTILLOT, V. E. & RENNE, P. R. 2003. On the ages of flood basalt events. *Comptes Rendus Geoscience*, 335, 113-140.
- CRANE, A. L., BAIROS-NOVAK, K. R., GOLDMAN, J. A. & BROWN, G. E. 2022. Chemical disturbance cues in aquatic systems: a review and prospectus. *Ecological Monographs*, 92, e01487.
- CRIBB, A. T. & BOTTJER, D. J. 2020. Complex marine bioturbation ecosystem engineering behaviors persisted in the wake of the end-Permian mass extinction. *Scientific Reports*, 10, 203.
- CUVILLIER-HOT, V., GAUDRON, S. M., MASSOL, F., BOIDIN-WICHLACZ, C., PENNEL, T., LESVEN, L., NET, S., PAPOT, C., RAVAUX, J. & VEKEMANS, X. 2018. Immune failure reveals vulnerability of populations exposed to pollution in the bioindicator species *Hediste diversicolor*. *Science of the Total Environment*, 613, 1527-1542.
- DAL CORSO, J., SONG, H., CALLEGARO, S., CHU, D., SUN, Y., HILTON, J., GRASBY, S. E., JOACHIMSKI, M. M. & WIGNALL, P. B. 2022. Environmental crises at the Permian–Triassic mass extinction. *Nature Reviews Earth & Environment*, 3, 197-214.

- DALE, H. 2019a. *The Impacts of Invertebrate Activities on Sediment Microbial Community and Functional Ecology*. University of Southampton.
- DALE, H., TAYLOR, J. D., SOLAN, M., LAM, P. & CUNLIFFE, M. 2019. Polychaete mucopolysaccharide alters sediment microbial diversity and stimulates ammonia-oxidising functional groups. *FEMS microbiology ecology*, 95, fiy234.
- DALE, H. J. 2019b. *The Impacts of Invertebrate Activities on Sediment Microbial Community and Functional Ecology. Doctoral Thesis*, University of Southampton.
- DALLAS, L. J., SHULTZ, A. D., MOODY, A. J., SLOMAN, K. A. & DANYLCHUK, A. J. 2010. Chemical excretions of angled bonefish *Albula vulpes* and their potential use as predation cues by juvenile lemon sharks *Negaprion brevirostris*. *Journal of Fish Biology*, 77, 947-962.
- DAMASHEK, J. & FRANCIS, C. A. 2018. Microbial nitrogen cycling in estuaries: from genes to ecosystem processes. *Estuaries and Coasts*, 41, 626-660.
- DANI, K. G. S. & LORETO, F. 2017. Trade-Off Between Dimethyl Sulfide and Isoprene Emissions from Marine Phytoplankton. *Trends in Plant Science*, 22, 361-372.
- DAVEY, J. T. 1994. The architecture of the burrow of *Nereis diversicolor* and its quantification in relation to sediment-water exchange. *Journal of Experimental Marine Biology and Ecology*, 179, 115-129.
- DAVIES, M. S. & HAWKINS, S. 1998. Mucus from marine molluscs. *Advances in marine biology*. Elsevier.
- DAVIS, A. R., COLEMAN, D., BROAD, A., BYRNE, M., DWORJANYN, S. A. & PRZESLAWSKI, R. 2013. Complex responses of intertidal molluscan embryos to a warming and acidifying ocean in the presence of UV radiation. *PloS one*, 8, e55939.
- DE MARCHI, L., PRETTI, C., CHIELLINI, F., MORELLI, A., NETO, V., SOARES, A. M. V. M., FIGUEIRA, E. & FREITAS, R. 2019. The influence of simulated global ocean acidification on the toxic effects of carbon nanoparticles on polychaetes. *Science of The Total Environment*, 666, 1178-1187.
- DE VOS, J. M., JOPPA, L. N., GITTLEMAN, J. L., STEPHENS, P. R. & PIMM, S. L. 2015. Estimating the normal background rate of species extinction. *Conservation Biology*, 29, 452-462.
- DEBOSE, J. L., LEMA, S. C. & NEVITT, G. A. 2008. Dimethylsulfoniopropionate as a foraging cue for reef fishes. *Science*, 319, 1356-1356.
- DERBY, C. D. 2000. Learning from spiny lobsters about chemosensory coding of mixtures. *Physiology & behavior*, 69, 203-209.
- DI VEROLI, G. Y., FORNARI, C., GOLDLUST, I., MILLS, G., KOH, S. B., BRAMHALL, J. L., RICHARDS, F. M. & JODRELL, D. I. 2015. An automated fitting procedure and software for dose-response curves with multiphasic features. *Scientific Reports*, 5, 14701.
- DIJK, B., LAURILA, A., ORIZAOLA, G. & JOHANSSON, F. 2016. Is one defence enough? Disentangling the relative importance of morphological and behavioural predator-induced defences. *Behavioral Ecology and Sociobiology*, 70, 237-246.
- DIRZO, R. & RAVEN, P. H. 2003. Global state of biodiversity and loss. *Annual review of Environment and Resources*, 28, 137-167.
- DONEY, S. C., BUSCH, D. S., COOLEY, S. R. & KROEKER, K. J. 2020. The impacts of ocean acidification on marine ecosystems and reliant human communities. *Annual Review of Environment and Resources*, 45.
- DONEY, S. C., FABRY, V. J., FEELY, R. A. & KLEYPAS, J. A. 2009. Ocean Acidification: The Other CO₂ Problem. *Annual Review of Marine Science*, 1, 169-192.
- DOREY, N., MELZNER, F., MARTIN, S., OBERHÄNSLI, F., TEYSSIÉ, J.-L., BUSTAMANTE, P., GATTUSO, J.-P. & LACQUE-LABARTHE, T. 2013. Ocean acidification and temperature

- rise: effects on calcification during early development of the cuttlefish *Sepia officinalis*. *Marine Biology*, 160, 2007-2022.
- DROSER, M. L. & BOTTJER, D. J. 1986. A semiquantitative field classification of ichnofabric. *Journal of Sedimentary Research*, 56.
- DUBOIS, M., GILLES, K. A., HAMILTON, J. K., REBERS, P. T. & SMITH, F. 1956. Colorimetric method for determination of sugars and related substances. *Analytical chemistry*, 28, 350-356.
- DUCROTOY, J.-P., MICHAEL, E., CUTTS, N., FRANCO, A., LITTLE, S., MAZIK, K. & WILKINSON, M. 2019. Temperate estuaries: their ecology under future environmental changes. *Coasts and Estuaries*. Elsevier.
- DUDMAN, K. & DE WIT, S. 2021. An IPCC that listens: introducing reciprocity to climate change communication. *Climatic Change*, 168, 1-12.
- DUPONT, C. L., MOFFETT, J. W., BIDIGARE, R. R. & AHNER, B. A. 2006. Distributions of dissolved and particulate biogenic thiols in the subarctic Pacific Ocean. *Deep Sea Research Part I: Oceanographic Research Papers*, 53, 1961-1974.
- DUPONT, S., ORTEGA-MARTINEZ, O. & THORNDYKE, M. 2010. Impact of near-future ocean acidification on echinoderms. *Ecotoxicology*, 19, 449-462.
- DUPORT, E., STORA, G., TREMBLAY, P. & GILBERT, F. 2006. Effects of population density on the sediment mixing induced by the gallery-diffuser *Hediste* (*Nereis*) *diversicolor* OF Müller, 1776. *Journal of Experimental Marine Biology and Ecology*, 336, 33-41.
- DURCHON, M. & PORCHET, M. 1971. Premières données quantitatives sur l'activité endocrine du cerveau des Néréidiens au cours de leur cycle sexuel. *General and Comparative Endocrinology*, 16, 555-565.
- EDELIN, E., LAMBERT, P., RIGAUD, C. & ELIE, P. 2006. Effects of body condition and water temperature on *Anguilla anguilla* glass eel migratory behavior. *Journal of Experimental Marine Biology and Ecology*, 331, 217-225.
- EKE, C. D., ANIFOWOSE, B., VAN DE WIEL, M. J., LAWLER, D. & KNAAPEN, M. A. 2021. Numerical Modelling of Oil Spill Transport in Tide-Dominated Estuaries: A Case Study of Humber Estuary, UK. *Journal of Marine Science and Engineering*, 9, 1034.
- EL IBRAHIMI, B., JMIAI, A., EL MOUADEN, K., BADDOUH, A., EL ISSAMI, S., BAZZI, L. & HILALI, M. 2019. Effect of solution's pH and molecular structure of three linear α -amino acids on the corrosion of tin in salt solution: A combined experimental and theoretical approach. *Journal of Molecular Structure*, 1196, 105-118.
- ENS, B., BUNSKOEKE, E., HOEKSTRA, R., HULSCHER, J., KERSTEN, M. & DEVLAS, S. 1996. Prey choice and search speed: why simple optimality fails to explain the prey choice of oystercatchers *Haematopus ostralegus* feeding on *Nereis diversicolor* and *Macoma balthica*. *Ardea*, 84, 73-90.
- ERWIN, D. H. 1994. The Permo-Triassic extinction. *Nature*, 367, 231.
- ESSELINK, P. & ZWARTS, L. 1989. Seasonal trend in burrow depth and tidal variation in feeding activity of *Nereis diversicolor*. *Marine Ecology Progress Series*, 243-254.
- EVANS, P., HERDSON, D., KNIGHTS, P. & PIENKOWSKI, M. 1979. Short-term effects of reclamation of part of Seal Sands, Teesmouth, on wintering waders and Shelduck. *Oecologia*, 41, 183-206.
- EVANS, S. 1969. Habituation of the withdrawal response in nereid polychaetes: 1. The habituation process in *Nereis diversicolor*. *The Biological Bulletin*, 137, 95-104.
- FABRY, V. J., SEIBEL, B. A., FEELY, R. A. & ORR, J. C. 2008. Impacts of ocean acidification on marine fauna and ecosystem processes. *Ices Journal of Marine Science*, 65, 414-432.
- FAIRHALL, A. 1973. Accumulation of fossil CO₂ in the atmosphere and the sea.
- FANG, X., MOENS, T., KNIGHTS, A., SOETAERT, K. & VAN COLEN, C. 2021. Allometric scaling of faunal-mediated ecosystem functioning: A case study on two bioturbators in contrasting sediments. *Estuarine, Coastal and Shelf Science*, 254, 107323.

- FARNSEY, S., KUHAJDA, B., GEORGE, A. & KLUG, H. 2016. *Fundulus catenatus* (Northern Studfish) Response to the Potential Alarm Cue Chondroitin Sulfate. *Southeastern Naturalist*, 15, 523-533, 11.
- FAUCHALD, K. & JUMARS, P. A. 1979. The diet of worms: a study of polychaete feeding guilds. *Oceanography and marine Biology annual review*.
- FAULKNER, A. E., HOLSTROM, I. E., MOLITOR, S. A., HANSON, M. E., SHEGRUD, W. R., GILLEN, J. C., WILLARD, S. J. & WISENDEN, B. D. 2017. Field verification of chondroitin sulfate as a putative component of chemical alarm cue in wild populations of fathead minnows (*Pimephales promelas*). *Chemoecology*, 27, 233-238.
- FEELY, R. A., SABINE, C. L., LEE, K., BERELSON, W., KLEYPAS, J., FABRY, V. J. & MILLERO, F. J. 2004. Impact of Anthropogenic CO₂ on the CaCO₃ System in the Oceans. *Science*, 305, 362-366.
- FENG, X., CHEN, Z.-Q., BENTON, M. J., SU, C., BOTTJER, D. J., CRIBB, A. T., LI, Z., ZHAO, L., ZHU, G. & HUANG, Y. 2022. Resilience of infaunal ecosystems during the Early Triassic greenhouse Earth. *Science advances*, 8, eabo0597.
- FERNANDES, S., SOBRAL, P. & COSTA, M. H. 2006. *Nereis diversicolor* effect on the stability of cohesive intertidal sediments. *Aquatic Ecology*, 40, 567-579.
- FERNER, M. C. & JUMARS, P. A. 1999. Responses of deposit-feeding spionid polychaetes to dissolved chemical cues. *Journal of Experimental Marine Biology and Ecology*, 236, 89-106.
- FERRARI, M. C. O., WISENDEN, B. D. & CHIVERS, D. P. 2010. Chemical ecology of predator–prey interactions in aquatic ecosystems: a review and prospectusThe present review is one in the special series of reviews on animal–plant interactions. *Canadian Journal of Zoology*, 88, 698-724.
- FEUGERE, L., ANGELL, L., FAGENTS, J., NIGHTINGALE, R., ROWLAND, K., SKINNER, S., HARDEGE, J., BARTELS-HARDEGE, H. & VALERO, K. C. W. 2021. Behavioural stress feedback loops in benthic invertebrates caused by pH drop-induced metabolites. *bioRxiv*, 2021.04.16.440165.
- FINE, M. & TCHERNOV, D. 2007. Scleractinian Coral Species Survive and Recover from Decalcification. *Science*, 315, 1811-1811.
- FLÜGEL, E. 2002. Triassic reef patterns.
- FOO, S., BYRNE, M., RICEVUTO, E. & GAMBI, M. 2018. The Carbon Dioxide Vents of Ischia, Italy, A Natural System to Assess Impacts of Ocean Acidification on Marine Ecosystems: An Overview of Research and Comparisons with Other Vent Systems: An Annual Review.
- FOOTE, M. 2000. Origination and extinction components of taxonomic diversity: general problems. *Paleobiology*, 26, 74-102.
- FORETICH, M. A., PARIS, C. B., GROSELL, M., STIEGLITZ, J. D. & BENETTI, D. D. 2017. Dimethyl sulfide is a chemical attractant for reef fish larvae. *Scientific reports*, 7, 1-10.
- FORM, A. U. & RIEBESELL, U. 2012. Acclimation to ocean acidification during long-term CO₂ exposure in the cold-water coral *Lophelia pertusa*. *Global Change Biology*, 18, 843-853.
- FOSTER, W. J., HIRTZ, J. A., FARRELL, C., REISTROFFER, M., TWITCHETT, R. J. & MARTINDALE, R. C. 2022. Bioindicators of severe ocean acidification are absent from the end-Permian mass extinction. *Scientific Reports*, 12, 1202.
- FRANKE, U. 2005. *Applications of planar oxygen optodes in biological aquatic systems*. PhD thesis. Univ. of Bremen.
- FRASER, W. T., LOMAX, B. H., JARDINE, P. E., GOSLING, W. D. & SEPHTON, M. A. 2014. Pollen and spores as a passive monitor of ultraviolet radiation. *Frontiers in Ecology and Evolution*, 2, 12.

- FREITAS, R., DE MARCHI, L., MOREIRA, A., PESTANA, J. L. T., WRONA, F. J., FIGUEIRA, E. & SOARES, A. M. V. M. 2017. Physiological and biochemical impacts induced by mercury pollution and seawater acidification in *Hediste diversicolor*. *Science of The Total Environment*, 595, 691-701.
- FREITAS, R., PIRES, A., MOREIRA, A., WRONA, F. J., FIGUEIRA, E. & SOARES, A. M. V. M. 2016. Biochemical alterations induced in *Hediste diversicolor* under seawater acidification conditions. *Marine Environmental Research*, 117, 75-84.
- FUJITA, K., HIKAMI, M., SUZUKI, A., KUROYANAGI, A., SAKAI, K., KAWAHATA, H. & NOJIRI, Y. 2011. Effects of ocean acidification on calcification of symbiont-bearing reef foraminifers. *Biogeosciences*, 8, 2089-2098.
- GALASSO HL, R. M., LEFEBVRE S, ALIAUME C, CALLIER MD. 2018. Body size and temperature effects on standard metabolic rate for determining metabolic scope for activity of the polychaete *Hediste (Nereis) diversicolor*. *PeerJ*, 6.
- GALÍ, M. & SIMÓ, R. 2015. A meta-analysis of oceanic DMS and DMSP cycling processes: Disentangling the summer paradox. *Global Biogeochemical Cycles*, 29, 496-515.
- GARCÍA, E., CLEMENTE, S. & HERNÁNDEZ, J. C. 2018a. Effects of natural current pH variability on the sea urchin *Paracentrotus lividus* larvae development and settlement. *Marine environmental research*, 139, 11-18.
- GARCÍA, E., HERNÁNDEZ, J. C. & CLEMENTE, S. 2018b. Robustness of larval development of intertidal sea urchin species to simulated ocean warming and acidification. *Marine environmental research*, 139, 35-45.
- GATTUSO, J.-P. & BUDDEMEIER, R. W. 2000. Calcification and CO₂. *Nature*, 407, 311.
- GAZEAU, F., PARKER, L. M., COMEAU, S., GATTUSO, J.-P., O'CONNOR, W. A., MARTIN, S., PÖRTNER, H.-O. & ROSS, P. M. 2013. Impacts of ocean acidification on marine shelled molluscs. *Marine Biology*, 160, 2207-2245.
- GIBBIN, E. M., CHAKRAVARTI, L. J., JARROLD, M. D., CHRISTEN, F., TURPIN, V., N'SIALA, G. M., BLIER, P. U. & CALOSI, P. 2017. Can multi-generational exposure to ocean warming and acidification lead to the adaptation of life history and physiology in a marine metazoan? *JOURNAL OF EXPERIMENTAL BIOLOGY*, 220, 551-563.
- GILLET, P., MOULOUD, M., DUROU, C. & DEUTSCH, B. 2008. Response of *Nereis diversicolor* population (Polychaeta, Nereididae) to the pollution impact—Authie and Seine estuaries (France). *Estuarine, Coastal and Shelf Science*, 76, 201-210.
- GLUD, R. N. 2008. Oxygen dynamics of marine sediments. *Marine Biology Research*, 4, 243-289.
- GODBOLD, J. A., BULLING, M. T. & SOLAN, M. 2011. Habitat structure mediates biodiversity effects on ecosystem properties. *Proc Biol Sci*, 278, 2510-8.
- GODBOLD, J. A. & SOLAN, M. 2013. Long-term effects of warming and ocean acidification are modified by seasonal variation in species responses and environmental conditions. *Philosophical Transactions of the Royal Society B: Biological Sciences*, 368, 20130186.
- GODBOLD, J. A., SOLAN, M. & KILLHAM, K. 2009. Consumer and resource diversity effects on marine macroalgal decomposition. *Oikos*, 118, 77-86.
- GOGINA, M., ZETTLER, M. L., VANAVERBEKE, J., DANNHEIM, J., VAN HOEY, G., DESROY, N., WREDE, A., REISS, H., DEGRAER, S. & VAN LANCKER, V. 2020. Interregional comparison of benthic ecosystem functioning: Community bioturbation potential in four regions along the NE Atlantic shelf. *Ecological Indicators*, 110, 105945.
- GOLDENBERG, S. U., NAGELKERKEN, I., MARANGON, E., BONNET, A., FERREIRA, C. M. & CONNELL, S. D. 2018. Ecological complexity buffers the impacts of future climate on marine consumers. *Nature Climate Change*, 8, 229-233.
- GOMES, A., CORREIA, A. T. & NUNES, B. 2019. Worms on drugs: ecotoxicological effects of acetylsalicylic acid on the Polychaeta species *Hediste diversicolor* in terms of

- biochemical and histological alterations. *Environmental Science and Pollution Research*, 26, 13619-13629.
- GRASBY, S. E., BEAUCHAMP, B. & KNIES, J. 2016. Early Triassic productivity crises delayed recovery from world's worst mass extinction. *Geology*, 44, 779-782.
- GRAVINESE, P. 2017. *Ocean acidification impacts the embryonic development and hatching success of the Florida stone crab, Menippe mercenaria*.
- GUNDERSON, A. R., ARMSTRONG, E. J. & STILLMAN, J. H. 2016. Multiple Stressors in a Changing World: The Need for an Improved Perspective on Physiological Responses to the Dynamic Marine Environment. *Annual Review of Marine Science*, 8, 357-378.
- HALLAM, A. & WIGNALL, P. B. 1997. *Mass extinctions and their aftermath*, Oxford University Press, UK.
- HANCOCK, A. M., KING, C. K., STARK, J. S., MCMINN, A. & DAVIDSON, A. T. 2020. Effects of ocean acidification on Antarctic marine organisms: A meta-analysis. *Ecology and Evolution*, 10, 4495-4514.
- HANSEN, K. & KRISTENSEN, E. 1998. The impact of the polychaete *Nereis diversicolor* and enrichment with macroalgal (*Chaetomorpha linum*) detritus on benthic metabolism and nutrient dynamics in organic-poor and organic-rich sediment. *Journal of Experimental Marine Biology and Ecology*, 231, 201-223.
- HARDEGE, J., MÜLLER, C. & BECKMANN, M. 1997. A waterborne female sex pheromone in the ragworm, *Nereis succinea* (Annelida, Polychaeta). *Polychaete Res*, 17, 18-21.
- HARDEGE, J. D. 1999. Nereidid polychaetes as model organisms for marine chemical ecology. *Hydrobiologia*, 402, 145-161.
- HARDEGE, J. D., MÜLLER, C. T., BECKMANN, M., BARTELSHARDEGE, H. D. & BENTLEY, M. G. 1998. Timing of reproduction in marine polychaetes: The role of sex pheromones. *Ecoscience*, 5, 395-404.
- HARLEY, M. B. 1950. Occurrence of a filter-feeding mechanism in the polychaete *Nereis diversicolor*. *Nature*, 165, 734-735.
- HARTIN, C. A., BOND-LAMBERTY, B., PATEL, P. & MUNDRA, A. 2016. Ocean acidification over the next three centuries using a simple global climate carbon-cycle model: projections and sensitivities. *Biogeosciences*, 13, 4329-4342.
- HAY, M. E. 2009. Marine chemical ecology: chemical signals and cues structure marine populations, communities, and ecosystems. *Annual Review of Marine Science*, 1, 193-212.
- HEDMAN, J. E., GUNNARSSON, J. S., SAMUELSSON, G. & GILBERT, F. 2011. Particle reworking and solute transport by the sediment-living polychaetes *Marenzelleria neglecta* and *Hediste diversicolor*. *Journal of Experimental Marine Biology and Ecology*, 407, 294-301.
- HEIP, C. & HERMAN, R. 1979. Production of *Nereis diversicolor* OF Müller (Polychaeta) in a shallow brackish-water pond. *Estuarine and Coastal Marine Science*, 8, 297-305.
- HENDRIKS, I. E., DUARTE, C. M. & ÁLVAREZ, M. 2010. Vulnerability of marine biodiversity to ocean acidification: a meta-analysis. *Estuarine, Coastal and Shelf Science*, 86, 157-164.
- HERRINGSHAW, L. G., CALLOW, R. H. & MCILROY, D. 2017. Engineering the Cambrian explosion: the earliest bioturbators as ecosystem engineers. *Geological Society, London, Special Publications*, 448, 369-382.
- HESSELBERG, T. 2007. Biomimetics and the case of the remarkable ragworms. *Die Naturwissenschaften*, 94, 613-21.
- HEUGENS, E. H., HENDRIKS, A. J., DEKKER, T., STRAALLEN, N. M. V. & ADMIRAAL, W. 2001. A review of the effects of multiple stressors on aquatic organisms and analysis of uncertainty factors for use in risk assessment. *Critical reviews in toxicology*, 31, 247-284.

- HIDDINK, J. G., BURROWS, M. T. & GARCÍA MOLINOS, J. 2015. Temperature tracking by North Sea benthic invertebrates in response to climate change. *Global Change Biology*, 21, 117-129.
- HOEGH-GULDBERG, O. & BRUNO, J. F. 2010. The impact of climate change on the world's marine ecosystems. *Science*, 328, 1523-1528.
- HOEGH-GULDBERG, O., CAI, R., POLOCZANSKA, E.S., BREWER, P.G., SUNDBY, S., HILMI, K., FABRY, V.J., AND JUNG S. 2014. The Ocean. . In: *Climate Change 2014: Impacts, Adaptation, and Vulnerability. Part B: Regional Aspects. Contribution of Working Group II to the Fifth Assessment Report of the Intergovernmental Panel on Climate Change*, [Barros, V.R., C.B. Field, D.J. Dokken, M.D. Mastrandrea, K.J. Mach, T.E. Bilir, M. Chatterjee, K.L. Ebi, Y.O. Estrada, R.C. Genova, B. Girma, E.S. Kissel, A.N. Levy, S. MacCracken, P.R. Mastrandrea, and L.L. White (eds.)].
- HOFMANN, G. E., SMITH, J. E., JOHNSON, K. S., SEND, U., LEVIN, L. A., MICHELI, F., PAYTAN, A., PRICE, N. N., PETERSON, B. & TAKESHITA, Y. 2011. High-frequency dynamics of ocean pH: a multi-ecosystem comparison. *PLoS one*, 6, e28983.
- HOFMANN, R., BUATOIS, L. A., MACNAUGHTON, R. B. & MÁNGANO, M. G. 2015. Loss of the sedimentary mixed layer as a result of the end-Permian extinction. *Palaeogeography, Palaeoclimatology, Palaeoecology*, 428, 1-11.
- HOLAN, J. R., KING, C. K., PROCTOR, A. H. & DAVIS, A. R. 2019. Increased sensitivity of subantarctic marine invertebrates to copper under a changing climate - Effects of salinity and temperature. *Environmental Pollution*, 249, 54-62.
- HÖNISCH, B., RIDGWELL, A. J., SCHMIDT, D. N., THOMAS, E., GIBBS, S., SLUIJS, A., ZEEBE, R., KUMP, L. R., MARTINDALE, R. C., GREENE, S. E., KIESSLING, W., RIES, J. B., ZACHOS, J., ROYER, D. L., BARKER, S., MARCHITTO, T. M., MOYER, R., PELEJERO, C., ZIVERI, P., FOSTER, G. & WILLIAMS, B. 2012. The Geological Record of Ocean Acidification. *Science*, 335, 1058-1063.
- HOPE, J. A., MALARKEY, J., BAAS, J. H., PEAKALL, J., PARSONS, D. R., MANNING, A. J., BASS, S. J., LICHTMAN, I. D., THORNE, P. D., YE, L. & PATERSON, D. M. 2020. Interactions between sediment microbial ecology and physical dynamics drive heterogeneity in contextually similar depositional systems. *Limnology and Oceanography*, 65, 2403-2419.
- HOWARTH, C. & VINER, D. 2022. Integrating adaptation practice in assessments of climate change science: The case of IPCC Working Group II reports. *Environmental Science & Policy*, 135, 1-5.
- HU, M., TSENG, Y.-C., SU, Y.-H., LEIN, E., LEE, H.-G., LEE, J.-R., DUPONT, S. & STUMPP, M. 2017. Variability in larval gut pH regulation defines sensitivity to ocean acidification in six species of the Ambulacraria superphylum. *Proceedings of the Royal Society B: Biological Sciences*, 284, 20171066.
- HUBLEY, M. J., LOCKE, B. R. & MOERLAND, T. S. 1996. The effects of temperature, pH, and magnesium on the diffusion coefficient of ATP in solutions of physiological ionic strength. *Biochimica et Biophysica Acta (BBA) - General Subjects*, 1291, 115-121.
- HUETTEL, M. & GUST, G. 1992. Impact of bioturbation on interfacial solute exchange in permeable sediments. *Marine ecology progress series*, 253-267.
- HUIJBERS, C. M., NAGELKERKEN, I., LÖSSBROEK, P. A., SCHULTEN, I. E., SIEGENTHALER, A., HOLDERIED, M. W. & SIMPSON, S. D. 2012. A test of the senses: fish select novel habitats by responding to multiple cues. *Ecology*, 93, 46-55.
- HULSWAR, S., SIMO, R., GALÍ, M., BELL, T., LANA, A., INAMDAR, S., HALLORAN, P. R., MANVILLE, G. & MAHAJAN, A. S. 2021. Third Revision of the Global Surface Seawater Dimethyl Sulfide Climatology (DMS-Rev3). *Earth Syst. Sci. Data Discuss.*, 2021, 1-56.
- IPCC 2013a. Climate Change 2014: Synthesis Report. Contribution of Working Groups I, II and III to the Fifth Assessment Report of the Intergovernmental Panel on Climate Change

- [Core Writing Team, R.K. Pachauri and L.A. Meyer (eds.)]. . *IPCC, Geneva, Switzerland*, 151.
- IPCC 2013b. Climate Change 2014: Synthesis Report. Contribution of Working Groups I, II and III to the Fifth Assessment Report of the Intergovernmental Panel on Climate Change [Core Writing Team, R.K. Pachauri and L.A. Meyer (eds.)]. *IPCC, Geneva, Switzerland*, 151.
- IPCC 2014. Climate Change 2014: Synthesis Report. Contribution of Working Groups I, II and III to the Fifth Assessment Report of the Intergovernmental Panel on Climate Change [Core Writing Team, R.K. Pachauri and L.A. Meyer (eds.)]. *IPCC, Geneva, Switzerland*, 151.
- IPCC 2022. *Climate Change 2022: Mitigation of Climate Change. Contribution of Working Group III to the Sixth Assessment Report of the Intergovernmental Panel on Climate Change* [P.R. Shukla, J. Skea, R. Slade, A. Al Khourdajie, R. van Diemen, D. McCollum, M. Pathak, S. Some, P. Vyas, R. Fradera, M. Belkacemi, A. Hasija, G. Lisboa, S. Luz, J. Malley, (eds.)], Cambridge, UK and New York, NY, USA.
- JABLONSKI, D. 1994. Extinctions in the fossil record. *Philosophical Transactions of the Royal Society of London. Series B: Biological Sciences*, 344, 11-17.
- JARDINE, P. E., FRASER, W. T., LOMAX, B. H., SEPTON, M. A., SHANAHAN, T. M., MILLER, C. S. & GOSLING, W. D. 2016. Pollen and spores as biological recorders of past ultraviolet irradiance. *Scientific Reports*, 6, 39269.
- JOACHIMSKI, M., LAI, X., SHEN, S., JIANG, H., LUO, G., CHEN, B., CHEN, J. & SUN, Y. 2012. *Climate warming in the latest Permian and the Permian-Triassic mass extinction*.
- JOHNSON, B. R. & ATEMA, J. 1986. CHEMICAL STIMULANTS FOR A COMPONENT OF FEEDING BEHAVIOR IN THE COMMON GULF-WEED SHRIMP LEANDER TENUICORNIS (SAY). *The Biological Bulletin*, 170, 1-10.
- KAMIO, M. & DERBY, C. D. 2017. Finding food: how marine invertebrates use chemical cues to track and select food. *Natural product reports*, 34, 514-528.
- KAMIO, M., YAMBE, H. & FUSETANI, N. 2021. Chemical cues for intraspecific chemical communication and interspecific interactions in aquatic environments: applications for fisheries and aquaculture. *Fisheries Science*.
- KICKLIGHTER, C. E., KAMIO, M., NGUYEN, L., GERMANN, M. W. & DERBY, C. D. 2011. Mycosporine-like amino acids are multifunctional molecules in sea hares and their marine community. *Proceedings of the National Academy of Sciences of the United States of America*, 108, 11494-11499.
- KITTREDGE, J. S., TAKAHASHI, F. T., LINDSEY, J. & LASKER, R. 1974. Chemical signals in the sea: marine allelochemicals and evolution. *Fishery Bulletin*, 72, 1.
- KLEYPAS, J. A. & LANGDON, C. 2006. Coral reefs and changing seawater carbonate chemistry. *Coastal and Estuarine Studies: Coral Reefs and Climate Change Science and Management*, 61, 73-110.
- KNOLL, A. H., BAMBACH, R. K., PAYNE, J. L., PRUSS, S. & FISCHER, W. W. 2007. Paleophysiology and end-Permian mass extinction. *Earth and Planetary Science Letters*, 256, 295-313.
- KOLKOVSKI, S., ARIELI, A. & TANDLER, A. 1997. Visual and chemical cues stimulate microdiet ingestion in sea bream larvae. *Aquaculture International*, 5, 527-536.
- KOWALEWSKY, S., DAMBACH, M., MAUCK, B. & DEHNHARDT, G. 2005. High olfactory sensitivity for dimethyl sulphide in harbour seals. *Biology Letters*, 2, 106-109.
- KRISTENSEN, E. 1981. Direct measurement of ventilation and oxygen uptake in three species of tubicolous polychaetes (*Nereis* spp.). *Journal of comparative physiology*, 145, 45-50.
- KRISTENSEN, E. 1983. Ventilation and oxygen uptake by three species of *Nereis* (Annelida: Polychaeta). I. Effects of hypoxia. *Mar. Ecol. Prog. Ser.*, 12, 289-297.

- KRISTENSEN, E. 1984. Life cycle, growth and production in estuarine populations of the polychaetes *Nereis virens* and *N. diversicolor*. *Ecography*, 7, 249-250.
- KRISTENSEN, E. 1985. Oxygen and Inorganic Nitrogen Exchange in a "Nereis virens" (Polychaeta) Bioturbated Sediment-Water System. *Journal of Coastal Research*, 1, 109-116.
- KRISTENSEN, E. 2000. Organic matter diagenesis at the oxic/anoxic interface in coastal marine sediments, with emphasis on the role of burrowing animals. *Life at interfaces and under extreme conditions*. Springer.
- KRISTENSEN, E. 2005. *Interactions between macro-and microorganisms in marine sediments*, American Geophysical Union.
- KRISTENSEN, E., AHMED, S. I. & DEVOL, A. H. 1995. Aerobic and anaerobic decomposition of organic matter in marine sediment: which is fastest? *Limnology and oceanography*, 40, 1430-1437.
- KRISTENSEN, E. & KOSTKA, J. 2005. Macrofaunal Burrows and Irrigation in Marine Sediment: Microbiological and Biogeochemical. *Interactions between Macro-and Microorganisms in Marine Sediments*. Washington, DC: American Geophysical Union, 125-157.
- KRISTENSEN, E., NETO, J. M., LUNDKVIST, M., FREDERIKSEN, L., PARDAL, M. Â., VALDEMARSEN, T. & FLINDT, M. R. 2013. Influence of benthic macroinvertebrates on the erodability of estuarine cohesive sediments: Density- and biomass-specific responses. *Estuarine, Coastal and Shelf Science*, 134, 80-87.
- KRISTENSEN, E., PENHA-LOPES, G., DELEFOSSE, M., VALDEMARSEN, T., QUINTANA, C. O. & BANTA, G. T. 2012. What is bioturbation? The need for a precise definition for fauna in aquatic sciences. *Marine Ecology Progress Series*, 446, 285-302.
- KROEKER, K. J., KORDAS, R. L., CRIM, R., HENDRIKS, I. E., RAMAJO, L., SINGH, G. S., DUARTE, C. M. & GATTUSO, J.-P. 2013. Impacts of ocean acidification on marine organisms: quantifying sensitivities and interaction with warming. *Global change biology*, 19, 1884-1896.
- LAFFOLEY, D. & BAXTER, J. M. 2016. *Explaining ocean warming: Causes, scale, effects and consequences*, IUCN Gland, Switzerland.
- LANGENBUCH, M. & PÖRTNER, H.-O. 2002. Changes in metabolic rate and N excretion in the marine invertebrate *Sipunculus nudus* under conditions of environmental hypercapnia: identifying effective acid—base variables. *Journal of Experimental Biology*, 205, 1153-1160.
- LAST, K. S. 2003. An actograph and its use in the study of foraging behaviour in the benthic polychaete, *Nereis virens* Sars. *Journal of Experimental Marine Biology and Ecology*, 287, 237-248.
- LAWRENCE, A. 1996. Environmental and endocrine control of reproduction in two species of polychaete: potential bio-indicators for global climate change. *Journal of the Marine Biological Association of the United Kingdom*, 76, 247-250.
- LAWRENCE, A. & SOAME, J. 2009. The endocrine control of reproduction in Nereidae: a new multi-hormonal model with implications for their functional role in a changing environment. *Philosophical Transactions of the Royal Society B: Biological Sciences*, 364, 3363-3376.
- LAWRENCE, A. J. & SOAME, J. M. 2004. The effects of climate change on the reproduction of coastal invertebrates. *Ibis*, 146, 29-39.
- LEIS, J. M., SIEBECK, U. & DIXSON, D. L. 2011. How Nemo finds home: the neuroecology of dispersal and of population connectivity in larvae of marine fishes. Oxford University Press.

- LEUNG, J. Y. S., RUSSELL, B. D. & CONNELL, S. D. 2020. Linking energy budget to physiological adaptation: How a calcifying gastropod adjusts or succumbs to ocean acidification and warming. *Science of The Total Environment*, 715, 136939.
- LEUNG, J. Y. S., ZHANG, S. & CONNELL, S. D. 2022. Is Ocean Acidification Really a Threat to Marine Calcifiers? A Systematic Review and Meta-Analysis of 980+ Studies Spanning Two Decades. *Small*, 18, 2107407.
- LEVY, H. M., SHARON, N., RYAN, E. M. & KOSHLAND, D. E. 1962. Effect of temperature on the rate of hydrolysis of adenosine triphosphate and inosine triphosphate by myosin with and without modifiers. Evidence for a change in protein conformation. *Biochimica et Biophysica Acta*, 56, 118-126.
- LEWIS, C., CLEWOW, K. & HOLT, W. V. 2013. Metal contamination increases the sensitivity of larvae but not gametes to ocean acidification in the polychaete *Pomatoceros lamarckii* (Quatrefages). *Marine Biology*, 160, 2089-2101.
- LIENART, G. D., MITCHELL, M. D., FERRARI, M. C. & MCCORMICK, M. I. 2014. Temperature and food availability affect risk assessment in an ectotherm. *Animal Behaviour*, 89, 199-204.
- LIPPS, J. H. & SIGNOR, P. W. 2013. *Origin and early evolution of the Metazoa*, Springer Science & Business Media.
- LIU, J., OU, Q., HAN, J., LI, J., WU, Y., JIAO, G. & HE, T. 2015. Lower Cambrian polychaete from China sheds light on early annelid evolution. *The Science of Nature*, 102, 34.
- LOMAS, M. W., MARK TRICE, T., GLIBERT, P. M., BRONK, D. A. & MCCARTHY, J. J. 2002. Temporal and spatial dynamics of urea uptake and regeneration rates and concentrations in Chesapeake Bay. *Estuaries*, 25, 469-482.
- LONSDALE, J.-A., LEACH, C., PARSONS, D., BARKWITH, A., MANSON, S. & ELLIOTT, M. 2022. Managing estuaries under a changing climate: A case study of the Humber Estuary, UK. *Environmental Science & Policy*, 134, 75-84.
- LONSDALE, J. M., S. & T. JEYNES 2013. Sediment Management in the Humber Estuary: Dredging and Disposal Strategies – Study in the framework of the Interreg IVB project TIDE: TIDE - Tidal River Development.
- LOUGH, J. M., ANDERSON, K. D. & HUGHES, T. P. 2018. Increasing thermal stress for tropical coral reefs: 1871–2017. *Scientific Reports*, 8, 6079.
- LU, Y., YUAN, J., LU, X., SU, C., ZHANG, Y., WANG, C., CAO, X., LI, Q., SU, J. & ITTEKKOT, V. 2018. Major threats of pollution and climate change to global coastal ecosystems and enhanced management for sustainability. *Environmental Pollution*, 239, 670-680.
- LUNT, J. & SMEE, D. L. 2015. Turbidity interferes with foraging success of visual but not chemosensory predators. *PeerJ*, 3, e1212-e1212.
- MAIR, P. & WILCOX, R. 2020. Robust statistical methods in R using the WRS2 package. *Behavior research methods*, 52, 464-488.
- MALARKEY, J., BAAS, J. H., HOPE, J. A., ASPDEN, R. J., PARSONS, D. R., PEAKALL, J., PATERSON, D. M., SCHINDLER, R. J., YE, L., LICHTMAN, I. D., BASS, S. J., DAVIES, A. G., MANNING, A. J. & THORNE, P. D. 2015. The pervasive role of biological cohesion in bedform development. *Nature Communications*, 6, 6257.
- MANGUM, C. P. & COX, C. D. 1971. ANALYSIS OF THE FEEDING RESPONSE IN THE ONUPHID POLYCHAETE DIOPATRA CUPREA (BOSC). *The Biological Bulletin*, 140, 215-229.
- MARINELLI, R. L., LOVELL, C. R., WAKEHAM, S. G., RINGELBERG, D. B. & WHITE, D. C. 2002. Experimental investigation of the control of bacterial community composition in macrofaunal burrows. *Marine Ecology Progress Series*, 235, 1-13.
- MARTIN, R. A. 2007. A review of behavioural ecology of whale sharks (*Rhincodon typus*). *Fisheries Research*, 84, 10-16.

- MARTIN, W. R. 2009. Chemical processes in estuarine sediments. *Elements of Physical Oceanography: A derivative of the Encyclopedia of Ocean Sciences*, 445.
- MARUBINI, F., FERRIER-PAGES, C. & CUIF, J. P. 2003. Suppression of skeletal growth in scleractinian corals by decreasing ambient carbonate-ion concentration: a cross-family comparison. *Proceedings of the Royal Society of London. Series B: Biological Sciences*, 270, 179-184.
- MASS, T., GIUFFRÉ, A. J., SUN, C.-Y., STIFLER, C. A., FRAZIER, M. J., NEDER, M., TAMURA, N., STAN, C. V., MARCUS, M. A. & GILBERT, P. U. 2017. Amorphous calcium carbonate particles form coral skeletons. *Proceedings of the National Academy of Sciences*, 114, E7670-E7678.
- MASUKO, T., MINAMI, A., IWASAKI, N., MAJIMA, T., NISHIMURA, S.-I. & LEE, Y. C. 2005. Carbohydrate analysis by a phenol-sulfuric acid method in microplate format. *Analytical biochemistry*, 339, 69-72.
- MATHURU, A. S., KIBAT, C., CHEONG, W. F., SHUI, G., WENK, M. R., FRIEDRICH, R. W. & JESUTHASAN, S. 2012. Chondroitin fragments are odorants that trigger fear behavior in fish. *Current Biology*, 22, 538-544.
- MAYES, W., BATTY, L., YOUNGER, P., JARVIS, A., KÖIV, M., VOHLA, C. & MANDER, U. 2009. Wetland treatment at extremes of pH: a review. *Science of the total environment*, 407, 3944-3957.
- MEADOWS, P., TAIT, J. & HUSSAIN, S. 1990. Effects of estuarine infauna on sediment stability and particle sedimentation. *Hydrobiologia*, 190, 263-266.
- MEADOWS, P. S. & TAIT, J. 1989. Modification of sediment permeability and shear strength by two burrowing invertebrates. *Marine Biology*, 101, 75-82.
- MELZNER, F., MARK, F. C., SEIBEL, B. A. & TOMANEK, L. 2020. Ocean Acidification and Coastal Marine Invertebrates: Tracking CO₂ Effects from Seawater to the Cell. *Annual Review of Marine Science*, 12, 499-523.
- MELZNER, F., STANGE, P., TRÜBENBACH, K., THOMSEN, J., CASTIES, I., PANKNIN, U., GORB, S. N. & GUTOWSKA, M. A. 2011. Food supply and seawater pCO₂ impact calcification and internal shell dissolution in the blue mussel *Mytilus edulis*. *PloS one*, 6, e24223.
- MERMILLOD-BLONDIN, F., FRANÇOIS-CARCAILLET, F. & ROSENBERG, R. 2005. Biodiversity of benthic invertebrates and organic matter processing in shallow marine sediments: an experimental study. *Journal of experimental marine biology and ecology*, 315, 187-209.
- MEYSMAN, F. J. R., MIDDELBURG, J. J. & HEIP, C. H. R. 2006. Bioturbation: a fresh look at Darwin's last idea. *Trends in Ecology & Evolution*, 21, 688-695.
- MICHAELIDIS, B., OUZOUNIS, C., PALERAS, A. & PÖRTNER, H. O. 2005. Effects of long-term moderate hypercapnia on acid-base balance and growth rate in marine mussels *Mytilus galloprovincialis*. *Marine Ecology Progress Series*, 293, 109-118.
- MICHAUD, E., ALLER, R. C. & STORA, G. 2010. Sedimentary organic matter distributions, burrowing activity, and biogeochemical cycling: Natural patterns and experimental artifacts. *Estuarine, Coastal and Shelf Science*, 90, 21-34.
- MOFFITT, S. E., HILL, T. M., ROOPNARINE, P. D. & KENNETT, J. P. 2015. Response of seafloor ecosystems to abrupt global climate change. *Proceedings of the National Academy of Sciences*, 112, 4684-4689.
- MÖLLER, P. 1985. Production and Abundance of Juvenile *Nereis diversicolor*, and Oogenic Cycle of Adults in Shallow Waters of Western Sweden. *Journal of the Marine Biological Association of the United Kingdom*, 65, 603-616.
- MOLTEDO, G., MARTUCCIO, G., CATALANO, B., GASTALDI, L., MAGGI, C., VIRNO-LAMBERTI, C. & CICERO, A. M. 2019. Biological responses of the polychaete *Hediste diversicolor* (O.F.Müller, 1776) to inorganic mercury exposure: A multimarker approach. *Chemosphere*, 219, 989-996.

- MORAES, T. B., RIBAS FERREIRA, J. L., DA ROSA, C. E., SANDRINI, J. Z., VOTTO, A. P., TRINDADE, G. S., GERACITANO, L. A., ABREU, P. C. & MONSERRAT, J. M. 2006. Antioxidant properties of the mucus secreted by *Laeonereis acuta* (Polychaeta, Nereididae): A defense against environmental pro-oxidants? *Comparative Biochemistry and Physiology Part C: Toxicology & Pharmacology*, 142, 293-300.
- MOREIRA, S. M., LIMA, I., RIBEIRO, R. & GUILHERMINO, L. 2006. Effects of estuarine sediment contamination on feeding and on key physiological functions of the polychaete *Hediste diversicolor*: laboratory and in situ assays. *Aquatic toxicology*, 78, 186-201.
- MOUNEYRAC, C., MASTAIN, O., AMIARD, J., AMIARD-TRIQUET, C., BEAUNIER, P., JEANTET, A.-Y., SMITH, B. & RAINBOW, P. 2003. Trace-metal detoxification and tolerance of the estuarine worm *Hediste diversicolor* chronically exposed in their environment. *Marine Biology*, 143, 731-744.
- MURPHY, E. A. & REIDENBACH, M. A. 2016. Oxygen transport in periodically ventilated polychaete burrows. *Marine biology*, 163, 208.
- MUTALIPASSI, M., FINK, P., MAIBAM, C., PORZIO, L., BUIA, M. C., GAMBI, M. C., PATTI, F. P., SCIPIONE, M. B., LORENTI, M. & ZUPO, V. 2020. Ocean acidification alters the responses of invertebrates to wound-activated infochemicals produced by epiphytes of the seagrass *Posidonia oceanica*. *Journal of Experimental Marine Biology and Ecology*, 530-531, 151435.
- MUUS, B. J. 1967. *The fauna of Danish estuaries and lagoons: distribution and ecology of dominating species in the shallow reaches of the mesohaline zone*, Høst.
- NAGELKERKEN, I. & MUNDAY, P. L. 2016. Animal behaviour shapes the ecological effects of ocean acidification and warming: moving from individual to community-level responses. *Global Change Biology*, 22, 974-989.
- NEUDECKER, S. Growth and survival of scleractinian corals exposed to thermal effluents at Guam. 4. International Coral Reef Symposium, Manila (Philippines), 18-22 May 1981, 1981.
- NEVITT, G. A. 2008. Sensory ecology on the high seas: the odor world of the procellariiform seabirds. *Journal of Experimental Biology*, 211, 1706-1713.
- NEVITT, G. A., VEIT, R. R. & KAREIVA, P. 1995. Dimethyl sulphide as a foraging cue for Antarctic procellariiform seabirds. *Nature*, 376, 680-682.
- NGATIA, L., III, J. G., MORIASI, D. & TAYLOR, R. 2019. Nitrogen and Phosphorus Eutrophication in Marine Ecosystems. *Monitoring of Marine Pollution*. IntechOpen.
- NIELSEN, S. S. 2017. *Food analysis laboratory manual*, Springer.
- NOGUEIRA, A. F. & NUNES, B. 2021. Effects of paracetamol on the polychaete *Hediste diversicolor*: occurrence of oxidative stress, cyclooxygenase inhibition and behavioural alterations. *Environmental Science and Pollution Research*, 28, 26772-26783.
- ORR, J. C., FABRY, V. J., AUMONT, O., BOPP, L., DONEY, S. C., FEELY, R. A., GNANADESIKAN, A., GRUBER, N., ISHIDA, A., JOOS, F., KEY, R. M., LINDSAY, K., MAIER-REIMER, E., MATEAR, R., MONFRAY, P., MOUCHET, A., NAJJAR, R. G., PLATTNER, G.-K., RODGERS, K. B., SABINE, C. L., SARMIENTO, J. L., SCHLITZER, R., SLATER, R. D., TOTTERDELL, I. J., WEIRIG, M.-F., YAMANAKA, Y. & YOOL, A. 2005. Anthropogenic ocean acidification over the twenty-first century and its impact on calcifying organisms. *Nature*, 437, 681.
- PANDORI, L. L. M. & SORTE, C. J. B. 2019. The weakest link: sensitivity to climate extremes across life stages of marine invertebrates. *Oikos*, 128, 621-629.
- PARSONS, D., SCHINDLER, R., HOPE, J., MALARKEY, J., BAAS, J. H., PEAKALL, J., MANNING, A., YE, L., SIMMONS, S., PATERSON, D., ASPDEN, R., BASS, S., DAVIES, A., LICHTMAN, I.

- D. & THORNE, P. 2016. The role of biophysical cohesion on subaqueous bed form size. *Geophysical Research Letters*, 43, 1566-1573.
- PEDRO, C. A., BRUNO, C. S., SARLY, M. S., MEIRELES, G., MOUTINHO, A., NOVAIS, S. C., MARQUES, J. C. & GONÇALVES, S. C. 2022. Are tolerance processes limiting the responses of *Hediste diversicolor* to cadmium exposure? A multimarker approach. *Aquatic Toxicology*, 252, 106300.
- PENN, J. L. & DEUTSCH, C. 2022. Avoiding ocean mass extinction from climate warming. *Science*, 376, 524-526.
- PEREIRA, H. M., LEADLEY, P. W., PROENÇA, V., ALKEMADE, R., SCHARLEMANN, J. P., FERNANDEZ-MANJARRÉS, J. F., ARAÚJO, M. B., BALVANERA, P., BIGGS, R. & CHEUNG, W. W. 2010. Scenarios for global biodiversity in the 21st century. *Science*, 330, 1496-1501.
- PETSIOS, E., THOMPSON, J. R., PIETSCH, C. & BOTTJER, D. J. 2017. Biotic impacts of temperature before, during, and after the end-Permian extinction: A multi-metric and multi-scale approach to modeling extinction and recovery dynamics. *Palaeogeography, Palaeoclimatology, Palaeoecology*.
- PIMM, S., RAVEN, P., PETERSON, A., ŞEKERCIOĞLU, Ç. H. & EHRLICH, P. R. 2006. Human impacts on the rates of recent, present, and future bird extinctions. *Proceedings of the National Academy of Sciences*, 103, 10941-10946.
- PIMM, S. L., RUSSELL, G. J., GITTLEMAN, J. L. & BROOKS, T. M. 1995. The future of biodiversity. *Science*, 269, 347-350.
- PIRES, A., FIGUEIRA, E., SILVA, M. S. S., SÁ, C. & MARQUES, P. A. A. P. 2022. Effects of graphene oxide nanosheets in the polychaete *Hediste diversicolor*: Behavioural, physiological and biochemical responses. *Environmental Pollution*, 299, 118869.
- PISCHEDDA, L., CUNY, P., ESTEVES, J. L., POGGIALE, J.-C. & GILBERT, F. 2012. Spatial oxygen heterogeneity in a *Hediste diversicolor* irrigated burrow. *Hydrobiologia*, 680, 109-124.
- PISCHEDDA, L., POGGIALE, J.-C., CUNY, P. & GILBERT, F. 2008. Imaging oxygen distribution in marine sediments. The importance of bioturbation and sediment heterogeneity. *Acta biotheoretica*, 56, 123-135.
- PORTEUS, C. S., HUBBARD, P. C., UREN WEBSTER, T. M., VAN AERLE, R., CANÁRIO, A. V. M., SANTOS, E. M. & WILSON, R. W. 2018. Near-future CO₂ levels impair the olfactory system of a marine fish. *Nature Climate Change*, 8, 737-743.
- PÖRTNER, H.-O., LANGENBUCH, M. & MICHAELIDIS, B. Effects of CO₂ on marine animals: Time scales, processes, and limits of adaptation. SCOR/IOC Symposium: Oceans in a high CO₂ world. Paris 2004. 2004.
- PÖRTNER, H.-O., ROBERTS, D. C., ADAMS, H., ADLER, C., ALDUNCE, P., ALI, E., BEGUM, R. A., BETTS, R., KERR, R. B. & BIESBROEK, R. 2022. Climate change 2022: Impacts, adaptation and vulnerability. *IPCC Sixth Assessment Report*.
- PÖRTNER, H.-O., ROBERTS, D. C., MASSON-DELMOTTE, V., ZHAI, P., TIGNOR, M., POLOCZANSKA, E. & WEYER, N. 2019. The ocean and cryosphere in a changing climate. *IPCC Special Report on the Ocean and Cryosphere in a Changing Climate*.
- PÖRTNER, H. 2001. Climate change and temperature-dependent biogeography: oxygen limitation of thermal tolerance in animals. *Naturwissenschaften*, 88, 137-146.
- PÖRTNER, H. O. & BOCK, C. 2000. A contribution of acid-base regulation to metabolic depression in marine ectotherms. *Life in the Cold*. Springer.
- PÖRTNER, H. O. & FARRELL, A. P. 2008. Physiology and climate change. *Science*, 690-692.
- PÖRTNER, H. O., LANGENBUCH, M. & MICHAELIDIS, B. 2005. Synergistic effects of temperature extremes, hypoxia, and increases in CO₂ on marine animals: From Earth history to global change. *Journal of Geophysical Research: Oceans*, 110.

- POULIN, R. X., LAVOIE, S., SIEGEL, K., GAUL, D. A., WEISSBURG, M. J. & KUBANEK, J. 2018. Chemical encoding of risk perception and predator detection among estuarine invertebrates. *Proceedings of the National Academy of Sciences*, 115, 662-667.
- POWERS, S. P. & KITTINGER, J. N. 2002. Hydrodynamic mediation of predator-prey interactions: differential patterns of prey susceptibility and predator success explained by variation in water flow. *Journal of Experimental Marine Biology and Ecology*, 273, 171-187.
- PROFANT, V., JOHANNESSEN, C., BLANCH, E. W., BOUŘ, P. & BAUMRUK, V. 2019. Effects of sulfation and the environment on the structure of chondroitin sulfate studied via Raman optical activity. *Physical chemistry chemical physics*, 21, 7367-7377.
- PRUSS, S. B., BOTTJER, D. J., CORSETTI, F. A. & BAUD, A. 2006. A global marine sedimentary response to the end-Permian mass extinction: Examples from southern Turkey and the western United States. *Earth-Science Reviews*, 78, 193-206.
- PRZESLAWSKI, R., BYRNE, M. & MELLIN, C. 2015. A review and meta-analysis of the effects of multiple abiotic stressors on marine embryos and larvae. *Global change biology*, 21, 2122-2140.
- RAVEN, J., CALDEIRA, K., ELDERFIELD, H., HOEGH-GULDBERG, O., LISS, P., RIEBESELL, U., SHEPHERD, J., TURLEY, C. & WATSON, A. 2005. *Ocean acidification due to increasing atmospheric carbon dioxide*, The Royal Society.
- REDDIN, C. J., NÄTSCHER, P. S., KOCSIS, Á. T., PÖRTNER, H.-O. & KIESSLING, W. 2020. Marine clade sensitivities to climate change conform across timescales. *Nature Climate Change*, 10, 249-253.
- RETALLACK, G., VEEVERS, J. & MORANTE, R. 1996. *Global coal gap between Permian--Triassic extinction and Middle Triassic recovery of peat-forming plants*.
- RHOADS, D. & YOUNG, D. 1970. The Influence of Deposit-feeding Organisms on Sediment Stability and Community Trophic Structure. *Journal of Marine Research*, 28, 150-178.
- RIEBESELL, U., ZONDERVAN, I., ROST, B., TORTELL, P. D., ZEEBE, R. E. & MOREL, F. M. 2000. Reduced calcification of marine plankton in response to increased atmospheric CO₂. *Nature*, 407, 364-367.
- RIES, J. B. 2011. A physicochemical framework for interpreting the biological calcification response to CO₂-induced ocean acidification. *Geochimica et Cosmochimica Acta*, 75, 4053-4064.
- RIES, J. B., COHEN, A. L. & MCCORKLE, D. C. 2009. Marine calcifiers exhibit mixed responses to CO₂-induced ocean acidification. *Geology*, 37, 1131-1134.
- RITTSCHOFF, D. 1990. Peptide-mediated behaviors in marine organisms Evidence for a common theme. *Journal of Chemical Ecology*, 16, 261-272.
- RITTSCHOFF, D. & COHEN, J. H. 2004. Crustacean peptide and peptide-like pheromones and kairomones. *Peptides*, 25, 1503-1516.
- ROGGATZ, C. C., LORCH, M., HARDEGE, J. D. & BENOIT, D. M. 2016. Ocean acidification affects marine chemical communication by changing structure and function of peptide signalling molecules. *Global change biology*, 22, 3914-3926.
- ROMANO, C., GOUDEMAND, N., VENNEMANN, T. W., WARE, D., SCHNEEBELI-HERMANN, E., HOCHULI, P. A., BRÜHWILER, T., BRINKMANN, W. & BUCHER, H. 2012. Climatic and biotic upheavals following the end-Permian mass extinction. *Nature Geoscience*, 6, 57.
- ROSSI, T., NAGELKERKEN, I., SIMPSON, S. D., PISTEVOS, J. C., WATSON, S.-A., MERILLET, L., FRASER, P., MUNDAY, P. L. & CONNELL, S. D. 2015. Ocean acidification boosts larval fish development but reduces the window of opportunity for successful settlement. *Proceedings of the Royal Society B: Biological Sciences*, 282, 20151954.
- ROUSE, G. & PLEIJEL, F. 2001. *Polychaetes*, Oxford university press.

- SCAPS, P. 2002. *A review of the biology, ecology and potential use of the common ragworm Hediste diversicolor (O.F. Müller) (Annelida: Polychaeta)*.
- SCHAUM, C. E., BATTY, R. & LAST, K. S. 2013. Smelling Danger - Alarm Cue Responses in the Polychaete *Nereis (Hediste) diversicolor* (Müller, 1776) to Potential Fish Predation. *PLOS ONE*, 8, e77431.
- SCHEIFFARTH, G. 2001. The diet of Bar-tailed Godwits *Limosa lapponica* in the Wadden Sea: combining visual observations and faeces analyses. *Ardea*, 89, 481-494.
- SCHMIDT, G. A. 1999. Forward modeling of carbonate proxy data from planktonic foraminifera using oxygen isotope tracers in a global ocean model. *Paleoceanography*, 14, 482-497.
- SCHÖTTLER, U. 1979. On the anaerobic metabolism of three species of *Nereis* (Annelida). *Mar Ecol Prog Ser*, 1, 249-254.
- SEDDON, A. W., FESTI, D., ROBSON, T. M. & ZIMMERMANN, B. 2019. Fossil pollen and spores as a tool for reconstructing ancient solar-ultraviolet irradiance received by plants: an assessment of prospects and challenges using proxy-system modelling. *Photochemical & Photobiological Sciences*.
- ŞENGÖR, A. C., ATAYMAN, S. & ÖZEREN, S. 2008. A scale of greatness and causal classification of mass extinctions: Implications for mechanisms. *Proceedings of the National Academy of Sciences*, 105, 13736-13740.
- SHEN, J., FENG, Q., ALGEO, T. J., LI, C., PLANAVSKY, N. J., ZHOU, L. & ZHANG, M. 2016. Two pulses of oceanic environmental disturbance during the Permian–Triassic boundary crisis. *Earth and Planetary Science Letters*, 443, 139-152.
- SHEN, S.-Z., CROWLEY, J. L., WANG, Y., BOWRING, S. A., ERWIN, D. H., SADLER, P. M., CAO, C.-Q., ROTHMAN, D. H., HENDERSON, C. M., RAMEZANI, J., ZHANG, H., SHEN, Y., WANG, X.-D., WANG, W., MU, L., LI, W.-Z., TANG, Y.-G., LIU, X.-L., LIU, L.-J., ZENG, Y., JIANG, Y.-F. & JIN, Y.-G. 2011. Calibrating the End-Permian Mass Extinction. *Science*, 334, 1367-1372.
- SHEPHERD, J. G., BREWER, P. G., OSCHLIES, A. & WATSON, A. J. 2017. Ocean ventilation and deoxygenation in a warming world: introduction and overview. The Royal Society Publishing.
- SHNIT-ORLAND, M. & KUSHMARO, A. 2009. Coral mucus-associated bacteria: a possible first line of defense. *FEMS microbiology ecology*, 67, 371-380.
- SHRIVASTAVA, S., STEWARDSON, M. J. & ARORA, M. 2021. Influence of Bioturbation on Hyporheic Exchange in Streams: Conceptual Model and Insights From Laboratory Experiments. *Water Resources Research*, 57, e2020WR028468.
- SILVA, M. S. S., PIRES, A., ALMEIDA, M. & OLIVEIRA, M. 2020. The use of *Hediste diversicolor* in the study of emerging contaminants. *Marine Environmental Research*, 159, 105013.
- SIMÃO, A. M. S., BOLEAN, M., HOYLAERTS, M. F., MILLÁN, J. L. & CIANCAGLINI, P. 2013. Effects of pH on the production of phosphate and pyrophosphate by matrix vesicles' biomimetics. *Calcified tissue international*, 93, 222-232.
- SIX, K. D., KLOSTER, S., ILYINA, T., ARCHER, S. D., ZHANG, K. & MAIER-REIMER, E. 2013. Global warming amplified by reduced sulphur fluxes as a result of ocean acidification. *Nature Climate Change*, 3, 975-978.
- SNELL, T. W., KUBANEK, J., CARTER, W., PAYNE, A. B., KIM, J., HICKS, M. K. & STELZER, C.-P. 2006. A protein signal triggers sexual reproduction in *Brachionus plicatilis* (Rotifera). *Marine Biology*, 149, 763-773.
- SOKOLOVA, I. M., FREDERICH, M., BAGWE, R., LANNIG, G. & SUKHOTIN, A. A. 2012. Energy homeostasis as an integrative tool for assessing limits of environmental stress tolerance in aquatic invertebrates. *Marine environmental research*, 79, 1-15.

- SOLAN, M., BATTY, P., BULLING, M. T. & GODBOLD, J. A. 2008. How biodiversity affects ecosystem processes: implications for ecological revolutions and benthic ecosystem function. *Aquatic Biology*, 2, 289-301.
- SOLAN, M. & HERRINGSHAW, L. G. 2008. Bioturbation in aquatic environments: linking past and present. *Aquatic Biology*, 2, 201-205.
- SONG, H., WIGNALL, P. B., CHU, D., TONG, J., SUN, Y., SONG, H., HE, W. & TIAN, L. 2014. Anoxia/high temperature double whammy during the Permian-Triassic marine crisis and its aftermath. *Scientific Reports*, 4, 4132.
- SONG, H., WIGNALL, P. B., TONG, J., BOND, D. P. G., SONG, H., LAI, X., ZHANG, K., WANG, H. & CHEN, Y. 2012. Geochemical evidence from bio-apatite for multiple oceanic anoxic events during Permian-Triassic transition and the link with end-Permian extinction and recovery. *Earth and Planetary Science Letters*, 353-354, 12-21.
- SONG, H., WIGNALL, P. B., TONG, J. & YIN, H. 2013. Two pulses of extinction during the Permian-Triassic crisis. *Nature Geoscience*, 6, 52.
- SPALDING, C., FINNEGAN, S. & FISCHER, W. W. 2017. Energetic costs of calcification under ocean acidification. *Global Biogeochemical Cycles*, 31, 866-877.
- SPALDING, C. & HULL, P. M. 2021. Towards quantifying the mass extinction debt of the Anthropocene. *Proceedings of the Royal Society B: Biological Sciences*, 288, 20202332.
- SPERO, H. J., BIJMA, J., LEA, D. W. & BEMIS, B. E. 1997. Effect of seawater carbonate concentration on foraminiferal carbon and oxygen isotopes. *Nature*, 390, 497.
- STABILI, L. 2019. The mucus of marine invertebrates. *Enzymatic Technologies for Marine Polysaccharides*, 151.
- STABILI, L., ACQUAVIVA, M., BIANCOLINO, F., CAVALLO, R., DE PASCALI, S., FANIZZI, F., NARRACCI, M., CECERE, E. & PETROCELLI, A. 2014. Biotechnological potential of the seaweed *Cladophora rupestris* (Chlorophyta, Cladophorales) lipidic extract. *New Biotechnology*, 31, 436-444.
- STÅHL-DELBANCO, A. & HANSSON, L.-A. 2002. Effects of bioturbation on recruitment of algal cells from the "seed bank" of lake sediments. *Limnology and Oceanography*, 47, 1836-1843.
- STANLEY, S. M. 2016. Estimates of the magnitudes of major marine mass extinctions in earth history. *Proceedings of the National Academy of Sciences*, 113, E6325-E6334.
- STECKBAUER, A., RAMAJO, L., HENDRIKS, I., FERNANDEZ, M., LAGOS, N., PRADO, L. & DUARTE, C. M. 2015. Synergistic effects of hypoxia and increasing CO₂ on benthic invertebrates of the central Chilean coast. *Frontiers in Marine Science*, 2.
- STEWART, R. I. A., DOSSENA, M., BOHAN, D. A., JEPPESEN, E., KORDAS, R. L., LEDGER, M. E., MEERHOFF, M., MOSS, B., MULDER, C., SHURIN, J. B., SUTTLE, B., THOMPSON, R., TRIMMER, M. & WOODWARD, G. 2013. Chapter Two - Mesocosm Experiments as a Tool for Ecological Climate-Change Research. In: WOODWARD, G. & O'GORMAN, E. J. (eds.) *Advances in Ecological Research*. Academic Press.
- STRADER, M. E., WONG, J. M. & HOFMANN, G. E. 2020. Ocean acidification promotes broad transcriptomic responses in marine metazoans: a literature survey. *Frontiers in Zoology*, 17, 7.
- STURDIVANT, S. K., DIAZ, R. J. & CUTTER, G. R. 2012. Bioturbation in a declining oxygen environment, in situ observations from Wormcam. *PloS one*, 7, e34539.
- SUN, Y., JOACHIMSKI, M. M., WIGNALL, P. B., YAN, C., CHEN, Y., JIANG, H., WANG, L. & LAI, X. 2012. Lethally Hot Temperatures During the Early Triassic Greenhouse. *Science*, 338, 366-370.
- SUTRISNO, R., SCHOTTE, P. M. & WISENDEN, B. D. 2014. Chemical arms race between predator and prey: a test of predator digestive countermeasures against chemical labeling by dietary cues of prey. *Journal of freshwater ecology*, 29, 17-23.

- TAL, A. B., SHENKAR, N., PAZ, A., CONLEY, K., SUTHERLAND, K. & YAHIEL, G. 2021. High mucous-mesh production by the ascidian *Herdmania momus*. *Marine Ecology Progress Series*, 663, 223-228.
- TAPPIN, D., PEARCE, B., FITCH, S., DOVE, D., GEAREY, B., HILL, J., CHAMBERS, C., BATES, R., PINNION, J. & DIAZ DOCE, D. 2011. *The Humber regional environmental characterisation*, Marine Aggregate Levy Sustainability Fund.
- TIMMERMAN, K., BANTA, G. T. & GLUD, R. N. 2006. Linking *Arenicola marina* irrigation behavior to oxygen transport and dynamics in sandy sediments. *Journal of Marine Research*, 64, 915-938.
- TOLHURST, T. J., GUST, G. & PATERSON, D. M. 2002. The influence of an extracellular polymeric substance (EPS) on cohesive sediment stability. In: WINTERWERP, J. C. & KRANENBURG, C. (eds.) *Proceedings in Marine Science*. Elsevier.
- TWITCHETT, R. J. & BARRAS, C. G. 2004. Trace fossils in the aftermath of mass extinction events. *Geological Society, London, Special Publications*, 228, 397-418.
- TWITCHETT, R. J., LOOY, C. V., MORANTE, R., VISSCHER, H. & WIGNALL, P. B. 2001. Rapid and synchronous collapse of marine and terrestrial ecosystems during the end-Permian biotic crisis. *Geology*, 29, 351-354.
- UTHICKE, S., PECORINO, D., ALBRIGHT, R., NEGRI, A. P., CANTIN, N., LIDDY, M., DWORJANYN, S., KAMYA, P., BYRNE, M. & LAMARE, M. 2013. Impacts of ocean acidification on early life-history stages and settlement of the coral-eating sea star *Acanthaster planci*. *PLoS One*, 8, e82938.
- VAN BREUGEL, Y., SCHOUTEN, S., TSIKOS, H., ERBA, E., PRICE, G. D. & SINNINGHE DAMSTÉ, J. S. 2007. Synchronous negative carbon isotope shifts in marine and terrestrial biomarkers at the onset of the early Aptian oceanic anoxic event 1a: Evidence for the release of ^{13}C -depleted carbon into the atmosphere. *Paleoceanography and Paleoclimatology*, 22.
- VARGAS, C. A., CUEVAS, L. A., BROITMAN, B. R., SAN MARTIN, V. A., LAGOS, N. A., GAITÁN-ESPITIA, J. D. & DUPONT, S. 2022. Upper environmental pCO_2 drives sensitivity to ocean acidification in marine invertebrates. *Nature Climate Change*, 12, 200-207.
- VELEZ, Z., HUBBARD, P. C., HARDEGE, J. D., BARATA, E. N. & CANÁRIO, A. V. M. 2007. The contribution of amino acids to the odour of a prey species in the Senegalese sole (*Solea senegalensis*). *Aquaculture*, 265, 336-342.
- VILA-VIÇOSA, D., TEIXEIRA, V. H., SANTOS, H. A. F. & MACHUQUEIRO, M. 2013. Conformational Study of GSH and GSSG Using Constant-pH Molecular Dynamics Simulations. *The Journal of Physical Chemistry B*, 117, 7507-7517.
- VON EUW, S., ZHANG, Q., MANICHEV, V., MURALI, N., GROSS, J., FELDMAN, L. C., GUSTAFSSON, T., FLACH, C., MENDELSON, R. & FALKOWSKI, P. G. 2017. Biological control of aragonite formation in stony corals. *Science*, 356, 933-938.
- WAKISAKA, N., MIYASAKA, N., KOIDE, T., MASUDA, M., HIRAKI-KAJIYAMA, T. & YOSHIHARA, Y. 2017. An Adenosine Receptor for Olfaction in Fish. *Current Biology*, 27, 1437-1447.e4.
- WANG, H., HAGEMANN, A., REITAN, K. I., HANDÅ, A., UHRE, M. & MALZAHN, A. M. 2020. Embryonic and larval development in the semelparous Nereid polychaete *Hediste diversicolor* (OF Müller, 1776) in Norway: Challenges and perspectives. *Aquaculture Research*, 51, 4135-4151.
- WANG, Y., SADLER, P. M., SHEN, S.-Z., ERWIN, D. H., ZHANG, Y.-C., WANG, X.-D., WANG, W., CROWLEY, J. L. & HENDERSON, C. M. 2014. Quantifying the process and abruptness of the end-Permian mass extinction. *QUANTIFYING THE END-PERMIAN MASS EXTINCTION. Paleobiology*, 40, 113-129.

- WIDDICOMBE, S. & NEEDHAM, H. 2007. Impact of CO₂-induced seawater acidification on the burrowing activity of *Nereis virens* and sediment nutrient flux. *Marine ecology progress series*, 341, 111-122.
- WIDDICOMBE, S. & SPICER, J. I. 2008. Predicting the impact of ocean acidification on benthic biodiversity: What can animal physiology tell us? *Journal of Experimental Marine Biology and Ecology*, 366, 187-197.
- WIGNALL, P. B. 2001. Large igneous provinces and mass extinctions. *Earth-Science Reviews*, 53, 1-33.
- WIGNALL, P. B. & NEWTON, R. 2003. Contrasting deep-water records from the Upper Permian and Lower Triassic of South Tibet and British Columbia: evidence for a diachronous mass extinction. *Palaios*, 18, 153-167.
- WIGNALL, P. B., SUN, Y., BOND, D. P., IZON, G., NEWTON, R. J., VÉDRINE, S., WIDDOWSON, M., ALI, J. R., LAI, X. & JIANG, H. 2009. Volcanism, mass extinction, and carbon isotope fluctuations in the Middle Permian of China. *science*, 324, 1179-1182.
- WIGNALL, P. B. & TWITCHETT, R. J. 1996. Oceanic anoxia and the end Permian mass extinction. *Science*, 272, 1155-1158.
- WINN, P., YOUNG, R. & EDWARDS, A. 2003. Planning for the rising tides: the Humber estuary Shoreline Management Plan. *Science of the total environment*, 314, 13-30.
- WITTMANN, A. C. & PÖRTNER, H.-O. 2013. Sensitivities of extant animal taxa to ocean acidification. *Nature Climate Change*, 3, 995.